

Sourcing and Dynamic of Mercury in Arctic Seals

Perspectives for a changing Arctic

by Marianna Pinzone





Sourcing and Dynamic of Mercury in Arctic Seals

A Doctoral thesis by Marianna Pinzone

University of Liege
Faculty of Sciences
Freshwater and Oceanic sScience Unit of reSearch (FOCUS)
Laboratory of Oceanology

September 2021

Dissertation presented in fulfillment for the degree of Doctor of Sciences

Supervisor : Dr. Krishna Das, University of Liège

Jury

Pr. Sylvie Gobert (Jury president), University of Liège (ULiege)

Pr. Bruno Delille (Jury secretary), University of Liège (ULiege)

Pr. David Amouroux, IPREM, (CNRS-UPPA, France)

Pr. Lars-Eric Heimbürger, Institut Méditerranéen d'Océanologie (MIO, France)

Pr. Cathy Debier; Catholic University of Louvain (UCLouvain)

Pr. Krishna Das (Supervisor), University of Liège (ULiege)

Cover picture : Hooded seal *Cystophora cristata* on the drift-ice of the Greenland Sea, March 2018. © Fredrik Markussen

Abstract

Mercury (Hg) is considered one of the top 10 chemicals of modern public health concern. After the implementation of the Minamata convention in 2017, efforts were mostly directed to the understanding of Hg cycling in marine environment impacted by climate change. **The Arctic region** is a hotspot of Hg contamination studies, being a major sink and source for the global Hg cycle. Although evidences exist about a shift in Hg bioaccumulation in Arctic wildlife over time, scientists were not able to effectively link it with climate change. The remote position of some regions of the Arctic brought to a paucity of data. For example, Total-Hg (THg) temporal and spatial trends in marine and terrestrial predators living in **the Greenland Sea** are wildly missing. Forecasting of future THg trends is especially important for Arctic marine predators like marine mammals, whose Hg concentrations often surpass suggested toxicological thresholds.

The assessment of Hg sources and pathways in the marine environment, remains a complex challenge despite its recognized toxicity, both for wildlife and humans. **Stable isotope ratios** of carbon (C), nitrogen (N), sulphur (S) and Hg are valid tracers of Arctic marine predators' trophic ecology, as well as Hg sourcing and cycling in the ocean. They are often studied separately, leaving the interpretation of the data at times incomplete and limiting the understanding of the complexity of the natural world.

The main goal of this work was to understand the main factors governing Hg pollution of marine predators in a changing Arctic. We focused on Greenland Sea true seals because of their diverse trophic ecologies and distribution. **The hooded seal** *Cystophora cristata*, **harp seal** *Pagophilus groenlandicus* and the **ringed seal** *Pusa hispida* are the most common specie in the area. As such they represent the main food source of local apex predators like polar bears and humans.

We applied a **multivariate approach** integrating C, N and S stable isotopes as proxies of seal ecology, Hg stable isotopes as proxies of Hg sources and Hg concentrations as proxies of levels of exposure. We set **3 specific questions**: **(1)** which are the main sources of Hg in Arctic marine predators? **(2)** Which factors influence the most Hg bioaccumulation and biomagnification in Arctic marine food webs? And **(3)** Which consequences can be drawn for the health of Arctic marine food webs in the framework of climate change?

Our main findings indicate that **(1) local Hg sources** are far more important in governing Hg bioaccumulation and biomagnification in Arctic marine food webs, than environmental Hg levels; and **(2)** while environmental change at global levels is determining a **decrease in Hg emissions and accumulation** in marine species from **oceanic food webs**, ongoing **changes across Arctic coasts** are **enhancing the risk of Hg exposure to inshore food webs**.

Acknowledgements

This work would have not been possible without the help of many exceptional people. Because of them, during these last five years I've laughed, I've learned, but more importantly, I've grown into the person and researcher I am today. My most sincere gratitude goes to:

My family. My mother, Nicola, Giulia, Giuseppe and Olivia, who taught me to dream big, and supported my intention to leave Italy and find my own path. Because of you, I never feel alone, wherever I am in the world. Marie-Christine, Nicolas and Salomé, who taught me to believe in myself and my work. A particular thanks to Nicolas for printing every article I publish and ask for an autograph and making me feel special, as well as for understanding from A to Z what it means to make research your reason for living. My dad, Maria Pia, Chiara, Giorgia, Valerio, Danilo, Giorgina, Davide and Francesco, for always showing an eager interest in my work and asking many, many... too many questions about fish, sharks and dolphins.

The students and friends I had the chance to supervise or collaborate with. I would like to thank Carmen Bâlon, Thomas Bawin, Chester Gan, Julian Garcia, Kshanika Piyumi Guruge, Diletta Lugli, Liz Loutrage, Davi Munhoz, Marie Petitguyot, Marine Pils, Elodie Robert, Alexis Trinquet and the 2016/2017 and 2017/2018 classes from the Arctic Biology course of the Arctic University of Norway – UiT (Tromsø), for their precious contribution during sampling, analysis and data interpretation.

My numerous collaborators. All of my gratitude goes to Prof. Rune Dietz, Prof. Christian Sonne, Dr. Igor Eulaers and Dr. Jean-Pierre Desforges from Aarhus University (Denmark), for their warm welcome in Roskilde, huge help for sample collection and for sharing their incredible knowledge about Hg cycling in Arctic wildlife.

Many thanks to Dr. Tore Haug from the Institute of Marine Research (IMR, Tromsø, Norway), Dr. Mario Acquarone and Prof. Lars Folkow (UiT, Tromsø, Norway) for sharing the numerous samples of free-ranging and captive Greenland Sea seals, without which I would never have been able to obtain these very important results.

Sincere thanks to Prof. Erling S. Nordøy from UiT (Tromsø, Norway) for helping me with sampling collection, and - more importantly - for allowing me to join twice the incredible journey to the Arctic onboard of the RV Helmer Hanssen.

Many thanks to Dr. David Amouroux, Sylvain Bérail, Emmanuel Tessier and the all team at the IPREM Institute of the Université de Pau et des Pays de l'Adour (UPPA) (Pau, France), for their kind welcome, patience and assistance during training and analysis of mercury speciation and stable isotopes. I remember my stay in Pau as a very valuable period of technical and theoretical learning.

Finally, I would like to thank Dr. Bruno Delille for his guidance and collaboration with regards to extraction of climate change variables and integration with mercury data. I greatly value the expertise gained through this collaboration.

The funding agencies that have made this work possible. The PhD was funded the Belgian Fonds National pour la Recherche Scientifique F.R.S. - FNRS through the FRIA PhD fellowship, as well as the F.R.S.-FNRS Research Credit scholarship (IsoArctic project), the FOCUS Research Unit at ULiege (IceBio project) and the Fédération Wallonie-Bruxelles (FWB) and ULiège COVID-19 financial aids. In addition, my deepest gratitude goes to all the additional funds that allowed the realization of field missions and the participation to scientific congresses: the Agathon de Potter price, the Patrimoine fund of the University of Liege and the FNRS grants for Scientific meetings in and outside Europe.

My colleagues (past and present) of the laboratory of Oceanology (ULiège, Belgium) and the FOCUS Research Unit, whom I am lucky enough to call friends: France Collard, Alice Cransveld, Patrick Dauby, Cédric Delforge, Paulo Dorneles, Baptiste Le Bourg, Laurence Lefebvre, Benjamin Lejeune, Mariella Lunetta, Michel Marengo, Janeide Padilha, Dorothée Pête, Carolina Pizzocchero, François Remy, Joseph Schnitzler and Nicolas Sturaro. Thank you all for the memorable moments spent together like the coffee breaks, the Friday's pizza and the long scientific chats. You all contributed to make me the researcher I am today.

A special thought to Renzo Biondo, who made me feel a little bit at home sharing with me the Italian culture and spirit, trained me for total-mercury analysis and followed my every step when I first started to work at the laboratory. I have learned so much thanks to you. You will always be in my heart.

A special thanks to France Damseaux, la twin, for sharing this great yet difficult PhD journey together. For supporting me all the way, at each difficult moment, and to understand my every feeling without me even needing to tell them out loud.

Special thanks to Dr. Gilles Lepoint for introducing and training me to the analysis of stable isotopes, his supervision, emotional support and critical help. For being my office-neighbor and enduring my loud talks and music during your afternoon naps.

Many thanks to Dr. Loïc Michel, for being my stable isotopes guru, for sharing his experience and passion about the scientific career. I am proud to have made you a seal chick too.

My greatest thanks to **Madame Chef** Sylvie Gobert, for welcoming me with open arms at the laboratory of Oceanology, and for always involving me in many different activities. Thanks to you I learned a lot and felt like an active member of the laboratory from the very beginning.

My sincere gratitude for the members of **my thesis committee**, Bruno Frédéricich, Gilles Lepoint, Thierry Jauniaux, Célia Joaquim-Justo and Krishna Das who helped me, guided me and supported me throughout these 4 years. I am very grateful for all your valid inputs and the interesting discussions about my results.

My outmost gratitude to the **jury members** for accepting our invitation and take the time to evaluate and discuss my work: Sylvie Gobert, Bruno Delille, David Amouroux, Lars-Eric Heimbürger and Katy Debier.

To the best promoter of the world, Krishna Das. She believed in me when I did not and always pushed me to be the better and stronger version of myself. Thanks to you I have realized my dream.

To the loves of my life. My husband Gaetan Hug, for his assistance with the English-proofing of the manuscript, all the cooking and patience demonstrated during the writing of the thesis. For always following (physically and emotionally) my dreams and being the most lovable, understanding human being I know. Because of you, I am not scared of anything.

My daughter, Aurora Tiaré Hug. When I look into your eyes I see the northern lights and the sea. Your cheerfulness and stubbornness are the reasons that motivate me to continue in the field of research and contribute, even if little, to save this wonderful planet we leave in.

Abbreviations and acronyms

AMAP: Arctic Monitoring and Assessment Program

AMDEs: Atmospheric Mercury Depletion Events

AO: Arctic Oscillation

C: Carbon

Cc: *Cristophora cristata*

CRM: Certified Reference Material

DMHg: Dimethyl-Mercury

DOC/DOM: Dissolved Organic Carbon/Matter

DOLT: Dogfish Liver Certified Reference Material for Trace Metals and other Constituents

DORM: Dogfish protein Certified Reference Material for Trace Metals and other Constituents

ERM: European Reference Material

Fe: Iron

FYI: First Year Ice

GC-ICPMS: Gas Chromatography-Inductively Coupled Plasma Mass Spectrometry

HB: Hot block

HCl: Chloridric acid

HNO₃: Nitric acid

IDA: Isotope Dilution Analyses

iHg: Inorganic Mercury

IPD: Isotope Pattern Deconvolution

IRB: Iron Reducing Bacteria

IRM: Internal Reference Material

IRMM: Institute for Reference Materials and Measurements

IUCN: International Union for Conservation of Nature

LMMs: Linear Mixing Models

LOD: Limit of Detection

LOQ: Limit of Quantification

MC-ICPMS: Multicollector-Inductively Coupled Plasma Mass Spectrometry

MDF: Mass Dependent Fractionation

MIZ: Marginal Ice Zone

MeCo: Methylcobalamin

MeHg: Methylated Mercury (monomethyl or dimethyl mercury)

merA: Mercuric Reductase

MIE: Magnetic Isotope Effect

MIF: Mass Independent Fractionation
MMHg: Methylmercury
MYI: Multi-Year Ice
MW: Microwave
N: Nitrogen
NaBEt₄: Sodium tetraethyl borate
NFS: Nuclear Field Shield effect
NIES: National Institute for Environmental Studies
NIST: National Institute of Standards and Technology
IAEA: International Atomic Energy Agency
IRM: Internal Reference Material
NAO: North Atlantic Oscillation
NRCC: National Research Council of Canada
ID: Isotope Dilution
PCA: Principal Component Analysis
Pg: *Pagophilus groenlandicus*
Ph: *Pusa hispida*
POC: Particulate Organic Carbon
RDA: Redundancy Analysis
S: Sulphur
SEA: Standard Ellipse Area
SIA: Stable Isotope Analysis
SIBER: Stable Isotope Bayesian Ellipses models in R
SnCl₂: Stannous Chloride (II)
SRB: Sulphate Reducing Bacteria
SSE: Self-Shielding Effect
TEF: Trophic Enrichment Factor
THg: Total Mercury
TMAH: Tetramethylammonium hydroxide
TMS: Trophic Magnification Slope
IUPAC: International Union of Pure and Applied Chemistry
LMWOC: Low-Molecular-Weight Organic Compounds
UNEP: United Nations Environment Program
WHO: World Health Organization

§ : paragraph

Table of Contents

Abstract

Acknowledgements

Abbreviations and acronyms

General background and objectives.....x

Chapter 1 General Introduction..... 1

1.	Mercury	2
1.1.	Mercury global cycle	2
1.2.	Mercury cycle in the marine environment.....	4
1.3.	Mercury bioaccumulation in the food web	8
1.4.	Mercury toxicity.....	12
2.	Mercury in the Arctic.....	15
2.1.	The Arctic region	15
2.2.	Sea-ice and its role for Arctic marine food webs.....	19
2.3.	Mercury cycling in the Arctic	21
2.4.	A changing Arctic	26
3.	Stable isotopes as chemical tracers	30
3.1.	Stable isotopes of carbon, nitrogen and sulphur.....	31
3.2.	Stable isotopes of mercury.....	33
3.3.	Hg MDF and MIF in marine ecosystems and predators	36

Chapter 2 General Material & Methods..... 38

1.	Model species.....	39
1.1.	The hooded seal	40
1.2.	The harp seal	41
1.3.	The ringed seal	43
2.	Sampling site.....	44
3.	Ethical statement.....	45
3.1.	Captivity	45
3.2.	In-situ harvesting.....	46
4.	Sampling	46
4.1.	Partners	46
4.2.	Seals in captivity	48
4.3.	Tissue bank sampling.....	49
4.4.	Free-ranging seals	49
5.	Seals aging	51
5.1.	Teeth analysis.....	52
5.2.	Standard length.....	52
5.3.	Pelage.....	52
6.	Samples preparation	53
7.	Analytical technics.....	54
7.1.	THg concentrations.....	54
7.2.	Carbon, nitrogen and sulphur stable isotopes analysis.....	54
7.3.	Hg speciation	55
7.4.	Mercury stable isotopes	58
8.	Statistics.....	61
8.1.	Lipids correction	61
8.2.	Exploratory data analysis	61
8.3.	Calculation of SIBER niches	61
9.	Constrains	62

Chapter 3 Carbon, Nitrogen and Sulphur isotopic fractionation in captive subadult hooded seal <i>Cystophora cristata</i>: application for diet analysis	63
Abstract.....	64
1. Introduction.....	65
2. Materials and Methods	67
2.1. Sampling and captivity.....	67
2.2. Samples preparation.....	68
2.3. Stable isotope analysis	68
2.4. Isotope fractionation calculation.....	68
2.5. Statistical analyses.....	69
3. Results	69
3.1. Biometric analysis	69
3.2. Stable isotope ratios	70
3.3. Experimentally-estimated TEFs.....	71
3.4. Comparison with model-estimated TEFs.....	71
4. Discussion.....	72
4.1. Comparison with the literature.....	72
4.2. Comparison between tissues	74
4.3. Assessment of model efficiency in calculating isotopic fractionation	77
5. Conclusions.....	79
Chapter 4 Using Hg stable isotopes to assess Hg dynamic in Arctic seals: new insights from a captive experiment on hooded seal <i>Cystophora cristata</i>	80
Abstract.....	81
1. Introduction.....	82
2. Material and method.....	84
2.1. Samples collection and preparation	84
2.2. Mercury species analysis.....	84
2.3. Mercury stable isotopes analysis.....	85
2.4. TEF quantification	85
2.5. Statistical analyses.....	85
3. Results	86
3.1. Mercury species profile.....	86
3.2. Mercury stable isotopes analysis.....	87
3.3. TEFs.....	88
4. Discussion.....	89
4.1. Bioaccumulation of mercury.....	89
4.2. Mass-dependent fractionation of mercury isotopes reflects speciation and transformation in tissues.....	90
4.3. Mass-Dependent Fractionation of mercury isotopes does not reflects sources and trophic transfer	92
4.4. Information about mercury sources is preserved from prey to predator.....	93
4.5. Age influence mercury metabolism and TEFs.....	94
5. Conclusions.....	96
Chapter 5 Terrestrial versus marine: discrimination of Hg sources in Arctic true seals by a multi-isotopic approach.....	97
Abstract.....	98
1. Introduction.....	99
2. Material and methods	101
2.1. Sampling protocol	101
2.2. Total-mercury and stable isotopes analysis.....	102
2.3. Statistical analyses.....	103
2.4. Data interpretation.....	105

3.	Results.....	107
3.1.	Multivariate analysis	107
3.2.	SIBER	107
3.3.	Stable isotope ratios	107
3.4.	Mercury levels.....	108
4.	Discussion.....	110
4.1.	Habitat use is the most important factor influencing the multi-isotopic composition of Arctic true seals.....	110
4.2.	Offshore versus coastal habitat use	112
4.3.	Habitat use influences Hg sources	114
4.4.	Habitat use influences Hg pathways	115
4.5.	Habitat use influences levels of Hg exposure	116
5.	Conclusions.....	120
Chapter 6 Impact of environmental changes on Hg temporal trends in Arctic true seals.....		121
	Abstract.....	122
1.	Introduction.....	123
2.	Material and methods	125
2.1.	Sampling	125
2.2.	Analysis.....	125
2.3.	Correction of $\delta^{13}\text{C}$ values	125
2.4.	Extraction of biological and climatic variables	126
2.5.	Statistics analysis.....	126
3.	Results.....	129
3.1.	Linear Mixing Models (LMMs).....	129
3.2.	Hg stable isotopes' trends.....	129
4.	Discussion.....	131
4.1.	Mercury trends in ringed seals	131
4.2.	Mercury trends in hooded seals	135
4.3.	Temporal trends of mercury sources.....	136
5.	Conclusions.....	141
Chapter 7 General Discussion.....		142
1.	The Arctic: a hotspot for Hg pollution studies.....	143
2.	Spatial Hg trends in Arctic seals: what are we missing?	144
3.	Trophic level, metabolism or habitat use?.....	146
3.1.	Higher trophic level does not mean higher mercury	146
3.2.	Specialized nursing does not put seals at risk.....	146
3.3.	Different habitat use, different mercury sources.....	147
4.	Hg sources in seals from the Greenland Sea.....	149
4.1.	Local or global?	150
5.	Present and future dynamic of mercury in Greenland sea marine predators.....	156
5.1.	A changing Arctic	156
5.2.	Offshore foodwebs.....	158
5.3.	Coastal food webs	159
Take home message		163
References.....		164
ANNEX.....		209

General background and objectives

Mercury (Hg) is considered one of the top 10 chemicals of public health concern by the World Health Organization (Jonsson et al., 2017). Since the discovery of its strong toxic effects on the health of poisoned consumers in the 50s, its direct production was banned in many parts of the world (Mason et al., 2012). In August 2017, the “Minamata Convention on Mercury” was finally ratified, signaling the urgent need for mitigation of Hg emissions at global scale (Chen et al., 2018).

The Arctic region is at the center of this problem, since it is a well-known sink and source for the global Hg cycle (Kirk et al., 2012). The particular geochemistry of the Arctic Ocean with its position, gentle shelves, strong water column stratification, ice cover, and surface circulation systems, are all factors exacerbating the remobilization of Hg in the natural ecosystems (Outridge et al., 2008). The ongoing climate-driven environmental changes add up to the complexity of Arctic Hg chemistry. Indeed, warming of the Arctic environment was strongly associated with changes in rates of Hg uptake by marine food webs (Sundseth et al., 2015). Additionally, the new discoveries related to the importance of Arctic tundra and permafrost as storages of globally-produced Hg, bring new concerns about the potential increase of Hg terrestrial reemissions to the ocean as a consequence of climate change (Douglas and Blum, 2019; Liu et al., 2018).

In this framework, Arctic marine predators like marine mammals seem to be the most sensitive to the increase of Hg concentrations in the environment (McKinney et al., 2015). Specifically, they have shown a 10x increase over the past 150 years, with an average rate of increase of 1 to 4 % per year (Dietz et al., 2009). As a consequence, Hg levels in their tissues have reached the point where adverse health effects might be expected (Braune et al., 2011).

Such trends are not consistent on a panarctic scale since they differ temporally and spatially and from a species to the other.

The reasons **why** such spatial and temporal inconsistency exists and why Arctic marine mammals seem to be more concerned by Hg increase than other organisms are still unclear.

Until now, most of the focus was given to the levels of pollution rather than the sources of Hg from the environment. However marine mammals like true seals present such complex life styles, ecologies and physiologies, which did not allow to effectively link climate change to Hg pollution.

Stable isotope ratios of carbon (C) and nitrogen (N) are confirmed valid tracers of Arctic marine predators' trophic ecology. The amelioration of analytical techniques allowed to extend isotopic analysis also to more complicated elements like S and Hg. Sulphur (S) stable isotopes consist in a powerful addition to trophic analysis, since it is less modified by environmental and metabolic processes (Connolly et al., 2004). On the other hand, discoveries made through the analysis of Hg stable isotopes boosted the understanding of Hg sourcing and cycling in the oceans (Tsui et al., 2019).

Several studies demonstrated how the interpretation of isotopic data can be complicated by **intrinsic factors** (e.g. age, diet, etc.), as well as **external factors** (e.g. sea-ice, riverine run-off, temperatures, etc.). There is thus a blatant need for additional studies on physiologically complex animals like marine mammals.

The main objective of this thesis is to assess the main factors influencing Hg sources and accumulation pathways in Arctic marine predators. We set two specific questions:

1. Which are the main **Hg sources** to Arctic marine predators?
2. Which factors influence the most Hg bioaccumulation and biomagnification by Arctic marine food webs?

We structured the thesis to test the following intrinsic and external factors:

- **Tissues' metabolism** (*Chapter 3 & 4*);
- **Species trophic ecology** (diet, habitat use, distribution, etc.) (*Chapter 5*);
- **Environmental change** (sea ice cover, temperature, prey biomass, etc.) (*Chapter 6*).

Our **final goal** is to understand the consequences of climate change on the levels of Hg exposure in Arctic animals and human communities at large.

We integrate **Hg levels** and **C, N, S and Hg stable isotopes** with environmental parameters (ice cover, temperature, etc.) in time and space, in **multivariate models in R** (PCA, RDA, SIBER and LMMs). We conduct the analysis on muscle of **three sentinel species of Arctic true seals**: the hooded seal *Cystophora cristata*, the harp seal *Pagophilus groenlandicus* and the ringed seal *Pusa hispida* from the Greenland Sea.

Thanks to numerous collaborations, we had access to a large number of samples of hooded, harp and ringed seals living and breeding along the **Eastern coast of Greenland Sea** (Fram Strait, Greenland Sea and Denmark Strait). These species are the most common in the region and present distinct trophic ecologies, geographical ranges and physiological adaptations (Rosing-Asvid, 2010). Moreover, they are harvested by Scandinavian and indigenous populations (Steiner et al., 2019).

Quantifying the impact of climate change on Hg trends in these three species is imperative for the health assessment of Greenland Sea marine predators, as well as **human communities**. Due to its remoteness and low human presence, the **Greenland Sea** is one of the least studied areas in the Arctic. Yet, satellite-based estimates show how it is one of the most impacted regions by climate change (Meredith et al., 2019).

The thesis is structured as follows:

- Chapter 1: This chapter presents a general introduction on Hg pollution worldwide and in the Arctic region, together with the ongoing climate change and the application of C, N, S and Hg stable isotopes.
- Chapter 2: This chapter presents the general materials and methods used in this thesis. We describe sampling collection, Hg speciation and stable isotope analysis, the SIBER and multivariate statistical approaches.
- Chapter 3: This chapter presents the influence of physiological factors (e.g. age, tissue metabolism) on C, N and S isotopic incorporation in Arctic seals. The study was conducted on captive hooded seal pups that were exposed to a controlled diet for 2 years.
- Chapter 4: This chapter presents the influence of physiological factors (e.g. age, tissues' metabolism and detoxification role) on Hg isotopic incorporation in Arctic seals. The study was conducted on captive hooded seal pups that were exposed to a controlled diet for 2 years.
- Chapter 5: This chapter presents the influence of ecological factors (habitat use, prey choice, hunting behavior) on Hg sourcing and accumulation in Arctic seals. The study was conducted on wild hooded, harp and ringed seals sampled between 2008 and 2019 along the Eastern coast of Greenland;
- Chapter 6: This chapter presents the influence of environmental factors (e.g. sea ice cover, temperature, prey biomass, etc.) on temporal trends of Hg levels in Arctic seals. The study was conducted on wild hooded, harp and ringed seals sampled between 1985 and 2019 along the Eastern coast of Greenland;
- Chapter 7: This chapter presents a final general discussion about the main outcomes of our analysis. We discuss about Hg sources in Arctic true seals at local and global scale and depict Hg dynamic in Arctic marine food webs in a context of present and future climate change.

Chapter 1

General Introduction

1. MERCURY

Mercury (or Hg from the Greek “*hydrargyros*”, silver) is a heavy, silvery-white liquid element with an atomic number of 80 and an atomic mass of 200.59 g mol⁻¹ (Liu et al., 2012). In the periodic table of elements, Hg is classified as a transitional metal (d-block), the only one in liquid form at standard temperature and pressure conditions (25°C and 1bar, IUPAC (SATP)) (McNaught and Wilkinson, 1997). Hg freezing point is at -38.8°C and its boiling point is at 356.7°C. Hg presents three oxidation states: Hg⁰ (metallic), Hg¹⁺ (mercurous) and Hg²⁺ (mercuric), with the monovalent form being rare owing to its instability (Liu et al., 2012). The standard reduction potential for the Hg⁰ / Hg²⁺ redox pair (E⁰ = 0.851 V; Lide, 2007) is in the range of commonly encountered environmental redox conditions (as defined by E^h), resulting in dynamic reduction and oxidation cycling in atmospheric, aquatic, and terrestrial compartments. In terms of reactivity and binding, Hg is considered a soft acid and, therefore, according to the Hard–Soft Acid–Base Theory, forms stable bonds and compounds with soft bases such as thiols, sulfides, and other ligands containing reduced Sulphur (Lehnher, 2014).

1.1. Mercury global cycle

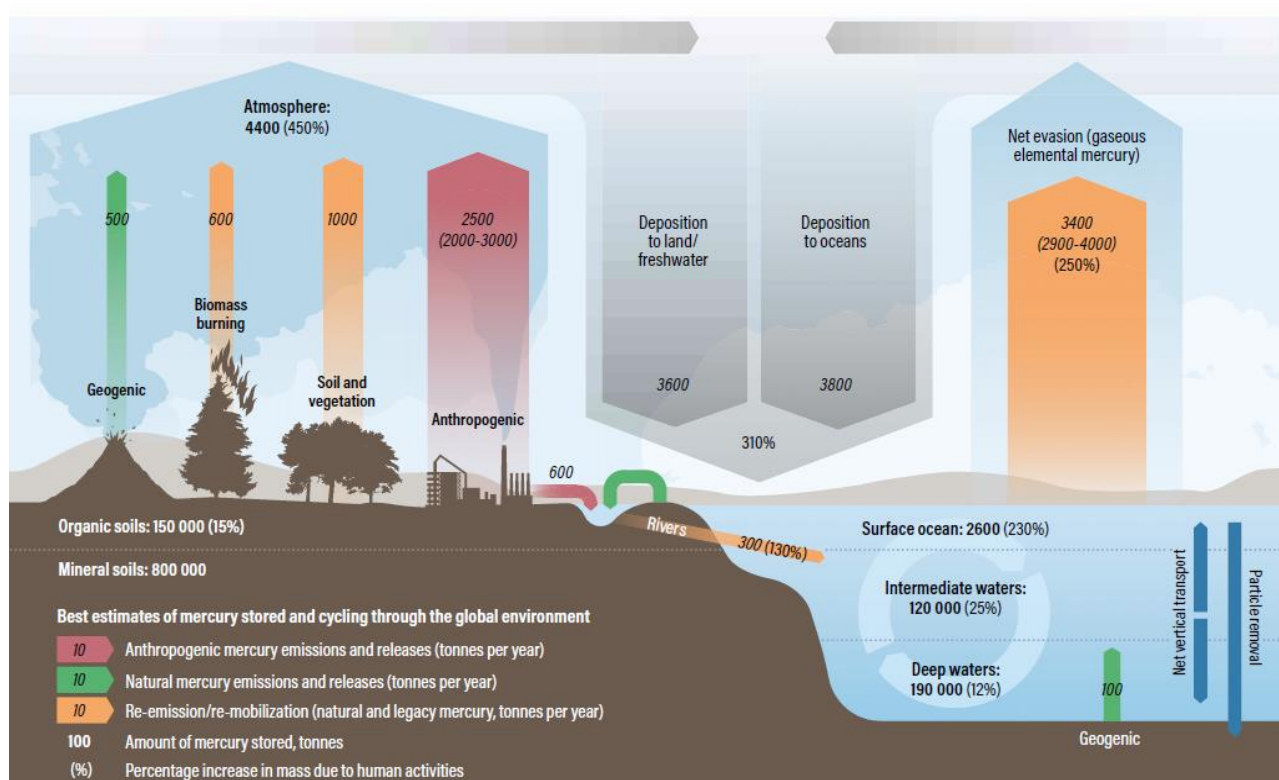


Figure 1.1. Global mercury (Hg) budget reported in the latest “Global Mercury Assessment” report (UNEP, 2018). The arrows represent the processes (emission/deposition) of Hg transport in the environment. Numbers represent the amount (in tons per year = Mg y⁻¹) of Hg fluxes. Percentages in brackets represent the increase in Hg due to human activities since the pre-anthropogenic and preindustrial periods (set as 1450 AD). Figure copyright: Outridge et al., 2018.

Hg is a natural occurring, ubiquitous element. Due to its physio-chemical characteristics, it can be transported over long distances and accumulated in areas far away from its original source (UNEP, 2013). Emission into the atmosphere is the primary pathway of mercury global circulation and entering in the environment (UNEP, 2013). Environmental mercury has both natural and anthropogenic origin (Figure 1.1). Natural sources include geologic activities (volcanic and geothermal) and reemission of Hg from terrestrial environments via biomass burning, rock weathering, exchange of Hg⁰ at air-water air-land or snow-ice interfaces (Liu et al., 2012). The oceans represent 70 % of the planetary surface (Mason and Sheu, 2002). Therefore, they are considered as the major input of Hg into the atmosphere, with an estimated yearly contribution of 52 % of total Hg production through volatilization of Hg in/from marine environments (e.g. air-surface layers exchange, hydrothermal vents) (Pirrone and Mason, 2009). The latest Hg reports estimate that about 600 Mg y⁻¹ of Hg emissions in the environment are of natural origin (UNEP, 2018).

Anthropogenic sources of Hg include (UNEP, 2018):

- artisanal and small-scale gold mining (38 %),
- fossil fuel combustion (like coal, 21 %),
- smelting of metals (15 %),
- waste incineration (7 %), and
- the chloro-alkali production (0.68 %) (Liu et al., 2012; UNEP, 2013).

Today the largest producers of Hg are (UNEP, 2018):

- East and Southeast Asia (39 %),
- Southern America (18.4 %), and
- the sub-Saharan Africa (16.2 %), and
- the ensemble of the 27 EU countries plus the UK (3.5 %).

Recent Hg global budget models estimate that human activities have increased current atmospheric Hg concentrations by about 450 % (representing a 5.5 fold increase) above natural levels (before 1450 AD, pre-anthropogenic and pre-industrial periods) (Outridge et al., 2018). The latest estimates show that nowadays between 2 000 to 3 000 Mg y⁻¹ of Hg emissions in the environment are of anthropogenic origin (Figure 1.1; UNEP, 2018).

The dominant species of Hg in the environment are 3: elemental mercury (Hg⁰), divalent mercury (Hg²⁺) and methylated mercury (monomethyl-Hg or MMHg, and dimethyl-Hg or DMHg). Each of them plays a crucial role in the biogeochemical cycle of Hg. In the literature MMHg and DMHg are often considered together and referred to as MeHg. We will also use this nomenclature throughout the entire thesis. Hg⁰ is the most volatile, composing >95 % of Hg found in air. Due to its relatively low deposition velocity (0.8 to 1.6 years) (Selin, 2009), it circulates in the atmosphere over long distances (Pirrone et al., 2010). Hg²⁺ is the most reactive reservoir of Hg in air (although representing less than 5 %), as well as the other compartments of the environment. Having strong affinity for a vast range of

inorganic and organic ligands, it is readily deposited in water and soil (Jonsson et al., 2014a). DMHg is quite soluble and volatile and is easily photodegraded. To this day, there is no data showing that DMHg can be bioaccumulated (Lehnherr, 2014). Conversely, MMHg is considered as relatively lipid soluble and can be bioaccumulated by living organisms and biomagnified along the food web (National Research Council, 2000a). MMHg is the form of most concern for aquatic ecosystems.

1.2. Mercury cycle in the marine environment

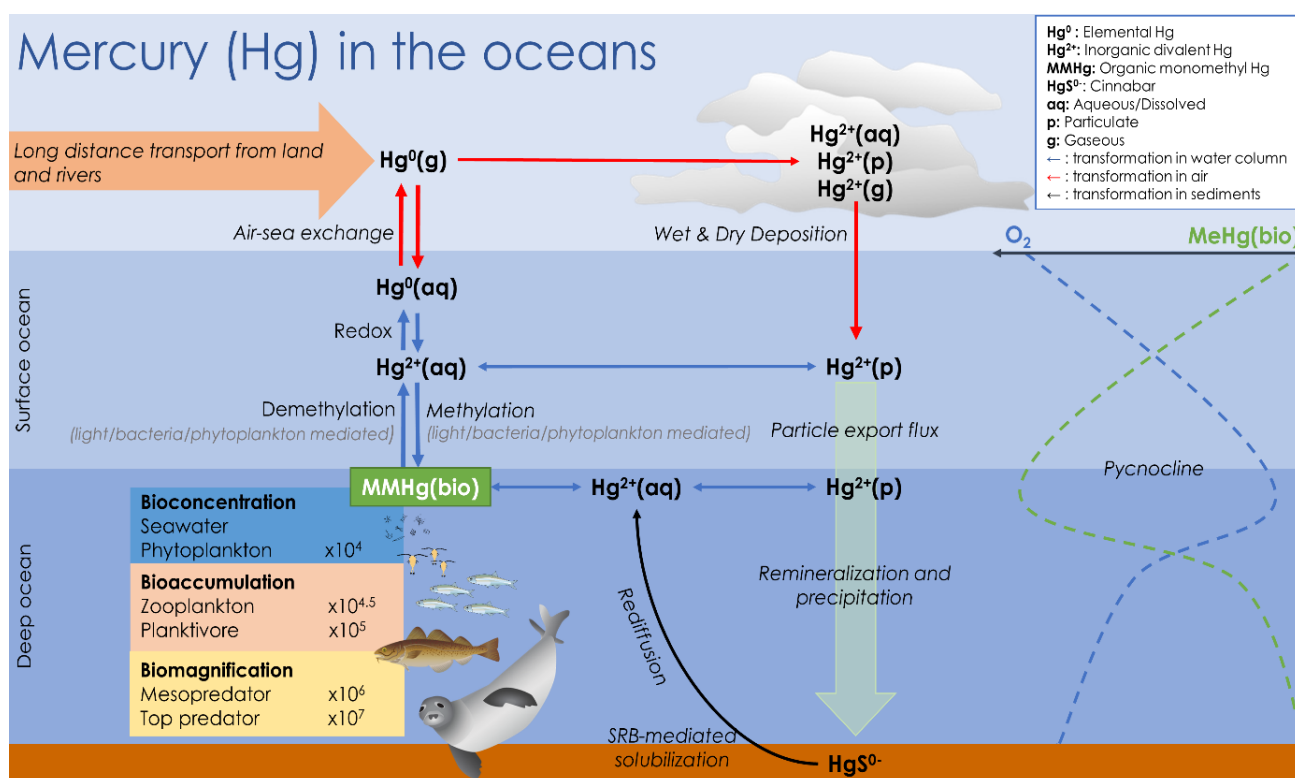


Figure 1.2. Simplified Hg cycle in the marine environment. Red arrows show air-water processes, the blue arrows show processes undergoing in the water column, while black arrows show processes at the water-sediments interface. Since poorly understood, Hg processes related to dimethyl-Hg (DMHg) are neglected. Figure modified from Petrova, 2020.

Mercury enters the marine environment through local and long-range sources (Figure 1.2). Direct atmospheric deposition is the dominant source of long-range transported Hg (~ 90 %) (Mason et al., 2012). Hg^0 can be oxidized to Hg^{2+} by strong oxidants such as ozone and halogens (e.g. Br radicals) through various gas-, aerosol-, and aqueous-phase reactions (Lehnherr, 2014). Hg^{2+} is quickly taken up in rain water, snow, or absorbed onto small particles, and is rapidly removed by the atmosphere and deposited in the ecosystems through wet and dry deposition (Mason and Sheu, 2002). In contrast to Hg^0 and Hg^{2+} , direct anthropogenic sources of MeHg are scarce (Bravo and Cosio, 2020).

Once deposited, Hg^{2+} has two fates: it is either mobilized by ocean circulation, binding to abundant ligands such as chloride and dissolved organic matter (DOM), or it is reduced to Hg^0 and evade again to the atmosphere (Bowman et al., 2020). In seawater, Hg undergoes different transformations (oxidation, reduction, methylation and demethylation) (Liu et al., 2012). The most important process concerning marine biota is the methylation of aqueous Hg^{2+} to MMHg and DMHg. Indeed, Hg^{2+} constitutes the main source of MeHg in the oceans (Yu et al., 2016). Previous publications suggested that DMHg readily degrades in marine waters, especially in the presence of sunlight, but more recent studies have provided conflicting results that suggest higher stability (Balcom et al., 2015; Black et al., 2009). Kirk et al. (2012) reported that DMHg might constitute up to 80 % of MeHg in seawater. Even if DMHg is not expected to bioaccumulate or to occur in concentrations of concern for human or wildlife health (Douglas et al., 2012), its degradation is hypothesized to be an important source for MMHg (Baya, 2015; Jonsson et al., 2016). Anyhow, the formation and degradation pathways of DMHg remain poorly understood (Kirk et al., 2012).

The following paragraphs will mostly focus on the cycle of MMHg in the marine environment. The levels of MMHg in the oceans are governed by several biotic and abiotic processes (Bowman et al., 2020; Bravo and Cosio, 2020). Abiotic reactions are mainly induced by photochemistry and occur in the photic zone of the water column (Lehnherr and St. Louis, 2009; Vost et al., 2012). The biotic reactions occur in the water column as well as at the sea bottom, and are carried out mostly by bacteria and phytoplankton (Bowman et al., 2020). These processes do not depend only on the amount of Hg^{2+} bioavailable for methylation (Jonsson et al., 2014a; Schaefer et al., 2011), but also on many environmental parameters and the availability of Hg^{2+} methylating microorganisms (Paranjape and Hall, 2017).

1.2.1. Surface waters

At the surface, where light influx is not limited, photochemical reductions are the main mechanism (80 % in certain typical areas) responsible for Hg abiotic processing (Du et al., 2019; Luo et al., 2020). The process of Hg photomethylation mostly implies the transfer of methyl groups in the form of methylcarbanion (CH^{3-}), radical ($-\text{CH}_3$) or carbonium ion (CH^{3+}) to Hg^{2+} (Vost et al., 2012). Such reaction requires the availability of methyl-donor compounds, such as: methylcobalamin (MeCo), methyl-iodide (Me_3I), methyl-tin (Me_3Sn), fulvic and/or humic acids (Chen et al., 2008; Cossa et al., 2009). Several mechanisms are instead recognized to cause abiotic MMHg photodemethylation:

- -OH induced (Chen et al., 2003),
- singlet oxygen ($^1\text{O}_2$) induced (Zhang and Hsu-kim, 2010),
- excited triplet of DOM (3DOM*) induced (Qian et al., 2014),
- direct photolysis (Tai et al., 2014).

The latter is believed to be the main pathway in environmental waters (Tai et al., 2017). During direct photolysis, MMHg photodegradation is induced by ultraviolet light, with UV-A and UV-B from 280 to 400 nm being the most efficient wavelengths (Lehnerr and St. Louis, 2009; Li et al., 2010).

The rates of Hg photomethylation and demethylation are not influenced only by the intensity of light influxes, but also by other environmental parameters including pH, temperature, redox potential in sediments and, the most important one, the availability of Hg binding ligands (Hsu-Kim et al., 2013; Liem-Nguyen et al., 2017). For example, a larger proportion of sulphur-containing ligands, as found in freshwater bodies, is synonym of faster photodegradation compared to the DOM/chloride complexes rich seawaters (Zhang and Hsu-kim, 2010). Indeed, the high stability of chloride compounds such as methyl-chloride (CH_3HgCl) makes MMHg degradation more difficult (Whalin et al., 2007). Low pH and low dissolved organic carbon (DOC) content are considered favorable for the photo-degradation of MMHg (Klapstein and Driscoll, 2018). In the case of DOC for example, it creates strong bounds with Hg controlling its distribution and availability, but also provides highly redox active radicals that may serve as reductants or oxidants during photochemical reactions (French et al., 2014). Several mechanisms controlling the photodegradation of MeHg are uncertain and still under study (Li and Cai, 2013).

1.2.2. Deep oxic waters and anoxic waters

Until recently, biotic methylation mediated by anaerobic bacteria was considered as the main MMHg formation route in subsurface and bottom marine waters (Gilmour et al., 2013, 2011). However, several studies have recently demonstrated how oxic subsurface waters is where most of MMHg production takes place (Balcom et al., 2015; Heimbürger et al., 2015; Monperrus et al., 2007).

Biotic methylation occurs in the oxic layers of most ocean basins (Bowman et al., 2019; Cossa et al., 2011b; Heimbürger et al., 2015, 2010; Rosati et al., 2018; Soerensen et al., 2016b; Wang et al., 2012, 2018), during remineralization of suspended OM or in association with nutrient maxima and oxygen utilization (Blum et al., 2013; Masbou et al., 2015b; Munson et al., 2018). In both oxic and anoxic water layers, most of MMHg biotic production and degradation is induced by bacteria (Villar et al., 2020). By now scientists determined more than 54 microbes that are capable of processing Hg (Du et al., 2019). The principal groups are (Bravo and Cosio, 2020) (Figure 1.3):

- sulphate and iron reducing bacteria (SRB and IRB, respectively),
- methanogens, and
- syntrophs.

The capacity for Hg methylation by bacteria was connected to the expression of a two-gene cluster (*hgcA* and *hgcB*) (Parks et al., 2013).

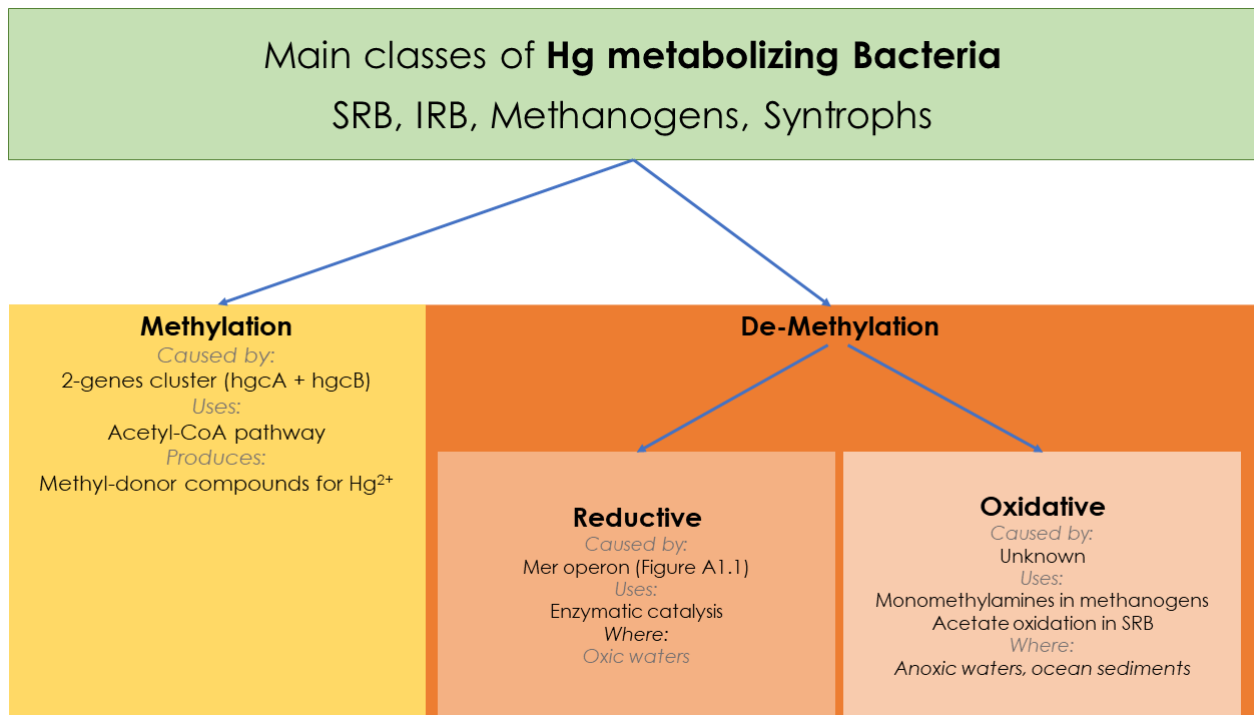


Figure 1.3. Summary of all methylating and demethylating processes induced by bacteria in the oceans.

A screening of all available metagenomes found *hgcAB* genes in nearly all anoxic environments (Podar et al., 2015), as well as in oxic subsurface waters of the global ocean (Villar et al., 2020). The gene *hgcA* encodes a corrinoid protein that is essential for the biosynthesis of the folate branch of acetyl-CoA pathway, whereas the gene *hgcB* encodes a ferredoxin-like protein thought to be an electron donor to *hgcA* (Parks et al., 2013). Both provide methyl groups required for Hg²⁺ methylation, although it is not clear whether MMHg production is a controlled or an accidental metabolic process (Gionfriddo et al., 2016).

Bacteria degrade MMHg via two main processes (Figure 1.3), which are distinguished by the gaseous carbon products of the degradation process (Paranjape and Hall, 2017):

- Oxic waters: reductive demethylation,
- Anoxic waters and ocean sediments: oxidative demethylation (Ma et al., 2019).

Reductive demethylation is carried out by bacteria possessing the *mer* operon, occurring mostly in the aerobic zone (Boyd and Barkay, 2012; Du et al., 2019). The *mer* operon includes genes that encode several proteins controlling binding, transfer and breakdown to Hg²⁺ or MMHg (see Annex to Chapter 1, §1) (Boyd and Barkay, 2012). It seems to be a direct protective mechanism against Hg toxicity (Pedrero et al., 2012). Oxidative demethylation instead is mostly operated by anaerobic bacteria in anoxic conditions (Lu et al., 2016). This process is still poorly understood but it possibly occurs as a by-product of bacterial metabolism (Marvin-Dipasquale et al., 2000).

Few studies suggest that phytoplankton and its metabolites could also have a role in MMHg processing (Gregoire and Poulain, 2014; Lee and Fisher, 2017; Schartup et al., 2020). The

abundance and size of phytoplankton seems to directly boost the remineralization and production of MMHg in oxic waters (Heimbürger et al., 2010). Small-phytoplankton blooms occur deeper in the photic zone closer to the MMHg maximum, enhancing biological uptake of MMHg at the base of the food web (Heimbürger et al., 2015). Another study conducted in the Arctic, proposes that Hg^{2+} could even be methylated by zooplankton intestinal microbial communities, however further studies are needed to confirm this hypothesis (Pućko et al., 2014).

1.3. Mercury bioaccumulation in the food web

1.3.1. Bioaccumulation and bioamplification in the food web

Primary producers are considered the main Hg access to marine food webs (Lee and Fisher, 2016; Pickhardt et al., 2018, 2002). In addition to the *mer* system, other mechanisms of Hg uptake by microorganisms are:

- passive permeation,
- facilitated permeation (specific transmembrane proteins), and
- active transport (ATP-driven ion pumps) (Hsu-Kim et al., 2013; Zhou et al., 2017).

When concentrations of either Hg^{2+} or MMHg in an organism exceed those in the water this process is called bioconcentration (Vost et al., 2012). Phytoplankton is known to concentrate 10^4 - 10^6 higher Hg levels than ambient water. This accumulation represents the largest relative increase in MMHg levels at any point in a food web (Schartup et al., 2018; Zhang et al., 2019).

The rates of Hg uptake by primary producers is favored in the presence of specific ligands, which are more readily absorbed than others. For example, neutral complexes of HgCl_2 can cross biological membranes more rapidly than ionic Hg^{2+} . In the same way thiol-complexed Hg is more easily taken up and methylated by bacteria (Kidd et al., 2012). DOM plays conflicting roles in Hg uptake, depending on its form and redox conditions of different aquatic systems (Buckman et al., 2019; French et al., 2014; Haitzer et al., 2002; Lee and Fisher, 2017; Ndu et al., 2012).

Although bioconcentration is the main uptake route at the base of the food web, primary to tertiary consumers can be exposed to Hg through both water and diet, with the relative importance of dietary exposure increasing with an organism trophic level (Vost et al., 2012). Such process is known as bioaccumulation. In the oceans, Hg^{2+} concentration are usually ~20 times higher than MMHg (Mason et al., 2012). However, the ability to form lipophilic complexes with chloride ions is greater for MMHg (100 %) than for Hg^{2+} (45 %) (Altunay et al., 2019). This results in MMHg being the preferentially bioaccumulated form due to a better efficiency in the trophic transfer (Lavoie et al., 2013). Although Hg^{2+} and MMHg are assimilated equally, the latter is concentrated in the cytoplasm and associated with the soluble fraction of phytoplankton, whereas Hg^{2+} mainly remains adsorbed on the cell

membrane (Morel et al., 1998). This different distribution in the unicellular organisms brings the efficiency of MMHg assimilation to be 4x greater than Hg^{2+} (Morel et al., 1998).

Once in the organism, the complexation of MMHg with amino acids containing thiol groups (e.g. cysteine and methionine) or non-sulphured amino acids (e.g. histidine), will regulate Hg solubility in the gastrointestinal tract and its subsequent assimilation by the body (Sonne et al., 2009a). This specific selectivity of Hg compounds explains the exponential increase of MMHg fractions (and decrease of Hg^{2+}) with trophic levels observed along food webs. MMHg constitutes between 20 and 50 % of accumulated Hg in phytoplankton, more than 75 % in second trophic level organisms (e.g. zooplankton) and 90 to 100 % in muscle of predators such as fish or marine mammals (Kidd et al., 2012; Wagemann et al., 1998).

Hg exposure to higher trophic levels does not depend only on environmental concentrations of this element, but also on foraging strategies (e.g. benthic or pelagic) (Pinzone et al., 2019) and geographical distribution (Cransveld et al., 2017). Overall, fish-rich diets have been associated with higher Hg levels in marine mammals' tissues, while diets composed by higher amounts of invertebrates like cephalopods or mollusks have been associated with lower Hg levels in favor of higher Cd levels (Brown et al., 2016; López-Berenguer et al., 2020; Pinzone et al., 2015).

The rates of Hg bioaccumulation and biomagnification will then depend on a vast number of physiological and ecological factors, characteristic to each marine species (Lavoie et al., 2013; Smylie et al., 2016). Indeed, Hg concentrations are known to increase with body size, weight and age, with older organisms usually presenting higher levels of Hg in their tissues (Hammerschmidt and Fitzgerald, 2006).

1.3.2. Monomethyl-mercury accumulation and detoxification in marine predators

Hg concentrations in higher trophic level species are controlled by numerous processes including:

- the amount of bioavailable Hg and/or MMHg at the bottom of the food web,
- species-specific processes controlling bioaccumulation and dilution, and
- food web length, structure and type (Kirk et al., 2012).

For marine predators (e.g. large fish, seabirds or marine mammals) diet represents the main pathway of exposure to Hg. After prey digestion, MMHg is absorbed through the intestine walls and transported by the blood stream towards all the other tissues (Figure 1.4). The primary target of MMHg in the body are sulfhydryl (thiol; -SH) groups of low- and high-weight biological ligands (Ajsuvakova et al., 2020). MMHg complexation with these molecules appears to regulate the accumulation and elimination in the different organs (Bridges and Zalups, 2010; Wagemann et al., 1998).

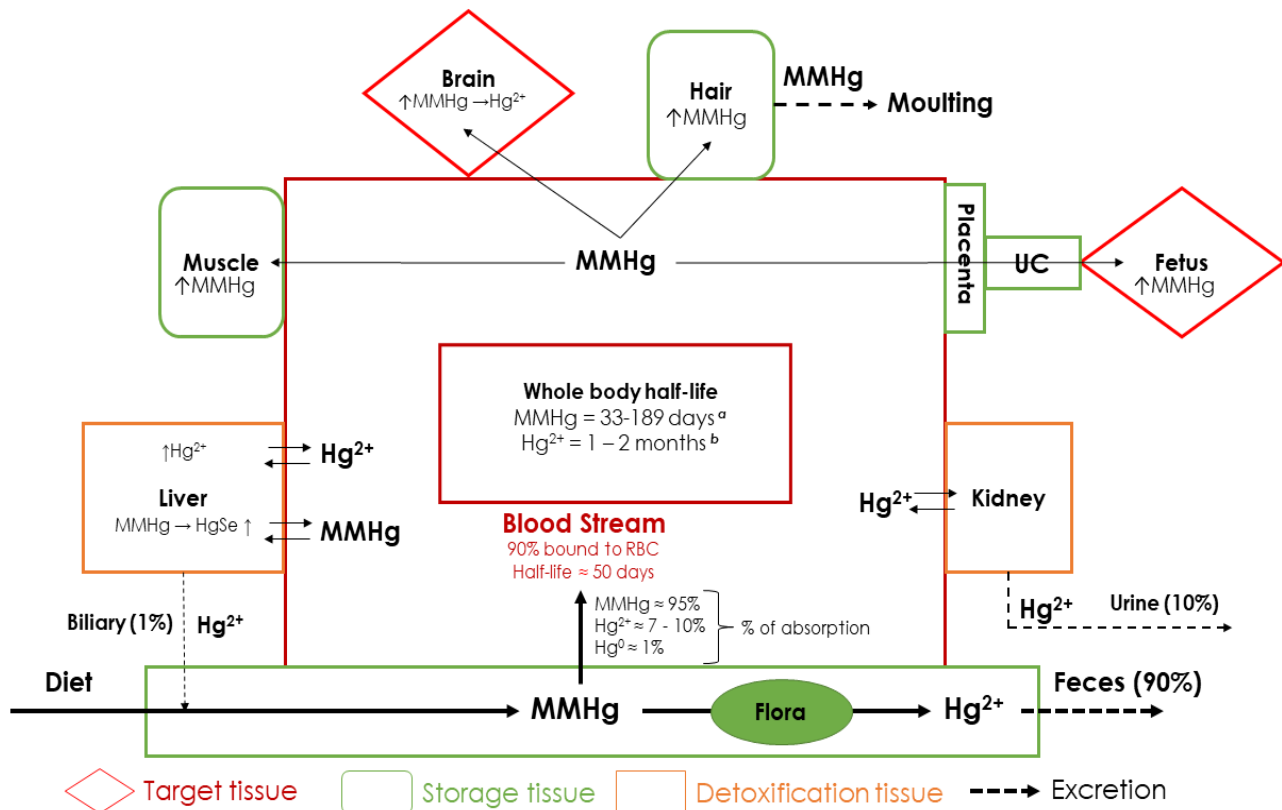


Figure 1.4. Simplified schematics of the distribution of monomethyl-Hg (MMHg) and inorganic Hg (Hg^{2+}) in humans and mammalian predators. Red diamonds represent the target tissues of Hg toxicity. Orange squares represent detoxifying tissues. Green squares represent storage tissues where MMHg is accumulated over time. Excretion is represented by dotted arrows; assimilation and transfer through continuous arrows. Figure taken and modified from Clarkson et al., 2007; National Research Council, 2000b. Absorption % were extracted by: Gentès et al., 2015; Maury-Brachet et al., 2006; Park and Zheng, 2012. a = half-life calculated on hair, b = half-life calculated in whole blood (Nordberg and Fowler, 2019).

Some examples are:

- Cysteine (Cys) and Cys-containing enzymes,
- Glutathione (GSH)
- Albumin
- Hemoglobin of red blood cells (Hong et al., 2012).

Blood, which is responsible of transporting Hg by thiol-conjugate ligands (Bridges and Zalups, 2010; Clarkson et al., 2007), is an equilibrium vector between Hg uptake, tissue storage and remobilization due to the continuous inter-organ circulation of Hg (Clarkson, 2007).

At first, Hg is distributed to liver and kidney, which are key organs for the metabolism of Hg within the body, and consequently for Hg detoxification. Kidney is the major target organ of inorganic Hg. The proximal tubule is the primary target site of Hg^{2+} , where mercury salts are absorbed and accumulated (Rice et al., 2014). Inorganic Hg salts are not lipid soluble and do not cross the blood-brain barrier or blood-placenta barrier. Inorganic Hg salts are mainly excreted in the urine and feces (1 % of body burden / day, Figure 1.4) (Park and Zheng, 2012).

Liver is the organ where dietary MMHg is demethylated in Hg^{2+} and made inert, through the co-precipitation of Hg^{2+} with Se to form HgSe granules or tiemanite (Wagemann et al., 1998). This process is confirmed to occur in predators strongly exposed to Hg such as seabirds, seals and whales (Bolea-Fernandez et al., 2019; Eagles-Smith et al., 2009; Li et al., 2020; Lyytikäinen et al., 2015; Perrot et al., 2015; Renedo et al., 2021). Its occurrence in fish instead, is quite debated due to contrasting results in the literature (Cransveld et al., 2017; Gentès et al., 2015; Kwon et al., 2014; Wang et al., 2013; Wang and Wang, 2017). This efficient detoxification process allows to reduce Hg bioavailability and thus its toxicity (Ewald et al., 2019). As a consequence of the complexity of Hg dynamics in the organism, it is still not clear if MMHg demethylation only takes place in liver or in several other organs and tissues. Due to the high fractions of Hg^{2+} in livers of marine mammals and seabirds, liver is considered the main organ responsible for MMHg demethylation (Kehrig et al., 2015; Wagemann et al., 1998). However, previous studies on striped dolphins and marine fish investigated the formation of HgSe also in other organs (kidney, lung, spleen, pancreas, muscle and brain) and confirmed the presence of HgSe in all the examined tissues, suggesting that Se could be involved in the detoxification process of Hg in tissues other than just the liver (Nakazawa et al., 2011; Wang and Wang, 2017). HgSe accumulate as inert crystals in the tissues for life, while the remaining demethylated Hg^{2+} is excreted through urines and feces (Figure 1.4).

While Se binding appears to act as a defensive mechanism against the direct toxic effects of Hg exposure, it may also cause indirect physiological problems (Kershaw and Hall, 2019). Indeed, Spiller (2018) suggested that the “protective effect” of Se against Hg toxicity may in fact negatively lead to a Se deficient state. As a result, MMHg is now recognized as a highly specific, irreversible inhibitor of selenoenzymes (Spiller, 2018).

MMHg can also be directly stored - definitely or temporarily - in “storage tissues” such as muscle, skin appendages (nails, claws, feathers, hairs, etc.) and transferred to the offspring (fetuses or eggs) (Cizdziel et al., 2003; Clarkson et al., 2007).

MMHg excretion occurs mostly through the fecal pathway, followed by urines (% values in Figure 1.4) (National Research Council, 2000b). Humans, marine mammals and seabirds can also excrete MMHg through replacement of hair and feathers, which constitutes an effective excretory pathway (Bond et al., 2015; Magos and Clarkson, 2008; Renedo et al., 2017a). Baleen and toothed whales have no fur and are thus private of this Hg excretion route (Dietz et al., 2013). The biological half-life of MMHg in the mammalian body is 39 to 70 days depending on body burden (Park and Zheng, 2012).

1.4. Mercury toxicity

The earliest recorded event of mercury poisoning was the death of emperor Ying Zheng, the first emperor to unify China (259 – 210 B.C.), who reportedly died of swallowing Hg pills meant to make him immortal (Zhao et al., 2006). In the 18th and 19th centuries many poisonings occurred among hat makers (the “Mad Hatter disease”), miners or building constructors that were using gold amalgam used for gilding (Rice et al., 2014). In the 1950-70s, MMHg was routinely used as a fungicide or heavily produced as industrial waste (Hsu-Kim et al., 2018). This resulted in a number of poisoning catastrophes. In Japan, industrial spills in the Bay of Minamata and the Agano river, caused exposure to high-levels of MMHg in the human population living in Minamata and Niigata (Harada, 1995). These accidents led to fatalities and devastating neurological damage, particularly in newborns and fetuses (Rice et al., 2014). The Minamata poisoning accident was so devastating that intoxication symptoms are still been observed today within the populations inhabiting the coasts of the Shiranui Sea (Takaoka et al., 2017). In the 70s the use and emission of MMHg and other Hg compounds was ultimately banned (Angot et al., 2018; Chen et al., 2018). Today, Mercury is ranked third by the US Government Agency for Toxic Substances and Disease Registry among the most toxic elements or substances on the planet “to be dumped into our waterways and soil, spilled into our atmosphere, and consumed in our food and water” (Rice et al., 2014). After decades of research, development, and multi-stakeholder efforts, the Minamata Convention on Mercury, a multilateral agreement to mitigate human health impacts from mercury pollution, entered into force in August 2017 (Kwon et al., 2020). The objective of the Convention is to “protect human health and the environment from anthropogenic emissions and releases of mercury and mercury compounds”, and it sets out a range of measures to meet that objective. These include the control of the supply and trade of mercury, including setting limitations on specific sources of mercury (UN Environment, 2017).

While all species of Hg have intrinsic toxic properties, MMHg is the form of most concern for marine biota and humans consuming seafood (Grandjean et al., 2010). The current understanding of Hg toxicity derives from various laboratory studies on model species, and in humans (Chakrabarti et al., 1998; Mergler et al., 2007). For marine mammals, controlled experiments to establish any definite causal relation between Hg and any physiological problem are rare. The first attempt was conducted on harp seals *Phoca groenlandicus* in the 1970s (Ronald et al., 1977). However, they used very high concentrations that are not commonly found in the environment. After that, few other investigations have been carried out in an attempt to evaluate contaminant effects at ambient environmental levels (Basu et al., 2010, 2006; Das et al., 2008; Ostertag et al., 2014). Only recently, and in areas where Hg environmental levels are extremely elevated, Hg²⁺ was also proposed to potentially cause severe toxic effects in marine predators, (Park and Zheng, 2012).

Hg toxicity is expressed at different levels. Because of its high affinity of several molecules present in the body, Hg can act as competitor for binding receptors or catalyst enzymes (Clarkson and Magos,

2006). In this way Hg creates a cascade of effects, encompassing the molecular, cellular and systemic compartments of the organism (Figure 1.5).

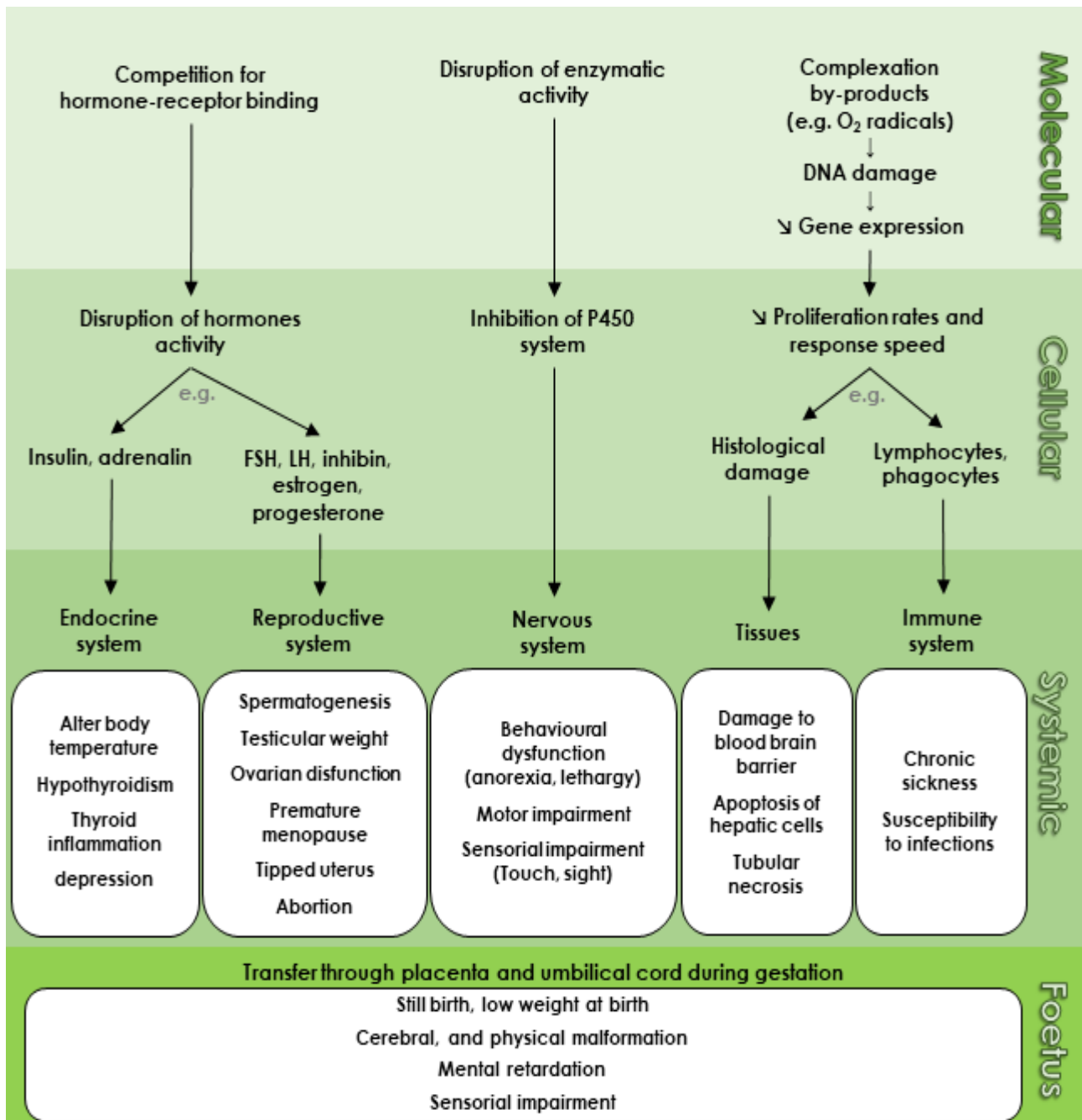


Figure 1.5. Summary of Hg toxicity in the body. White boxes indicate the health consequences of Hg toxicity. References: endocrine system (Choi et al., 2017; Kershaw and Hall, 2019); reproductive system (Bjørklund et al., 2019; Fossato da Silva et al., 2011; Khan et al., 2004); nervous system (Jackson, 2018; López-Berenguer et al., 2020; Rice et al., 2014; Yee and Choi, 1996); tissues (Choi et al., 2017; Zalups, 2000); Immune system (Kershaw and Hall, 2019); fetus (Broussard et al., 2002; Yoshida, 2002).

Knowledge gaps

Although much is known about the clinical signs of acute Hg toxicity, the consequences of chronic exposure to low levels of Hg are not well characterized (Desforges et al., 2021b). Nowadays, most organisms (including humans) are exposed to Hg at low levels on a continuous basis and such exposures may have subtle yet detrimental sub-clinical effects (Karagas et al., 2012; Pereira et al., 2019). Although the Minamata poisoning happened in 1956, 2271 patients were officially diagnosed with symptoms of Hg toxicity (called “Minamata disease”) until 2011 (Takaoka et al., 2017; Yorifuji and Tsuda, 2014).

The lack of controlled experiments at low concentrations limits our knowledge of Hg basal metabolism and detoxification within the organisms. Recent findings have shown how factors like levels of environmental pollution, age and habitat use influence Hg detoxification activity by tissues and speciation within the organisms (Bolea-Fernandez et al., 2019; Li et al., 2020; Perrot et al., 2015; Pinzone et al., 2021a). Arctic marine mammals like hooded seals *Cystophora cristata* present in physiological specializations apt to assure their survival in the cold (Blix, 2016). The intense metabolic changes they undergo during key stages of life (e.g. nursing, growing, etc.) could exacerbate inter-organ Hg processing and result in higher health risk at both individual and population level (Desforges et al., 2021a).

→ Chapter 4

2. MERCURY IN THE ARCTIC

2.1. The Arctic region

The definition of the Arctic region is not straightforward. The geographical definition comprises the region north of the Arctic Circle (66°32'N), which encircles the area of the midnight sun (polar day). However, from an environmental point of view, defining the Arctic solely on the basis of the Arctic Circle makes little sense (AMAP, 1997a). A big part of the samples analyzed in this work was collected in the framework of the Arctic Monitoring and Assessment Plan (AMAP) program. As such, throughout the entire thesis we will define as “Arctic” the core area covered by the AMAP assessment (Red line, Figure 1.6). In this definition the Arctic boundary was set between 60°N and the Arctic Circle, with some modifications: in the North Atlantic, the southern boundary follows 62°N and includes the Faroe Islands, the White Sea, the Labrador Sea and Greenland Sea. In the Bering Sea area, the southern boundary is the Aleutian chain. Finally, on the American side, the southern boundary is represented by the Hudson Bay (AMAP, 1997a).

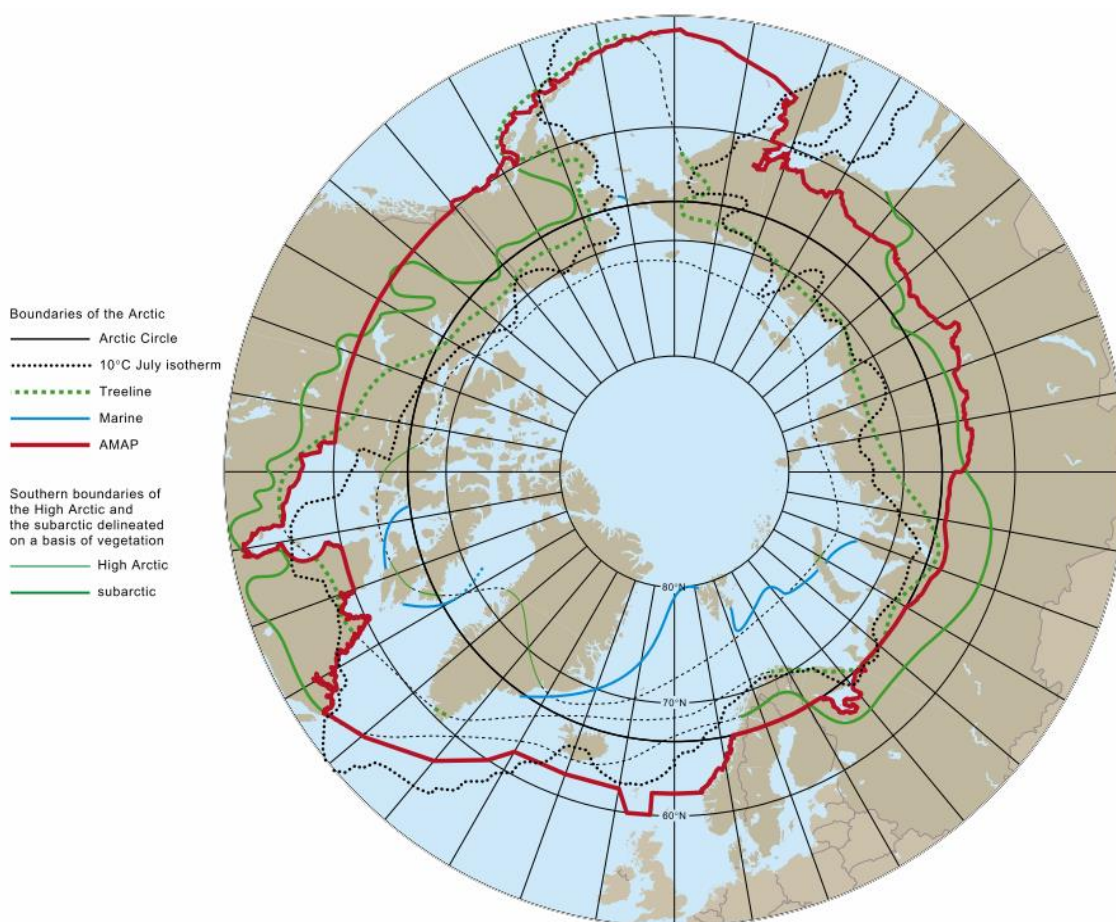


Figure 1.6. Arctic delimitations defined by latitudes (black line), temperature (dotted black line), trees distribution (dotted green line), vegetation (light green line - High Arctic, dark green line - Low Arctic), the Arctic Ocean delimitation (blue line) and the AMAP definition (Red line). Reproduced from (AMAP, 1997a).

The Arctic region derives its name from the stellar constellation of Ursa major, the Great Bear (from *Arctos* in Greek for bear) (AMAP, 1997a). It is the vast polar region located at the northern extremity of the Earth (Figure 1.7A), comprising a deep, ice covered, and nearly isolated ocean, the Arctic Ocean. This ocean is surrounded by the northernmost coasts of Eurasia and North America: Russia, Canada, Denmark (Greenland), Norway (Svalbard), Finland, Sweden and the USA (Alaska) (AMAP, 1997a). It contains 1 % of global seawater volume, covering about 14 million km² (Figure 1.7A) (McClelland et al., 2012). Sea ice, permafrost, glaciers, ice sheets, and river and lake ice are all characteristic parts of the Arctic's physical geography, supporting and shaping Arctic ecosystems and inhabitants (ACIA, 2005).

The average depth of the Arctic Ocean is 1 038 m. The deepest point is Molloy Hole in the Fram Strait, at about 5 550 m (Stewart and Jamieson, 2019). Continental shelves (average depth of 150m) around the deep central basin occupy slightly more than half of the ocean's area (9.5 million km²) (Jakobsson, 2002). This is a significantly larger proportion than in any other oceans, corresponding to about 15 % of the world's shelf seas (Woodgate, 2013). The Arctic Ocean is connected to the Atlantic Ocean through the Barents Sea and the Fram Strait (AMAP, 1997a). It is connected to the Pacific Ocean via the narrow and shallow (50m) Bering Strait (Figure 1.7A). Rivers account for about 11 % of the global freshwater input into the Arctic; also a higher proportion compared with other oceans (AMAP, 1997a; McClelland et al., 2012).

In addition to the important riverine discharge, the Arctic Ocean is characterized by higher precipitation versus evaporation. These two factors in conjunction with the sea ice freeze/melt cycle, lead to a strong stratification of Arctic Ocean's water layers (Rudels, 2012). As proposed by Rudels (2009), the Arctic Ocean water column can be separated in 4 layers (Figure 1.7B):

- **0 – 50m:** Polar Mixed Layer (yellow), composed by low salinity;
- **100 – 250m:** Pacific and Atlantic halocline (light blue and brown), with salinity increasing with depth;
- **400 – 700m:** the Atlantic layer (light blue); and
- **700 – 5500m:** Arctic deep water (dark blue) (Rudels, 2009).

Being a very large region, the Arctic encompasses diverse climatic conditions. Mean annual surface temperatures range from 4°C in Reykjavik, to -18°C over the central Arctic Ocean, or -28.1°C over the crest of the Greenland Ice Sheet (about 71° N and over 3 000 m elevation) (ACIA, 2005). Also, precipitation rates are quite diverse, ranging from an average annual precipitation of 150 mm in the central Arctic, to 600 to 900 mm yr⁻¹ in the North Atlantic (Boisvert et al., 2018).

Arctic weather and climate do not change only spatially, but can vary greatly from year to year. Such differences are partly due to the poleward intrusion of warm ocean currents such as the Gulf Stream and the southward extension of cold air masses (Rudels, 2012).

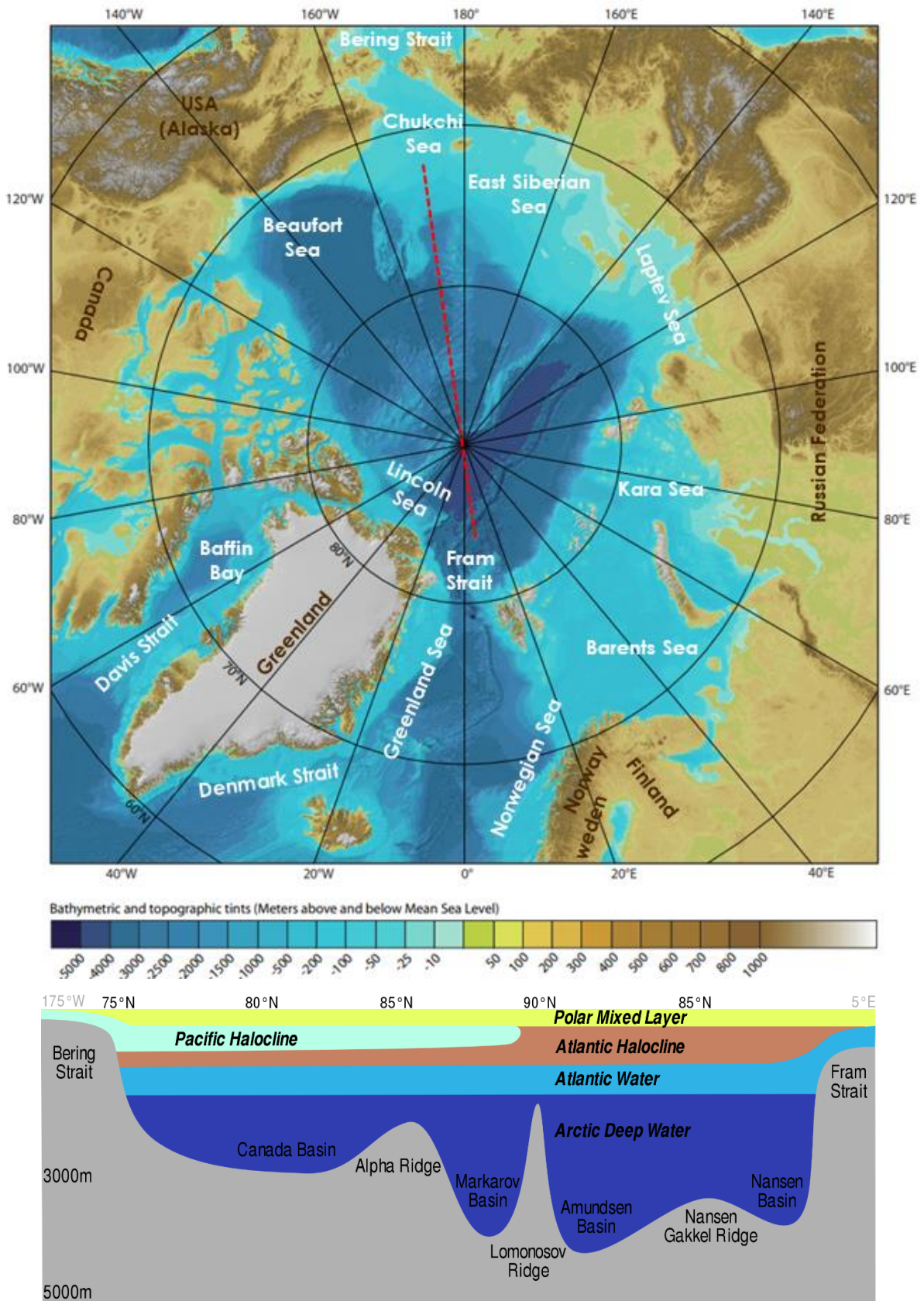


Figure 1.7. (A) Map of the Arctic Ocean. Modified by the International Bathymetric Chart of the Arctic Ocean (IBCAO) (Jakobsson et al., 2020). The red dotted line represents the transect shown at the bottom. **(B)** Vertical section of the 4 water masses of the Arctic Ocean. Figure credits: [Brn-Bld, CC BY-SA 3.0](#), via [Wikimedia Commons](#).

Cyclic patterns also shape climate patterns: the North Atlantic Oscillation (NAO) (Hurrell et al., 2003) strongly influences winter weather patterns from Greenland to Central Asia; whereas the Pacific Decadal Oscillation has a similar influence in the North Pacific and Bering Sea (Kim et al., 2020). Arctic oceanic processes and surface currents initiate a large-scale movement of water (Figure 1.8), driven by temperature and salinity differences (thermohaline circulation or the global Conveyor Belt, Lozier, 2010), driving the circulation of oceanic water masses around the world and consequently the global climate system (Armitage et al., 2020; Budikova, 2009).



Figure 1.8. The major physical pathways (wind, rivers and ocean currents) that transport contaminants to the Arctic. Reproduced from Macdonald et al., 2005.

Light radiation levels change drastically between seasons (Blix, 2005). Above the 72°33' latitude, the Arctic is characterized by the alternation of a period of 24h continuous darkness (November to January) named the “Polar Night”, followed by a period of 24h continuous sunlight (or “Polar Day”, March to September) (Burn, 1995).

The most important feature of the Arctic Ocean is the presence of sea ice. Around 8 million km² are covered all year round (“perennial pack ice”); however, the total sea ice extent varies seasonally and yearly. The yearly peak of maximum extent is generally around the month of March (~ 15 million km²), while the minimum is in September (~7 million km²; ACIA, 2005). The ice is in constant motion, following the major currents, and growing in thickness as it moves along. On a basin-wide scale, sea ice in the Arctic Ocean moves with two predominant drift systems (Figure 1.8): the transpolar drift and the Beaufort Gyre (Figure 1.8; ACIA, 2005). The transpolar drift pushes the ice from the Siberian coast region (where is formed) across the Arctic Ocean and eventually through the Fram Strait (ACIA, 2005). This trip can take up to 6 years, allowing the ice to grow as thick as 3 meters or more. As a result, the thickest sea ice (4 to 6 m) is located north of the coasts of Canada and Greenland, while the thinnest sea ice (0 to 2 m) extends along the coasts of Siberia (ACIA, 2005). Changes in the relative strength of the Beaufort Gyre and the Transpolar Drift are important controls on the extent and distribution of multi-year ice (MYI) (AMAP, 2017).

2.2. Sea-ice and its role for Arctic marine food webs

Sea-ice and the marginal ice zone (MIZ) supports a large amount of algae, like *Nitzschia frigida* or *Melosira arctica* between the ice-obliged species, and *Chaetoceros* spp and *Thalassiosira* spp among the pelagic ones (Figure 1.9; AMAP, 1997b). Arctic marine primary production is characterized by short and intense algal blooms that follow the ice edge as it melts and break ups (Søreide et al., 2006). They usually start in April/May at the southernmost fringes of the first-year ice (FYI) and around September near the multi-year ice (MYI) packs in the far north (Søreide et al., 2006). Arctic sea-ice algae and sub-ice phytoplankton account for 57 % of the total annual primary production in the Arctic Ocean (Schartup et al., 2020). Ice algae are therefore a crucial seasonal food source for 1st order consumers such as sympagic (ice-associated) invertebrates as well as pelagic zooplankton and benthic communities (Kohlbach et al., 2016; Legendre et al., 1992). Through trophic interactions, sympagic production is funneled to higher trophic levels. Indeed, top predators such as the beluga or polar bears, indirectly rely on sea-ice derived OM (Brown et al., 2018, 2017). Direct dependence of consumers to sea ice-derived OM has been highlighted using stable isotopes ratios, fatty acids (included but not limited to highly branched isoprenoids such as IP25) but also compound-specific isotope analysis of fatty acid trophic markers (Kohlbach et al., 2019; Steiner et al., *Submitted*).

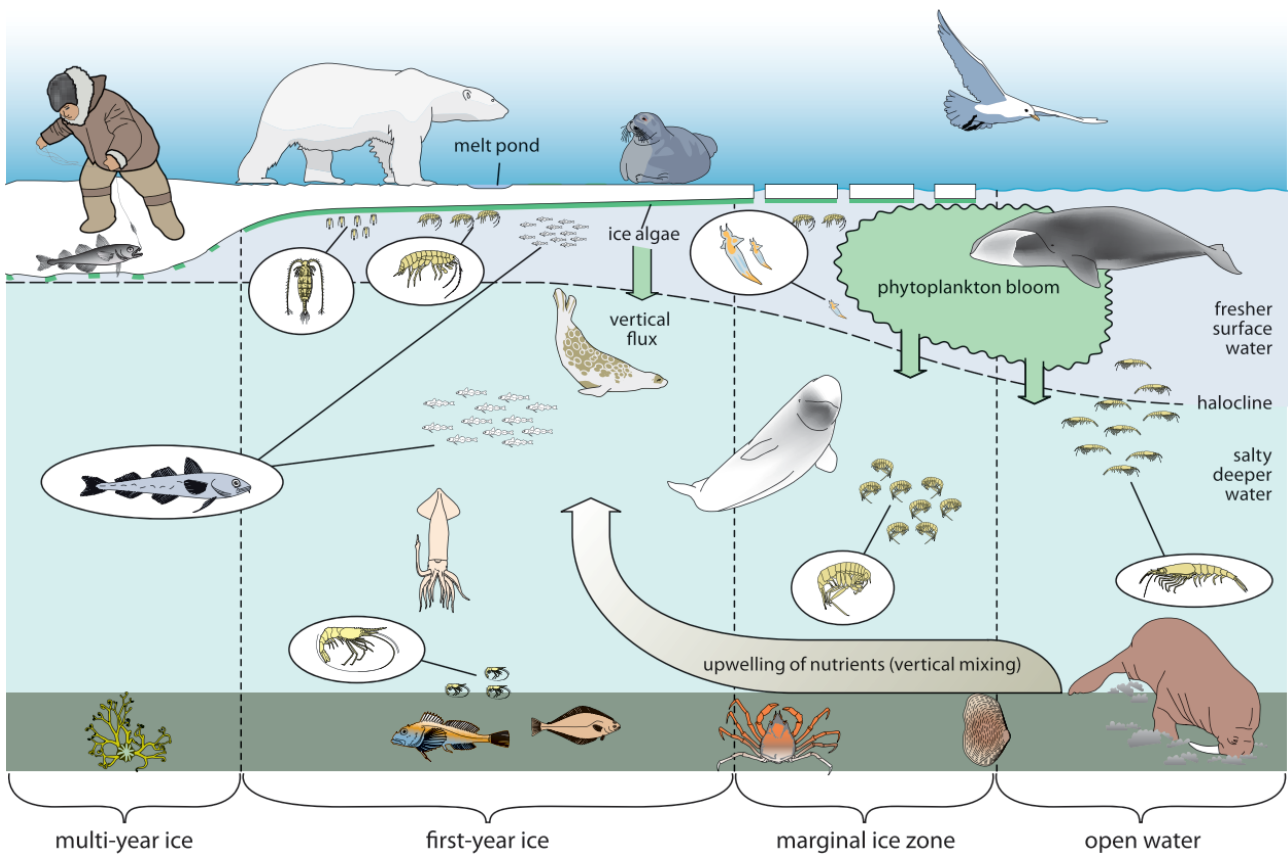


Figure 1.9. The Arctic marine food web. Reproduced from AMAP, 2012.

Indirectly, many secondary level predator species such as the ivory gulls *Pagophila eburnea*, baleen whales (e.g. bowhead whale *Balaena mysticetus*) and fish such as the capelin *Mallotus villosus*, Arctic cod *Arctogadus glacialis* and polar cod *Boreogadus saida* depend on an ice-associated invertebrates based diet (AMAP, 2012).

Sea ice provides a physical surface for third to higher level predators. Among those are marine and terrestrial mammals like the polar bear *Ursus maritimus* and the arctic fox *Alopex lagopus*, or seabirds like the guillemot *Cepphus spp* (AMAP, 2012). These animals use sea-ice for resting, nursing, hunting and as migratory corridors (Kovacs et al., 2011). Some species of pinnipeds are sea-ice obliged for a part of their life. Walrus *Odobenus rosmarus* give birth, mate on sea-ice and use it seasonally to reach bivalve beds too far from shore. The bearded seal *Erignathus barbatus*, requires FYI pans in spring time for raising pups and molting (Kovacs et al., 2011). The ringed seal *Pusa hispida* is ice-associated all year round, requiring stable ice for breeding, molting, resting and hunting on sympagic prey. Some other species like the ribbon seal *Histiophoca fasciata*, harp seal *Pagophilus groenlandicus* and the hooded seal *Cystophora cristata* all depend on pack ice for breeding.

Finally, sea-ice is strongly essential for Arctic indigenous people (Figure 1.9). Marine mammals constitute the basement of indigenous traditional food. The importance of traditional food varies from one area to the other. For example, in 2005, the majority (68 %) of adults in Inuit Nunangat were still

relying on traditional food, with at least half of the meat and fish consumed in each family being country food (ICC Canada, 2014). However, in Greenland the consumption of local food by Inuit has been reduced by 50 % over the last years, representing only 10 to 20 % of an adult's diet (Hansen et al., 2016).

2.3. Mercury cycling in the Arctic

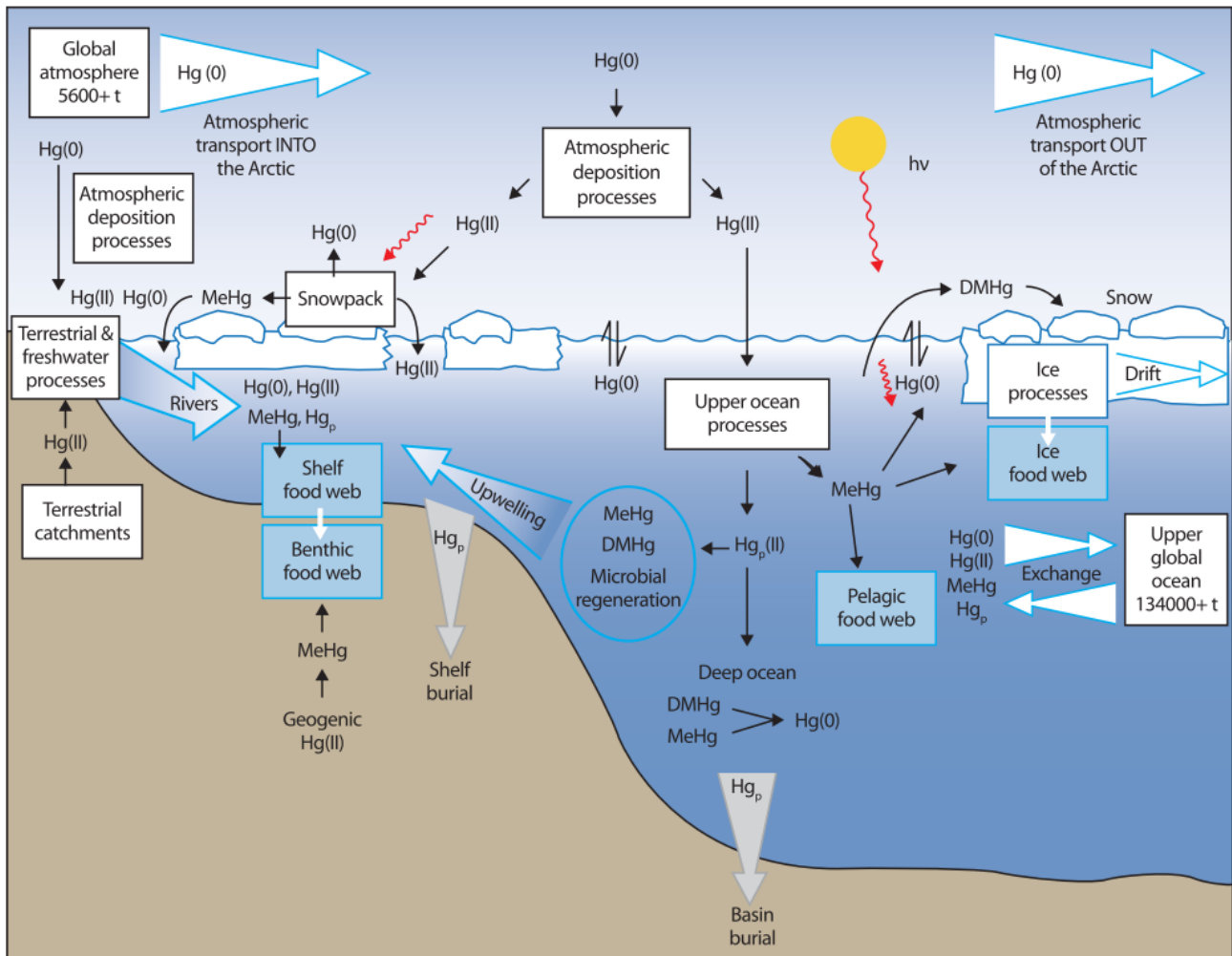


Figure 1.10. The mercury cycle in the Arctic Ocean. Rectangular boxes show system processes, like food webs or atmospheric deposition chemistry. Large shaded arrows refer to atmospheric or oceanic transport processes that exchange Hg with the global environment and move Hg between reservoirs within the Arctic Ocean. Small black arrows refer to chemical processes that produce changes between Hg species. Reproduced from AMAP, 2011.

2.3.1. The most recent discoveries

The Arctic Ocean is considered the major sink of the global Hg cycle (Figure 1.10; Dastoor and Durnford, 2013). Arctic terrestrial ecosystems were recently indicated as important source of Hg to marine biota (Dastoor and Durnford, 2013). Stable isotope data suggest that, through year round Hg⁰

deposition and summer vegetation uptake, the Arctic tundra can store-up to half the world's soil Hg (Obrist et al., 2017). On the other hand, Schuster et al. (2018) estimated that the Northern Hemisphere permafrost regions contain 793 ± 461 Gg of Hg, indicating that permafrost soils store nearly twice as much Hg as all other soils, the ocean, and the atmosphere combined. These recent findings add up to the complexity of Hg cycling in the Arctic Ocean, bringing enormous new implications for the comprehension of the potential impact of climate change on Hg exposure to marine biota (Schuster et al., 2018).





2.3.2. Sources of mercury in the Arctic Ocean

There are no Hg point sources in the Arctic, therefore all anthropogenic Hg that is deposited in this region virtually derives from lower latitudes (AMAP, 2011). Overall, the largest contributors of anthropogenic Hg to the Arctic are:

- East Asia (10 to 15 %)
- Europe (2 to 3 %),
- North America (2 to 2.5 %) and
- South Asia (1.5 to 2 %) (AMAP, 2011; Durnford et al., 2010).

Hg enters the Arctic Ocean via a number of different pathways, including the atmosphere, river exports and ocean currents (Table 1.1) (AMAP, 2011). It is estimated that 2/3 of Hg deposited in the Arctic is natural or re-emitted (40 to 45 % from land and 30 to 34 % from oceans), whereas 20 to 28 % is from anthropogenic sources (Durnford et al., 2010).

Table 1.1. Hg budget in the Arctic Ocean (70° – 90°N). Inputs and outputs (as Mg yr⁻¹) are presented in order of importance. Values are extracted from (Fisher et al., 2012; Outridge et al., 2008). The large difference in Hg inputs from the Pacific and Atlantic oceans reflects the water budget for the Arctic Ocean, which receives approximately 4x more water from the Atlantic Ocean than from the Pacific Ocean (Outridge et al., 2008). * Includes terrestrial run-off from tundra and permafrost.

 Hg Inputs 		 Outputs 	
1. Rivers*	80 Mg yr⁻¹	1. Evasion from ocean surface	90 Mg yr⁻¹
2. Atmosphere:	45 Mg yr⁻¹	2. Particle settling	43 Mg yr⁻¹
<i>Direct deposition</i>	<i>25 Mg yr⁻¹</i>	3. Ocean circulation	6 Mg yr⁻¹
<i>Meltwater inputs of atmospheric Hg</i>	<i>20 Mg yr⁻¹</i>		
3. Coastal erosion	15 Mg yr⁻¹		
4. Pacific inflow	3.9 Mg yr⁻¹		
5. Atlantic inflow	44 Mg yr⁻¹		
Total of inputs :	≈ 190 Mg yr⁻¹	Total of outputs :	≈ 140 Mg yr⁻¹

The contribution of anthropogenic Hg from different source regions is impacted by weather fronts, such as the Arctic front, which have an important influence on the long-range transport of aerosols (Fisher et al., 2011).

2.3.3. Atmospheric Mercury Depletion Events (AMDEs)

Atmospheric Mercury Depletion Events (AMDEs) are a phenomenon occurring in polar regions at spring time, during which the oxidation of Hg^0 and subsequent deposition of Hg^{2+} into the marine environment is enhanced (Poulain et al., 2015). The initiation of AMDEs requires the presence of Hg in the atmosphere, cold temperatures, a stable inversion layer, sunlight and reactive halogens. Thus, the Arctic Ocean during springtime provides the optimal physical and chemical conditions required for atmospheric transformation and deposition of Hg (Steffen et al., 2007). The fact that AMDEs are only reported during polar springtime suggests that sea-ice or, more specifically, refreezing ice in open leads provides a halogens (Br^- , BrO^- , Cl^- and ClO^-) source that drives AMDEs chemistry (Kirk et al., 2012; Steffen et al., 2007). Aspmo et al. (2006) showed that indeed Hg^0 concentrations are higher and more variable over the Arctic Ocean, particularly in regions with greater ice cover ($1.82 \pm 0.24 \text{ ng m}^{-3}$), than over the open North Atlantic Ocean ($1.53 \pm 0.12 \text{ ng m}^{-3}$) (Aspmo et al., 2006). During AMDEs, atmospheric ozone is broken down, causing Hg^0 to bind with the halogen compounds and be oxidized in Hg^{2+} , which in turn is readily scavenged by snow and ice surfaces (Douglas et al., 2017; Wang et al., 2019).

Snowpack characteristics and local environmental conditions influence Hg^{2+} remobilization time (Faïn et al., 2008; Sherman et al., 2010). H_2O_2 in pH-neutral snow, HO_2^- , humic acids, oxalic acid and sulfite-based compounds promote Hg^{2+} reduction within the snowpack and its consequent remobilization as Hg^0 to the atmosphere (Faïn et al., 2008). Halides, such as Cl^- and Br^- stabilize Hg^{2+} in snow (Faïn et al., 2008; Kirk et al., 2012). In general 20 to 50 % of deposited Hg^{2+} during ADMEs is immediately photo-reduced and again volatilized (Sherman et al., 2010). Therefore, even if Hg atmospheric deposition in the Arctic is generally less important than at temperate latitudes or in industrialized regions of the world, this might change seasonally and spatially based on the intensity of AMDEs and ice composition. In coastal marine sites and over FYI, where snow-pack halogen concentrations are frequently high, AMDEs might be stronger than in offshore waters or in areas covered by multi-year ice (Kirk et al., 2012; Moore et al., 2014).

2.3.4. Sea-ice, water column and bottom sediments

In general, Arctic Ocean THg seawater concentrations are similar to those measured in the North Atlantic ($0.487 \pm 0.32 \text{ ng L}^{-1}$), North Pacific ($0.23 \pm 0.17 \text{ ng L}^{-1}$), Southern Ocean ($0.2 \pm 70.09 \text{ ng L}^{-1}$),

and Mediterranean Sea ($0.26 \pm 0.10 \text{ ng L}^{-1}$) (Kirk et al., 2012). However, in the Arctic Ocean the extent and concentration of sea-ice influence both the rates of air-water Hg exchange as well as Hg photochemistry in the water column (DiMento et al., 2019; Vancoppenolle et al., 2013). As in other regions of the world, in the Arctic euphotic zone Hg transformation pathways are mostly governed by both biotic and abiotic processes (Figure 1.10). However, the presence of ice affects the rates of a process *versus* the other, acting as both physical and biological influencing factor (DiMento et al., 2019). In ice-covered areas and seasons, ice-associated microbial activity is the most important path, while in summer and ice-free areas, photoreactions balance the biotic ones (Barkay and Poulain, 2007; Point et al., 2011). Less sea-ice usually determines higher evasion rates of DMHg or dissolved Hg^0 to the atmosphere, and higher rates of MMHg demethylation in subsurface waters (Lehnherr et al., 2011; Schartup et al., 2020).

The mechanism of sea-ice production and melting creates a highly stratified surface water column that has been proposed to enhance MMHg production (Schartup et al., 2020). Several studies showed a positive correlation between chlorophyll *a* (a proxy for primary production) and MMHg concentration in arctic sea-ice as well as subsurface waters, suggesting that MMHg in polar region is mostly biologically produced (Sunderland and Schartup, 2016; Wang et al., 2018). This implies that MMHg produced in sea-ice and bioaccumulated by sea-ice algae may contribute disproportionately to MMHg levels in Arctic marine biota (Schartup, 2016).

Even if water column mixing and resuspension of stored Hg in sea bottom sediments are not usually recognized as major pathways of Hg exposure to marine food web, they acquire a big importance in the Arctic (AMAP, 2011). First, the general oligotrophy of the Arctic central basin leads to an exceptionally low particulate export, which may mean that bio-active elements like Hg tend to recycle within the stratified polar mixed layer rather than transfer to deeper waters through particle flux (Douglas et al., 2012). Secondly, the characteristic dominance of gentle continental shelves in the Arctic Ocean (>50 % of total area) favors the bottom/water Hg exchange processes, exacerbating its reemission from the sea bottom (Douglas et al., 2012).

2.3.5. Accumulation within the Arctic food web

Hg biomagnification in the Arctic food web shows a step-wise increase from one trophic level to the next, as in other regions of the world (Figure 1.11; Kirk et al., 2012). Hg levels in primary producers and consumers are quite homogenous on a panarctic scale. However, tertiary to apex predators show strong spatial variability. Hg levels are higher in Northern America and Western Greenland than in the European Arctic (e.g. Eastern Greenland), as a consequence of the different level of industrialization and human development between these regions (Dietz et al., 2013). This trend was confirmed for belugas (Stern, 2010), seabirds (Albert et al., 2021), polar bears (Routti et al., 2011) and ringed seals

(Rigét et al., 2011). Habitat segregation between or within species, and animals' trophic ecology also influences Hg exposure (Stevick et al., 2002). Several studies reported that higher Hg levels are generally found in offshore species, followed by sympagic and coastal animals (Loseto et al., 2008a). On a temporal scale, Hg levels in Arctic marine predators have shown a 10x increase over the past 150 years, with an average rate of increase of 1 to 4 % per year (Dietz et al., 2009). In the same study, they proposed that ~ 90 % of the Hg currently present in Arctic animals originates from anthropogenic sources (Dietz et al., 2009). Although there is no consistent trend across species and tissues for the entire Arctic, there is a clear east-to-west gradient of temporal Hg trends. The Canadian and Western Greenland regions of the Arctic show the larger increases in biota THg concentrations with respect to the Northern Atlantic Arctic (Rigét et al., 2011).

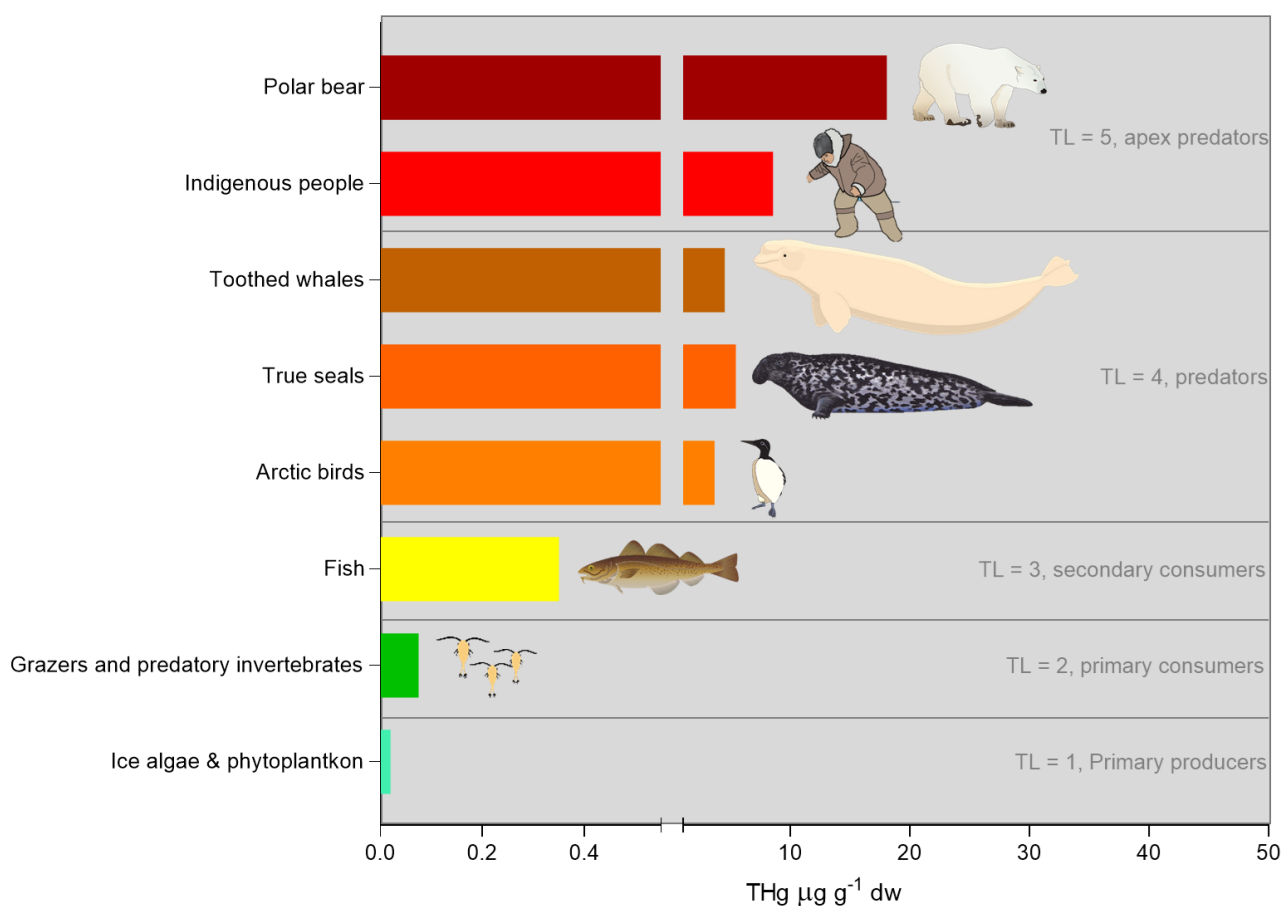


Figure 1.11. Literature THg concentrations range (in $\mu\text{g g}^{-1} \text{ dw}$) across the Arctic marine food web. All the seven functional groups are represented over the y axis, spanning over five trophic levels (TL) (Legendre et al., 1992). TL 1 : THg = $0.02 \mu\text{g g}^{-1} \text{ dw}$ (bulk) (Loseto et al., 2008b); TL2 : THg = 0.02 to $0.2 \mu\text{g g}^{-1} \text{ dw}$ (whole body) (Atwell et al., 1998; Loseto et al., 2008b); TL3 : THg = 0.2 to $0.5 \mu\text{g g}^{-1} \text{ dw}$ (muscle) (Loseto et al., 2008b); TL4 : THg = 1.1 to $15 \mu\text{g g}^{-1} \text{ dw}$ (muscle) (Albert et al., 2021; Loseto et al., 2008a; this study); TL 5 – THg = 2.1 to $31 \mu\text{g g}^{-1} \text{ dw}$ (hair) (Dietz et al., 2011; Rigét et al., 2011; Weihe et al., 2005). Most of TL 4 to TL 5 organisms surpass the U.S. EPA guideline of $1 \mu\text{g g}^{-1} \text{ dw}$ (FAO/WHO, 2003).

2.4. A changing Arctic

The Arctic is one of the regions on Earth which is more affected by climate-driven environmental change (Overland et al., 2019). Environmental change can affect the ecosystem at multiple levels: physical, chemical and biological.

2.4.1. Main physical changes

- Atmosphere: Since 1980, the rise in annual average temperature in the Arctic has been twice the global mean, with higher increases in the cold season (Symon, 2011). Specifically, a 2.7°C increase was observed between 1971 and 2017, with a 3.1°C increase in winter and 1.8°C increase in summer (AMAP, 2017). In addition, scientists observed changes in precipitation rates and types, with a shift towards more rain *versus* snow, and a strong annual increase (1.5 to 2.0 % / year) in annual precipitation (Bintanja, 2018).
- Terrestrial ecosystems: the first 10 to 20cm of permafrost are warming up, enhancing thawing during summer period (AMAP, 2019; Schaefer et al., 2020). Model projections estimate a 30 to 99 % reduction in the area Arctic permafrost by 2100, assuming anthropogenic greenhouse gases emissions continue at current rates (Schuster et al., 2018).
- Marine ecosystems: the most concerning changes comprises sea-ice extent, thickness and melting onset. Summer sea-ice extent (September) is currently declining at 12 % per decade (Symon, 2011). Since 2010, we experienced the two lowest records for minimum sea-ice extent in summer: 3.39 million km² in 2012 and 3.74 million km² in 2020 (Lannuzel et al., 2020). Arctic sea ice maximums (March) in 2015, 2016, 2017 and 2018 were the lowest since the 80s (AMAP, 2019). Since 1958, the average sea-ice thickness has declined by >60 % (>2 m) (AMAP, 2017). Recent models project worst trends at high latitudes (1.3m thinner) than lower ones (0.3 m thinner) (Tedesco et al., 2019). Between 2002 and 2017, the Arctic has lost more than 50 % of its oldest MYI and is undergoing a regime shift from a system dominated by MYI (until 2011) to a system dominated by seasonal ice FYI (Schartup et al., 2020). Melt onset trends show considerable advances on a panarctic scale with marked regional differences (Kodaira et al., 2020). The strongest change since 1979 has occurred in the Barents Sea and East Greenland Sea (25 and 30 days earlier melting onset, respectively), followed by the Baffin Bay, Kara Sea, Hudson Bay (22, 15, and 10 days, respectively) and the Central Arctic Sea (5 days) (Tedesco et al., 2019). Such shift is believed to accelerate in the next 100 years reaching a 1.5 months delay for freeze-ups and 1 month advance for ice breakups, leading to a much shorter ice season (Tedesco et al., 2019).

2.4.2. Impacts on Arctic marine food webs

The alteration of sea-ice cover and dynamic determines a bottom-up cascade of changes, which are altering the intensity of cryo-pelagic and cryo-benthic coupling (Kohlbach et al., 2019).

- Primary producers: The deeper and more intense penetration of sunlight in seawater is leading to the increase in primary productivity (up to 500 % in the Bering Sea in 2018) (Kearney et al., 2019). At the same time, variation in sea-ice was linked to a shift in ice microalgae biodiversity, size, as well as timing and intensity of algal blooms (Schartup et al., 2020; Tedesco et al., 2019).
- Primary to tertiary consumers: The shift in algal communities pushes grazers (mostly *calanus* sp.) to move from being sympagic towards a more coastal habitat use (Li et al., 2009). More than 20 new fish species were cataloged in the Chukchi-Beaufort region in the last 15 years (Wassmann et al., 2011). All these changes might modify the energy fluxes at the base of food web and enact the deterioration of nutritional status for secondary to tertiary consumers (Mckinney et al., 2013).
- Top predators: At the top of the food web, numerous studies linked the decrease in ice cover and thickness with shifts in marine mammals' trophic behavior. These include: the worsening of ringed seals nutritional status (Najbjerg et al., 2017), the shift in polar bears feeding ecology (Mckinney et al., 2013), the change of thick-billed murre (*Uria lomvia*) diet from cod- to capelin-dominated in the last 20 years (Gaston et al., 2003), the decrease in nestling survival in black-legged kittiwakes (*Rissa tridactyla*) and Northern fulmars (*Fulmaris glacialis*) (Gaston et al., 2005), and the >80 % decline in Ivory gulls (*Pagophila eburnea*) population in Canadian Arctic (Gaston et al., 2005). The survival of such species might be threatened as a consequence of ice-changing conditions through many processes like habitat loss and fragmentation, longer fasting period, higher energy expenditure for hunting, birth rates decrease or newborns survival (Burek et al., 2008; Laidre et al., 2015; Mckinney et al., 2013; Stirling et al., 2008).

Arctic environmental changes can alter Hg exchange processes between atmospheric, terrestrial and aquatic reservoirs (Budikova, 2009). Arctic biological changes instead can alter Hg exposure and biomagnification within marine food webs (McKinney et al., 2015). As such, the major concern of modern Arctic research is to understand the drivers and extent of Hg fate in the changing marine ecosystems (Stern et al., 2011).

2.4.3. Impacts on Hg marine chemistry

- Alteration of terrestrial inputs of modern and legacy Hg

The shorter period of ice and snow cover supports higher sediment bacterial activity in wetlands and therefore higher rates of Hg²⁺ methylation (Sundseth et al., 2015). The enhanced frequency of forest and ground fires, exacerbates the mobilization of Hg and C stored in soils and vegetation into the air

(Stern et al., 2011). The higher temperatures might enhance snow melting and spring freshwater runoff, leading to a more important seasonal transfer of land-produced MMHg to coastal seas (Mu et al., 2020; Schaefer et al., 2020). Increase permafrost thawing may lead to peaks of Hg inputs in Arctic estuaries (Schaefer et al., 2020). The modelled loss of permafrost in the next 180 years is expected to increment the bioavailability of modern and legacy terrestrial Hg inputs into the Arctic Ocean (Lim et al., 2019; Mu et al., 2020).

– Alteration of Hg methylation associated to sea-ice

The reduction in sea-ice extent is believed to affect Hg dynamics across the air–seawater interface, increasing the deposition of Hg²⁺ directly on seawater rather than on sea-ice (Schartup et al., 2018; Sunderland and Schartup, 2016). MMHg has been observed to build up under sea-ice such that during the melting season there is a large pool of MMHg potentially available to take part in photochemical reactions (Sunderland and Schartup, 2016). Under such a scenario, photodemethylation rates, which are proportional to MMHg concentration, would be high during ice-free season but negligible at other times (Lehnherr et al., 2011). If the spatial extent and duration of ice cover continues to decline as is widely predicted, a new scenario might emerge where there is no longer a build-up of MMHg under the ice and photodemethylation would occur at a slower rate and for a longer time, completely altering actual annual MMHg photodemethylation fluxes (Stern et al., 2011).

Ice-associated primary productivity is believed to be the major source of MMHg at the base of the Arctic marine food web (Soerensen et al., 2016a). The shift in biomass and diversity of primary producers in ice-free conditions, is believed to exacerbate the rates of Hg methylation and bioavailability for primary consumers (Schartup et al., 2020).

Finally, the shift from a stable MYI dominated Arctic to a halogen-rich FYI dominated one, is believed to enhance the release of e.g. reactive Br⁻ into the marine boundary layer, leading to higher rates of AMDEs' Hg deposition (Stern et al., 2011).

– Renewed bioavailability of oceanic legacy Hg

Legacy mercury represents Hg produced in the past, which was deposited in the Arctic and is stored today mostly in the inorganic form, not directly available for uptake by food webs (Pollman and Engstrom, 2020). The oceanic basins of the Arctic are a potential enormous source of legacy Hg (Dastoor and Durnford, 2013). The central Arctic Ocean basins and Hudson Bay contain large total (inorganic) Hg inventories in seawater as a result of anthropogenic inputs over the past 200 years, as well as natural background Hg reservoirs (Chen et al., 2018). The biologically-unassimilated fraction of Hg is at least two orders of magnitude greater than the small amount (0.1 % to 1 % of total mass) in marine biota (Stern et al., 2011). Climate-driven alteration of oceanic circulation or vertical mixing within the water column might cause re-emission of such Hg and exacerbate the rates of exposure to Arctic organisms.

Knowledge Gaps

If the consequences of sea-ice alteration on Hg uptake by primary consumers can be directly observed, it is not so easy to do so for higher trophic levels (Hazen et al., 2019). In the framework of climate change and its potential impact on Hg accumulation in Arctic marine predators, there are today two main scientific questions which need to be answered:

The new discoveries about the role of permafrost and tundra within the Arctic Hg cycling raise concerns about how important terrestrial inputs are with regards to marine predators' rates of exposure to Hg.

→ [Chapter 5](#)

The spatial and species-specific inconsistency of Hg temporal trends in Arctic biota opens the discussion about which factors might really influence levels of Hg exposure. The physical, chemical and biological changes brought by climate change logically affect Hg cycling in the Arctic marine ecosystem, but which one has the greatest effect in marine predators like marine mammals is still an open question.

→ [Chapter 6](#)

→ [Chapter 7](#)

3. STABLE ISOTOPES AS CHEMICAL TRACERS

Isotopes are forms of the same element that differ in their atomic mass (Sharp, 2007). The atomic mass of an element is determined by the sum of the number of protons and the number of neutrons (Fry, 2006). Stable isotopes usually present a limited number of neutrons in excess. A larger abundance of neutrons with regards to protons, might lead to instability of the nucleus and its break-up over time, as it happens with radio-active isotopes (e.g. ^{14}C , used for fossil dating; Alves et al., 2018). A particular element can have more than one stable isotope. The lighter isotopes (with lower atomic mass) are usually the most abundant in nature (Table 1.2).

Table 1.2. Mean natural abundances of the stable isotopes used in this thesis (C, N, S and Hg), with their relative International Reference Standards.

Element	Isotope	Abundance (%)	Isotopic ratios (R)	International Primary Reference Standard
Carbon	^{12}C	98.89	$^{13}\text{C}/^{12}\text{C}$	Vienna Pee Dee Belemnite (vPDB)
	^{13}C	1.11		
Nitrogen	^{14}N	99.63	$^{15}\text{N}/^{14}\text{N}$	Atmospheric Air (AIR)
	^{15}N	0.37		
Sulphur	^{32}S	95.02	$^{34}\text{S}/^{32}\text{S}$	Vienna Canyon Diablo Troilite (vCDT)
	^{33}S	0.75		
	^{34}S	4.21		
	^{36}S	0.02		
Mercury	^{196}Hg	0.155	—	NIST-SRM-3133 UM-Almaden
	^{198}Hg	10.04	$^{198}\text{Hg}/^{196}\text{Hg}$	
	^{199}Hg	16.94	$^{199}\text{Hg}/^{198}\text{Hg}$	
	^{200}Hg	23.14	$^{200}\text{Hg}/^{198}\text{Hg}$	
	^{201}Hg	13.17	$^{201}\text{Hg}/^{198}\text{Hg}$	
	^{202}Hg	29.73	$^{202}\text{Hg}/^{198}\text{Hg}$	
	^{204}Hg	6.83	$^{204}\text{Hg}/^{198}\text{Hg}$	

The formation of a bond with a heavy isotope requires more energy than the formation of a bond with a light isotope. At the opposite, it is more difficult to break a chemical bond with a heavy isotope than with a light isotope (Fry, 2006). For this reason, light and heavy isotopes react differently during chemical reactions, often resulting in a product with a higher fraction of lighter over heavier isotope than the original substrate. This kinetic process is unidirectional and commonly referred to as mass-dependent isotopic fractionation (MDF; Fry, 2006).

It is described by the isotopic fractionation factor α :

$$\alpha_{A/B} = \frac{R_A}{R_B} \quad (1.1)$$

where R_A and R_B are the ratios of the heavy to light isotopes in the molecules or substances A and B, respectively. Because α is very close to 1, the very useful relationship is derived:

$$10^3 \ln \alpha_{A/B} \approx \delta_A - \delta_B = \Delta_{A-B} \quad (1.2)$$

Where Δ_{A-B} is the fractionation between substance A and B, reflecting equilibrium or kinetic partitioning (Yin et al., 2010). Equilibrium fractionation arises during isotope exchange when the forward and backward reaction rates of the isotope that lead to isotope redistribution are identical (Yin et al., 2010).

In ecological studies the abundance of the heavy with respect to the light isotope is defined as isotopic ratio (R). Variations in environmental and biological isotopic ratios are represented in the literature in δ notation (Equation 1.3; Coplen, 2011). The δ values denote a difference in measurement made relative to standards during the actual analysis.

$$\delta^H X = \left[\left(\frac{R_{sample}}{R_{standard}} - 1 \right) \right] \times 1000 \quad (1.3)$$

In this definition, the δ notation is specified for a particular element ($X = H, C, N, O$ or S), the superscript H gives the heavy isotope mass of that element (e.g. ^{13}C , ^{15}N or ^{34}S), and R is the ratio of the heavy isotope to the light isotope for the element (e.g. $^{13}C/^{12}C$, $^{15}N/^{14}N$ or $^{34}S/^{32}S$). The multiplication x1000 helps amplifying the small neutron-related isotope differences. The unit of δ is therefore “‰” or “permille” (also per mill), from the Latin “parts per thousand” (Coplen, 2011).

With the exception of hydrogen which has a very broad range, most δ values range between -100 and $+50$ ‰ for natural samples. Negative δ values indicate relatively less heavy isotope than is present in the standard (Fry, 2006). Standards instead have a δ value of 0 ‰ because they contain nonzero amounts of heavy and light isotopes. Therefore, a δ value of 0 ‰ in a sample means no difference from the standard. Samples with higher δ values are relatively enriched in the heavy isotope and are “heavier.” Samples with lower δ values are relatively enriched in the light isotope and are “lighter” (Fry, 2006).

3.1. Stable isotopes of carbon, nitrogen and sulphur

The analysis of carbon (C), nitrogen (N) and sulphur (S) stable isotopes has by now proven to be a successful tool in ecological and trophic studies of marine food webs and predators like marine mammals (Newsome et al., 2010; Peterson and Fry, 1987). Studying the ecology of a species signifies

describing its relation with the environment it inhabits and with the other organisms that may or may not compete for the same biotic and abiotic resources (Middelburg, 2014; Newsome et al., 2007). Species' trophic ecology focuses instead specifically on the use of resources to meet the energy requirements (Boecklen et al., 2011).

The investigation of trophic ecology using stable isotope ratios is based on the principle that the isotopic composition in the tissues of an organism results from the combination of the stable isotope ratios of the various assimilated food items (Fry, 2006). In comparison with traditional dietary analyses (e.g. stomach contents and fecal analyses), stable isotope analysis provides information about the assimilated food and not only the ingested one (Jardine et al., 2006). Moreover, this technique allows to work on live and healthy animals as this analysis may be done on small amount of various tissues (e.g. hair and blood; Jardine et al., 2006). Stable isotope analysis can also provide different time scales of diet integration by using different tissues with different turnover times (Dalerum and Angerbjörn, 2005; Martínez Del Rio et al., 2009).

C marine cycle is complex and may lead to several chemical reactions and physical process that may influence the isotopic compositions of the molecules in the water column. Most of the C isotope fractionation ($^{13}\text{C}/^{12}\text{C}$; $\delta^{13}\text{C}$) occurs at the base of food webs, during photosynthesis or respiration processes (Kelly, 2000). $\delta^{13}\text{C}$ values at the base of the marine food web are quite variable (e.g. phytoplankton: -34.6‰ to 18‰) and depend on HCO_3^- , O_2 or CO_2 abundances, nutrients availabilities, temperature, primary growth rates, but also on species-specific metabolic capacities (McMahon et al., 2013a; Michel et al., 2019). In the Arctic Ocean for example, $\delta^{13}\text{C}$ values can range between $-29.0 \pm 3.1\text{‰}$ in the pelagic *Calanus glacialis* to $-22.1 \pm 0.4\text{‰}$ in the sympagic *Apherusa glacialis* (Kohlbach et al., 2016). Organisms relying on ice-derived C being generally more enriched in ^{13}C than those relying on C from pelagic origins (Michel et al., 2019; Yunda-Guarin et al., 2020). Therefore, $\delta^{13}\text{C}$ is generally used to determine the origin of primary sources of carbon in food webs or feeding areas. $\delta^{13}\text{C}$ values do not change a lot between one trophic level to the other (generally only $\sim 1\text{‰}$) and are conserved along the food web (McConnaughey and McRoy, 1979).

Similarly to $\delta^{13}\text{C}$ values, S isotopic composition ($^{34}\text{S}/^{32}\text{S}$; $\delta^{34}\text{S}$) is used to refine the discrimination between primary producers or between benthic and pelagic sources (Connolly et al., 2004; Fry and Chumchal, 2011). The complexity of S sources in the water column explains the large fractionation range of S stable isotopes in the marine environment (Norici et al., 2005). Producers that predominantly utilize seawater sulphates, such as pelagic microalgae and phytoplankton, tend to be enriched in ^{34}S ($\sim 18\text{‰}$) (Connolly et al., 2004; Trust and Fry, 1992). Those using sedimentary sulfides such as marsh plants on the coasts or anaerobic bacteria found in the sea bottom, are instead more depleted in ^{34}S (-10 to $+5\text{‰}$) (Connolly et al., 2004; Croisetière et al., 2009). In sea ice, $\delta^{34}\text{S}$ values show high variability with values ranging between $+10.6$ to 23.6‰ as a result of ice thermodynamic growth and the structure of brine inclusions networks (Carnat et al., 2018). In the Antarctic food web, $\delta^{34}\text{S}$ values of food sources span from $5.6 \pm 2.7 \text{‰}$ in sympagic algae, to $18.5 \pm 0.8\text{‰}$ in suspended

particulate organic matter (SPOM) (Michel et al., 2019). In the organisms, S is usually only present in S-containing amino acids like cysteine and methionine, and therefore its isotopic analysis exclusively represents protein pathways derived from diet (Vander Zanden et al., 2015). Therefore, as for C, $\delta^{34}\text{S}$ values do not show trophic enrichment (maximum observed difference between trophic levels: $\sim 2\text{‰}$) (McCutchan et al., 2003; Pinzone et al., 2017). For this reason, C and S isotopic compositions might result in large differences between different habitats (pelagic vs. benthic), distribution (coastal vs. offshore), latitudes (Doi et al., 2004; Michel et al., 2019; Pizzochero et al., 2018; Włodarska-Kowalczyk et al., 2019), but would not allow to assess species trophic position.

Conversely to C and S, an enrichment in N heavier isotopes (^{15}N) is observed along the food web, resulting in higher $\delta^{15}\text{N}$ values going from the bottom to the top (Hansson et al., 1997; Post, 2002). This important fractionation is caused by nitrification and denitrification during N assimilation through several important metabolism functions such as protein synthesis or excretion of nitrogenous waste products by the organism (Blackstock, 1989; Cantalapiedra-Hijar et al., 2015). This results in a trophic shift between prey and predator, which for seals typically ranges between $+2.2$ to $+4.3\text{‰}$ (Beltran et al., 2016; Lesage et al., 2002a). For this reason, $\delta^{15}\text{N}$ values can help assessing the trophic position of a species within the food web.

Since N isotopic composition is strongly influenced by the organisms' metabolism, $\delta^{15}\text{N}$ values can also be used to discriminate between different physiological statuses of the animals (Hertz et al., 2015). Indeed, it has already been observed how fasting, nursing or pregnancy would determine an increase in $\delta^{15}\text{N}$ values in the tissues of marine mammals (Cherel et al., 2015; Doi et al., 2017; Habran et al., 2019; Lübcker et al., 2020; McHuron et al., 2019). In the same way, the higher metabolic rates in growing birds, fish (Martínez Del Rio et al., 2009; Newsome et al., 2016; Ramos and Gonzalez-Solis, 2012; Wolf et al., 2009b) and marine mammals like seals might cause a larger enrichment in the heavier isotope (^{15}N) (e.g. 4‰ in hooded seal pups) (Pinzone et al., 2017). Therefore, knowing in advance the fractionation extent between diet and a particular tissue type is necessary for a meaningful interpretation (Hobson et al., 1996).

3.2. Stable isotopes of mercury

A rapidly emerging and successful tool in the field of environmental chemistry is the measurement of natural variations in the isotopic composition of Hg (Blum and Bergquist, 2007). Indeed, Hg has seven stable isotopes with a 4 % relative mass difference (196, 198, 199, 200, 201, 202, and 204 amu; Table 1.2). The longest-lived radioactive isotope is ^{194}Hg , which has a half-life of 520 years (Blum and Johnson, 2017). Many biotic and abiotic reactions can potentially invoke Hg isotope fractionation (Blum and Bergquist, 2007).

As for C, N and S, Hg isotope ratios are reported as δ values in permille (‰), relative to the average ratios measured in the NIST-3133 Hg reference material:

$$\delta^{xxx}Hg(\text{‰}) = \left\{ \left[\frac{\left(\frac{xxxHg}{198Hg} \right)_{unknown}}{\left(\frac{xxxHg}{198Hg} \right)_{NIST - 3133}} \right] - 1 \right\} \times 1000 \quad (1.4)$$

where xxx is the mass of a Hg isotope between 196 and 204 amu (Bergquist and Blum, 2007a). The use of ^{198}Hg (instead of ^{196}Hg) as the denominator in $\delta^{xxx}\text{Hg}$ values was recommended and universally adopted early in the history of Hg isotope studies, because of the very low abundance of ^{196}Hg (Blum et al., 2014). Conversely, the use of ^{204}Hg , was discarded because this isotope has a potential isobaric interference with ^{204}Pb during the analysis (Blum et al., 2014).

As for the other elements, Hg stable isotopes undergo mass-dependent fractionation, which is commonly defined as given below:

$$\delta^{202}Hg = \left\{ \left[\frac{\left(\frac{^{202}Hg}{^{198}Hg} \right)_{sample}}{\left(\frac{^{202}Hg}{^{198}Hg} \right)_{NIST - 3133}} \right] - 1 \right\} \times 1000 \quad (1.5)$$

Many *in vivo* and *in vitro* studies showed that it happens as a consequence of several biotic and abiotic processes in the environment and within the organism: microbial reduction of Hg^{2+} (Kritee et al., 2008), dark abiotic reduction of Hg^{2+} (Zheng and Hintelmann, 2010), microbial demethylation of MeHg (Kritee et al., 2009), photoreduction of Hg^{2+} (Bergquist and Blum, 2007a; Zheng et al., 2018; Zheng and Hintelmann, 2009), photodemethylation of MeHg (Bergquist and Blum, 2007a; Chandan et al., 2015), photo-microbial reduction of Hg^{2+} (Kritee et al., 2018), photo-microbial demethylation of MeHg (Kritee et al., 2018), abiotic dark oxidation of dissolved Hg^0 in the presence of DOM (Zheng et al., 2019), dark microbial methylation of Hg^{2+} (Rodríguez-González et al., 2009), binding of aqueous Hg^{2+} to thiol groups (Wiederhold et al., 2010), and photooxidation of Hg^0 in the presence of halogens (Sun et al., 2016). Some studies reported the occurrence of Hg isotopic fraction between trophic levels at the top of the food web (Perrot et al., 2015, 2010), as a result of metabolic transformation of Hg compounds within organisms' tissues (Tsui et al., 2019).

The odd-mass ^{199}Hg and ^{201}Hg and the even-mass ^{200}Hg and ^{204}Hg isotopes undergo an additional fractionation, which does not depend on mass differences: the mass-independent fractionation or MIF. In the literature odd and even MIF are indicated with big delta (Δ) and are calculated as follows:

$$\Delta^{199}Hg \approx \delta^{199}Hg - (\delta^{202}Hg_{measured} \times 0.2520) \quad (1.6)$$

$$\Delta^{200}Hg \approx \delta^{200}Hg - (\delta^{202}Hg_{measured} \times 0.5024) \quad (1.7)$$

$$\Delta^{201}Hg \approx \delta^{201}Hg - (\delta^{202}Hg_{measured} \times 0.7520) \quad (1.8)$$

$$\Delta^{204}Hg \approx \delta^{204}Hg - (\delta^{202}Hg_{measured} \times 1.4930) \quad (1.9)$$

Two mass-independent mechanisms are responsible for causing MIF: the nuclear field shift effect (NFS) and the magnetic isotope effect (MIE) (Buchachenko, 2013). A third minor mechanism has been recently observed: the self-shielding effect (SSE) (Obrist et al., 2018; Renedo, 2017).

NFS depends on the nuclear volume and nuclear charge radius. It is associated to the fact that odd isotopes are smaller than even ones (Yang and Liu, 2016). This leads to a higher nuclear charge density that influences the basal energy of the atom and its reactivity in chemical reactions (Yang and Liu, 2016). MIE is induced by light exposure. Nuclides with an odd number of protons and neutrons are characterized by a non-zero nuclear spin that induces a magnetic moment in the nuclei during kinetic reactions (Buchachenko, 2001). The resulting radicals can undergo spin conversion and will more likely recombine, causing additional fractionation (the resulting MIF) (Buchachenko, 2009). On the other hand, even isotopes will lead to the production of radicals without magnetic nuclei that will directly become the products (Buchachenko, 2009).

The potential mechanisms causing even MIF have not been identified yet: one possibility is that they are related to oxidation of Hg^0 by halogen radicals in the atmosphere (Sun et al., 2016). However, SSE was recently observed and associated with even MIF (Cai and Chen, 2015). Mead et al. (2013) suggested that this mechanism could be linked to Hg structure and its capacity of light absorption. Briefly, the different abundance and mass of the seven Hg isotopes lead to a different behavior during photo-excitation by light absorption (Mead et al., 2013). Because of their higher mass and abundance, isotopes like ^{200}Hg and ^{204}Hg will be capable of “shielding” themselves and attenuate photo-excitation, while rare Hg isotopes like ^{196}Hg will be more easily photo-excited inducing an unusual isotopic fractionation that does not depend on mass (Mead et al., 2013).

Primary Hg sources are generally associated with near-zero odd MIF. NVF usually causes relatively small MIF, whereas the largest odd MIF signatures are associated with MIE by photochemical reactions (Obrist et al., 2018). Photochemical demethylation of MeHg to Hg^0 can lead to a large enrichment of odd-mass Hg isotopes in the residual MeHg that is preserved along the aquatic food chain (Bergquist and Blum, 2007a). On the other hand, photo-reduction of Hg^{2+} complexes in snow was shown to lead to large depletions of odd-mass isotopes in residual snow (Sherman et al., 2010). Even MIF has recently been observed mainly in atmospheric samples (up to +1.24‰) (Cai and Chen, 2015). Research has demonstrated that the 200 and 204 even MIF are often opposite: Hg^{2+} in precipitation usually present positive $\Delta^{200}\text{Hg}$ values and concurrent negative $\Delta^{204}\text{Hg}$, while the complementary pool of atmospheric Hg^0 shows negative $\Delta^{200}\text{Hg}$ and concurrent positive $\Delta^{204}\text{Hg}$ (Obrist et al., 2018).

3.3. Hg MDF and MIF in marine ecosystems and predators

Since Hg stable isotopes undergo MDF and MIF as a consequence of biotic and abiotic processes occurring in the environment, they reflect a perfect tracer of Hg sourcing in the marine ecosystem and dynamics within the food web (Tsui et al., 2019). In the last twenty years the numbers of publications on the application of *in vivo* Hg stable isotopes analysis has quadrupled (Meng et al., 2020).

Because $\Delta^{199}\text{Hg}$ and $\Delta^{201}\text{Hg}$ values are not influenced by organisms' metabolism and do not change from one trophic level to the other, they can be successfully use to trace MeHg or Hg^{2+} sources from the environment even in apex predators (Cransveld et al., 2017; Kwon et al., 2014; Le Croizier et al., 2020). For example, Hg MIF measured in fish tissues have efficiently helped separating MeHg source in these animals based on their habitat and distribution. In coastal/estuarine areas in the Gulf of Mexico, San Francisco Bay or in Norwegian fjords, $\Delta^{199}\text{Hg}$ values range between 0.6 and 1.0‰ (Bolea-Fernandez et al., 2019; Gehrke et al., 2011; Kwon et al., 2014; Perrot et al., 2019; Senn et al., 2010). Offshore fish and sharks from the Pacific and Indian Oceans present instead $\Delta^{199}\text{Hg}$ values between 2.5 to 5.5‰ (Blum et al., 2013; Le Croizier et al., 2020; Motta et al., 2019). Blum et al. (2013) observed a vertical gradient in the water column, with sub-surface pelagic fish showing higher $\Delta^{199}\text{Hg}$ values than deep species feeding below the photic zone (Blum et al., 2013).

Also the source of Hg^{2+} from which MeHg is produced can influence $\Delta^{199}\text{Hg}$ values (Tsui et al., 2019). Hg^{2+} derived from dry deposition can be imprinted with slightly negative $\Delta^{199}\text{Hg}$ (Zheng et al., 2016), Hg^{2+} from industrial sources can have near-zero $\Delta^{199}\text{Hg}$ (Lepak et al., 2015; Wiederhold et al., 2015) and Hg^{2+} from wet deposition (e.g., into large lakes and ocean) can have variable positive $\Delta^{199}\text{Hg}$ (Gratz et al., 2010).

Also Hg MDF (mostly represented by $\delta^{202}\text{Hg}$) reflects the Hg isotope values of MeHg in the ambient environment and can be used to study Hg biochemical cycling in the marine ecosystem (Tsui et al., 2019). However, since Hg MDF is caused by a large number of processes, the range of $\delta^{202}\text{Hg}$ values found in aquatic ecosystems is very wide (-2 to 1.5‰) and their interpretation remains quite complex (Yin et al., 2014). In addition, the general consensus today is that significant prey-predator Hg MDF may occur in the higher trophic levels of food webs, so that $\delta^{202}\text{Hg}$ values can also be used to trace food web Hg trophic transfer in these species (Perrot et al., 2010; Tsui et al., 2019). In the same way, MDF can occur during Hg uptake and metabolism (transfer, transformation and excretion) within seabirds, marine mammals and fish (Feng et al., 2015; Man et al., 2019; Pinzone et al., 2021a; Wang and Tan, 2019). MeHg demethylation it is recognized as the most important mechanism of internal Hg MDF in different organs. MDF preferentially involves lighter Hg isotopes and generates newly formed iHg having a lower $\delta^{202}\text{Hg}$ (Perrot et al., 2015). The remaining non demethylated MeHg will then have a higher $\delta^{202}\text{Hg}$ compared to the initially bioaccumulated MeHg (Perrot et al., 2015; Renedo et al., 2021). The extension of Hg MDF can change based on Hg environmental levels (Pinzone et al., 2021a) or animals' age, as it was shown between adult and young pilot whales (Li et al., 2020).

Knowledge Gaps

Extensive literature exists on the application of C, N, S and Hg stable isotopes to study marine predators' trophic ecology and Hg sources. With regards to Hg stable isotopes, several works focused on Northern marine mammals, including the Baikal seal, ringed seal from Alaska, beluga whales and polar bears from the Pacific Arctic, and North Atlantic pilot whales (Bolea-Fernandez et al., 2019; Li et al., 2020; Masbou et al., 2018, 2015a; Perrot et al., 2015, 2012). These works confirmed that the application of Hg stable isotopes is the future of Hg contamination analysis in Arctic marine wildlife.

At the same time however, such research demonstrated how the interpretation of isotopic data cannot be overly simplified. They showed how Hg MIF and MDF might be caused by intrinsic factors (e.g. age, diet, etc.) in one species, while being influenced by external factors (e.g. sea-ice, riverine run-off, temperatures, etc.) in another.

There is a blatant need for additional studies on physiologically complex animals like marine mammals. This is especially true when considering how much Arctic marine mammals like true seals seem affected by changes in local Hg pollution and cycling, as a result of ongoing climate change.

→ Chapter 3

→ Chapter 4

Chapter 2







General Material & Methods

1. MODEL SPECIES

The bio-indicator models we selected for this study are the hooded seal *Cystophora cristata* (Erxleben 1777), harp seal *Pagophilus groenlandicus* (Erxleben 1777) and ringed seal *Pusa hispida* (Schreber 1775), because:

- they are the three most common true seals (*Phocidae*) in our sampling area, the Greenland Sea;
- they are marine tertiary predators, representing the perfect link between the lower trophic levels they feed upon and Arctic apex predators for which they constitute the most important food source;
- they show completely different trophic ecologies, distribution and physiological adaptations (Table 2.1), and are presently being harvested by both traditional and commercial hunters.

Table 2.1 Summary of morphological, ecological and distribution characteristics of our bio-indicators. When possible, numerical data are presented as average (max recorded value). Information extracted by: Bengtsson et al., 2020; Blix, 2005; Born et al., 2004, 1998; Folkow et al., 2010, 2004; Hammill and Smith, 1991; Haug et al., 2017a; Kovacs, 2018, 2015; Lavigne, 2018; Lindström et al., 2013; Lydersen et al., 1997; Matley et al., 2015; Potelev et al., 2014; Reeves, 2014; Rosing-Asvid, 2010; Siegstad et al., 2014; Teilmann et al., 1999.

<p>Hooded seal <i>Cystophora cristata</i> (<i>Cc</i>)</p>  	<p>Harp seal <i>Pagophilus groenlandicus</i> (<i>Pg</i>)</p>  	<p>Ringed seal <i>Pusa hispida</i> (<i>Ph</i>)</p>  
<p>Morphology</p> <ul style="list-style-type: none"> • Male: 260cm (271cm), 300kg (461kg); • Females: 220cm, 200kg; • Newborns: 100cm, 23 to 35kg; <p>Fur at birth: post-natal hair (shedding after 2 years);</p> <p>Breeding: March, drifting pack-ice of the West Ice;</p> <p>Lactation: 4 days, 10L milk / day, pups gain 7 kg/day;</p> <p>Weaning: 2 weeks;</p> <p>Diving depth: 700m (1200m)</p> <p>Diet:</p> <ul style="list-style-type: none"> • <u>Adults:</u> Greenland halibut, batoids (rays, etc.), catfish, cod, redfish <i>Sebastes spp.</i>, squids and blue whiting <i>Micromesistius poutassou</i>; • <u>Pups:</u> small fish such as capelin, herring and polar cod, along with squids and amphipods <i>Themisto spp.</i> <p>Distribution: Arctic, sub-Arctic, North-Atlantic Ocean</p> <p>Status: protected since 2016</p>	<p>Morphology</p> <ul style="list-style-type: none"> • Male: 170cm, 135kg; • Females: 170cm, 120kg; • Newborns: 80cm, 11kg; <p>Fur at birth: lanugo (shedding after 3 weeks);</p> <p>Breeding: March – April, drifting pack-ice of the West Ice;</p> <p>Lactation: 12 days, pups gain 2.2 kg/day;</p> <p>Weaning: 6 weeks;</p> <p>Diving depth: 50m (300m)</p> <p>Diet:</p> <ul style="list-style-type: none"> • <u>Adults:</u> capelin <i>Mallotus villosus</i>, sandeel <i>Ammodytes sp.</i>, polar cod <i>Boreogadus saida</i> and arctic cod <i>Arctogadus glacialis</i>, etc.; • <u>Pups:</u> invertebrates like Euphausiids <i>Thyanoessa spp.</i> and pelagic Amphipods <i>Parathemisto spp.</i> <p>Distribution: Arctic, sub-Arctic, North-Atlantic Ocean</p> <p>Status: Not protected</p>	<p>Morphology</p> <ul style="list-style-type: none"> • Adults: 110 to 160cm, 50 to 110kg; • Newborns: 65cm, 4.5kg; <p>Fur at birth: lanugo (shedding after 2 to 3 weeks);</p> <p>Breeding: April, fast-ice, Scoresby Sound, King Oscar Fjord;</p> <p>Lactation: 6 to 7 weeks, pups gain up to 0.4kg kg/day;</p> <p>Weaning: 2 to 3 weeks;</p> <p>Diving depth: <50m (200m)</p> <p>Diet:</p> <ul style="list-style-type: none"> • <u>Adults:</u> pelagic amphipods; polar cod <i>Boreogadus saida</i>, Arctic cod <i>Arctogadus glacialis</i>, and more temperate species like capelin <i>Mallotus villosus</i> and redfish <i>Sebastes spp.</i>; • <u>Pups:</u> small fish such as capelin, herring and polar cod, along with squids and amphipods <i>Themisto spp.</i> <p>Distribution: Arctic, fjords of Greenland Sea</p> <p>Status: Not protected</p>

1.1. The hooded seal

The hooded seal *Cystophora cristata* derives its name from the inflatable nasal sac which is developed only in males (Jefferson *et al.*, 2015). This sac reaches full size only at sexual maturity and is used for display during courtship fighting (Blix, 2005). Adult hooded seals are silver grey in color, with the face usually black and irregular black spots all over the body (Kovacs, 2018). Pups' pelage instead is blue on the back and silver-grey on the belly (Kovacs, 2018).

Hooded seals occur in the North Atlantic, Arctic and subarctic waters (Figure 2.1). Three distinct subpopulations are recognized: one is located in the Canadian waters, one in the Davis Strait and one in the Greenland Sea (West of Jan Mayen Island) (Kovacs, 2016). There is interchange between the seals from Eastern and Western Greenland outside of breeding and molting season, but it varies a lot from year to year. Genetically, the hooded seal is considered as a panmictic population (Coltman *et al.*, 2007).

The Greenland Sea subpopulation breeds on the drifting pack of the West Ice. Females congregate at the breeding grounds from mid-March (Vacquie-Garcia *et al.*, 2017). Births occur between the space of 2 to 3 days around the end of March. Pups are born in an advanced developmental stage as they have already deposited a thin layer of blubber (≥ 2 cm) and shed their lanugo in uterus (Blix, 2005; Kovacs, 2018).

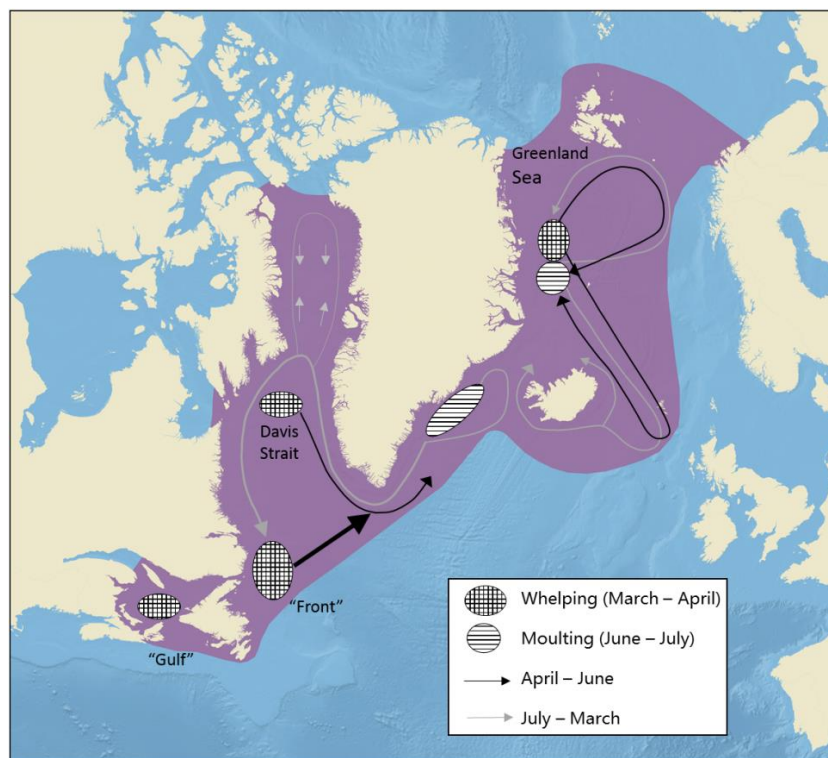


Figure 2.1. Hooded seal *C. cristata* distribution and range. Black arrows represent spring hunting, while grey ones represent fall/winter hunting. Moulting areas are represented by horizontal lines, whelping / "breeding" grounds are checkered. Reproduced from nammco.no.

Hooded seal present the shortest period of lactation among all mammals (4 days only) (Lydersen et al., 1997). Mating takes place immediately after suckling period (Rosing-Asvid, 2010). Weaned pups will fast on ice for 2 weeks, relying on their blubber body reserves, before going to the water and learn how to swim, dive and forage (Folkow et al., 2010). Afterwards, adults head North of their respective breeding areas for the annual molt in the Fram Strait and then continue their migration to feeding areas (Garde, 2013).

The majority of hooded seals undertake very long hunting migrations: some of them migrate along the coast of Eastern Greenland reaching also the Blossville Coast and Iceland (Vacque-Garcia et al., 2017). Others swim East to Svalbard, the Faroe Island, the Norwegian coasts and the Shetland areas. On occasion, subadults of hooded seals are spotted in the North Sea, the French coast (Calais), down to Portugal and the Mediterranean Sea (Andersen et al., 2009; Folkow et al., 1996). Adult hooded seals are specialized benthic-pelagic divers, exploiting the continental slope (Rosing-Asvid, 2010). Pups instead find most of their food in upper water layers (Folkow et al., 2010).

Today the total hooded seal population size consists approximately of 675 000 individuals, showing an important decrease in the last 15 years. The hooded seal population of the Greenland Sea has decreased by 43 % (3.7 % decrease / year) over the same time span (Kovacs, 2016). The first large estimate was conducted in 1946 and counted 1 136 055 individuals. The last survey in 2019 counted 77 300 (95 % CI: 60 100 – 94 600) (ICES, 2019). This stock is less than 10 % of its abundance observed 60 years ago (Øigård et al., 2014). Overhunting was clearly involved in the collapse of this stock as quotas were being set for a population size much larger than it actually was (Stenson, 2014). Total catches in the 50s comprised between 40 000 and 50 000 individuals, in the 2000s between 1000 and 7000, in 2019 only 23 seals (from Norway) (ICES, 2019).

1.2. The harp seal

The Harp seal *Pagophilus groenlandicus* does not show a strong sexual dimorphism. Both males and females are silver grey with a black face and a black harp-shaped marking on the back. Pups are born with a white/yellowish coat (lanugo) that they keep for 2 to 4 weeks, before going through a series of pelts (Blix, 2005).

Harp seals inhabit the North Atlantic and Arctic Oceans, from Northern Russia to Eastern Canada and the United States (Figure 2.2). Three distinct subpopulations are recognized: one is located in the White Sea in Russia, one on the West Ice in the Greenland Sea, one in the Northwest Atlantic (Lavigne, 2018). They separate during breeding and molting, but their ranges overlap for the rest of the year. Genetic analysis revealed that the breeding groups in the Northwest Atlantic (Gulf of St. Lawrence and the Front of Labrador and Newfoundland) are one group and that the animals that breed in the White Sea and those in the Greenland Sea are another group (Kovacs, 2015).

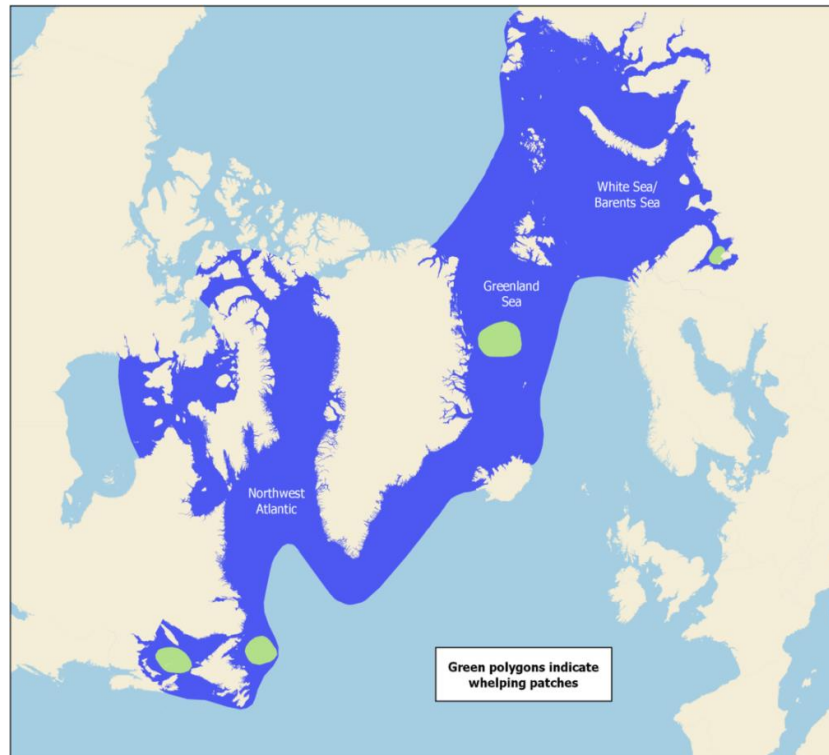


Figure 2.2. Harp seal *P. groenlandicus* range and distribution. Whelping patches are represented by green polygons. Reproduced from nammco.co.

In the Greenland Sea, female and male harp seals congregate together from March to April on the drifting pack-ice (Haug et al., 2017b). Birth occurs in vast herds, highly synchronized between the end of March and the beginning of April. During nursing, pups deposit a 5cm blubber layer that allows him to survive the post-weaning fast (Rosing-Asvid, 2010). After weaning, pups stay on ice for up to 6 weeks, losing up to half their body mass (Ofteidal et al., 1996; Storeheier and Nordøy, 2001). At the beginning they are helpless, but they learn gradually to swim and catch food (Malde, 2019). The development of these capacities is in line with the shredding of lanugo and the growth of greyish and black-spotted postnatal hair (Malde, 2019). This is lost only during molting season of their second year of life. At sexual maturity the seals get a black pattern on their back (saddlebacks) which develops to a clear harp-shaped spot in older adults (Lavigne, 2018). Females mate immediately after weaning and leave shortly after to replenish body mass lost during nursing. Males migrate directly to molting grounds. Males start molting around mid-May, while females around July (Haug et al., 2013, 2004). After molting, the large majority of the Greenland Sea stock migrates to the Barents Sea, where they remain until fall. However, some individuals go to Svalbard or all the way to the Kara Sea (Russia, Figure 2.2) (Haug et al., 2004; Lindstrøm et al., 2013; Potelev et al., 2014). Harp Seals are generalist pelagic hunters that remain within the continental shelf area, with recorded dives of around 20 minutes in winter, and 2 to 15 minutes in summer (Folkow et al., 2004; Rosing-Asvid, 2010).

The global estimate for harp seal numbers is close to 9 million animals, making the harp seal the most abundant pinniped species in the Northern hemisphere (Kovacs, 2015). The breeding group in the West Ice near Jan Mayen counts 426 808 (95 % CI: 313 005 – 540 612) with a pup production of 66 407 (95 % CI: 51 605 – 81 209) per year (Haug et al., 2006; Øigård et al., 2009). Total allowable catch (TAC) was around 6 000 in 2019 (Biuw et al., 2018). In the Greenland Sea the latest 2019 WGHARP report shows that the rate of increase is considerably lower than previous estimates, with estimated abundances being stable or slightly decreasing since the early 2000s (ICES, 2019).

1.3. The ringed seal

The Ringed seal *Pusa hispida* is the smallest of all phocids (Reeves, 2014; Rosing-Asvid, 2010). There are currently five recognized subspecies of ringed seal (Figure 2.3): the circumpolar Arctic Ringed Seal (*P. h. hispida*), the Okhotsk Ringed Seal (*P. h. ochotensis*), the Baltic Ringed Seal (*P. h. botnica*), the Ladoga Seal (*P. h. ladogensis*), and the Saimaa Seal (*P. h. saimensis*) (Lowry, 2016). The genus name has been recently changed from *Phoca* to *Pusa*, but it not yet fully recognized, mostly because of contrasting molecular and genetic works (Lowry, 2016).

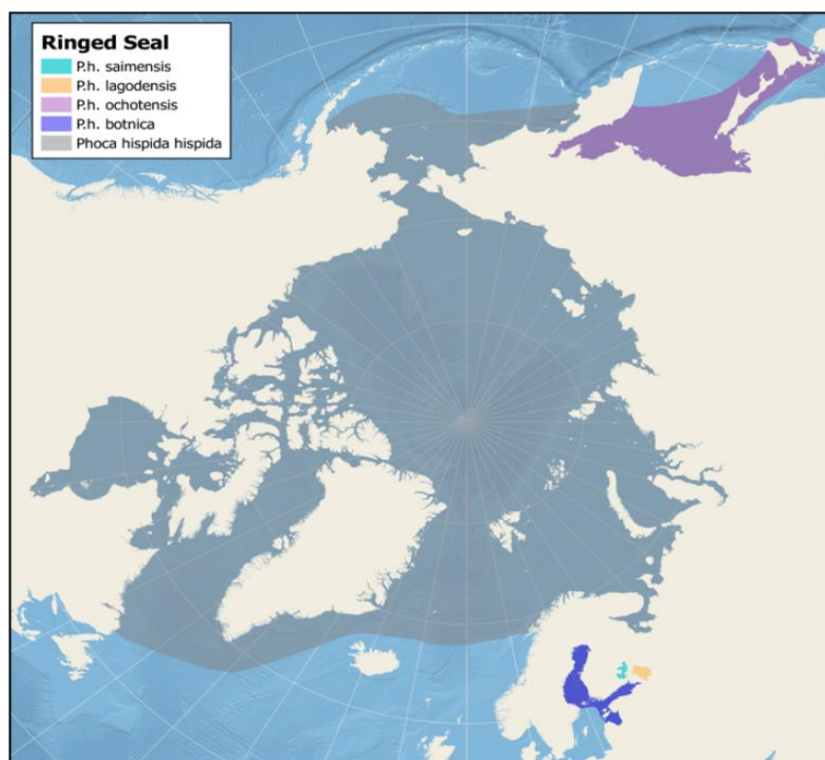


Figure 2.3. Ringed seal *P. hispida* distribution and range. The colors represent the five recognized subpopulations of this species around the Northern hemisphere. Reproduced from nammco.no.

During breeding periods, ringed seals create breeding lairs comprising a cave dug into a snowdrift (Stirling and Smith, 2004). They also have to create breathing holes in the ice that can be even 2 m thick, in order to ensure continuous access to food and protection from predators like polar bears (Hammill and Smith, 1991; Kelly et al., 2010). There is a large variability in pups' size at weaning across the entire Arctic distribution (Blix, 2005). Mating is believed to take place after weaning. However, the distribution of adults after mating vary greatly. Some remain within the fjords year-round, some venture in the Greenland Sea towards the Fram Strait and Svalbard, following the ice-packs (Freitas et al., 2008; B. P. Kelly et al., 2010). Molting occurs over several months: end of April to mid-June with peak in May for pups, mid-May to mid-July with peak in June for adults (Carlens et al., 2006; Lowry, 2016).

Ringed seals are considered mostly as generalist and sympagic feeders that feed under the ice or in the upper part of the water column (Born et al., 2004; Teilmann et al., 1999). Prey choice might change with season and geographic region (Bengtsson et al., 2020; Matley et al., 2015).

The worldwide population size and trend of ringed seals is not accurately known. Estimates of circa 1 450 000 seals for the entire Arctic population were proposed by the 2016 IUCN Red List, with the global population size reaching over 3 million animals (Lowry, 2016). Extremely scattered information is available for ringed seals in the Greenland Sea because of the vast geographic area occupied by the species (Ferguson et al., 2005). The latest count along the East coast of Greenland was conducted in 1984, within Scørensby Sound and King Oscar Fjords (Born et al., 1998). They measured nearly 30 000 seals, mostly on ridged 1-year-old ice covered with snow. Because of their distribution ringed seals can be hunted year-round, even during the dark months. As such, this is the most consumed species by Northern peoples. There are no national restrictions on seal hunting in Greenland: the general annual harvest averaged 79 206 seals between 1993 and 2009 (Cumming, 2015). In the Scoresby Sound catch statistics reported an average of 5 380 seals hunted per year in 2015, and 7 567 seals in 2018 ([NAMMCO catches database](#)).

2. SAMPLING SITE

The study area covers the Atlantic sector of the Arctic Ocean: the Greenland Sea, the Norwegian Sea, the Barents Sea, The Denmark Strait and the Fram Strait (Figure 2.4). The colors represented in this figure will be used throughout the entire manuscript: blue for hooded seals, red for harp seals and green for ringed seals.

Sampling was conducted along the breeding and molting grounds of the Eastern coast of Greenland. Hooded and harp seals were sampled offshore, on the drift ice. Ringed seals were sampled on land fast ice in the Scoresby Sound: at Ittoqqortoormiit and Kap Tobin specifically.

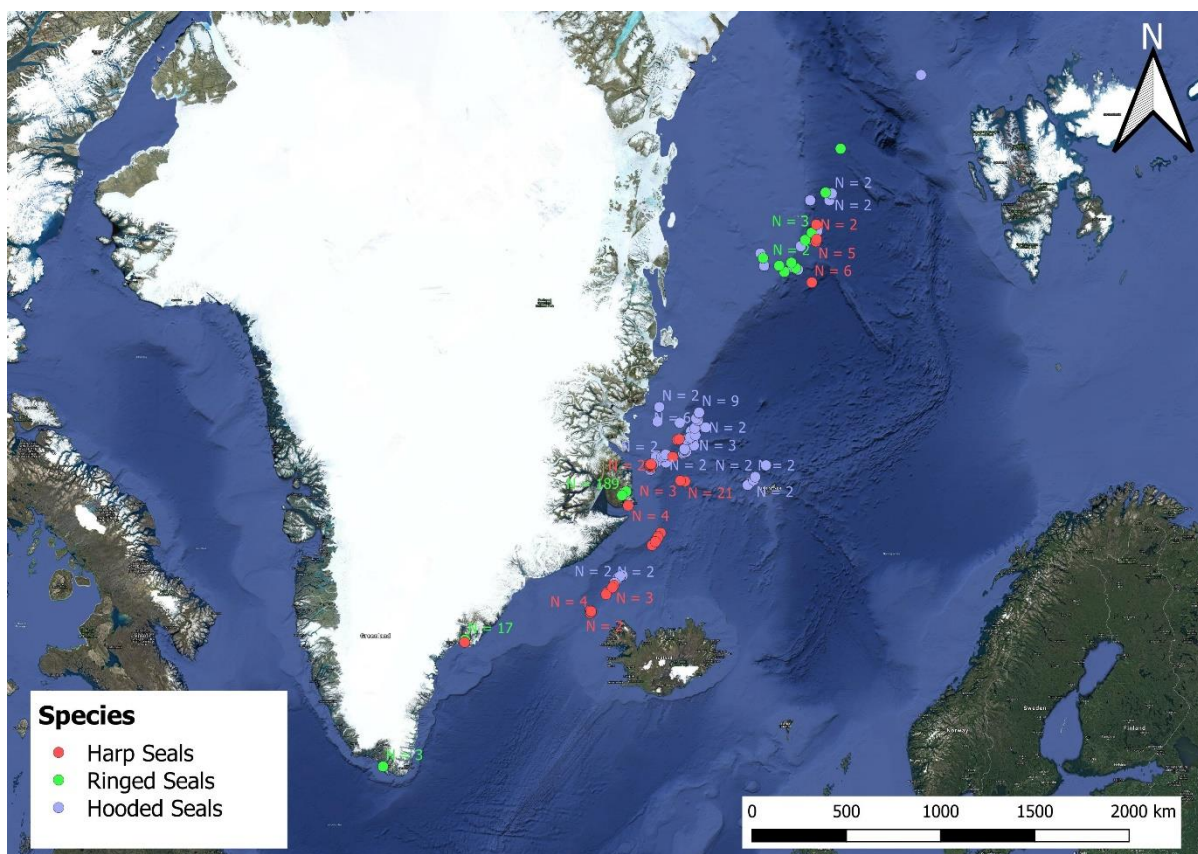


Figure 2.4. Sampling locations for all seals measured in this thesis. Harp seals are represented by green dots; ringed seals are represented by red dots; hooded seals are represented by blue dots. Samples that were taken at the same coordinates were grouped together and labelled with the total sample number. As QGIS required coordinates in decimal degrees, initial latitude and longitude coordinates that were recorded in the DMS (degrees, minutes, and seconds) format were converted using the formulae (Hours + Minutes/60) and [(Hours + Minutes/60) * -1] respectively. Maps were created using QGIS software for Windows platform (version 3.4.1-Madeira), downloaded from the [QGIS programme website](#). Google Satellite and its corresponding coordinate system was used as the base layer in all map figures.

3. ETHICAL STATEMENT

3.1. Captivity

Tissues from captive seals derives from several physiological studies at the University of Tromsø. The captivity experiment was approved by the Norwegian Food Safety Authority (permit n°2012/030044). The animal facility approved for such captivity experiment (Norwegian Animal Research Authority, approval #089) was situated at the Department of Arctic and Marine Biology (DAMB), UiT - The Arctic University of Tromsø (UiT). Experiments were undertaken under Norwegian Animal Research Authority permit (no 5399, 5422 and 5843). Animals were primarily used for experiments other than those reported here and tissues were harvested from them at the termination of these (Alvira-Iraizoz and Nordøy, 2019; Geiseler et al., 2016).

3.2. *In-situ* harvesting

Hunting of free-ranging seals was conducted as part of an extensive scientific sampling program for a number of studies that included toxicological, virologic and physiological investigations on the same animals (Alvira-Iraizoz and Nordøy, 2019; de la Vega et al., 2020; Hoff et al., 2017; Malde, 2019; Pinzone et al., 2021b; Schots et al., 2017; Sonne et al., 2018). Permission for a limited scientific catch (< 50 animals each year) of harp and hooded seals was obtained from the Ministry of Foreign Affairs of Denmark (Utenrigsministeriet) in a verbal note (JTHAV J. nr. 12/1352 nr. 2017-1054 and nr. 2019-9877) and from the Norwegian Directorate of Fisheries (letter ref. 17/497 and 18/14793). Adult seals shooting was done in accordance to Norwegian Sealing Regulations (Forskrift for utøvelse av selfangst i Vesterisen og Østisen: FOR-2003-02-11-151) (Norwegian Ministry of Trade and Industry, 2003). Seal pups capture and also followed the protocol in accordance with the Norwegian Animal Welfare Act (LOV-2018-06-15-38, §12) (Norwegian Ministry of Agriculture and Food, 2009), Directive 2010/63/EU of the European Parliament (CELEX 32010L0063, Annex IV) (European Parliament and The Council, 2010) and Norwegian Regulations for Use of Animals in Research (FOR-2017-04-05-451, Appendix C) (National legislation - NORWAY, 2017).

4. SAMPLING

4.1. Partners

Samples were gathered thanks to the collaboration of several partners (Table 2.2):

– Tissue bank samples

Ringed, hooded and harp seals harvested between 1985 and 2018 were accessed at **Aarhus University** (Roskilde, Denmark) in collaboration with Prof. Rune Dietz, Prof. Christian Sonne, Dr. Igor Eulaers and Dr. Jean-Pierre Desforges and the **AMAP** assessment program. Hooded and harp seals harvested between 2000 and 2010 were accessed at the Institute of Marine Research (**IMR**, Tromsø, Norway) in collaboration with Dr. Tore Haug.

– Free-ranging seals

Harp and hooded seals harvested from 2017 to 2019 were accessed *in-situ* thanks to the collaboration with Prof. Erling S. Nordøy from (**UiT**, Tromsø, Norway).

– Captive seals

Samples of tissues from captive hooded seal pups were accessed thanks to the collaboration with Dr. Mario Aquarone and Prof. Lars Folkow from (**UiT**, Tromsø, Norway).

Table 2.2. Sampling design for our 3 model species. The sampling year, area, technic and collaboration are reported. The number of sampled seals (*n*) is shown as N AdM, N AdF, N SubAd, N Yea (**total N for the year**). **AdM** = Adult male, **AdF** = Adult Female, **SubAd** = Subadult, **Yea** = Yearling. GLGs = Growth Layer Groups counting. Details about collaborations are given in paragraph 4.1 (page 8).

Year	<i>n</i>	Area	Technic	Aging	Collaboration
Hooded seal <i>Cystophora cristata</i>					
1985	0, 0, 2, 9 (11)	Ammassalik – Denmark Strait	Tissue Bank	GLGs	Aarhus University
1987	2, 4, 3, 2 (11)	Ammassalik – Denmark Strait	Tissue Bank	GLGs	Aarhus University
2001	7, 4, 18, 1 (30)	West Ice – Greenland Sea	Tissue Bank	GLGs	IMR
2002	1, 1, 5, 1 (8)	West Ice – Greenland Sea	Tissue Bank	GLGs	IMR
2007	11, 17, 6, 9 (43)	West Ice – Greenland Sea	Tissue Bank	GLGs	IMR
2008	1, 2, 17, 0 (20)	West Ice – Greenland Sea	Tissue Bank	GLGs	IMR
2014	0, 0, 6, 0 (6)	UiT facilities	Captive seals	Standard length	UiT
2015	0, 5, 0, 0 (5)	West Ice – Greenland Sea	Tissue Bank	Standard length	Aarhus University
2017	1, 0, 3, 4 (8)	West Ice – Greenland Sea	Free-ranging seals	Standard length	UiT
2018	1, 5, 0, 5 (11)	West Ice – Greenland Sea	Free-ranging seals	Standard length	UiT
2019	5, 0, 0, 0 (5)	West Ice – Greenland Sea	Free-ranging seals	Standard length	UiT
TOT	158				
Ringed seal <i>Pusa hispida</i>					
1985	0, 4, 8, 0 (12)	Ammassalik – Denmark Strait	Tissue Bank	GLGs	Aarhus University
1987	3, 0, 0, 0 (3)	Ammassalik – Denmark Strait	Tissue Bank	GLGs	Aarhus University
1994	6, 5, 11, 1 (23)	Ammassalik – Denmark Strait	Tissue Bank	GLGs	Aarhus University
2000	4, 6, 8, 0 (18)	Ittoqqortoormiit – Scoresby Sound	Tissue Bank	GLGs	Aarhus University / AMAP
2002	5, 7, 10, 5 (27)	Greenland Sea – Scoresby Sound	Tissue Bank	GLGs	IMR / Aarhus University / AMAP
2004	6, 3, 8, 0 (17)	Ittoqqortoormiit – Scoresby Sound	Tissue Bank	GLGs	Aarhus University / AMAP
2006	9, 8, 6, 0 (23)	Ittoqqortoormiit – Scoresby Sound	Tissue Bank	GLGs	Aarhus University / AMAP
2008	6, 5, 9, 0 (20)	Ittoqqortoormiit – Scoresby Sound	Tissue Bank	GLGs	Aarhus University / AMAP
2010	6, 12, 11, 1 (30)	Ittoqqortoormiit – Scoresby Sound	Tissue Bank	GLGs	Aarhus University / AMAP
2012	7, 8, 15, 2 (32)	Ittoqqortoormiit – Scoresby Sound	Tissue Bank	GLGs	Aarhus University / AMAP
2014	6, 6, 6, 0 (18)	Ittoqqortoormiit – Scoresby Sound	Tissue Bank	GLGs	Aarhus University / AMAP
2016	5, 2, 9, 3 (19)	Ittoqqortoormiit – Scoresby Sound	Tissue Bank	GLGs	Aarhus University / AMAP
2018	5, 5, 10, 0 (20)	Ittoqqortoormiit – Scoresby Sound	Tissue Bank	GLGs	Aarhus University / AMAP
TOT	262				
Harp seal <i>Pagophilus groenlandicus</i>					
2001	7, 3, 12, 0 (22)	West Ice – Denmark Strait	Tissue Bank	GLGs	IMR
2015	5, 0, 0, 3 (8)	West Ice – Greenland Sea	Tissue Bank	GLGs	Aarhus University / AMAP
2017	1, 1, 3, 5 (10)	West Ice – Greenland Sea	Free-ranging seals	Pelage	UiT
2018	0, 9, 0, 14 (23)	West Ice – Greenland Sea	Free-ranging seals	Pelage	UiT
TOT	63				

4.2. Seals in captivity

Eight hooded seal newborns were captured in March 2012 on the whelping grounds along the pack-ice of the Greenland Sea, North-West of Jan Mayen Island. Sampling was conducted during a research cruise with R/V *Helmer Hanssen*. Seals were captured with the use of a hoop-net and brought onboard, where they were kept in 1.5 by 2.5 m pens during the transit back to Tromsø (Norway). The captivity experiment was situated at the Department of Arctic and Marine Biology (DAMB), UiT - the Arctic University of Tromsø (UiT) (Figure 2.5). For 2 years, all seals were fed on a constant diet of freshly frozen, thawed Norwegian Spring Spawning herring *Clupea harengus*, in quantities appropriate for the sustainment of a correct development and a natural growth curve based on animals' mass (2kg / animal per day) (Gentry and Holt, 1982). In this regard, food was also supplemented with a vitamin complex (Seatabs MA III, Pacific Research Labs, Inc., Vashon Island, WA, USA). Herring were purchased from the same company each year (Pelagia – Seafood from Norway, MSC-C-50933, FAO 27): they were thus sampled in the same area (Northeast Atlantic), in the same period (February to March), following the same protocol for both fishing and storing conditions (<https://pelagia.com/products/spring-spawning-herring/>). All fish used for the experiment belonged to the same length range (25 to 30 cm). The indoor light regime simulated that of outdoor natural light-darkness cycles at 70°N latitude. Seals were maintained in two indoor 40 000 L (1.5 m deep) seawater pools with a wooden ledge along one side on which the animals could haul out at will. Two seals (K5 and K6) were euthanized after 1 year (March 2013) for other physiological studies at the UiT; and were not available for our analysis. The remaining 6 seals were euthanized in 2015 and different organs were collected for analysis.



Figure 2.5. Hooded seal *C. cristata* feeding. Feeding occurred twice a day. Each animal was called out of the water and fed with ca. 1kg of Norwegian spawning herring *C. harengus* ($n = 4$ fish per seal). Vitamins were added in the mouth of each herring before feeding.

At the termination of those experiments, the seals were euthanized in accordance with a permit issued by the National Animal Research Authority of Norway (NARA permit no. 5399, 5422 and 5843): the seals were sedated by intramuscular injection of zolazepam/tiletamine (Zoletil Forte Vet., Virbac S.A., France; 1.5 to 2.0 mg kg⁻¹ body mass), then anaesthetized using an endotracheal tube to ventilate lungs with 2 to 3 % isoflurane (Forene, Abbott, Germany) in air. When fully anaesthetized, they were euthanized by exsanguination via the carotid arteries.

Muscle, liver, kidney, whole blood and hair of hooded seals and herring (entire fish, $n = 15$ in 2014 and $n = 15$ in 2018) were collected after dissection and stored in the freezers of the Department of Arctic Marine Biology at UiT.

4.3. Tissue bank sampling

Sampling from tissue banks was conducted over several missions in Denmark and Norway. Hooded and harp seal samples were collected at the Institute of Marine Research (IMR) in Tromsø (Norway), in April 2018. Ringed seal tissues were mostly collected at Aarhus University (Denmark) in November 2017, May 2018 and February 2019.

Tissue bank samples of muscle, hair, kidney and liver were stored at -30°C. Once unfrozen, around 10 g of tissue were extracted from each tissue-bank specimen, with the use of a sterilized stainless-steel scalpel. The sample was then rinsed with milliΩ water to eliminate remaining blood. Samples were stored in Minigrip® polyethylene plastic bags and stored again at -30°C.

4.4. Free-ranging seals

Sampling of seals was conducted on the pack-ice of the Greenland Sea (69°10'N/16°36'W to 71°15'N/19°44'W, Figure 2.4) onboard of the university vessel RV “Helmer Hanssen” and in collaboration with Prof. Erling S. Nordøy from the AMB Department of UiT. Fieldwork occurred during the breeding season of harp and hooded seals three consecutive years:

- from the 6th and the 19th of April 2017,
- from the 19th of March to the 2nd of April 2018, and
- from the 15th to the 30th of March 2019.

Adult and subadult seals were shot to the head from the bow of the ship using 6.5 x 55 mm expanding ammunition causing immediate death. They were subsequently brought on board with the help of a metallic crane, before bleeding of arterial veins of the front flippers. Seal pups were caught on the ice and sedated with an intramuscular (I.M.) injection of Zoletil Forte Vet. (100 mg ml⁻¹ – tiletamine /

zolazepam – 2.0 to 2.5 mg kg⁻¹). They were further catheterized into the extradural-intervertebral vein onboard the ship, to inject a lethal dose of pentobarbital (15 to 20 mg kg⁻¹).

After death, each seal was weighted. Adults and subadults were weighted using the metal crane, whereas pups were put again in the hoop-net and weighted onboard. The weight of the net was measured every three or four animals and then subtracted to obtain seal net body mass. Standard length was measured keeping the meter in a straight line from the nose to the tip of the tale. For the measurement of the Curvilinear (“Zoological”) length instead the meter would follow the dorsal contour of the animal. Other information was additionally recorded like the girth, namely the pectoral body circumference (under the flippers), the sex, sampling date, position, air temperature, ice type and sea depth (Table 2.3).

Table 2.3. Biometric information of hooded, ringed and harp seals analyzed in this work. Data of standard length (SL, in cm), girth (in cm), body mass (BM, in kg) and blubber thickness (BT, in mm) are reported by age groups: AdF, Adult Females; AdM, Adult Males; SubAd, subadults; Yea, Yearlings. Data are shown as Average (Median) ± Standard Deviation, (Min – Max) *n*.

Age group	SL (cm)	Girth (cm)	BM (kg)	BT (mm)
Hooded seal				
AdF N = 38	181 (187) ± 27 (101 - 220) 34	126 (128) ± 21 (65 - 173) 33	146 (145) ± 50 (20 - 250) 36	36 (34) ± 50 (18 - 69) 31
AdM N = 29	213 (220) ± 24 (119 - 235) 29	152 (154) ± 16 (86 - 175) 29	214 (220) ± 50 (47 - 300) 29	51 (50) ± 13 (47 - 300) 29
SubAd N = 54	139 (138) ± 21 (104 - 204) 54	101 (100) ± 16 (75 - 154) 54	68 (56) ± 33 (28 - 194) 53	30 (29) ± 11 (10 - 57) 49
Yea N = 33	106 (104) ± 17 (87 - 169) 33	81 (79) ± 14 (57 - 120) 31	35 (32) ± 18 (18 - 109) 32	32 (30) ± 13 (15 - 74) 19
Harp seal				
AdF N = 17	165 (162) ± 9 (66 - 180) 17	125 (123) ± 11 (57 - 143) 13	126 (125) ± 27 (16 - 168) 16	49 (50) ± 12 (10 - 70) 16
AdM N = 9	170 (169) ± 10 (154 - 186) 9	131 (127) ± 13 (118 - 158) 9	125 (123) ± 27 (91 - 174) 9	46 (43) ± 9 (37 - 65) 9
SubAd N = 15	138 (140) ± 16 (112 - 167) 15	103 (103) ± 12 (80 - 132) 15	67 (69) ± 20 (37 - 119) 15	40 (38) ± 7 (27 - 54) 15
Yea N = 19	92 (95) ± 7 (79 - 104) 19	77 (78) ± 12 (56 - 95) 17	26 (27) ± 7 (11 - 37) 18	42 (40) ± 15 (14 - 80) 16
Ringed seal				
AdF N = 59	114 (112) ± 10 (85 - 140) 59	99 (94) ± 11 (84 - 120) 10	50 (49) ± 14 (34 - 70) 11	40 (40) ± 8 (20 - 61) 46
AdM N = 60	122 (122) ± 11 (102 - 146) 60	75 (100) ± 7 (86 - 110) 13	42 (50) ± 7 (37 - 61) 13	40 (40) ± 11 (20 - 70) 50
SubAd N = 98	109 (109) ± 13 (81 - 150) 98	78 (78) ± 6 (70 - 87) 13	25 (23) ± 6 (17 - 35) 13	37 (40) ± 7 (25 - 56) 80
Yea N = 12	90 (88) ± 15 (66 - 117) 12	15 (72) ± 4 (67 - 76) 5	28 (18) ± 2 (16 - 21) 5	34 (35) ± 5 (27 - 40) 11

Dissection of each seal was conducted on the bridge of the vessel. Once tissues were extracted they were brought in the wet lab where they were weighted and rinsed with mineralized water to remove the blood. The origin of the sample was chosen in compliance with standard dissection protocols for marine mammals (IJsseldijk et al., 2020; Jauniaux et al., 2002). Muscle and hair were systematically sampled on the left ventral side of the animal; whereas liver and kidney were sampled from the left bottom lobe. Around 10 g of tissue were cut out and stored in Sarstedt polyethylene plastic bags (PP – 60/85 mm, several dimensions) that were previously labelled. We also collected brain, lung, heart, mammalian gland, blubber, umbilical cord, blood, spleen and milk. All samples were stored on board in -20°C freezers.

During each dissection stomach content was investigated for the presence of prey, macro-plastics and parasites (Pinzone et al., 2021b). Once back in Tromsø, samples were stored in the freezers of the Department of Arctic Marine Biology at UiT.

After all fieldworks (tissue bank, captivity and *in-situ* harvesting), samples were transferred to the University of Liège (Belgium) in a 3 layers packaging, following the EU Commission Regulation N° 142/2011 for the import/export of animal by-products and derived products not intended for human consumption (EU Commission, 2020; EU Parliament, 2009), the WHO regulations for the transport of dangerous goods (UNECE, 2015) and infectious substances (WHO, 2015). Transport was done in rigid and isolated foam boxes and kept at -20°C with the use of Techni Ice (ISO 9001, Techni Ice Australia P/L).

5. SEALS AGING

Seals were separated in different age classes, adult males (“AdM”), adult females (“AdF”), subadults (“SubAd”) and yearlings (“Yea”):

- Yea = 0 to 1 years old,
- SubAd = 1 to sexual maturity,
- Adults = from sexual maturity onwards.

Hooded seal males are believed to mature between 4 and 6 years of age, whereas females mature between 3 and 5 years of age (Kovacs, 2018). Harp seals of both sexes mature between 6 and 8 years of age (Lavigne, 2018). In ringed seals instead, sexual maturity is reached between 3 to 5 years of age in females and between 5 to 7 years of age in males (Hammill, 2018).

Because the large number of sampling partners, distinct age calculations were conducted: teeth analysis, calculation via the standard length or visual estimation using pelages.

5.1. Teeth analysis

The age of seals collected from tissue banks, was already available from previously published works (Dietz et al., 2013, 2011; Rigét et al., 2011, 2005; Sonne et al., 2009b). It was performed following Dietz et al. 1991 (Dietz et al., 1991), by counting annual layering in the cementum of the canine or premolar teeth. Briefly, the canine teeth were extracted from the jaws after boiling (max. 10 minutes) and placed in 5 % HNO₃. Teeth were then store in 80 % alcohol to avoid splitting or cracking and prevent bacterial growth, before being decalcified (Dietz et al., 1991). Prior to sectioning, they were soaked for 24 hours in tap water to hydrate the alcohol-fixed tissue. Toluidine blue was used as the staining agent during sectioning of the teeth. Age determination was then conducted counting the growth layer groups (GLGs) of the cementum in the lower third of the tooth (Dietz et al., 1991).

For hooded, harp and ringed seals whose GLG-calculated age was not available, we used either the standard length or the pelage's type and coloring as explained hereby.

5.2. Standard length

We estimated the age of captive hooded seals using the two equations developed especially for this species by Wiig in 1985 (Wiig, 1985):

$$\text{for females: } L_x = 200 (1 - e^{-0.202 (x + 0.61)})^{0.336} \quad (2.1)$$

$$\text{for males: } L_x = 221.1 (1 - e^{-0.129 (w + 0.61)})^{0.309} \quad (2.2)$$

5.3. Pelage

We estimated the age of free-ranging harp seals looking at the type and color of their pelage (Figure 2.6). This technique allows an approximate and quick estimation of seal life stage in species where the fur pattern shifts over time. Harp seal pups present a white-yellowish lanugo hair in the first 20 days of life ("whitecoats"). Between 20 and 30 days of life they start to shred the lanugo on their pectoral flippers and head ("ragget jackets") (Lavigne, 2018). After 30 days they usually present the new post-natal hair on almost all the body ("beater"). In adult harp seals (> 5 years old), a harp-shaped spot is clear on their back (Lavigne, 2018).



Figure 2.6. Greenland Sea harp seal *Pagophilus groenlandicus* pelage types. Figure **A** shows pups at different stages of lanugo shredding in their first weeks of life. Figure **B** shows the classic black head and harp shape shown by adult individuals. Pictures credits: **(A)** Marianna Pinzone, 2017; **(B)** Fredrik Markussen, 2018.

6. SAMPLES PREPARATION

The outer exposed tissue layer was cut away from thawed tissue samples to minimize possible contamination and changes due to handling and storage. Between 6 and 10 g of thawed tissue (muscle, liver, kidney, red blood cells and hair) were dissected using a ceramic knife (or scissors), placed in plastic tubes and accurately weighted to the nearest 0.1 mg. Tubes were then placed at -80°C overnight before freeze-drying for 48h (Alpha 1 - 4 LD plus, Christ, Germany). Liver and kidney were freeze-dried longer due to their high fat content. Tubes were then weighted again to determine the water content of each sample and the wet weight/dry weight ratio (Table A2.1).

Samples of hair were washed ultrasonically with reagent grade acetone (acetone for trace analysis ≥ 99.8 % purity, ARISTAR®, VWR) and were rinsed repeatedly with milliΩ water (18.2 MΩ cm⁻¹) to remove exogenous contaminants, blood and fat residuals, according to the method recommended by the International Atomic Energy Agency (Katz and Chatt, 1988):

- First bath: 10 minutes in milliΩ water,
- Second bath: 10 minutes in acetone,
- Third bath: 10 minutes in milliΩ water,

A second series of bath was given to samples particularly covered in blood and fat residues. A maximum of 2 acetone baths were given because of its potential to alter the isotopic composition of the samples. Hair samples were lyophilized for 24h.

Muscle, liver and kidney samples were ground to a fine powder using a ceramic mortar and pestle, while hairs were cut with ceramic scissors in the smallest size possible.

7. ANALYTHICAL TECHNIQS

This part encompasses the technics used through the entire thesis. Details about specific sampling or analysis will be presented separately in the following chapters.

7.1. THg concentrations

This analysis was conducted at the laboratory of Oceanology (ULiège). Total Hg (THg) concentrations were determined directly on powder samples by atomic absorption spectroscopy (AAS) on a Tri-cell Direct Mercury Analyzer 80 (DMA-80 evo, Milestone, Italy), in compliance with the US EPA 7473 protocol validated for biological solid samples and solutions. Depending on the tissue considered, different quantities of material were loaded in quartz boats. All quantities were adapted to fall within a specific range of Hg that fits the standard curves (5 to 30 ng or 100 to 300 ng Hg) and recorded to the nearest 0.01 mg. Analysis' quality assurance included using blanks (HCL 1 %), standard solutions (100 ng Hg ml⁻¹, Merck) and certified reference materials (CRMs) at the beginning and end of each batch: DORM-2, DOLT-3, NIES-13 (Table 2.4). THg recovery of CRMs ranged from 74 % to 118 %, averaging 99.3 ± 2.2 %. T-Hg concentration is expressed ng g⁻¹ dry weight (dw).

Table 2.4. CRMs and Hg Standard concentrations for the ensemble of THg analysis run in this work. THg Results are expressed as mean ± 1SD (standard deviation). Recovery % are given as Mean (MIN – MAX). DOLT-3 and DORM-2 certified materials were obtained from the National Research Council of Canada (CNRC), NIES-13 was obtained by the National Institute for Environmental Studies (NIES) of Japan.

CRM	Composition	Certified (ng g ⁻¹ dw)	<i>n</i>	Measured (ng g ⁻¹ dw)	Recovery %
DOLT-3	Tuna fish liver	3370 ± 140	12	3442 ± 198	102 (93 – 110)
DORM-2	Tuna fish muscle	4640 ± 260	28	4595 ± 398	99 (85 – 118)
NIES-13	Human hair	4420 ± 200	12	4379 ± 404	99 (74 – 108)
Hg Standard	100 ng Hg ml ⁻¹	100	36	97 ± 6	97 (74 – 107)

7.2. Carbon, nitrogen and sulphur stable isotopes analysis

This analysis was conducted at the laboratory of Oceanology (ULiège). Freeze-dried samples were weighed in tin capsules using a microbalance (accuracy 0.01 mg). In order to optimize the combustion of the sample approximatively the same mass of tungsten was added in each capsule. Stable isotope measurements were performed with an isotope ratio mass spectrometer (IsoPrime100, Isoprime, United Kingdom) coupled to an N-C-S elemental analyzer (Vario MICRO cube, Elementar, Germany)

for automated analyses. Isotope ratios were expressed using the δ notation (in parts per thousands, ‰), according to equation 1.3 (Chapter 1, §3).

As international standards used for correcting our isotope ratios were Vienna Pee Dee Belemnite (for carbon), Atmospheric Air (for nitrogen) and Vienna Canyon Diablo Troilite (for Sulphur) (Table 2.5). IAEA (International Atomic Energy Agency, Vienna, Austria) certified reference materials for sucrose (IAEA-C₆; $\delta^{13}\text{C} = -10.8 \pm 0.5\text{‰}$; mean \pm standard deviation), ammonium sulphate (IAEA-N₁; $\delta^{15}\text{N} = 0.4 \pm 0.2\text{‰}$; mean \pm standard deviation) and silver sulphide (IAEA-S₁; $\delta^{34}\text{S} = -0.3\text{‰}$) were used as primary analytical standards. Sulphanilic acid (Sigma-Aldrich; $\delta^{13}\text{C} = -25.6 \pm 0.4\text{‰}$; $\delta^{15}\text{N} = -0.13 \pm 0.4\text{‰}$; $\delta^{34}\text{S} = 5.9 \pm 0.5\text{‰}$; mean \pm standard deviation) was used as a secondary analytical standard. Standard deviations on multiple batch repeat measurements of secondary and internal laboratory standards analyzed interspersed with samples (one repeat of each standard every 12 analyses) were 0.2‰ for $\delta^{13}\text{C}$ and $\delta^{15}\text{N}$ and 0.4‰ for $\delta^{34}\text{S}$.

Table 2.5. Certified and measured $\delta^{13}\text{C}$, $\delta^{15}\text{N}$, $\delta^{34}\text{S}$ and C/N ratio of the primary and secondary standards analysed in this work. Values are shown as mean \pm 1SD (standard deviation). Such information is given separately for each batch analysed in Table A2.2.

	Reference values			C/N
	$\delta^{13}\text{C}$ (‰)	$\delta^{15}\text{N}$ (‰)	$\delta^{34}\text{S}$ (‰)	
IAEA-C₆- CH₁₂H₂₂O₁₁ (sucrose)	-10.80 \pm 0.5	–	–	–
IAEA-N₁- (NH₄)₂SO₄	–	0.40 \pm 0.2	–	–
IAEA-S₁- Ag₂S	–	–	-0.30	–
Sulphanilic Acid- C₆H₇NO₃S	-25.62 \pm 0.4	-0.13 \pm 0.5	5.87 \pm 0.50	5.14
	Measured values			
	$\delta^{13}\text{C}$ (‰)	$\delta^{15}\text{N}$ (‰)	$\delta^{34}\text{S}$ (‰)	C/N
IAEA-C₆- CH₁₂H₂₂O₁₁ (sucrose)	-10.8 \pm 0.1	–	–	–
IAEA-N₁- (NH₄)₂SO₄	–	0.4 \pm 0.1	–	–
IAEA-S₁- Ag₂S	–	–	-0.1 \pm 0.5	–
Sulphanilic Acid- C₆H₇NO₃S	-25.8 \pm 0.2	-0.5 \pm 0.4	5.9 \pm 0.6	5.0 \pm 0.1

7.3. Hg speciation

This analysis was performed in collaboration with the IPREM (Institut Pluridisciplinaire de Recherche sur l'Environnement et les Matériaux) of the University of Pau (UPPA) under the supervision of David Amouroux and Emmanuel Tessier. Hg extraction was done with two different methods (Table 2.6):

- For hair, where the presence of keratin might give a strong matrix effect on both the digestion and isotopic dilution processes, we conducted an acid digestion using nitric acid HNO₃-6N 50 % (307mL H₂OmQ + 196mL HNO₃ 65 %, INSTRA quality);

- For the other tissues we conducted an alkaline digestion by tetramethylammonium hydroxide TMAH 25 % ((CH₃)₄NOH in H₂O, Sigma Aldrich).

Between 0.005 and 0.5 g were digested in 5 mL of reagent. The amount of sample to digest was decided based on the previously measured THg concentrations. This allows to: (1) calculate the volume to apply for the digestive solutions (TMAH or HNO₃ 6N) and (2) optimize the extraction of Hg from the biological matrices. Solutions were left to rest overnight in digestion vials (CEM) at room temperature.

Microwave assisted extraction was performed using a CEM MW system (Discover SP-D, CEM Corporation) coupled to an autosampler Explorer 4872 96 (USA). The extraction was carried out in CEM Pyrex vessels as follows:

- 1 minute of warming up to 75°C,
- 4 minutes at constant temperature with magnetic agitation to homogenise the samples, and
- 2 minutes of cooling with pressurized air.

Temperature was controlled continuously during the entire process, to avoid exceeding the 80 to 85°C. If needed, extracts were centrifuged (3 minutes at 2000rpm) after digestion, to separate biological remains from the solutions. All samples were extracted in triplicates.

Prior to Hg species analyses, samples were derivatized at pH 4 by ethylating, using sodium tetraethyl borate (NaBEt₄, 5 %). This was done in order to volatilize ethylated forms of Hg and extract in isoctane by mechanical shaking using an orbital shaker during 20 minutes.

Hg species concentrations were quantified by species-specific isotopic dilution mass spectrometry analysis (SIDMS) as previously described (Renedo et al., 2017b). More specifically, each sample was spiked with known amounts of two isotope tracers (in this case ¹⁹⁹iHg and ²⁰¹MeHg), to quantify the natural isotopic abundance of the studied endogenous species (²⁰²iHg and ²⁰²MeHg) (Clémens et al., 2012). Quantification was then conducted with the single-IDA method, based on the measurement of the mixed isotope ratios (Clémens et al., 2012; Rodríguez-González et al., 2005). Single-IDA model consists on the specific measurement of Hg species separately (Table 2.6): only two isotopes are considered for the quantification of each Hg species ($R^{202/201}$ for MeHg and $R^{202/199}$ for iHg) (Renedo et al., 2017b). The values obtained from the used CRMS and the QA/QC overview of the analysis did not justify the use of IPD (Isotope Pattern Deconvolution). Spiking was conducted before digestion for hair tissue (acid digestion), while for muscle, liver and kidney it was done afterwards.

Table 2.6. Details of samples preparation for Hg speciation analysis with GC-ICPMS Trace Ultra GC. Volumes used during digestion, spiking and derivation are presented in italic light grey, between brackets as ng mL⁻¹. TMAH: tetramethylammonium hydroxide; NaBEt₄ = sodium tetraethyl borate; MMHg = monomethyl-Hg; iHg = inorganic Hg.

Sample origin	Sample content	Digestion	Isotopic spike	Time of spike	pH 4 derivation
Seals	Liver	Basic extraction <i>(4mL of TMAH)</i>	40µL ²⁰¹ MMHg (<i>1 ng mL⁻¹</i>) + 30 µL ¹⁹⁹ iHg (<i>25 ng mL⁻¹</i>)	After digestion	NaBEt ₄ , 5 % + 400 µL of isooctane
	Muscle	Basic extraction <i>(4mL of TMAH)</i>	25µL ²⁰¹ MMHg (<i>25 ng mL⁻¹</i>) + 40 µL ¹⁹⁹ iHg (<i>1 ng mL⁻¹</i>)	After digestion	NaBEt ₄ , 5 % + 400 µL of isooctane
	Kidney	Basic extraction <i>(4mL of TMAH)</i>	25µL ²⁰¹ MMHg (<i>25 ng mL⁻¹</i>) + 40 µL ¹⁹⁹ iHg (<i>1 ng mL⁻¹</i>)	After digestion	NaBEt ₄ , 5 % + 400 µL of isooctane
	Hair	Acid extraction <i>(5 mL of HNO₃ 6N)</i>	75 - 200µL Mixed spike* <i>(²⁰¹MMHg 50 ng mL⁻¹ + ¹⁹⁹Hg 12.5 ng mL⁻¹)</i>	Before digestion	NaBEt ₄ , 5 % + 300 - 400 µL of isooctane*
Herring	Muscle	Basic extraction <i>(4mL of TMAH)</i>	20µL ²⁰¹ MMHg (<i>25 ng mL⁻¹</i>) + 60 µL ¹⁹⁹ iHg (<i>1 ng mL⁻¹</i>)	After digestion	NaBEt ₄ , 5 % + 400 µL of isooctane
ERM464-1	Tuna fish Muscle	Acid extraction <i>(5 mL of HNO₃ 6N)</i>	40µL ²⁰¹ MMHg (<i>25 ng mL⁻¹</i>) + 25 µL ¹⁹⁹ iHg (<i>1 ng mL⁻¹</i>)	After digestion	NaBEt ₄ , 5 % + 500 µL of isooctane
DOLT-4	Dogfish Liver	Acid extraction <i>(5 mL of HNO₃ 6N)</i>	30µL ²⁰¹ MMHg (<i>25 ng mL⁻¹</i>) + 50 µL ¹⁹⁹ iHg (<i>1 ng mL⁻¹</i>)	After digestion	NaBEt ₄ , 5 % + 500 µL of isooctane
NIES-13	Human hair	Acid extraction <i>(5 mL of HNO₃ 6N)</i>	630µL Mixed spike <i>(²⁰¹MMHg 50 ng mL⁻¹ + ¹⁹⁹Hg 12.5 ng mL⁻¹)</i>	Before digestion	NaBEt ₄ , 5 % + 500 µL of isooctane
Blank TMAH	TMAH	Basic extraction <i>(4mL of TMAH)</i>	5 µL ¹⁹⁹ iHg (<i>1 ng mL⁻¹</i>)	After digestion	NaBEt ₄ , 5 % + 400 µL of isooctane
Blank HNO₃ 6N	HNO ₃ 6N	Acid extraction <i>(5 mL of HNO₃ 6N)</i>	5 µL ¹⁹⁹ iHg (<i>1 ng mL⁻¹</i>)	After digestion	NaBEt ₄ , 5 % + 400 µL of isooctane

* Based on THg concentrations measured with the DMA80 evo at ULiège.

Hg species analysis was carried out by GC-ICPMS Trace Ultra GC equipped with a Triplus RSH autosampler coupled to an ICP-MS XSeries II (Thermo Scientific, USA) as detailed in previous works (Renedo et al., 2017b).

The quality assurance protocol included the analysis of 3 replicates for each sample, the use of blanks (Table 2.7) and CRMs with the same proportion of MMHg and iHg as our samples: ERM-464-1 (tuna fish muscle, ERM®), DOLT-4 (dogfish liver, CNRC), and NIES-13 (Human hair, NIES). Quantification of iHg was strongly affected by the matrix of the samples. Thus, all concentrations were corrected to compensate extraction imperfection.

Table 2.7. Certified values for Hg species (MMHg and iHg) and THg levels and values obtained during analysis with GC-ICPMS Trace Ultra GC. Hg concentrations are shown as mean \pm standard deviation in ng g^{-1} dry weight (dw). Recovery percentages are shown as Min – Max range in %.

CRM	Hg species	N	Certified values (ng.g^{-1} dw)	Measured values (ng.g^{-1} dw)	Recovery %
DOLT-4	MMHg	5	1330 \pm 120	1250 \pm 20	95 – 98
	iHg	5	1250 \pm 110	1280 \pm 30	88 – 90
	THg	6	2580 \pm 220	2530 \pm 50	67 – 72
ERM-464-1	MMHg	6	5120 \pm 160	5000 \pm 30	93 – 94
	iHg	6	120 \pm 60	190 \pm 20	140 – 168
	THg	6	5240 \pm 100	5300 \pm 50	94 – 96
NIES-13	MMHg	9	3800 \pm 400	3790 \pm 110	99 – 101
	iHg	9	620 \pm 40	631 \pm 3	101
	THg	8	4420 \pm 200	4420 \pm 120	97 – 104

7.4. Mercury stable isotopes

Sample preparation and Hg stable isotopes analysis (SIA) were performed in collaboration with the IPREM institute of the University of Pau (UPPA), under the supervision of David Amouroux and Sylvain Bérail. A different amount of powder sample was prepared for each tissue, based on the THg concentrations measured with the DMA80: between 0.05 and 0.1 g of hair, 0.1 g of muscle and kidney, and between 0.005 and 0.05g of liver. Matrix digestion was conducted in blue-cap 50mL falcon vials adding 3 mL of HNO_3 (69 %, INSTRA quality) and 1 mL of HCl (37 %, INSTRA quality). Samples were left to digest at room temperature, overnight. They were subsequently transferred to Savillex Teflon vessels for the mineralization step in the Hot block (HB). A first round of mineralization was done at 85°C during 24 h. After cooling, 1 mL of H_2O_2 (30 %, ULTREX quality) was added to the vessels before operating a second HB mineralization for other 24 h.

Hg isotopic analyses were performed in a Nu Plasma HR MC-ICPMS (Nu Instruments, UK using a continuous flow Cold Vapor Generation (CVG) (Renedo et al., 2021). The dissolved Hg^{2+} was reduced

into Hg^0 by tin chloride (SnCl_2), separated from the rest of the matrix in a custom quartz Gas Liquid Separator (GLS) and then transported by a continuous flow of Ar to the plasma torch of the MC-ICP-MS. A Desolvation Nebulizer System (DNS, Nu Instrument, UK) and a double entry torch were used for the simultaneous introduction of a NIST-SRM-997 thallium (Tl) isotopic standard to internally correct for instrumental mass bias as presented elsewhere (Renedo, 2017). Tl is used because its fractionation in the instrument is quite similar to Hg and it is located in the same mass range of the analyte. The solution is introduced continuously and the $^{205}\text{Tl}/^{203}\text{Tl}$ ratio is monitored. Then the instrumental mass-bias is calculated using the exponential fractionation law, as previously described (Bérail et al., 2017; Renedo et al., 2017b).

External mass bias correction was done using NIST 3133 and UM-Almaden (now distributed as NIST 8610) as secondary standards (Bérail et al., 2017; Cransveld et al., 2017; Renedo et al., 2021). Recoveries of extraction were verified for all samples by checking the signal intensity obtained on the MC-ICPMS for diluted extracts relative to NIST 3133 standard (with an approximate uncertainty of $\pm 15\%$).

Internal reproducibility of the analytical method was performed on the medium and long-term through repetition of the measurement of CRMs (ERM-464-1, DOLT-5 and NIES-13), the IRM NIST 8610 and selected seal samples. The long-term precision (2SD) for Hg isotopic values was satisfactory for the most analyzed reference samples: UM-Almaden (0.14 ‰ and 0.08 ‰, $n=52$), ERM-464-1 (0.15 ‰ and 0.13 ‰, $n = 13$), DOLT-5 (0.13 ‰ and 0.15 ‰, $n = 8$) and NIES-13 (0.12 ‰ and 0.17 ‰, $n = 3$) for $\delta^{202}\text{Hg}$ and $\Delta^{199}\text{Hg}$ values, respectively.

Since there are no certified reference isotopic values for the used reference materials except for UM-Almaden (NIST-8160), the accuracy of the method was approximate and based on published data in previous studies as reference (Table 2.8).

We used a standard-sample bracketing system to calculate δ values (in per mil, ‰) relative to the reference standard NIST SRM 3133 mercury spectrometric solution. Isotope ^{198}Hg was used as the reference for ratio determination of all other Hg isotopes. MDF was calculated using equation 1.5, odd MIF using equation 1.6 and 1.8, even MIF using equation 1.7 and 1.79 (Chapter 1, [§3.2](#)).

Table 2.8. Hg isotopic compositions of certified reference materials as found in the literature and measured in this thesis. Presented isotope ratios for the UM-Almaden secondary standard are averages of analytical session averages from November 2018 through November 2020. Presented isotope ratios for procedural standards are represented as average \pm 2SD (standard deviation) from the entire analytical session. N is the number of processed standards. The certified value was available only for NIST-8610; with regards to the other RCMs, isotope ratios derive from previous literature.

CRMs	Content	Reference	N	$\delta^{204}\text{Hg}$	$\delta^{202}\text{Hg}$	$\delta^{201}\text{Hg}$	$\delta^{200}\text{Hg}$	$\delta^{199}\text{Hg}$	$\Delta^{204}\text{Hg}$	$\Delta^{201}\text{Hg}$	$\Delta^{200}\text{Hg}$	$\Delta^{199}\text{Hg}$
NIST-8610 (UM Almaden)	Cinnabar	Certified	140	-0.82 \pm 0.07	-0.56 \pm 0.03	-0.46 \pm 0.02	-0.27 \pm 0.01	-0.17 \pm 0.01	-	-0.04 \pm 0.01	0.00 \pm 0.01	-0.03 \pm 0.02
		Measured	52	-0.78 \pm 0.19	-0.52 \pm 0.14	-0.44 \pm 0.12	-0.26 \pm 0.10	-0.16 \pm 0.09	0.00 \pm 0.11	-0.05 \pm 0.07	0.01 \pm 0.05	-0.03 \pm 0.08
ERM-464-1*	Tuna fish muscle	(Li et al., 2014)	3	0.94 \pm 0.06	0.7 \pm 0.04	2.49 \pm 0.06	0.43 \pm 0.05	2.55 \pm 0.08	-0.10 \pm 0.05	1.96 \pm 0.06	0 \pm 0.04	2.38 \pm 0.07
		(Perrot et al., 2010)	3	0.72 \pm 0.05	0.55 \pm 0.03	1.96 \pm 0.11	0.33 \pm 0.02	2.02 \pm 0.13	-	1.54 \pm 0.10	0.05 \pm 0.10	1.88 \pm 0.13
		(Epov et al., 2008)	/	-	0.59 \pm 0.20	2.23 \pm 0.18	0.37 \pm 0.14	2.33 \pm 0.11	-	1.79 \pm 0.08	0.07 \pm 0.08	2.18 \pm 0.08
		(Sherman and Blum, 2013)	9	-	0.68 \pm 0.06	2.48 \pm 0.03	0.43 \pm 0.05	2.57 \pm 0.08	-	1.97 \pm 0.03	0.09 \pm 0.04	2.40 \pm 0.07
		Measured (July 2020)	4	0.68 \pm 0.16	0.55 \pm 0.12	1.92 \pm 0.19	0.33 \pm 0.09	1.99 \pm 0.24	-0.14 \pm 0.10	1.51 \pm 0.12	0.06 \pm 0.04	1.86 \pm 0.21
		Measured (March - Nov 2020)	9	1.02 \pm 0.40	0.71 \pm 0.15	2.44 \pm 0.18	0.43 \pm 0.11	2.49 \pm 0.15	-0.04 \pm 0.35	1.90 \pm 0.09	0.07 \pm 0.05	2.31 \pm 0.13
DOLT-5	Dogfish liver	(Li et al., 2020)	8	-	0.12 \pm 0.08	0.60 \pm 0.12	0.11 \pm 0.10	0.67 \pm 0.10	-	0.51 \pm 0.10	0.05 \pm 0.06	0.64 \pm 0.10
		Measured	5	-0.23 \pm 0.12	-0.11 \pm 0.14	0.40 \pm 0.16	-0.04 \pm 0.10	0.52 \pm 0.18	-0.06 \pm 0.11	0.49 \pm 0.07	0.02 \pm 0.07	0.55 \pm 0.16
NIES-13	Human Hair	(Yamakawa et al., 2016)	11	2.6 \pm 0.16	1.89 \pm 0.10	2.77 \pm 0.10	0.98 \pm 0.08	2.13 \pm 0.07	-0.04 \pm 0.11	1.36 \pm 0.07	0.04 \pm 0.04	1.65 \pm 0.06
		Measured	3	2.74 \pm 0.10	1.91 \pm 0.12	2.76 \pm 0.11	0.99 \pm 0.10	2.05 \pm 0.17	-0.12 \pm 0.08	1.32 \pm 0.06	0.03 \pm 0.07	1.57 \pm 0.17

* The isotopic composition of ERM464-1 resulted significantly different between the 2019 and 2020 sessions of analysis; therefore, it is reported separately. In July 2019 the CRMs was prepared using both the Hot Block (HB) and High-Pressure Asher (HPA) techniques and did not show and difference. In March 2020 and November 2020, the CRM was mineralized with HB. All samples presented the same isotopic values but differed from 2019 samples. Both 2019 and 2020 CRM-464 derived from the same bottle.

8. STATISTICS

This part encompasses the general outline of data analysis and statistical protocols used throughout the entire thesis. Details will be presented separately in the following chapters.

8.1. Lipids correction

Before beginning the statistical analysis, we corrected the $\delta^{13}\text{C}$ values. Most studies on marine predators cite the importance of lipid extraction when trying to interpret differences in $\delta^{13}\text{C}$ values among tissues (Pinzone et al., 2015; Ruiz-Cooley et al., 2011). Indeed, lipids are depleted in ^{13}C relative to protein and carbohydrates (DeNiro and Epstein, 1978; Tieszen et al., 1983). Thus, they have the potential to lower $\delta^{13}\text{C}$ values in tissues if not removed (Post et al., 2007). The concentration of lipids varies among tissues according to species, but also according to temporal changes in ecology (Newsome et al., 2010). Therefore, we applied the lipid normalization equation (McConnaughey and McRoy, 1979) adapted by Post et al. (2007) for aquatic animals:

$$\delta^{13}\text{C}_{\text{normalised}} = \delta^{13}\text{C}_{\text{untreated}} - 3.32 + 0.99 \left(\frac{\text{C}}{\text{N}}\right) \quad (2.3)$$

Where the numerical values represent respectively the line ($b = -3.32$) and the intercept ($\alpha = 0.99$) of the regression line equation, and C:N the explanatory variable. This normalization was conducted only on samples presenting a C:N ratio between 3 and 4 (Post et al., 2007).

8.2. Exploratory data analysis

The ROUT method was used to identify outliers, with a maximum False Discovery Rate (FDR) $Q = 0.1\%$, since it allows to simultaneously check for the presence of outliers for multiple variables with different units (Motulsky and Brown, 2006). The distribution and homoscedasticity of our data were tested with the Shapiro-Wilk test, the Skewness, the Kurtosis and the comparison between the value of the Average and the Median. The results were used to decide which tests (parametric or non-parametric) to apply for the analysis of the variance. Principal Component Analysis (PCA) and Redundancy Analysis (RDA) were used to check similarity and codependency between our seal species, ecological and environmental factors.

8.3. Calculation of SIBER niches

Following Jackson et al. (2011) we used the Stable Isotopes Bayesian Ellipses (SIBER) package (version 2.1.5) in R (version 4.0.5; R Core Team 2018) to explore variations in C, N, S and Hg stable

isotopes (Jackson et al., 2011). SIBER was used to generate bivariate standard ellipses as proxies of the trophic and habitat resources of a consumer (Layman et al., 2007; Layman and Allgeier, 2012; Newsome et al., 2007). The geometric representation of a niche in SIBER is the standard ellipse area (SEA). As default, it encompasses 40 % of studied individuals and represents a bivariate equivalent of standard deviation. As such, it contains only the “typical” members of a population without being influenced by outlier individuals in the considered space (Newsome et al., 2007). For this reason, it can be used as a proxy of the habitat and resources most commonly used by the population (Layman and Allgeier, 2012). Niche areas of each species were also estimated using Bayesian modelling (SEA_B). SEA_B involves the use of an iterative model based on Bayesian inference to estimate the covariance matrix from the data (Das et al., 2017; Pinzone et al., 2019; Ryan et al., 2014). SEA_B is more effective at taking into account both natural and analytical variability in the data and provides a distribution of solutions rather than a single value, providing error estimates as well as pairwise comparisons (Pinzone et al., 2019).

9. CONSTRAINS

Because of the global pandemic of SARS-CoV-2, part of Hg speciation analysis was strongly delayed. For this reason, in this thesis we present results about MMHg and iHg only for Chapter 4. MMHg concentrations for Chapter 5 and 6 will be integrated later for publication in scientific journals.

Our initial goal was to study the influence of nursing period on Hg accumulation in Arctic marine mammals together with tissue metabolism, ecology and environmental changes. In order to properly interpret Hg remobilization within adult seals and transfer to newborns, data of MMHg concentrations were necessary. Because we could not get MMHg concentrations in time, we decided to exclude this chapter from the manuscript.

Because of time and budget constraints, Hg stable isotopes analysis was conducted on a subset of samples selected after the analysis of THg concentrations and C, N and S stable isotope ratios. Among those samples, 2 samples of harp seal newborns (ID: H6a-18 and H5a-18) and 1 hooded seal (ID: 5-2008) resulted in THg concentrations < than 130 ng g⁻¹ dw. This concentration consisted in the limit of detection for the Hg stable isotopes analysis with CVG-MC-ICPMS. Thus, no isotopic value could be quantified for these samples.

For the temporal study (Chapter 6), we selected samples which would represent the entire range of THg concentrations. We selected five individuals per year presenting the lowest THg value, the 25 % and 75 % THg quartiles, the median and the maximum THg value.

Chapter 3

Carbon, Nitrogen and Sulphur isotopic fractionation in captive subadult hooded seal *Cystophora cristata*: application for diet analysis

After : Pinzone M., Aquarone M., Huyghebaert L., Sturaro N., Michel L.N., Siebert U., Das K.
In Rapid Commun Mass Spectrom, 2017; 31:1720-1728. <https://doi.org/10.1002/rcm.7955>

ABSTRACT

Rationale: Intrinsic biogeochemical markers, such as stable isotope ratios of carbon, nitrogen and sulphur are increasingly used to trace trophic ecology of marine predators. However, insufficient knowledge of fractionation processes in tissues continues to hamper the use of these markers.

Main question: Which mechanisms affect C, N and S isotopic incorporation in a specialized Arctic true seal species?

Methods: We performed a controlled feeding experiment with 8 subadult hooded seals *Cystophora cristata* that were held on a herring-based diet *Clupea harengus* for 2 years. Stable isotope ratios were measured via isotope ratio mass spectrometry in 3 of their tissues and related to values of these markers in their diet.

Results: Diet-tissue isotope enrichment (trophic enrichment factor, TEF) values between dietary herring and seal tissues for C ($\delta^{13}\text{C}$ -TEF) were + 0.7 ‰ for red blood cells, + 1.9 ‰ for hair and + 1.1 ‰ for muscle. The TEFs for N ($\delta^{15}\text{N}$ -TEF) were + 3.3 ‰ for red blood cells, + 3.6 ‰ for hair and + 4.3 ‰ for muscle. For S, $\delta^{34}\text{S}$ -TEFs were +1.1 ‰ for red blood cells, + 1.0 ‰ for hair and + 0.9 ‰ for muscle.

Conclusions: These values were greater than those previously measured in adult seals. The cause of this enrichment may be related to the higher rate of protein synthesis and catabolism in growing animals. This study is the first report on S isotope enrichment values for a marine mammal species.

Keywords: isotope fractionation, hooded seal, discrimination model, growth.

1. INTRODUCTION

The analysis of C, N and S stable isotopes is routinely used to study marine mammal trophic ecology (Newsome et al., 2010). However, several studies have stressed the need for implementing modern isotopic knowledge with baseline information of elements processing in the organisms (Martínez Del Rio et al., 2009; Ramos and Gonzalez-Solis, 2012; Wolf et al., 2009b). This might be especially important in species with complex physiological adaptations, like Arctic marine mammals.

The hooded seal *Cystophora cristata* is one of the most physiologically specialized *Phocidae*, hunting and breeding in the cold Arctic and subarctic waters (Kovacs, 2016). In the last decade, a strong decrease in population numbers in combination with higher rates of subadults stranding out of the normal distribution range was observed (Bellido et al., 2009). Several studies have proposed that such phenomena may be caused by climate change (Friedlaender et al., 2006; Øigård et al., 2014; Stirling et al., 2008). The reason why this seems to affect hooded seals more than other species it is not clear yet. Only fragmented information about the physiology and ecology of this species are available in the literature.

Quantifying the extent of isotope fractionation (IF) observed between the different tissues of a consumer and its prey can allow to study C, N and S metabolization within an organism. IF results from the numerous metabolic processes linked with prey digestion and assimilation (Adams and Sterner, 2000). Such processes are commonly represented by the calculation of the trophic enrichment factor (TEF), which depicts the net isotopic difference between a consumer and its food source (Caut et al., 2009). In the literature, TEFs are commonly referred to as big delta “ Δ ” (Caut et al., 2009). However, the same term is used in this thesis to indicate the mass-independent fractionation (MIF) of Hg stable isotopes (Chapter 1, §3.2). In order to avoid confusion, we will refer to the TEF values of C, N and S as $\delta^{13}\text{C}$ -TEF, $\delta^{15}\text{N}$ -TEF and $\delta^{34}\text{S}$ -TEF, respectively.

Diet-tissue trophic enrichment factors can be estimated through controlled experiments in which organisms are fed a constant diet of known isotopic composition (Roth and Hobson, 1996). Since the turnover of stable isotopes within tissues varies accordingly to metabolic rates, measurement of such values in several tissues from the same individual can provide short, intermediate and long-term dietary information (Hobson et al., 1996). Tissues that are metabolically active (e.g. muscle, blood, kidney) can integrate a period of days to months; while hairs, skin, vibrissae, nails, which are considered as inert, reflect the diet and behavior during a year or even the entire life of the individual (Wolf et al., 2009a). Assessing differences and relationships among tissues allows the alternative use of non-destructive sampling of endangered species (Fossi and Marsili, 1997; Jaspers et al., 2007; Weijs et al., 2011).

The way in which stable isotopes fractionate between diet and the various tissues still remain poorly understood (Caut et al., 2009; Hobson et al., 1996; Lesage et al., 2002b). This greatly affects the correct use of recently-developed approaches such as the application of isotopic mixing models (e.g.

SIAR, MixSIAR), which strongly depend on TEF information. Several studies have shown how a moderate variation in fractionation estimates can lead to important differences in model outputs and, therefore, misleading conclusions (Bond and Diamond, 2011). This becomes especially important when TEF average values are used, or when there is not a good isotopic separation between the sources used for the model (Phillips et al., 2014).

The main objective of this study was to estimate C, N and, for the first time in marine mammals S-IF, in growing individuals of hooded seal *Cystophora cristata* (Erleben, 1777) kept in human care for 2 years under a diet exclusively based on herring *Clupea harengus* (Linnaeus, 1758).

Conversely to previous captive feeding reported in the literature, our animals were completely healthy individuals, which **avoided eventual effects of body condition** on IF results. Moreover, the 2-years-long experiment allowed to reach a complete diet-to-tissue equilibrium, **eliminating the influence of diet or distribution shifts** normally occurring in the wild. As such, we obtained **basal metabolic fractionation rates of growing hooded seals**, which may lead to a better interpretation of future ecological studies.

We also **compared our results with** the fractionation factors resulting from the application of two **models developed by Caut et al., 2009 and Healy et al., 2017** with the aim of assessing their use in marine mammal ecology.

2. MATERIALS AND METHODS

2.1. Sampling and captivity

In March 2012, 8 pups of hooded seals (4 females and 4 males) were caught using hoop nets on the pack-ice of the Greenland Sea (permit n.12/1352). The captivity experiment was conducted at the Department of Arctic and Marine Biology (DAMB), The Arctic University of Tromsø (UiT) and lasted in total 22 months (until February 2014) (Norwegian Animal Research Authority, approval #089).

Seals were fed on a constant diet of Norwegian Spring Spawning herring *Clupea harengus* supplemented with a vitamin complex. All fish used for the experiment belonged to the same length range (25 to 30 cm). The indoor light regime simulated that of outdoor natural light-darkness cycles at 70°N latitude. Seals were maintained in two indoor 40,000L (1.5 m deep) seawater pools with a wooden ledge along one side on which the animals could haul out at will. After 2 years, seals were euthanized and different organs were collected for analysis (Table 3.1). Two seals (K5 and K6) were euthanized after 1 year (March 2013) for other physiological studies at the UiT; and only blood was available for our analysis. After 3-4 hours (minimum) from blood collection the vials including the “Clot activator agent” (BD Vacutainer® red top serum) were passed in the centrifuge for 15 minutes at 3000 rounds/min to separate the Red Blood Cells (RBCs). Once the phases were completely separated RBCs were conserved at :20°C in the BD Vacutainer® vial. After death, the age of each seal was estimated using the two equations developed especially for hooded seals by Wiig (Wiig, 1985) (equation 2.1 and 2.2, Chapter 2 §5.2).

Table 3.1. List of the 8 hooded seals *C. cristata* sampled in the Greenland Sea in March 2012 and included in the captivity experiment, with all biometric information and the tissues on which the analysis was conducted. Standard length is expressed in cm, weight in kg. RBCs: Red Blood Cells.

Seal Id code	Sex	Weight	Standard Length	Tissues sampling day	Sampled Tissue		
					Muscle	Hair	RBCs
K1-12	F	77	144	14.02.14	✓	✓	✓
K2-12	F	103	NA ^a	28.02.14	✓	✓	✓
K3-12	F	88	138	27.02.14	✓	✓	✓
K4-12	M	81.5	144	19.02.14	✓	✓	✓
K5-12	M	85	148	02.12.13 ^b			✓
K6-12	F	93	148	04.12.13 ^b			✓
K7-12	M	75	NA ^a	21.02.14	✓		✓
K8-12	M	86	NA ^a	26.02.14	✓		✓

^a NA = Not available

^b Euthanized before in the framework of physiological studies at UiT.

2.2. Samples preparation

Between 6 and 10 g of thawed tissue were dissected using a ceramic knife (or scissors), placed in plastic tubes and accurately weighted to the nearest 0.1 mg. Tubes were then placed at -80°C. Samples of hair were washed ultrasonically three times (10 minutes each): a first and third time with MilliQ water (18.2MΩ-cm), a second with reagent grade acetone (acetone for trace analysis ≥ 99.8 % purity, ARISTAR®, VWR) to remove exogenous contaminants, blood and fat residuals, according to the method recommended by the International Atomic Energy Agency (Katz and Chatt, 1988). All tissues were freeze-dried for 24h (Alpha 1-4 LD plus, Christ, Germany). Samples were finally ground to a fine powder using a ceramic mortar and pestle, while hairs were cut with ceramic scissors in the smallest size possible.

2.3. Stable isotope analysis

Stable isotope ratios of N, C and S were measured in muscle, hair and RBCs of captive hooded seals, as well as muscle of herring, were measured using an isotope ratio mass spectrometer (IsoPrime100, IsoPrime, Cheadle, UK) coupled in continuous flow to an elemental analyzer (Vario MICRO cube, Elementar Analysensysteme GmbH, Hanau, Germany). Isotopic ratios were conventionally expressed in delta (δ) notation in ‰ (Coplen, 2011), according to equation 1.3 (Chapter 1, §3). Isotopic ratios were estimated relative to international standards as previously explained (Chapter 2, §7.2). Lipids extraction in herring muscle was not possible due to the small quantity of tissue material available for the analysis. Because of the large C/N variability found in these organisms we mathematically corrected for the C signature with the lipid normalization equation 2.4 (Chapter 2, §8.1).

2.4. Isotope fractionation calculation

The TEFs of N, C and S were calculated using the following equation:

$$\delta^nX\text{-TEF} = \delta^nX_p - \bar{\delta}^nX_f \quad (3.1)$$

Where δ^nX is the isotopic ratio of a particular element for a predator p , $\bar{\delta}$ is the average of stable isotope ratios X of all food items f used during captivity.

The TEFs measured on our captive hooded seals were compared with those resulting from the application of the regression models of Caut et al. (2009) and the Bayesian models of Healy et al. (2017) in order to check for their validity for species for which no measurement is available (Figure 3.2). Following Caut et al. we calculated $\delta^{13}\text{C}$ - and $\delta^{15}\text{N}$ -TEFs for muscle, air and red blood cells

through the application of their regression equations, which either considered all tissues together ($\delta^{13}\text{C-TEF} = -0.417\delta^{13}\text{C} - 7.878$ and $\delta^{15}\text{N-TEF} = -0.141\delta^{15}\text{N} + 3.975$) or each tissue separately ($\delta^{13}\text{C-TEF}_{\text{hair}} = -0.474\delta^{13}\text{C} - 9.064$, $\delta^{13}\text{C-TEF}_{\text{muscle}} = -0.366\delta^{13}\text{C} - 7.030$, $\delta^{13}\text{C-TEF}_{\text{RBC}} = 1.16 \pm 0.19\text{‰}$; $\delta^{15}\text{N-TEF}_{\text{muscle}} = -0.214\delta^{15}\text{N} + 3.938$, $\delta^{15}\text{N-TEF}_{\text{hair}} = 2.59 \pm 0.41\text{‰}$ and $\delta^{15}\text{N-TEF}_{\text{RBC}} = 2.06 \pm 0.23\text{‰}$) (Caut et al., 2009). The Bayesian model was instead used to calculate all TEFs for the different tissues using the newly developed DEsIR (Stable Isotope Discrimination Estimation In R) package (now renamed as SIDER) in the R v3.4.0 statistical environment (R Core Team, 2016) (Lazic, 2016). For the application of the Healy *et al.* method, several parameters needed to be specified as input information- such as *Cystophora cristata* habitat (“marine”), taxonomic class (“mammalia”), tissue (“blood”, “hair” or “muscle”) and diet type (“carnivore”) (Healy et al., 2017). Since no specific values for red blood cells were available in the literature, we used TEFs measured on whole blood to run the model.

2.5. Statistical analyses

The Shapiro-Wilk test was used to check for normality, while the Levene’s test was used to assess homogeneity of all sets of data. A one-way analysis of variance (ANOVA) followed by Dunnett’s pairwise multiple comparisons test ($p < 0.05$) was conducted to examine the variability of IF between the 3 tissues of hooded seals. Parametric Student t-tests ($p < 0.05$) were performed to compare delta values between each seal tissue and the muscle of herring. All statistical analyses were performed using GraphPad Prism version 6 for Mac (GraphPad Software, La Jolla CA, USA).

3. RESULTS

3.1. Biometric analysis

At the time of death, the 8 captive seals (4 males and 4 females) weighted 75 to 103kg, with lengths ranging from 138 to 148cm (Table 3.1). We applied the equation proposed by Wiig (Wiig, 1985) for hooded seals specifically, to estimate the age of all subadults except K2, K7 and K8, whose measurement of standard length was not available. These animals were estimated to be 19 to 22 months old.

3.2. Stable isotope ratios

No difference was found in all the considered parameters between the two seals euthanized in 2013 and those sacrificed in 2014 ($p > 0.05$); therefore, the 8 animals will be considered in our analysis as the same group. The stable isotope ratios of C, N and S and the C/N ratio of each tissue of hooded seals are presented in Table 3.2, together with the results of the ANOVA. Lipid-normalized $\delta^{13}\text{C}$ values of herring ($n = 15$) used to feed the seals during the experiment were -20.5 ± 1.2 ‰, the $\delta^{15}\text{N}$ values were 9.5 ± 0.5 ‰, and the $\delta^{34}\text{S}$ values were 17.2 ± 0.5 ‰. Their C/N ratios ranged from 5.2 to 11 (mean \pm SD = 7.0 ± 1.6). In captive seals the $\delta^{13}\text{C}$ values significantly differed among all tissues with hair being the most ^{13}C -enriched tissue, followed by muscle and RBCs. Muscle showed the highest $\delta^{15}\text{N}$ values, while hair and RBCs presented similar ranges. No difference was observed for $\delta^{34}\text{S}$ values among all three tissues.

Table 3.2. Carbon, nitrogen and sulphur isotope ratios and C/N ratios of muscle, hair and red blood cells (RBCs) of captive hooded seals. Stable isotope ratios are represented in δ notation (‰) as Mean \pm SD (Min – Max). n represents the number of samples in which the analysis was conducted for each tissue.

Values	Tissues			Inter-tissue ANOVA*
	Muscle	Hair	RBCs	
<i>n</i>	6	4	8	–
$\delta^{13}\text{C}$ value	-19.4 ± 0.1 (-19.5 to -19.1)	-18.7 ± 0.1 (-18.8 to -18.6)	-19.6 ± 0.1 (-19.7 to -19.5)	F = 182, p < 0.0001, df = 15
$\delta^{15}\text{N}$ value	13.8 ± 0.3 (13.4 – 14.5)	13.1 ± 0.2 (12.9 – 13.3)	12.8 ± 0.1 (12.5 – 13.0)	F = 26.15, p < 0.0001, df = 15
$\delta^{34}\text{S}$ value	18.2 ± 0.8 (17.1 – 19.3)	17.5 ± 0.1 (17.4 – 17.6)	18.0 ± 0.8 (16.7 – 19.4)	F = 0.818, p = 0.458, df = 15
C/N ratio	$3.2(3.3) \pm 0.05$ (3.3 – 3.4)	$3.1(3.1) \pm 0.04$ (3.0 – 3.1)	$3.3(3.2) \pm 0.01$ (3.3 – 3.3)	F = 106, p < 0.0001, df = 15

* Bold values represent a significant difference

A significant difference between captive seals and herring was found in hair $\delta^{13}\text{C}$ values ($p = 0.006$, $t = 3.042$, $df = 17$). For muscle, such difference was weaker ($p = 0.033$, $t = 2.300$, $df = 19$), while it did not exist for RBCs ($p = 0.067$, $t = 1.932$, $df = 21$). With regard to $\delta^{15}\text{N}$ values, a significant difference between seals and herring was found for all muscle ($p < 0.0001$, $t = 19.94$, $df = 19$), hair ($p < 0.0001$, $t = 14.14$, $df = 17$) and RBCs ($p < 0.0001$, $t = 18.97$, $df = 21$).

The C/N ratio varied very little within tissues, with hair presenting a significantly lower mean (3.0 to 3.1, $p < 0.0001$) than RBCs (3.3 to 3.3) and muscle (3.3 to 3.4). The seals-herring comparison of $\delta^{34}\text{S}$ values showed a significant difference in muscle ($p = 0.007$, $t = 3.043$, $df = 19$) and RBCs ($p = 0.008$, $t = 2.906$, $df = 21$) but not in hair ($p = 0.175$, $t = 1.416$, $df = 17$).

3.3. Experimentally-estimated TEFs

$\delta^{13}\text{C}$ -TEF (Figure 3.1) significantly varied among all tissues (ANOVA, $p < 0.0001$, $F = 184.5$) with hair showing the largest fractionation ($\delta^{13}\text{C}$ -TEF = 1.9 ± 0.1 ‰), followed by muscle ($\delta^{13}\text{C}$ -TEF = 1.1 ± 0.1 ‰) and RBCs ($\delta^{13}\text{C}$ -TEF = 0.8 ± 0.1 ‰) (Figure 1). $\delta^{15}\text{N}$ -TEF differed between muscle ($\delta^{15}\text{N}$ -TEF = 4.3 ± 0.4 ‰), which showed the largest fractionation, and the other two tissues ($\delta^{15}\text{N}$ -TEF of hair = 3.6 ± 0.3 ‰; $\delta^{15}\text{N}$ -TEF of RBCs = 3.3 ± 0.1 ‰) (ANOVA, $p < 0.00001$, $F = 26.15$). Hair and RBCs showed a less pronounced difference ($p = 0.049$). The $\delta^{34}\text{S}$ -TEF of muscle was 0.9 ± 0.8 ‰, the $\delta^{34}\text{S}$ -TEF of hair 0.4 ± 0.1 ‰ and the $\delta^{34}\text{S}$ -TEF of RBCs 1.0 ± 0.8 ‰. No difference was observed among any tissues for $\delta^{34}\text{S}$ -TEF (ANOVA, $p = 0.208$, $F = 1.766$).

3.4. Comparison with model-estimated TEFs

High variation was obtained between the TEFs measured in captive hooded seals and those resulting from the application of models (Figure 3.2). For muscle our $\delta^{15}\text{N}$ -TEFs resulted in the largest values, followed by the TEFs calculated by the Bayesian method of Healy et al. ($\delta^{15}\text{N}$ -TEF = 4.0 ± 1.1 ‰), the Caut et al. all-tissue regressions ($\delta^{15}\text{N}$ -TEF = 2.0 ± 0.1 ‰) and the Caut et al. tissue-specific regressions ($\delta^{15}\text{N}$ -TEF = 0.8 ± 0.1 ‰). For hair, our $\delta^{15}\text{N}$ -TEFs were the largest, followed by the TEFs of Healy et al. ($\delta^{15}\text{N}$ -TEF = 3.1 ± 0.0 ‰), the Caut et al. tissue-specific regressions ($\delta^{15}\text{N}$ -TEF = 2.6 ± 0.3 ‰) and the Caut et al. all-tissue regressions ($\delta^{15}\text{N}$ -TEF = 2.0 ± 0.02 ‰). For RBCs, the Healy et al. $\delta^{15}\text{N}$ -TEFs were the largest ($\delta^{15}\text{N}$ -TEF_{RBC} = 4.1 ± 1.0 ‰), followed by our measured values, the Caut et al. all-tissue regressions ($\delta^{15}\text{N}$ -TEF = 2.2 ± 0.02 ‰) and finally the Caut et al. tissue-specific regressions ($\delta^{15}\text{N}$ -TEF = 2.1 ± 0.1 ‰).

For muscle the $\delta^{13}\text{C}$ -TEFs calculated by the model of Healy et al. were the largest ($\delta^{13}\text{C}$ -TEF = 1.5 ± 1.4 ‰), followed by our measured values, the Caut et al. all-tissue model ($\delta^{13}\text{C}$ -TEF = 0.1 ± 0.04 ‰) and the Caut et al. tissue-specific model ($\delta^{13}\text{C}$ -TEF = -0.05 ± 0.04 ‰). For hair the $\delta^{13}\text{C}$ -TEFs calculated by the model of Healy et al. were the largest ($\delta^{13}\text{C}$ -TEF = 3.1 ± 0.0 ‰), followed by our measured values, the Caut et al. all-tissue model ($\delta^{13}\text{C}$ -TEF = -0.1 ± 0.04 ‰) and the Caut et al. tissue-specific model ($\delta^{13}\text{C}$ -TEF = -0.2 ± 0.04 ‰). Finally, the $\delta^{13}\text{C}$ -TEFs in RBCs were the largest in the Healy et al. model ($\delta^{13}\text{C}$ -TEF = 1.4 ± 1.3 ‰), followed by the Caut et al. tissue-specific model ($\delta^{13}\text{C}$ -TEF = 1.2 ± 0.2 ‰), our measurements and the Caut et al. all-tissue model ($\delta^{13}\text{C}$ -TEF = 0.3 ± 0.03 ‰).

Overall, the Bayesian model developed by Healy et al. (2017) resulted in TEFs included in the same range as the experimentally-calculated ones, while the equations of Caut et al. (2009) gave more different values, which in some cases also gave negative estimates.

4. DISCUSSION

4.1. Comparison with the literature

Prey-predator isotope fractionation occurs during the several biochemical pathways that a particular food item undergoes during digestion and assimilation by a predator (Bearhop et al., 2002). Within an organism N-IF occurs primarily during processes of **deamination and transamination of amino acids** from the assimilated food, for the synthesis of new body proteins (Germain et al., 2013; Hobson and Clark, 1992). During such processes, different nitrogenous waste products (e.g. NH_4^+) are formed and excreted as urea, uric acid or ammonia, causing consumer-diet ^{15}N enrichment (Hobson and Clark, 1992). This is in accordance with the significant difference found in $\delta^{15}\text{N}$ values between our hooded seals and their given diet. When comparing our results with the literature, the $\delta^{15}\text{N}$ -TEF in our hooded seals was larger than that of other seal species or animals (Germain et al., 2012). Taking RBCs as an example, the $\delta^{15}\text{N}$ -TEF found in previous captivity experiments ranged from 1.5 – 2.2‰ for captive harp and harbor seals to 2.5‰ in foxes, while our values are higher than 3.0‰ (Roth and Hobson, 2000, 1996).

The main process determining C-IF is respiration during which ^{12}C is lost as $^{12}\text{CO}_2$ through **oxidation of acetyl groups derived from the catabolism of lipids, proteins, and carbohydrates** (Hobson and Clark, 1992). Our $\delta^{13}\text{C}$ -TEF values of RBCs and muscle are comparable with those measured in other species of phocids (Beltran et al., 2016; Germain et al., 2012; Hobson et al., 1996; Kurle, 2002; Lesage et al., 2002b) or other terrestrial mammals (McCutchan et al., 2003; Roth and Hobson, 2000). However, hooded seal hair was significantly enriched in ^{13}C with respect to diet; in contrast to previous studies that manifest a generally less pronounced fractionation (Kelly, 2000). Very little is known on S metabolic pathways within the organisms. To our knowledge this is the first study to assess S fractionation values in animals with complex physiology such as *Phocidae*. The main **sources of S to a consumer are the organic S (contained in amino acids from the diet) and the inorganic S from the environment** (McCutchan et al., 2003). As for C, little or no fractionation is commonly associated with S assimilation into animals tissues and this is confirmed by the absence of significant increase in ^{34}S between hooded seal hair and herring (Hesslein et al., 1993). Nevertheless, we found a significant enrichment in ^{34}S in muscle and RBCs compared with diet, which is in the same range of S fractionation measured in muscle of various aquatic vertebrates (1.9 ± 1.4 ‰) (McCutchan et al., 2003).

Several factors may influence organisms' IF, such as what **taxonomic group** they belong to (Vanderklift and Ponsard, 2003; Zanden and Rasmussen, 2001). The higher fractionation of ^{15}N in our hooded seals with respect to terrestrial animals, as for example the red foxes analyzed by Roth and Hobson (Roth and Hobson, 2000), may be due to the particular physiological adaptations linked

with the diving behavior of marine mammals (Hobson et al., 1996). Indeed, seals' blood is far more enriched in hemoglobin and hematocrit than that of other non-diving homeotherms. It is possible that such differences in blood composition influence IF values (Hobson et al., 1996).

However, a difference in N fractionation is observed not only between our seals and other organisms, but also when comparing our results with values measured in other phocids (Beltran et al., 2016). One possibility is that the higher $\delta^{15}\text{N}$ -TEF values shown by hooded seals is a consequence of the **difference between diets** (Roth and Hobson, 2000). Indeed while our captive seals were fed with a mainly-protein-based diet (enriched in ^{13}C by about 4 ‰ over carbohydrates and by 6 ‰ over lipids), Beltran et al. (2016) used another nutrition strategy, consisting in a mix of commercial pellets, herring and capelin that possibly include higher proportions of carbohydrates (Beltran et al., 2016). Such variation may also be determining the seal-herring S enrichment observed in our study, since McCutchan et al. (2003) demonstrated that a diet high in proteins can increase the S fractionation rate of consumers with respect to diet.

Isotopic routing is considered as the dependency of consumers' isotopic composition on dietary proteins, carbohydrates and lipids (Ambrose and Norr, 1993). This process determines a particular isotope incorporation during the formation of a tissue, based on the isotopic nature of the nutrients assimilated through the diet (Kelly et al., 2010; Wolf et al., 2009a). Even if the precise mechanisms are still poorly known, a few studies demonstrated that **age** can influence N and, to a lesser degree, C routing during assimilation in consumers' tissues (Trueman et al., 2005). Young marine mammals such as seals undergo important physiological modifications regarding routing and rates of utilization of elements (Arnould et al., 2003; Kovacs and Lavigne, 1986). The incorporation of the isotope composition of the diet in growing predators depends more on the addition of new material to the tissue than on the replacement of materials exported from the tissue (Martínez del Rio and Carleton, 2012). This means that almost the totality of protein C and N assimilated by a young growing predator in the muscle derives from its prey (Kelly et al., 2010; Wolf et al., 2009a). Several studies have shown how growing birds and fish have higher rates of protein synthesis and catabolism that cause faster isotopic turnover and magnify the trophic effect, causing an even greater loss of the isotopically light N in urine (Alonso et al., 1991; Wolf et al., 2009a). These mechanisms could probably explain the greater $\delta^{15}\text{N}$ -TEF of our subadult hooded seals.

Independently of diet, the variability of N stable isotope composition between hooded seals and the other seals may be directly associated with the **health status** of these animals. In the case of a particular disease, a metabolic shift occurs toward utilizing more N for protein synthesis rather than urea production; as a consequence IF processes are directly affected (Reitsema, 2013). In humans for example, liver $\delta^{15}\text{N}$ values of cirrhotic patients result in a ^{15}N depletion of 3.2 ‰ with respect to healthy persons, without significant differences in $\delta^{13}\text{C}$ values (Petzke et al., 2006). While we conducted our captivity experiment on healthy captured seals, Hobson et al. (1996), Germain et al.

(2012 and 2013) and Beltran et al. (2016) measured their fractionation on subadult seals and sea lions in rehabilitation, and therefore with a poorer health status.

4.2. Comparison between tissues

For $\delta^{13}\text{C}$ -TEF, hair exhibited the greatest fractionation, followed by muscle and RBCs (Figure 3.1). In contrast, $\delta^{15}\text{N}$ -TEF was much higher in muscle than RBCs or hair. Finally, no differences were found in $\delta^{34}\text{S}$ -TEF between tissues. The **turnover rate of a tissue** influences elements incorporation rates and consequently IF processes. Indeed, Hobson and Clark (1992) found that the C turnover rate correlated linearly with the metabolic rate of tissues. For example, they found that in quails and American crows the half-life of C ranged from 2.6 days in liver, and 20 days in muscle, to circa 50 days in hair. Moreover, Pearson et al. (2003) showed that in warblers, the N half-life ranged from 0.5 to 1.7 days for plasma and from 7.5 to 28 days for whole blood. The higher tissue activity leads to quicker C or N incorporation with less metabolic changes of these elements, and results in a smaller IF (Pearson et al., 2003). Therefore, the higher $\delta^{13}\text{C}$ -TEF of hooded seal hair compared to muscle and RBCs may be a direct consequence of tissue turnover rates (Hobson and Clark, 1992; Pearson et al., 2003).

In addition, the **quantity of a certain element** determines the effects of fractionation processes. The higher the abundance of a specific compound available for biosynthesis the smaller the fractionation of its isotopic composition (Adams and Sterner, 2000; Robbins et al., 2005). When comparing the C/N ratios of our three tissues muscle and RBCs were very similar to each other, while hair presented much lower C/N value. The C/N ratios represent the quantity of C-containing molecules with respect to N in one sample (Cherel et al., 2005). Therefore, the lower C/N value results from the fact that hair is mostly composed by keratin, while blood and muscle present several C sources. The presence of a single C source forces the multiple usage of the same C pool by the hair tissue during its catabolism, leading to larger fractionation processes.

The pattern of variation for $\delta^{13}\text{C}$ -TEF seen in across tissues was not observed for $\delta^{15}\text{N}$ -TEF, with larger fractionation for N observed in muscle tissue than in hair. One possible explanation may be linked to the fact that the **different metabolic components** (e.g. lipids, proteins, carbohydrates, etc.) of cells, and at larger scale of tissues, do not have the same isotopic composition as a consequence of their varied histories (Hayes, 2001). For example, the C used for the production of fatty acids via the Acetyl-CoA route (oxidation of pyruvate to acetyl coenzyme A) is ^{13}C -depleted with respect to glucose; and this phenomenon explains the well-known ^{13}C depletion of lipids (Hayes, 2001). In addition, amino acids present a large variability in both their ^{13}C and ^{15}N isotopic signature, as shown in the collagen of pigs (Hare et al., 1991; Howland et al., 2003). Therefore, the selection of one specific

C, N or S “pool” for the metabolic renewal of a tissue will influence isotope incorporation rates, fractionation processes and ultimately tissues isotopic composition (Bearhop et al., 2002).

The **number of metabolic steps** that an element undergoes in a tissue may also determine variation of IF. The more elevated rates of protein metabolism for energy expenditure in muscle may determine a significant larger discrimination in this tissue. In captive hooded seals this is shown by the larger prey-predator ¹⁵N enrichment found in muscle with respect to RBCs or hair (Atherton and Smith, 2012). The same process can explain the fact that, even if no statistical difference is observed in S fractionation among hooded seal tissues, ³⁴S presented greater consumer-tissue enrichment in RBCs and muscle, than in hair. S is present in the mammalian body in four main **S-containing amino acids: methionine, cysteine, homocysteine, and taurine**. Only the first two are incorporated in proteins (Brosnan and Brosnan, 2006). Cysteine can be synthesized by the body starting from methionine, which is an essential amino acid assimilated through diet (Parcell and Cand, 2002). These two amino acids are integrated in numerous protein compounds in the different tissues based on metabolic requirements (Parcell and Cand, 2002).

In hair, for example, both cysteine and methionine are part of the filamentary complex of keratin (Bragulla and Homberger, 2009). Once incorporated into keratin they are no longer available for other metabolic processes (Bragulla and Homberger, 2009). This could result in the very low consumer-diet S fractionation in hooded seal hair. In RBCs and muscle, such amino acids are subjected to several changes during the formation of a vast set of proteins (vitamins, glutathione, etc.). Such proteins may play an important role, for example in the case of seals, in antioxidant response during diving hypoxia, and therefore result in larger fractionation rates (Kanatous et al., 2008; Vázquez-Medina et al., 2007). This is further confirmed in Figure 3.1 where RBCs and muscle present TEF values distributed along a range of 2.5 and 1.7‰, respectively, whilst hair is quite homogenous.

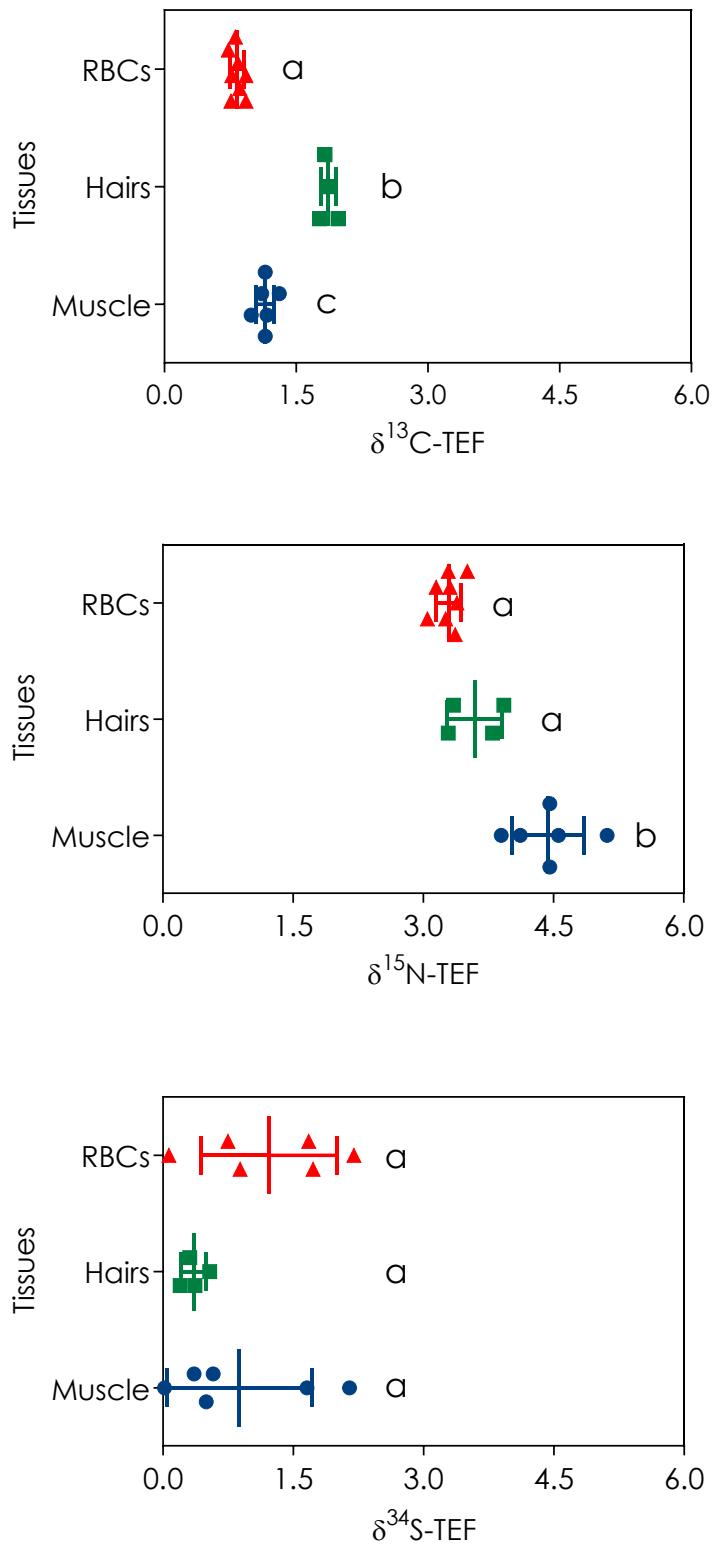


Figure 3.1. Calculation of isotopic fractionation (TEFs) factors of Carbon ($\delta^{13}\text{C}$ -TEF), Nitrogen ($\delta^{15}\text{N}$ -TEF) and Sulphur ($\delta^{34}\text{S}$ -TEF) in muscle ($n = 6$), hair ($n = 8$) and red blood cells (RBCs) ($n = 8$) of hooded seal subadults subjected to controlled feeding experiment. Values are presented as Mean (the middle bar \pm SD lines) in per mill (‰). Statistical groups are represented by the letters a, b and c.

4.3. Assessment of model efficiency in calculating isotopic fractionation

The large number of potential factors which seem to be influencing IF processes in young hooded seals really calls for further measurements, especially for growing individuals. However, in the case of marine mammals, captivity studies are limited by ethical and practical problems. In this direction Caut et al. (2009) and Healy et al. (2017) developed two models that allow TEFs to be calculated (called by Caut et al.: “*Discrimination factors*”; by Healy et al.: “*TDF Trophic Discrimination Factor*”) for animals for which no direct measurement exists (Caut et al., 2009; Healy et al., 2017). Two different statistical approaches are considered by these authors: the first model proposes the application of a multiple-regression Diet-Dependent Discrimination Factor method (DDDF) in which diet isotopic ratio is considered as the main factor controlling IF variation (Caut et al., 2009). Healy et al. instead use a Bayesian model (SIDER) to calculate IFs for birds and mammals through the incorporation of multiple sources of variation, among which are the phylogenetic structure and the error associated with measurements within a species (Healy et al., 2017). The application of the Caut *et al.* model to calculate hooded seal IFs of muscle, hair and blood gives very different results from those measured during our experiment (Figure 3.2). The $\delta^{15}\text{N}$ -TEF estimates were smaller than our values using either equations for all tissues pooled together, or using equations specific to each tissue. The $\delta^{13}\text{C}$ -TEF values were also smaller than those obtained in our experiment with the one exception of C-TEF calculated in RBCs by tissue-specific equations (Caut et al., 2009). The output of the Healy et al. model, instead, resulted in TEFs within the same range as those measured in this study (Healy et al., 2017). This shows that the hypothesis of Caut et al. that fractionation factors are mostly driven by the isotopic composition of preys does not seem to be appropriate for calculating the IF of seals, especially during the growing period (Caut et al., 2009). On the other hand, a comparatively more complex model considering multiple factors as drivers for fractionation does a rather good predictive job.

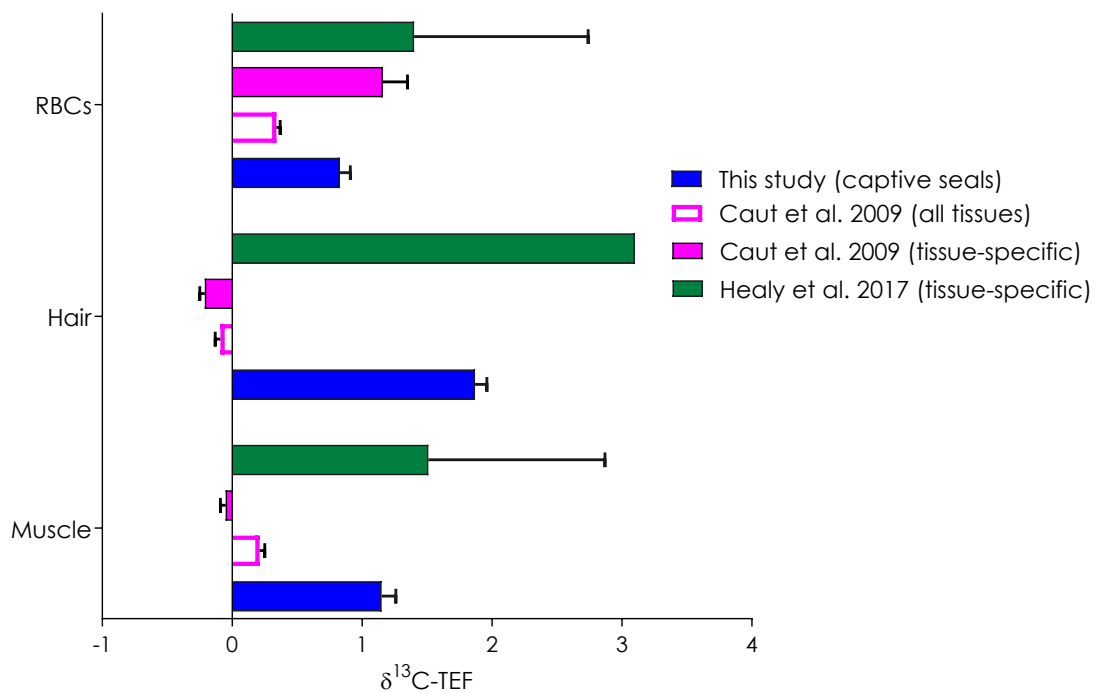
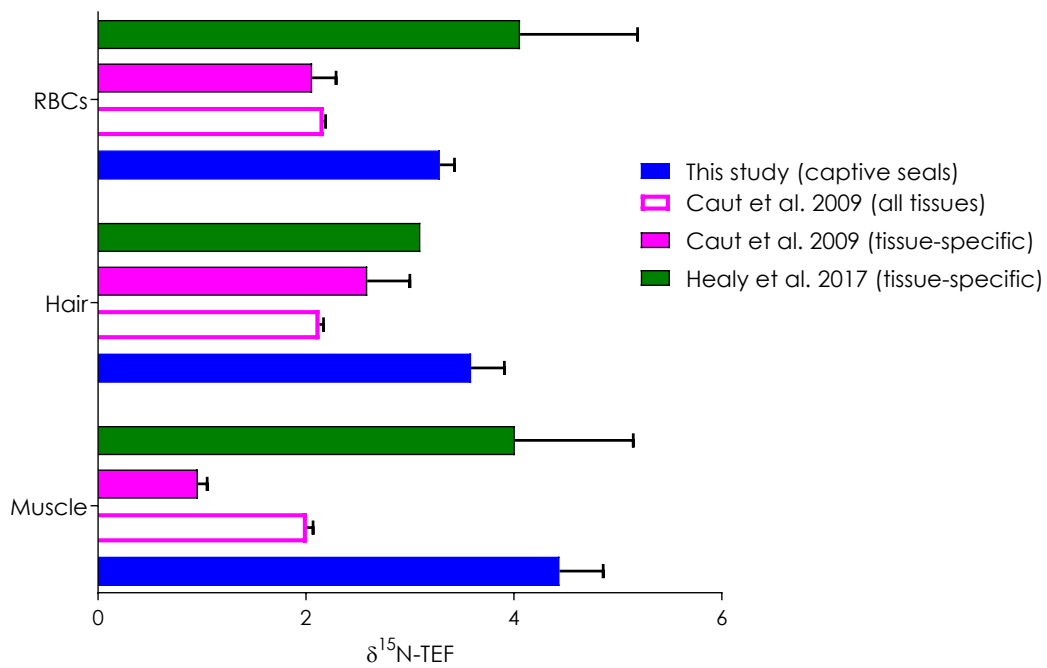


Figure 3.2. Comparison of the experimentally-estimated TEFs in this study for captive subadult hooded seals (blue) and the model-estimated TEFs resulting from the application of the Diet-based regression model of Caut et al., 2009 (filled and empty pink) and the Bayesian model of Healy et al., 2016 (green).

5. CONCLUSIONS

The main findings of this chapter can be summarized as follows:

1. This study shows how the “**growth effect**” on C and N-IF, already demonstrated in birds, fish and terrestrial small mammals, is exacerbated in physiologically-complex animals such as Arctic hooded seals. For the first time, it also demonstrates that S can present a significant isotopic enrichment from the diet to the consumer, as a result of diet composition or tissue metabolic needs.
2. The great N fractionation found in muscle raises concern about the study of seals ecology and distribution based on stable isotopes analysis. Indeed, we suggest that the application of the classic **3.5 ‰ N consumer-diet enrichment** to calculate predator trophic level or prey dietary proportion in growing marine mammals, leads to a **misleading** interpretation; a larger IF should be considered.
3. Since a small change in diet seems to greatly influence IF between two seal species, a **standardization of feeding protocols** may be needed for IF-related captive experiment with Phocidae. This could prevent misinterpretation of IF variation data between different species during comparison with the literature.
4. The large difference observed especially for N or C isotopic fractionation rates between the different tissues again confirms that: (1) between-tissue fractionation variability cannot be neglected when using “non-intrusive”, external tissues (e.g. hair) as a proxy of internal organs (e.g. muscle); and (2) in order to avoid errors in data analysis, captive feeding experiments on pinnipeds must be long enough to ensure that all the tissues with different metabolic rates have reached a complete **diet-to-tissue isotopic equilibrium**.

Chapter 4

**Using Hg stable isotopes to assess Hg dynamic in
Arctic seals: new insights from a captive experiment
on hooded seal *Cystophora cristata*.**

ABSTRACT

Rationale: An accurate interpretation of Hg isotopic data requires the consideration of several biotic factors such as age, diet, geographical range and tissue metabolic turnover. An *a priori* knowledge of the rates of prey-predator isotopic incorporation and Hg biomagnification is essential.

Main question: This study aims at assessing Hg stable isotopes incorporation and Hg biomagnification in a subarctic species of Phocidae: the hooded seal *Cystophora cristata*.

Methods: Six pups were caught in March 2012 in the breeding grounds of the Greenland Sea. They were kept in captivity for 2 years and fed on a continuous diet of Norwegian Spring Spawning (NSS) herring *Clupea harengus*. After 2 years they were euthanized and samples of muscle, liver, hair and muscle were collected. We measured THg, MMHg and iHg levels, and Hg stable isotopes ($\delta^{202}\text{Hg}$, $\Delta^{199}\text{Hg}$, $\Delta^{200}\text{Hg}$, $\Delta^{201}\text{Hg}$ and $\Delta^{204}\text{Hg}$) in these 4 tissues and herring muscle. We then calculated Hg isotopes Trophic Enrichment Factors (TEFs) and Hg Biomagnification Factors (BMFs) between each analyzed tissue and herring.

Results: $\delta^{202}\text{Hg}$ values ranged between 0.22‰ in kidney of hooded seal pups to 1.79‰ in hair, reflecting perfectly Hg speciation, distribution and detoxification processes in the different tissues of hooded seals. TEF of $\delta^{202}\text{Hg}$ values ranged from 0.80‰ in hair to -0.78‰ in kidney. $\Delta^{199}\text{Hg}$, $\Delta^{200}\text{Hg}$, $\Delta^{201}\text{Hg}$ and $\Delta^{204}\text{Hg}$ values and TEFs did not vary between herring and tissues of hooded seal. Our findings suggest that age is the major driver of changes in Hg internal metabolism and isotopic incorporation.

Conclusions: We assess for the first time TEFs of Hg stable isotopes in an Arctic true seal, without the effect of age, diet and distribution. Our results confirm the validity of Hg stable isotopes as a tracers of Hg environmental sources even in predators. Finally, we suggest muscle as the reliable tissue to trace Hg sources and trophic transfer on a spatial and temporal scale.

1. INTRODUCTION

The assessment of Hg sources and pathways in the marine environment, remains a complex challenge despite its recognized toxicity, both for wildlife and humans. This is especially relevant for Arctic true seals, which developed important physiological and ecological adaptations to survive in a cold and unstable environment (Blix, 2005).

The hooded seal *Cystophora cristata* is a subarctic true seal, which relies on drifting ice during breeding and molting season (Øigård et al., 2014). The hooded seal is one of the most contaminated Arctic true seals, presenting Hg concentrations in their tissues often surpassing the toxicity thresholds proposed for human and wildlife (Brunborg et al., 2006; Julshamn and Grahl-Nielsen, 2000; Nielsen and Dietz, 1990; Sonne et al., 2009b). The intense physiological and feeding adaptations of this species might be one of the reasons behind the heavier accumulation of Hg in their body compared to other seal species (Routti et al., 2018). This would make the hooded seal one of the species most at risk of adverse health effects related to Hg contamination (Dietz et al., 2013). Understanding the dynamics of Hg in the hooded seal is imperative for thorough health risk assessments at population scale (Dietz et al., 2019; Eagles-Smith et al., 2018).

The analysis of Hg stable isotopes is increasingly carried out in marine organisms to study Hg sources and trophic transfer (Kwon et al., 2020). An accurate interpretation of Hg isotopic data requires the consideration of several biotic factors such as sex, age, diet, habitat use and geographical distribution (Chapter 3). The intense metabolic changes hooded seal pups undergo during growth enhance prey-consumer isotopic enrichment compared to other seals species, but this question remains open in the case of Hg isotopes (Chapter 3).

Hg Trophic Enrichment factors (TEFs) (as C, N and S-TEFs) have the potential to reflect the intrinsic metabolization of a particular organism (Lesage et al., 2002a). Their quantification at a species-specific level is essential to correctly interpret the rates of Hg trophic transfer.

Several studies used Hg isotopes as a complementary ecological marker to study Hg bioaccumulation in polar bears, seals and pilot whales (Bolea-Fernandez et al., 2019; Perrot et al., 2015). However, while proven extremely valuable, these studies were conducted on wild animals. As such the effects of environmental processes on Hg MDF and MIF remained a confounding factor in the interpretation of Hg metabolism by the organisms.

The main objective of this chapter was to assess the factors influencing Hg metabolization in the organism of Arctic true seals. Based on previous literature and the results from chapter 3, our initial hypothesis was that the physiological specializations developed by hooded seals could lead to an exacerbation of Hg processing in the organism and higher bioaccumulation.

We measured Hg stable isotopes in several tissues of captive hooded seals kept on a continuous diet made of herrings. We studied Hg isotopic variability without the interference of diet, age or distribution, reflecting only the **basal metabolization of Hg within a specialized Arctic true seal**. Specifically, we wanted to answer 2 questions:

1. Can Hg Mass-Dependent Fractionation (MDF) reflect Hg metabolism within a consumer, and its transfer from the diet?
2. Can Hg odd and even Mass-Independent Fractionation (MIF) effectively show Hg sources from the environment without being altered throughout the food web?
3. Which are the main factors influencing Hg stable isotopes in hooded seals?

This study constitutes the **first quantification of Hg stable isotope TEFs** in an Arctic marine mammal species, the hooded seal *Cystophora cristata*.

2. MATERIAL AND METHOD

Ethical protocol, captivity and sampling are discussed in details in Chapter 2 (§3.1 and §4.2) and Chapter 3 (§2.1 and §2.2). Hereby, we will report only additional specific information about the technics used in this study.

2.1. Samples collection and preparation

To prevent the effect of age we only considered the 6 seals euthanized in 2014; namely after 2 years. These were K1-12, K2-12, K3-12, K4-12, K7-12 and K8-12 (Chapter 3, [Table 3.1](#)). K5-12 and K6-12 were excluded.

Because of the small sample quantity remaining after the analysis of C, N and S stable isotopes, we could not measure Hg concentrations and stable isotopes in red blood cells. We included samples of liver and kidney, since they are important organs for the metabolization of Hg in marine mammals.

Because there was no more herring left from 2012, we asked our collaborators at the Arctic University of Tromsø (UiT) to send us 15 additional herring for the measurement of Hg stable isotopes and species. These were purchased from the same company (Pelagia – Seafood from Norway), area (Northeast Atlantic) and period (February to March) than herring sampled in 2012. In this way we eliminated potential differences in Hg isotopes linked with diet.

2.2. Mercury species analysis

Total Hg concentration (hereafter expressed as ng g^{-1} dry weight, dw) were quantified by atomic absorption spectroscopy (AAS) on a Tri-cell Direct Mercury Analyzer 80 (DMA-80 Evo, Milestone, Italy), as described in Chapter 2 (§7.1). Hg species concentrations (inorganic Hg, iHg and monomethyl-Hg, MMHg) were quantified by species-specific isotopic dilution mass spectrometry analysis (SIDMS) after microwave-assisted extraction performed using a CEM MW system (Discover SP-D, CEM Corporation) coupled to an autosampler Explorer 4872 96 (USA). Hg species analysis was carried out by GC-ICPMS Trace Ultra GC equipped with a Triplus RSH autosampler coupled to an ICP-MS XSeries II (Thermo Scientific, USA) (Chapter 2, §7.3).

2.3. Mercury stable isotopes analysis

Hg isotopic analyses were performed in a Nu Plasma HR MC-ICPMS (Nu Instruments, UK using a continuous flow Cold Vapor Generation (CVG) after Hot block (HB) pre-digestion (Chapter 2, §7.4). Hg isotopic values were reported as delta (δ) notation values (in per mil, ‰), calculated relative to the bracketing standard NIST SRM-3133 CRM to allow interlaboratory comparisons. NIST SRM-997 thallium standard solution was used for the instrumental mass-bias correction using the exponential law (Chapter 2, §7.4). δ represents mass dependent fractionation (MDF) and Δ represents mass independent fractionation (MIF). Hg MDF, even and odd MIF were calculated as shown in Chapter 1, §3.2.

2.4. TEF quantification

The Trophic Enrichment Factor (TEF) were calculated to quantify Hg isotopic increment and accumulation rates respectively in the six captive hooded seal pups and herrings. TEF depicts the net isotopic difference between a consumer and its food source, and was calculated with equation 3.1 (Chapter 3, §2.4).

2.5. Statistical analyses

Data normality was tested with the Shapiro-Wilk test, recommended for small sample size. The skewness, kurtosis and Mean-Median difference were calculated in order to select which statistical tests to use (parametric vs. non-parametric). Even if most of the data followed a Gaussian distribution, the kurtosis and skewness often resulted very high (> 1), indicating an asymmetrical tendency of the curve. For many groups the Mean did not equal the Median. Because of all these reasons and the small sample size (e.g. $n = 4$ for hair), we decided to run non-parametric tests.

Pairwise comparisons were done with the Mann-Whitney test. Otherwise, the Kruskal-Wallis test followed by Dunnett's multiple comparison were performed. The Spearman rho (ρ) was used to assess correlation between parameters. At first, Hg stable isotope slopes were calculated fitting linear regressions; however, the resulting goodness of fit was quite low ($R^2 = 0.05$ to 0.2). The $\Delta^{199}\text{Hg}/\delta^{202}\text{Hg}$, $\Delta^{199}\text{Hg}/\Delta^{201}\text{Hg}$, $\Delta^{200}\text{Hg}/\delta^{202}\text{Hg}$ and $\Delta^{200}\text{Hg}/\Delta^{204}\text{Hg}$ slopes were therefore calculated as simple ratios. They will be referred to as "ratios" in the text, rather than "slopes".

All statistical analysis was conducted in GraphPad Prism version 8.4.2 for Windows (GraphPad Software, San Diego, California USA, www.graphpad.com). Family-wise significance and confidence level was set at $\alpha = 0.05$ (95 % confidence interval). However, due to the small N of certain groups and the large Hg isotopic variability, differences with p value > 0.01 were not interpreted.

3. RESULTS

3.1. Mercury species profile

Seal THg concentrations resulted in the following profile: Liver > Kidney > Hair > Muscle (Table 4.1), with significant differences between tissues (KW = 34.3, $p < 0.0001$). Muscle was significantly less concentrated than liver and kidney (Dunnett: $p = 0.0006$ and $p = 0.006$, respectively). Hooded seal liver and kidney were significantly more concentrated than herring (Dunnett: $p < 0.0001$ and $p < 0.0001$, respectively).

Seal MMHg concentrations resulted in the following profile: Hair > Liver > Kidney > Muscle (Table 4.1), with significant differences between tissue (KW = 30.1, $p < 0.0001$). Muscle resulted significantly less concentrated than hair (Dunnett: $p = 0.006$). Hooded seal hair and liver were significantly more concentrated than herring (Dunnett: $p < 0.0001$ and $p = 0.0003$, respectively).

Table 4.1. THg, MMHg and iHg concentrations (in $\text{ng g}^{-1} \text{dw}$), MMHg and iHg fractions (in %) and Hg stable isotope ratios (in ‰) measured in captive hooded seal *C. cristata* pups and their prey, the herring *C. harengus*. Results are shown as Mean (Median) \pm SD (Min – Max). *n* equals the number of organisms on which the analysis was conducted.

Animal Tissue	Hooded Seal				Herring Muscle
	Liver	Kidney	Muscle	Hair	
<i>n</i>	6	6	6	4	18
THg <i>ng g⁻¹ dw</i>	7875 (7349) \pm 3521 (2674 – 12624)	5376 (4676) \pm 2659 (2427 – 9152)	540 (574) \pm 110 (348 – 640)	1171 (1194) \pm 346 (622 – 1592)	108 (86.7) \pm 52.0 (47.8 – 191)
MMHg <i>ng g⁻¹ dw</i>	814 (881) \pm 150 (562 – 1014)	537 (529) \pm 110 (354 – 707)	453 (474) \pm 113 (270 – 588)	1070 (1104) \pm 318 (531 – 1484)	100 (73.8) \pm 50.7 (46.1 – 186)
iHg <i>ng g⁻¹ dw</i>	6686 (7019) \pm 3099 (1967 – 10026)	4454 (4122) \pm 1973 (1750 – 7363)	99.0 (102) \pm 27.5 (50.8 – 140)	114 (116) \pm 24 (74 – 147)	9.37 (6.36) \pm 5.72 (2.01 – 24.3)
fMMHg %	16.9 (13.8) \pm 8.59 (7.18 – 25.8)	16.4 (15.5) \pm 8.34 (5.67 – 24.8)	81.5 (81.2) \pm 5.28 (73.5 – 92.5)	89.8 (90.1) \pm 2.86 (85.7 – 93.2)	88.4 (91.5) \pm 9.45 (55.6 – 94.9)
fiHg %	85.7 (90.3) \pm 9.54 (67.3 – 91.5)	87.1 (88.5) \pm 7.08 (74.3 – 95.1)	18.5 (20.1) \pm 5.51 (9.75 – 24.6)	10.1 (9.9) \pm 2.83 (6.66 – 14.3)	1.35 (7.94) \pm 2.92 (3.71 – 16.6)
$\delta^{202}\text{Hg}$ ‰	0.71 (0.63) \pm 0.36 (0.50 – 0.97)	0.22 (0.17) \pm 0.26 (0.09 – 0.47)	1.20 (1.27) \pm 0.76 (0.75 – 1.74)	1.79 (1.72) \pm 0.45 (1.62 – 2.11)	1.00 (0.92) \pm 0.38 (0.79 – 1.46)
$\Delta^{199}\text{Hg}$ ‰	1.16 (1.13) \pm 0.13 (1.08 – 1.23)	1.08 (1.08) \pm 0.02 (1.06 – 1.09)	1.16 (1.14) \pm 0.12 (1.12 – 1.30)	1.12 (1.13) \pm 0.05 (1.10 – 1.15)	0.97 (0.91) \pm 0.35 (0.60 – 1.25)
$\Delta^{200}\text{Hg}$ ‰	0.02 (0.02) \pm 0.06 (-0.03 – 0.07)	-0.01 (-0.01) \pm 0.03 (-0.03 – 0.02)	0.06 (0.05) \pm 0.10 (0.01 – 0.17)	0.02 (0.02) \pm 0.04 (0.00 – 0.04)	0.03 (0.03) \pm 0.07 (-0.05 – 0.09)
$\Delta^{201}\text{Hg}$ ‰	0.99 (1.00) \pm 0.09 (0.91 – 1.03)	0.93 (0.92) \pm 0.04 (0.90 – 0.96)	1.00 (0.98) \pm 0.16 (0.93 – 1.19)	0.99 (0.98) \pm 0.05 (0.96 – 1.01)	0.81 (0.75) \pm 0.32 (0.59 – 1.07)
$\Delta^{204}\text{Hg}$ ‰	-0.04 (-0.03) \pm 0.15 (-0.16 – 0.05)	-0.03 (-0.01) \pm 0.11 (-0.11 – 0.04)	-0.01 (-0.02) \pm 0.16 (-0.10 – 0.16)	-0.08 (-0.07) \pm 0.06 (-0.11 to -0.04)	-0.05 (-0.04) \pm 0.16 (-0.24 – 0.06)

Seal iHg concentrations resulted in the following profile: Liver > Kidney >> Hair ~ Muscle (Table 4.1) with significant differences between tissue (KW = 32.3, $p < 0.0001$). Muscle was significantly less concentrated than liver (Dunnett: $p = 0.003$). The other tissues differed only weakly (Dunnett: $p > 0.01$). Hooded seal liver and kidney were significantly more concentrated than herring (Dunnett: $p < 0.0001$ and $p = 0.0001$, respectively).

Seal fMMHg resulted in the following profile: Hair > Muscle > Liver ~ Kidney (Table 4.1), with significant differences between tissues (KW = 34.1, $p < 0.0001$) (Figure 4.1). Hair had significantly higher fMMHg than liver and kidney (Dunnett: $p = 0.006$ and $p = 0.0001$, respectively). Hooded seals liver and kidney had significantly lower fMMHg than herring (Dunnett: $p < 0.0001$ and $p = 0.0002$, respectively).

Seal fiHg resulted in the following profile: Kidney ~ Liver > Muscle > Hair (Table 4.1). Kidney and liver presented significantly higher fiHg than muscle (KW = 27.5, $p < 0.0001$). Kidney and liver differed only weakly from hair (Dunnett: $p = 0.02$ for both). Hooded seals liver and kidney had significantly higher fiHg than herring (Dunnett: $p = 0.0005$ and $p = 0.0007$, respectively).

3.2. Mercury stable isotopes analysis

Raw values of Hg stable isotope delta values and ratios are presented in tables A4.1 and A4.2 (Annex to [Chapter 4](#)). $\delta^{202}\text{Hg}$ values differed strongly between tissues and organisms (KW = 29.6, $p < 0.0001$). $\delta^{202}\text{Hg}$ was significantly higher in muscle than liver ($p = 0.002$). Hair $\delta^{202}\text{Hg}$ was significantly higher than liver and kidney (Dunnett: $p = 0.010$ and $p < 0.0001$, respectively). $\delta^{202}\text{Hg}$ values significantly differed between seals kidney and herring ($p = 0.001$) and hair and herring ($p = 0.0004$). No difference was found for $\Delta^{199}\text{Hg}$, $\Delta^{201}\text{Hg}$ and $\Delta^{204}\text{Hg}$ values. $\Delta^{200}\text{Hg}$ values differed only between hooded seal muscle and kidney ($p = 0.003$).

$\Delta^{199}\text{Hg}/\delta^{202}\text{Hg}$ slope differed significantly between hair and kidney in seals ($p < 0.0001$) (Figure 4.2). $\Delta^{200}\text{Hg}/\delta^{202}\text{Hg}$ slope differed between kidney and the other tissues ($p = 0.035$). No difference was found for $\Delta^{199}\text{Hg}/\Delta^{201}\text{Hg}$ and $\Delta^{200}\text{Hg}/\Delta^{204}\text{Hg}$ slopes between seal tissues. Any difference was found between hooded seal tissues and their prey (Table 4.2).

A positive correlation was found between $\delta^{202}\text{Hg}$ values and fMMHg (Spearman $\rho = 0.643$, $p = 0.0003$, $R^2 = 0.567$) (Figure 4.1). A negative correlation was found between $\delta^{202}\text{Hg}$ values and fiHg (Spearman $\rho = -0.705$, $p < 0.0001$, $R^2 = 0.587$). A weak negative correlation was found between $\Delta^{199}\text{Hg}$ values and fiHg (Spearman $\rho = -0.382$, $p = 0.048$, $R^2 = 0.106$).

Table 4.2. Hg stable isotopes slopes calculated in captive hooded seal *C. cristata* pups and herring *C. harengus*. Statistical difference resulting from the Kruskal-Wallis test is represented in the last column. Bold letters indicate significant different groups, as indicated by the Dunnett's multiple comparisons test. When only one tissue is represented in bold, it means that that particular tissue differed from all the others.

Ratios	Hooded seal				Herring	Statistical difference
	Hair	Muscle	Liver	Kidney	Muscle	
$\Delta^{199}\text{Hg}/\delta^{202}\text{Hg}$	1.59±0.19	1.03±0.32	0.63±0.17	0.20±0.12	1.06±0.29	p < 0.0001, KW = 29.9
$\Delta^{199}\text{Hg}/\Delta^{201}\text{Hg}$	1.14±0.002	1.16±0.04	1.15±0.05	1.16±0.03	1.20±0.08	p = 0.080, KW = 8.23
$\Delta^{200}\text{Hg}/\delta^{202}\text{Hg}$	0.01±0.01	0.05±0.03	0.03±0.04	-0.05±0.08	0.03±0.04	p = 0.035, KW = 10.4
$\Delta^{200}\text{Hg}/\Delta^{204}\text{Hg}$	-0.34±0.35	-1.60±2.0	0.11±0.81	-0.06±0.97	-0.22±1.23	p = 0.350, KW = 4.42

3.3. TEFs

Raw values of Hg TEFs are shown in Table A4.2 and Table A4.3, in Annex to [Chapter 4](#). $\delta^{202}\text{Hg}$ -TEF ranged between -0.28‰ in kidney and 0.79‰ in hair, with significant differences between tissues (KW = 53.6, p < 0.0001; Table 4.3). $\Delta^{199}\text{Hg}$ -TEFs ranged 0.11‰ in kidney to 0.19‰ in hair, with only a weak difference (p = 0.023). $\Delta^{200}\text{Hg}$ -TEF ranged from -0.03‰ in kidney to 0.04‰ in muscle, with only a weak difference (p = 0.016). No differences were found between tissues for $\Delta^{201}\text{Hg}$ - and $\Delta^{204}\text{Hg}$ -TEF.

Table 4.3. Hg stable isotope TEFs in tissues of captive hooded seal *C. cristata* pups. Data are presented as Mean ± Standard Deviation (Min – Max) n.

	Tissue			
	Liver	Kidney	Muscle	Hair
$\delta^{202}\text{Hg}$ -TEF	-0.28 ± 0.18 (-0.5 to -0.03) 8	-0.78 ± 0.13 (-0.91 to -0.52) 7	0.20 ± 0.38 (-0.24 - 0.74) 8	0.79 ± 0.23 (0.62 - 1.11) 4
$\Delta^{199}\text{Hg}$ -TEF	0.16 ± 0.05 (0.10 - 0.26) 8	0.11 ± 0.01 (0.08 - 0.12) 7	0.19 ± 0.06 (0.15 - 0.33) 8	0.15 ± 0.03 (0.12 - 0.17) 4
$\Delta^{200}\text{Hg}$ -TEF	-0.01 ± 0.03 (-0.05 - 0.05) 8	0.02 ± 0.06 (-0.06 - 0.08) 7	0.04 ± 0.08 (-0.05 - 0.21) 8	-0.02 ± 0.03 (-0.06 - 0.01) 4
$\Delta^{201}\text{Hg}$ -TEF	0.18 ± 0.05 (0.10 - 0.22) 8	0.12 ± 0.02 (0.09 - 0.14) 7	0.19 ± 0.08 (0.12 - 0.38) 8	0.17 ± 0.03 (0.15 - 0.20) 4
$\Delta^{204}\text{Hg}$ -TEF	0.01 ± 0.07 (-0.11 - 0.10) 8	-0.03 ± 0.01 (-0.05 to -0.01) 7	0.03 ± 0.04 (-0.01 - 0.14) 8	-0.01 ± 0.02 (-0.03 - 0.02) 4

4. DISCUSSION

4.1. Bioaccumulation of mercury

The highest mean MMHg concentrations are found in hair, followed by muscle > liver > kidney. In contrast to iHg (kidney > liver > muscle > hair; Table 4.2). This is in agreement with previous studies on Hg bioaccumulation in Arctic seals (Dietz et al., 2013; Julshamn and Grahl-Nielsen, 2000; Nielsen and Dietz, 1990). **Differential tissue accumulation reflects the metabolic roles of hair, muscle, kidney and liver in seals** (Chapter 1, §1.3.2, Figure 1.4) (Capelli et al., 2008; Martínez-López et al., 2019; Trukhin and Simokon, 2018; Wagemann et al., 1998).

In seals, Hg is mostly assimilated through the diet (Dietz et al., 2019; Lehnert et al., 2018). The high similarity of thiol-containing Hg conjugates with certain endogenous molecules like amino acids or polypeptides, enhances the transport of Hg species within the body: MMHg through the blood, iHg through diffusion across the intestinal enterocytes in the small intestine and duodenum (Bridges and Zalups, 2017). In this way, 15 % of the assimilated iHg and 95 % of the assimilated MMHg are absorbed and taken up by tissues (Gentès et al., 2015; Park and Zheng, 2012).

Liver and kidney are key organs of Hg detoxification (Ewald et al., 2019; Nakazawa et al., 2011). Because of the elevated content in thiol-containing molecules (e.g. glutathione, cysteine, homocysteine, N-acetylcysteine, metallothionein, and albumin), kidney is the primary target for iHg and to a lesser extent MMHg (Zalups, 2000). Once in the organ, Hg undergoes a large series of transformation by some form of currently undefined complex ligand-exchange mechanisms (Bridges and Zalups, 2010). The proximal tubule is the primary site for the accumulation of newly formed iHg salts, before being slowly excreted through urine (Rice et al., 2014). This explains the larger proportion of iHg versus MMHg found kidney (Table 4.2).

Liver presents the second highest percentage of iHg versus MMHg (Table 4.2). In liver, dietary MMHg is demethylated to Hg^{2+} and made inert, through the co-precipitation of Hg^{2+} with Se and formation of HgSe (tiemanite) granules (Kehrig et al., 2016; Wang and Wang, 2017). In this way, Hg is accumulated as iHg throughout the entire life of the individual. The remaining small fraction of non-demethylated MMHg is transported away to other tissues like muscle (Wang and Tan, 2019).

Because of the strong affinity for sulfhydryl groups of proteins, MMHg is preferentially redistributed towards tissues like muscle, brain and hair (Bridges and Zalups, 2010). In true seals, **muscle and hair** are commonly considered as the storage tissues, where MMHg is accumulated temporarily or definitely (Lyytikäinen et al., 2015; Peterson et al., 2016a). As such, fMMHg results similar in these two tissue values (between 81 to 89 %). The time a tissue takes to completely renew its cellular composition (e.g. lipids, proteins, carbohydrates, etc.) is commonly referred to as “tissue turnover rate” (Mawson, 1955). High turnover rate tissues are those having an important metabolic role within the organism, like muscle, liver, blood, blubber, etc. These tissues are continuously renewed as a

necessity for the right functioning of animal's basal metabolism (Vander Zanden et al., 2015). Inert tissues like hair, nails, feathers, and bones have much longer turnover rates and, in the case of hair or feathers, might be renewed only once a year (Dauwe et al., 2003; Peterson et al., 2016b). Therefore, the slight difference in fMMHg between hair and muscle could result from the different turnover rates of these two tissues. Because of the fast turnover rate, MMHg would not have enough time to accumulate in hooded seal muscle compared to herring, because it would be continuously remobilized during tissue renewal. On the other hand, the slower turnover of hair, would allow longer input of MMHg over time, and result in higher fMMHg.

4.2. Mass-dependent fractionation of mercury isotopes reflects speciation and transformation in tissues

The positive correlation observed between MMHg and $\delta^{202}\text{Hg}$ values reflects the distinct distribution of Hg species in hooded seal tissues, as a result of their respective metabolic roles (Figure 4.1). Hair and muscle display the highest $\delta^{202}\text{Hg}$ values combined to a high fraction of MMHg. The opposite is observed in liver and kidney. **Hg MDF is thus proportional to MMHg fraction in the tissue of hooded seal subadults**, in agreement with previous studies on Hg dynamic (Perrot et al., 2015; Pinzone et al., 2021a; Renedo et al., 2018).

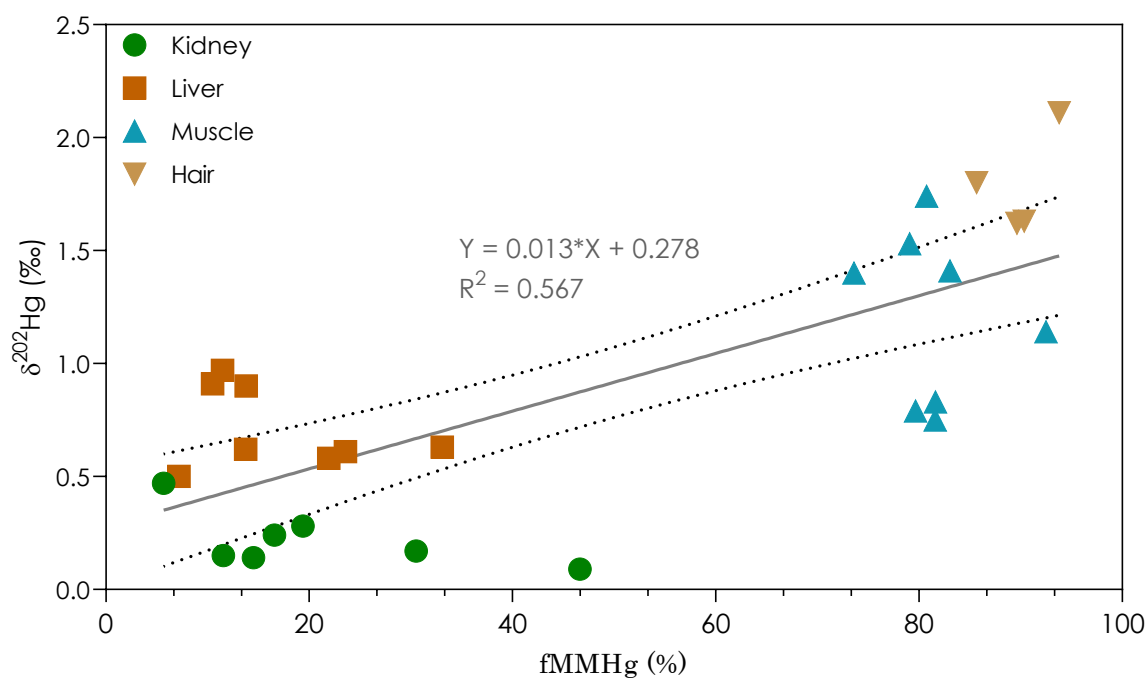


Figure 4.1. Spearman's correlation between Hg MDF (represented by $\delta^{202}\text{Hg}$, in ‰) and the fraction of MMHg (fMMHg, in %) in captive hooded seal *C. cristata*. Linear regression is represented by the straight grey line. Dotted lines show the 95 % confidence intervals. Kidney (green dot), Liver (dark-orange square), Muscle (turquoise triangle), Hair (gold down-triangle).

4.2.1. Liver and kidney

The largest Hg MDF occurring in marine predators like true seals and belugas (Perrot et al., 2015), long-finned pilot whales (Bolea-Fernandez et al., 2019; Li et al., 2020), Antarctic seabirds (Renedo et al., 2021) and European seabass (Pinzone et al., 2021a), is related to **hepatic MMHg demethylation**. Such process preferentially involves lighter Hg isotopes and generates newly formed iHg, characterized by lower $\delta^{202}\text{Hg}$ values (Perrot et al., 2015). The remaining non-demethylated MMHg has higher $\delta^{202}\text{Hg}$ compared to the initially bioaccumulated MMHg. This isotopically heavier fraction of MMHg is subsequently transferred to muscle and hair (Perrot et al., 2015). As the center of *in vivo* demethylation, liver will display lower $\delta^{202}\text{Hg}$ values than muscle and hair.

Kidney results as the most ^{202}Hg depleted tissue in hooded seals, even if $\delta^{202}\text{Hg}$ values are still positive (0.1 – 0.5 ‰) compared to the literature. As the target organ of both dietary iHg and iHg formed during MMHg breakdown in other tissues (Gentès et al., 2015), kidney could end up presenting even lower $\delta^{202}\text{Hg}$ values than liver. However, additional tissue-specific transformation processes could also contribute to the low renal $\delta^{202}\text{Hg}$ values (Li et al., 2020; Renedo et al., 2021).

Thiol-ligand Hg complexation in sediments and water solutions were previously proposed to cause Hg negative MDF ($\delta^{202}\text{Hg} = -0.3$ to -0.6‰) (Jiskra et al., 2012; Wiederhold et al., 2010). This seems to be linked with the preferential uptake of the lighter isotopes during sorption of Hg into thiol-binding complexes (Jiskra et al., 2012; Zheng et al., 2019). The high rates of Hg thiol-complexation occurring in kidney potentially justify the low renal $\delta^{202}\text{Hg}$ values of our captive hooded seals.

4.2.2. Muscle and hair

Hooded seal $\delta^{202}\text{Hg}$ values differ also between **hair and muscle**. A ^{202}Hg depletion in muscle relative to hair can well result from the lower fMMHg in muscle (as discussed earlier). However, the difference in fMMHg between muscle and hair is minimal compared to the difference in $\delta^{202}\text{Hg}$ values (≥ 1 ‰). One hypothesis is that this large shift could result from higher detoxification rates in hair with respect to muscle. As shown in Antarctic seabirds, the **molting** process favors the excretion of isotopically heavier MMHg (Renedo et al., 2021). This determines higher Hg MDF and $\delta^{202}\text{Hg}$ values in feathers (Renedo et al., 2018). The same could be proposed for hair of hooded seals.

The binding affinity between Hg^{2+} and Se is several orders of magnitude higher than that between Hg^{2+} and S (Melnick et al., 2010). As such, previous studies proposed that non-demethylated MMHg mobilized from the liver could be stored in muscle as both MMHg and iHg (Nakazawa et al., 2011). The occurrence of **HgSe-mediated detoxification processes in muscle** was proposed for striped dolphins, fish and pilot whales (Li et al., 2020; Nakazawa et al., 2011; Wang et al., 2013). Because HgSe in biological tissues are difficult to accurately quantify due to analytical challenges with solid precipitates, this hypothesis remains to be confirmed (Ewald et al., 2019). In long-finned pilot whale

muscle HgSe complexes are found depleted in ^{202}Hg with respect to MMHg, because of faster co-precipitation of lighter Hg isotopes during the formation of the tiemanite crystals (Bolea-Fernandez et al., 2019). The higher proportion of HgSe in muscle could also potentially explain why hooded seal muscle present lower $\delta^{202}\text{Hg}$ values than hair, **potentially supporting the occurrence of MMHg demethylation in muscle of this species.**

4.3. Mass-Dependent Fractionation of mercury isotopes does not reflect sources and trophic transfer

$\delta^{202}\text{Hg}$ are influenced not only by the metabolism but also by several environment processes, allowing its use to trace Hg contamination sources. As an example, the $\Delta^{199}\text{Hg}/\delta^{202}\text{Hg}$ ratio is commonly used to trace Hg formation processes in the environment (Blum et al., 2014). Bergquist & Blum (2007) found that progressive photochemical reduction of Hg^{2+} from an aqueous solution in the presence of terrestrial organic matter (OM) produced Hg^0 and residual Hg^{2+} that fell along a $\Delta^{199}\text{Hg}/\delta^{202}\text{Hg}$ line with a slope of 1.15 ± 0.07 (Mean \pm SE). Photochemical degradation of MeHg instead fell along a $\Delta^{199}\text{Hg}/\delta^{202}\text{Hg}$ line with a slope of 2.43 ± 0.10 (Mean \pm SE) (Bergquist and Blum, 2007b; Blum et al., 2014). However, since $\delta^{202}\text{Hg}$ changes a lot as a consequence of *in vivo* processing, questions arise about the use of $\Delta^{199}\text{Hg}/\delta^{202}\text{Hg}$ as environmental tracer. In this study, $\Delta^{199}\text{Hg}/\delta^{202}\text{Hg}$ ratios differ a lot between hooded seal tissues and herring. The $\Delta^{199}\text{Hg}/\delta^{202}\text{Hg}$ ratios obtained for herring, hooded seal muscle and hair are in the range of Hg^{2+} aqueous photochemical reduction, while $\Delta^{199}\text{Hg}/\delta^{202}\text{Hg}$ ratios found in liver and kidney are much smaller (Table 4.2). Such findings confirm **the impact of tissue metabolism on Hg isotopic composition** (Figure A4.1) and the **limited use of $\Delta^{199}\text{Hg}/\delta^{202}\text{Hg}$ as tracer of Hg sources from the environment.**

The great variability in Hg metabolism between hooded seal tissues might not only impact $\delta^{202}\text{Hg}$ values or $\Delta^{199}\text{Hg}/\delta^{202}\text{Hg}$ ratios, but also the rates of isotopic assimilation between prey and predator (Kwon et al., 2013). Even if the occurrence of Hg trophic MDF is still controversial, the consensus today is that it might indeed happen between apex consumers and their prey (Tsui et al., 2019, 2018). A significant positive MDF is observed between herring and hooded seal hair, while a significant negative MDF is observed between herring and hooded seal kidney (Figure 4.2). This indicates that **Hg trophic MDF effectively occurs in hooded seal pups** only in these 2 tissues. More importantly, our findings indicate that **the extent of Hg MDF between trophic levels varies depending on the analyzed tissue.**

Critical considerations about tissue selection in Hg stable isotopes studies are discussed in Annex to Chapter 4 (§1, [Page 220](#)).

4.4. Information about mercury sources is preserved from prey to predator

Conversely to Hg MDF, no correlation is observed between Hg odd and even MIF and fMMHg in all of hooded seal tissues. Hg stable isotope odd MIF is caused by photochemical processes in the environment and is not modified by *in vivo* metabolism (Gehrke and Blum, 2011; Tsui et al., 2019).

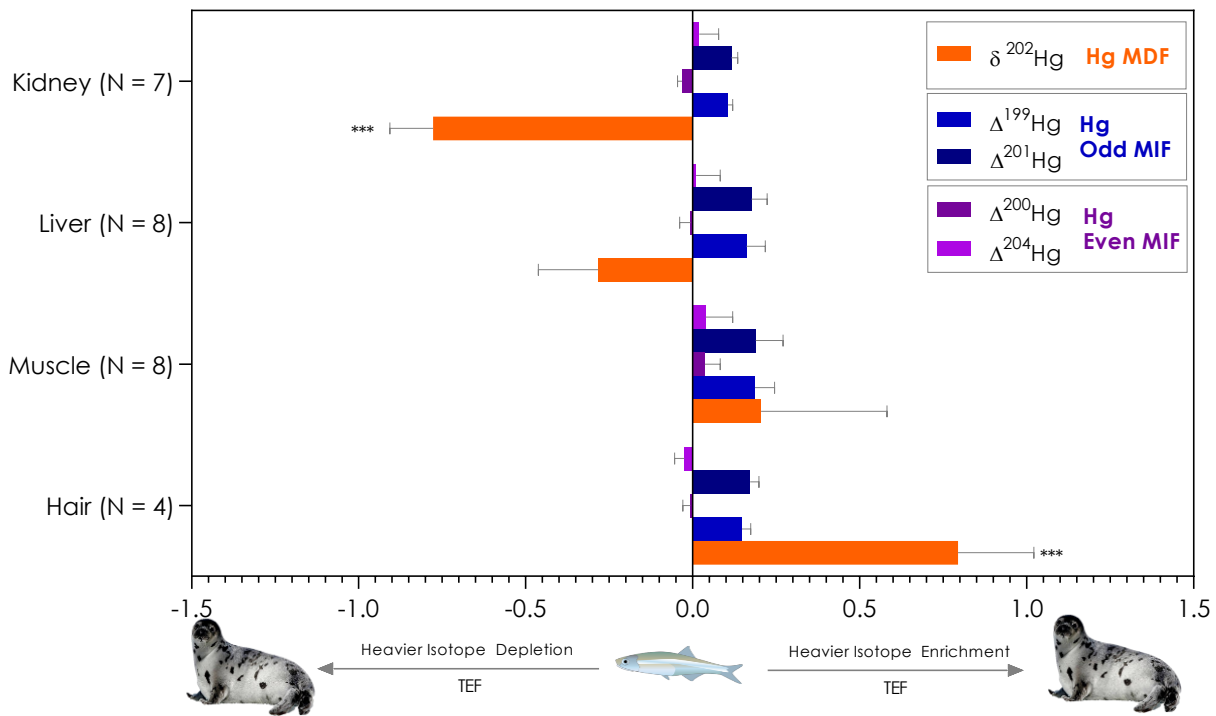


Figure 4.2. Trophic Enrichment Factors (TEFs) for Hg MDF (represented by $\delta^{202}\text{Hg}$, in orange), Hg odd MIF (represented by $\Delta^{199}\text{Hg}$ and $\Delta^{201}\text{Hg}$ in a blue palette) and Hg even MIF (represented by $\Delta^{200}\text{Hg}$ and $\Delta^{204}\text{Hg}$ in a purple palette). TEFs are calculated as the difference between Hg stable isotope values measured in tissues of captive hooded seals *C. cristata* and the mean of those measured in muscle of their diet (the herring, *C. harengus*). Bars represent mean with SD. Three asterisks = $p < 0.0001$, indicating a significant difference in Hg isotopic composition between hooded seals and prey. The Kruskal-Wallis significance was set at $\alpha = 0.05$. Raw TEF values can be found in Annex to Chapter 4, Table A4.2.

As such, $\Delta^{199}\text{Hg}$ values should not differ between tissues when animals are exposed to Hg originating from a single source point (Pinzone et al., 2021a). Even MIF ($\Delta^{200}\text{Hg}$ and $\Delta^{204}\text{Hg}$) has shown to occur mostly in atmospheric samples (e.g. rain, snow, etc.) and is not believed to happen as a consequence of biological processes (Cai and Chen, 2015). As such, $\Delta^{199}\text{Hg}$, $\Delta^{200}\text{Hg}$, $\Delta^{201}\text{Hg}$ and $\Delta^{204}\text{Hg}$ values should not vary from 1 trophic level to the other (Blum, 2011). No significant difference was found between herring and hooded seal $\Delta^{199}\text{Hg}$, $\Delta^{200}\text{Hg}$, $\Delta^{201}\text{Hg}$ and $\Delta^{204}\text{Hg}$ values, resulting in very negligible TEFs (Figure 4.2). Our findings confirm that **no MIF occurs between the diet and hooded seal tissues** (Tsui et al., 2019).

In the same way, $\Delta^{199}\text{Hg}/\Delta^{201}\text{Hg}$ ratio is similar between all hooded seals' tissues and herring, ranging between 1.15 ± 0.05 for kidney to 1.20 ± 0.08 for herring (Figure A4.1). This is consistent with $\Delta^{199}\text{Hg}/\Delta^{201}\text{Hg}$ ratios previously found in marine fish and consumers exploiting marine resources, and indicates that Hg in herring and hooded seals originated from photo-degradation of MMHg (Li et al., 2016a; Meng et al., 2020). This confirms the use of the **$\Delta^{199}\text{Hg}/\Delta^{201}\text{Hg}$ ratio as tracer of Hg environmental processing before accumulation by Arctic marine mammals** (Blum et al., 2014). The vast majority of samples analyzed in the literature ^{200}Hg and ^{204}Hg have been found to undergo MDF (Blum et al., 2014). However, the occurrence of even MIF was only observed in atmospheric samples until now (Cai and Chen, 2015). All $\Delta^{200}\text{Hg}$ and $\Delta^{204}\text{Hg}$ values obtained in this study are within measuring uncertainty ($< 0.2\%$); this is not enough to confirm the occurrence of the presence of even MIF. Anyway, the large variability in $\Delta^{200}\text{Hg}$ and $\Delta^{204}\text{Hg}$ raw values found in our samples suggests that the great range of $\Delta^{200}\text{Hg}/\delta^{202}\text{Hg}$ and $\Delta^{200}\text{Hg}/\Delta^{204}\text{Hg}$ ratios is not a result of internal metabolic MIF or MDF, but it might directly derive from the large environmental variability related with the several processes occurring in the atmosphere and at seawater-air boundary (Sun et al., 2019).

4.5. Age influence mercury metabolism and TEFs

In the previous chapter we have shown how the fast metabolism of young hooded seals might result in higher $\delta^{13}\text{C}$ -, $\delta^{15}\text{N}$ - and $\delta^{34}\text{S}$ -TEFs with regards to other Phocidae. This was linked on one side to the higher turnover rates of growing animals, and on the other to the extreme physiological adaptations of the hooded seals (Chapter 3). To our knowledge, Hg-TEF values in tissues of marine predators are not available yet in the literature. Few studies are available on Hg MDF and MIF in marine mammals (Bolea-Fernandez et al., 2019; Li et al., 2020), allowing to compare Hg stable ratios and concentrations measured in hooded seals with other species. Since no significant pattern was found for Hg even and odd MIF, we will focus mostly on Hg MDF ($\delta^{202}\text{Hg}$ values).

4.5.1. Liver and kidney

Captive hooded seal liver (L) and kidney (K) present higher $\delta^{202}\text{Hg}$ values than Baikal seals (L: -0.81 to -0.32% ; K: -0.82 to -0.26% ; Perrot et al., 2015), long-finned pilot whales (L: 1.23 to -0.23% ; K: -1.10 to -0.33% ; Bolea-Fernandez et al., 2019) and ringed seals from Alaska (L: -0.47 to 0.19% ; Masbou et al., 2015). This might be linked to the fact that the hooded seals sampled in this work were all subadults (Chapter 2, Table 2.1). Demethylation of MMHg in liver and Hg complexation with thiol-ligands in kidney are 2 detoxification mechanisms acquired with age as a consequence of the increasing exposure to this pollutant (Dietz et al., 2013; Martínez-López et al., 2019). Young marine mammals do not reach a specific threshold of hepatic and renal MMHg concentrations as adults do

(Bolea-Fernandez et al., 2019; Ewald et al., 2019). At young age, kidney seems to be as important as liver in stocking dietary Hg (mostly in the form of iHg). With time and the development of the hepatic cellular composition, a greater proportion of iHg accumulated in kidney is redistributed to liver, as a result of the increasing MMHg demethylation capacity (Ewald et al., 2019). In the same way, the rates of iHg complexation with thiol-ligands in kidney increases with life as an adaptation to prevent nephrotoxicity (Dietz et al., 2013). This is confirmed by the similar proportion of iHg and MMHg between liver and kidney of our hooded seals, young long-finned pilot whales and ringed seals (Bolea-Fernandez et al., 2019; Li et al., 2020). Liver of adult marine mammals presents instead higher Hg (all species) concentrations than kidney (Das et al., 2003). Lower rates of hepatic MMHg demethylation and thiol-complexation could result in the higher $\delta^{202}\text{Hg}$ values observed in liver and kidney of young hooded seals compared to adults. This suggests that **Hg stable isotopes in tissues of true seals are influenced by ontogenetic shifts in Hg detoxification capacity.**

Even if these hypotheses explain the difference in Hg MDF between hooded seals subadults and adult marine mammals, they do not justify why liver and kidney $\delta^{202}\text{Hg}$ values differ also between hooded seals, young Baikal seals and pilot whales. Part of Hg MDF that cannot be explained by metabolic activity, may relate to the **difference in foraging habitat and diet**. Our study is the first assessing Hg isotopic composition in captive animals on a constant diet, while all the other studies use samples of wild animals. Conversely to this study, Hg stable isotope ratios reported in these works might be influenced by shifts in diet, distribution and behavior.

4.5.2. Muscle and hair

$\delta^{202}\text{Hg}$ values in muscle of hooded seal subadults are similar to those measured in young long-finned pilot whales (0.95 to 1.31‰), but higher than adult long-finned pilot whales. Lower $\delta^{202}\text{Hg}$ values in muscle of adult whales are linked to the increased proportion of non-demethylated MMHg redistributed from liver to muscle and transformed in HgSe (Bolea-Fernandez et al., 2019). **Ontogenetic shifts in Hg detoxification in muscle** can then also explain the higher $\delta^{202}\text{Hg}$ values of hooded seal subadults compared to older pilot whales. However, no difference is found between $\delta^{202}\text{Hg}$ values of hooded seal subadults and Baikal seals of all ages (1.34 to 2.1‰). We can hypothesize **that age-related shifts in Hg speciation could be different between cetaceans and true seals**. This would indicate that the comparison of Hg stable isotopes between true seals and cetaceans should be taken with a lot of caution.

$\delta^{202}\text{Hg}$ values of hooded seal hair are lower than those found in adult Baikal seals (2.22 to 2.56‰; Perrot et al., 2015). As discussed earlier, molting leads to higher $\delta^{202}\text{Hg}$ values in feathers and potentially in hair (This chapter, §4.2). As for the other tissues, the **efficiency of Hg detoxification**

through molting is believed to increase with time (Lyytikäinen et al., 2015). This would result in a bigger enrichment in ^{202}Hg in hair of adult Baikal seals, compared to hooded seal subadults.

5. CONCLUSIONS

The **main goal** of this chapter was to assess the dynamic of Hg mass-dependent and mass-independent fractionation (MDF and MIF respectively) as a result of hooded seal species-specific basal metabolism, without the influence of diet, distribution nor age. Our **main findings** were:

1. Hg speciation and MDF ($\delta^{202}\text{Hg}$) reflect Hg distribution between the different tissues of hooded seals, as well as Hg detoxification rates. **Trophic Hg MDF** occurs between certain tissues (mostly hair) and their prey;
2. Hg odd and even MIF values ($\Delta^{199}\text{Hg}$, $\Delta^{201}\text{Hg}$, and $\Delta^{200}\text{Hg}$, $\Delta^{204}\text{Hg}$), ratios and TEFs are preserved from prey to consumer, validating their use as tracers of **Hg sources** in Arctic seals;
3. **Age** is the main driver of Hg internal metabolism and isotopic incorporation;
4. The interpretation of Hg isotopes depends on the analyzed **tissue**.

In the framework of this thesis we collected tissues from several years (1985 – 2019). Within each year seals were harvested before and after molting season. Based on previous considerations we have selected **muscle as monitoring tissue** of the following chapters. We consider it as the best tissue to trace Hg sources in marine predators, because it avoids the bias that sampling time and trophic transfer might bring in the interpretation of Hg isotope data in other tissues.

Chapter 5

Terrestrial *versus* marine: discrimination of Hg sources in Arctic true seals by a multi-isotopic approach

ABSTRACT

Rationale: Intrinsic biogeochemical markers, such as stable isotope ratios of carbon (C), nitrogen (N), sulphur (S) and mercury (Hg) are increasingly used to trace the effects of trophic ecology on Hg accumulation in marine predators. However, they are often used separately. This leaves the interpretation of the data at times incomplete. Using a multivariate approach could contend with the complexity of the natural world and reveal patterns that would not be detectable by univariate methods.

Main question: Are Arctic seals “what” or “where” they eat? Our main objective was to assess which factor influences the most Hg sourcing in Arctic marine predators and evaluate the consequences relative to the rates of exposure.

Methods: We measured THg levels, C, N, S and Hg stable isotopes in 3 true seal species living in the Greenland Sea: the hooded seal *Cystophora cristata*, the harp seal *Pagophilus groenlandicus* and the ringed seal *Pusa hispida*. They present distinct habitat use, diet and geographical distribution. We integrated all the measured parameters into a multivariate analysis and quantify species multi-isotopic niches (SEAs) with SIBER.

Results: The multi-isotopic niches of the 3 species resulted highly separated. Hooded seals presented the largest multivariate SEA (Mode, 95 % CI: 0.93, 0.60 – 1.41), a result of its highly distributed oceanic behavior. Harp seals presented the second largest SEA (Mode, 95 % CI: 0.31, 0.14 – 0.68), while ringed seals presented the smallest niche (Mode, 95 % CI: 0.22, 0.14 – 0.37) as a result of its strong territoriality within the Scoresby Sound. Ringed seals presented the highest THg levels ($1190 \pm 488 \text{ ng g}^{-1} \text{ dw}$), followed by hooded ($881 \pm 942 \text{ ng g}^{-1} \text{ dw}$) and harp seals ($407 \pm 289 \text{ ng g}^{-1} \text{ dw}$).

Conclusions: Our study showed how habitat use is the most important factor influencing Hg accumulation in Arctic true seals. A species like the ringed seal, which lives in the fjords on land fast ice, is more influenced by the enhanced MeHg production typical of these zones and accumulate higher levels of Hg compared to offshore hooded and harp seals.

Keywords: Hg sources; Arctic true seals; habitat use; Hg stable isotopes; trophic tracers; sea-ice.

1. INTRODUCTION

In the last 150 years a 10fold increase of total-mercury (THg) concentrations has been observed in the tissues of Arctic wildlife (Braune et al., 2011). This mostly concerns marine tertiary to apex predators like true seals, belugas and polar bears (Chapter 1, §2.3). The reason why Arctic marine mammals seem to be more exposed to such increase with respect to other animals remains unclear. The analysis of carbon (C), nitrogen (N) and sulphur (S) stable isotope ratios (expressed in δ notation in ‰, as $\delta^{13}\text{C}$, $\delta^{15}\text{N}$ and $\delta^{34}\text{S}$) is a recognized valuable tool for the assessment of marine mammals' ecology (Bowen and Iverson, 2013; Dehn et al., 2006; Hückstädt et al., 2012). At the same time, Hg stable isotope ratios are efficient proxies of Hg sources in marine food webs (Bergquist and Blum, 2009; Kwon et al., 2013; Tsui et al., 2019). $\delta^{202}\text{Hg}$, $\Delta^{199}\text{Hg}$ and $\Delta^{201}\text{Hg}$ values are often used to trace trophic position and discriminate marine sources (Masbou et al., 2018; Renedo et al., 2018). $\Delta^{200}\text{Hg}$ and $\Delta^{204}\text{Hg}$ values are increasingly being applied to trace atmospheric sources (Demers et al., 2013; Goix et al., 2019).

The exponential increase of SIA-based scientific studies also led to the development of ecological metrics and models to measure differences between individuals or groups (Cucherousset and Villéger, 2015) and quantify the isotopic and trophic diversity of a species (Parnell et al., 2013). For example, the Stable Isotopes Bayesian Ellipses model in R (SIBER) allows the use of stable isotope ratios to build geometric spaces (or “isospaces”) that can be used as proxies of species' or populations' ecological niches (Jackson et al., 2011). They are commonly referred to as “isotopic niches” (Jackson et al., 2011; Newsome et al., 2007). To our knowledge the SIBER package was considered only once in the literature to interpret Hg stable isotopes data (Cransveld et al., 2017). When only 2 or 3 stable isotope ratios are considered in the quantification of isospaces, the output might not reflect all the variables influencing the trophic ecology of a species (Cransveld et al., 2017). Metal isotope fractionation of biological systems occurs as a result of several processes. As such, it might result in a large variability of δ values for each specific element and an overlap of isotope signatures (Wiederhold, 2015). In organisms like marine mammals, where isotopic fractionation is influenced by many metabolic processes, there is a higher risk of this occurring very often, leading to uncomplete and speculative discussions (Newsome et al., 2010). Combining isotopic values of individual elements in a multi-dimensional space, would allow to increase the resolution of the isotopic signal and refine the interpretation of isotopic data (Boecklen et al., 2011).

In the literature, C, N, S and Hg stable isotopes are always used separately, either as tracers of marine mammals' trophic ecology (Blévin et al., 2020; Das et al., 2017; Matley et al., 2015; Pinzone et al., 2019) or Hg sourcing (Masbou et al., 2018; Perrot et al., 2012). Using a multivariate approach could contend with the complexity of simultaneously analyzing multiple variables (in this case C, N, S

and Hg stable isotopes) (Ramette, 2007). Generally, multivariate approaches are favored to multiple executions of univariate methods as they save time and conserve statistical power which is quickly lost through multiple testing (Buttigieg and Ramette, 2014). Moreover, taking multiple variables into account simultaneously may reveal patterns that would not be detectable by univariate methods. For example, Hg sourcing and accumulation in marine mammals is known to depend on several factors such as age, sex, nutritional status, key-period of life and geographical distribution (Das et al., 2004; Habran et al., 2013; Savery et al., 2013). Testing their effect on Hg concentrations separately, might mask synergetic effects given by the combination of two or more other factors.

The main objective of this chapter was to understand which factor influences the most Hg sources and accumulation in Arctic marine mammals. Based on previous literature, our initial hypothesis was that a larger species, feeding on higher trophic level prey like the hooded seal, could be at higher risk of Hg exposure (Loseto et al., 2008a).

To test our analysis, we measured THg levels, C, N, S and Hg stable isotopes in muscle tissue of 3 species of true seals living and breeding in the Greenland Sea: the hooded seal *Cystophora cristata*, the harp seal *Pagophilus groenlandicus* and the ringed seal *Pusa hispida*.

We wanted to answer **two specific questions**:

1. Which factor between age, nutritional status, sex, species, habitat use, sampling area and time influences the most Hg sources to Greenland Sea seals?
2. Which are the consequences on the levels of Hg bioaccumulation in hooded, harp and ringed seals?

2. MATERIAL AND METHODS

Details about the sampling and analysis are given in [chapter 2](#). Hereby, we will report only additional information about the specific technics used in this study.

2.1. Sampling protocol

Samples of muscle tissue were collected from 52 hooded seals *Cystophora cristata*, 134 ringed seals *Pusa hispida* and 42 harp seals *Pagophilus groenlandicus* harvested between 2008 and 2019 along the East coast of Greenland (68°05'N/15°45'W to 72°50'N/22°45'W). Hooded and harp seals were harvested offshore, on the drift ice of the Greenland Sea and Denmark Strait; while ringed seals were harvested on land fast ice in the Scoresby Sound (Ittoqqortoormiit or Kap Tobin, Figure 5.1). Muscle samples from 2008 to 2015 were gathered from the tissue banks of the Institute of Marine Research in Tromsø (Norway), the Arctic University of Norway UiT in Tromsø (Norway) and the Bioscience Department of the University of Aarhus in Roskilde (Denmark).

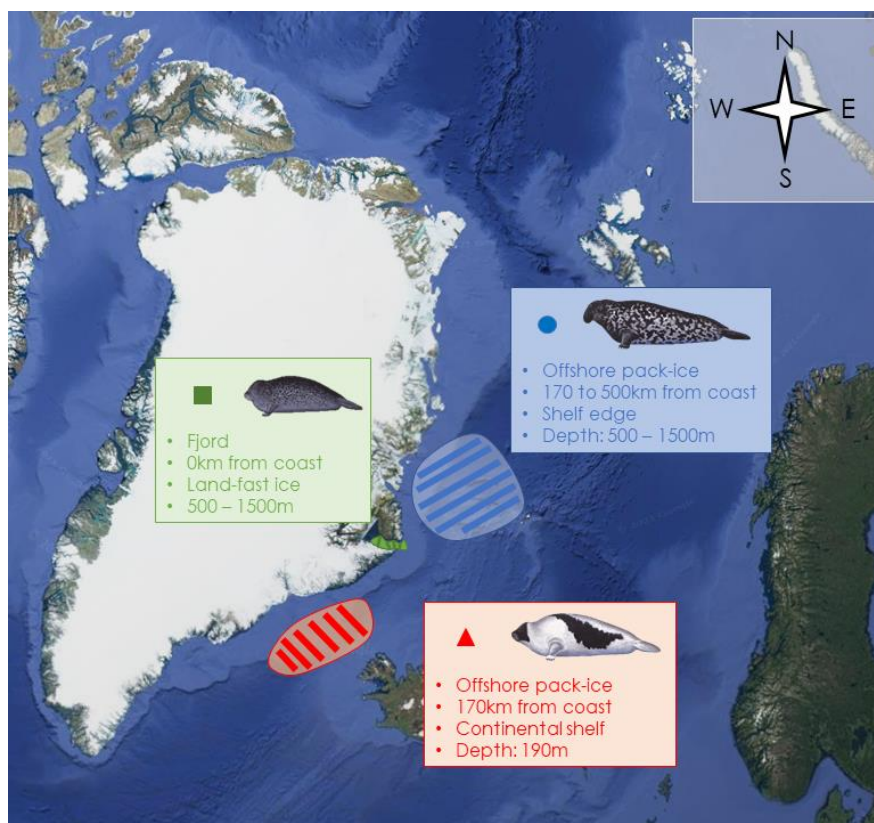


Figure 5.1. Map of the 3 sampling zones of this work: the Scoresby Sound (Green), offshore West Ice (Blue) and Denmark Strait (Red). Hooded seals were all sampled from the West Ice and are represented in blue. The harp seals were sampled from the Denmark Strait and are represented in red. Ringed seals were all sampled in the Scoresby Sound and are represented in green. The different habitat use are shown by shapes: circle for offshore / benthopelagic; triangle for offshore / pelagic; square for coastal / sympagic.

Muscle samples from 2015 to 2019 were collected from free-ranging animals during at-sea campaigns on board of the RV Helmer Hansen, in collaboration with the Arctic University of Tromsø (more details at [§4.1](#)). For tissue-bank individuals, age calculated by counting annual layering in the cementum of the canine or premolar teeth (Dietz et al., 1991). For free-ranging seals, age was estimated using animals' pelage coloring (Chapter 2, [§5](#)).

2.2. Total-mercury and stable isotopes analysis

Around 5mg of powder samples were weighted (nearest 0.01 mg) and analyzed for Total Hg concentration (THg, hereafter expressed as ng g⁻¹ dry weight, dw) using atomic absorption spectroscopy (AAS) on a Tri-cell Direct Mercury Analyzer 80 (DMA-80 evo, Milestone, Italy) (Chapter 2, [§7.1](#)).

Around 2.5mg of powder were weighted (nearest 0.001mg) and analyzed for C, N and S stable isotopes using an IRMS (IsoPrime 100, Isoprime, U.K.) coupled in continuous flow to an elemental analyzer (EA, Vario MICRO cube, Elementar, Germany) (Chapter 2, [§7.2](#)). The isotopic ratios were estimated relative to international references Vienna Pee Dee Belemnite (VPDB) for carbon, Atmospheric Air for nitrogen and Vienna Canyon Diablo Troilite (VCDT) for S as in equation 1.3 (Chapter 1, [§3.1](#)). Following international recommendations, the isotopic ratios (R) of N, C and S are expressed in delta (δ) notation in parts per thousand (‰) (Coplen, 2011). In order to correct for the bias given by the strong ¹³C depletion of lipids, we normalized $\delta^{13}\text{C}$ values using the equation 2.3 (Chapter 2, [§8.1](#)).

Hg isotopic analyses were performed on 0.1 to 0.15 g of seal muscle in a Nu Plasma HR MC-ICPMS (Nu Instruments, UK) using a continuous flow Cold Vapor Generation (CVG), after a 48h acid predigesting with Hot block (HB) (Chapter 2, [§7.4](#)). Hg isotopic values were reported as delta (δ) notation values (in per mil, ‰), calculated relative to the bracketing standard NIST SRM-3133 CRM to allow inter-laboratory comparisons. Isotope ¹⁹⁸Hg was used as the reference for ratio determination of all other Hg isotopes, using equation 1.4 (Chapter 1, [§3.2](#)). δ represents mass dependent fractionation (MDF) and Δ represents mass independent fractionation (MIF). Hg-MDF was calculated with equation 1.5. Hg odd MIF was calculated with equation 1.6 and 1.8. Hg even-MIF was calculated with equation 1.7 and 1.9 (Chapter 1, [§3.2](#)).

NIST SRM-997 thallium standard solution was used for the instrumental mass-bias correction using the exponential law (details in Chapter 2, [§7.4](#)). Internal reproducibility of the analytical method was performed on the medium and long-term through repetition of the measurement of CRMs (ERM-464-1, Tuna fish muscle), the IRM NIST 8610 and selected seal samples. Uncertainty for delta values was calculated using 2SD typical errors for each internal reference material. The long-term precision (2SD) for Hg isotopic values was satisfactory for the most analyzed reference samples: UM-Almaden (0.14

‰ and 0.08 ‰, $n = 42$) and ERM-464-1 (0.15 ‰ and 0.13 ‰, $n = 13$) for $\delta^{202}\text{Hg}$ and $\Delta^{199}\text{Hg}$ values, respectively.

2.3. Statistical analyses

In order to efficiently use multivariate analysis some assumptions must be met. Two of those are a Gaussian distribution of the data and the absence of co-linearity (or co-dependency) between the response variables (Buttigieg and Ramette, 2014). The ROUT method was used to identify outliers (Figure 5.2), with a maximum False Discovery Rate (FDR) $Q = 0.1\%$ (Motulsky and Brown, 2006). Normality of our data was tested with the Shapiro-Wilk test. The skewness, kurtosis and difference between resulting mean and median were additionally calculated in order to select which statistical tests to use (parametric vs. non-parametric). Even if most of the data were not normal, the kurtosis and skewness resulted <1 for most of data groups, indicating a symmetrical tendency of the curve and proximity to the Gaussian distribution. Variance of Hg stable isotopes between seal species was analyzed through a two-way ANOVA test, after normalization. Family-wise significance and confidence level was set at $\alpha = 0.05$ (95 % confidence interval) for all tests. The rest of covariance and variance analysis were conducted with non-parametric tests.

Spearman correlation matrices were computed for each species separately, between all the response variables considered in this study (Table A5.1). This allowed to screen for the presence of co-dependency and select the variables to use in the exploratory multivariate analysis (Table 5.1).

Table 5.1. Selected input parameters for the multivariate model.

Model's parameters	Measured Variables
Response variables:	$\delta^{13}\text{C}$, $\delta^{34}\text{S}$, $\delta^{15}\text{N}$, $\Delta^{199}\text{Hg}$, $\Delta^{200}\text{Hg}$, $\delta^{202}\text{Hg}$ and $\Delta^{204}\text{Hg}$
Explanatory numerical variables (or numerical factors):	blubber thickness, standard length, sampling month, sampling year
Explanatory nominal variables (or nominal factors):	species, sampling zone, age group and sex

Blubber thickness was used as a proxy of seal nutritional status (Derosus et al., 2020; Kauhala et al., 2019), while standard length as a proxy of seals age in addition to age groups (Chapter 2, §5) (Chabot and Stenson, 2002; Wiig, 1985). The Redundancy Analysis (RDA) was conducted to test the importance of both nominal and numerical factors at explaining our dataset (Ramette, 2007). The RDA inertia was used as QA of our analysis. This value is calculated as the proportion of constrained variables over the proportion of non-constrained ones.

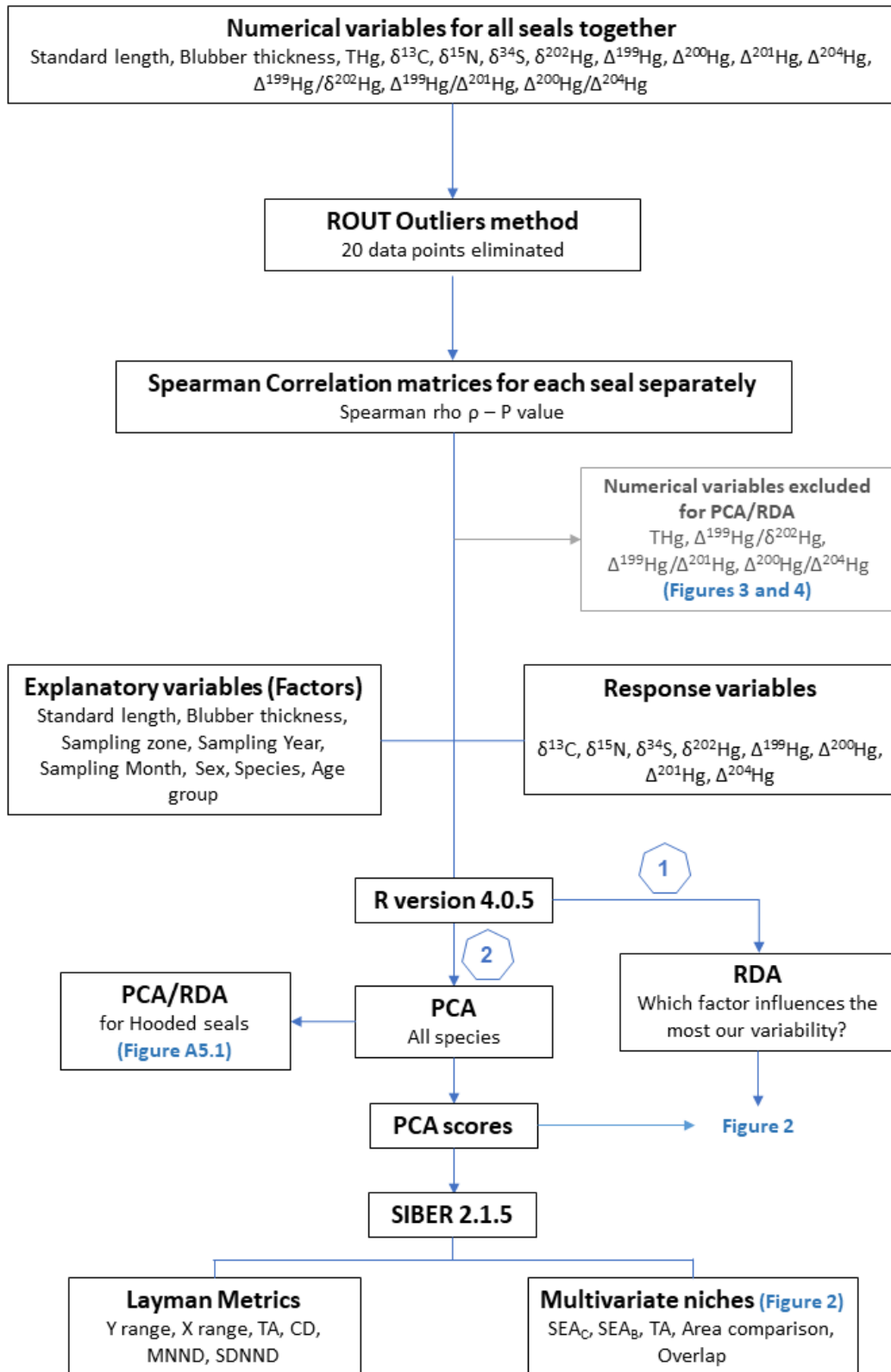


Figure 5.2. Schematics of the ensemble of descriptive and multivariate statistical analysis conducted for this chapter. SIBER metrics: SEA = Standard Ellipse Area; TA = Total Area. Layman metrics: CD = Mean distance to centroid; MNND = Mean nearest neighbor distance; SDNND = Standard Deviation of nearest neighbor distance.

The proportion of constrained variables indicate the amount of response variables which are affected by the selected factors. We validated our RDA analysis when the proportion of constrained variables was $\geq 80\%$.

The Principal Component Analysis was then used to summarize, in a low-dimensional space, the multi-isotopic variance in our three species (Buttigieg and Ramette, 2014). Several PCA runs were conducted in order to find the combination of factors and response variables that would explain most of the variability of our dataset (Figure 5.2). The Broken Stick method was used to estimate the number of informative PCs generated by the PCA (Buttigieg and Ramette, 2014).

The Stable Isotopes Bayesian Ellipses (SIBER) package (version 2.1.5) in R (version 4.0.5; R Core Team 2017) was used to quantify the differences between the multi-isotopic spaces of harp, hooded and ringed seals resulting from the PCA, through the generation of multivariate standard ellipses (SEA) and Layman metrics (Jackson et al., 2011; Layman et al., 2007). These ellipses would represent seals' ecological niches. They will include all the information relative to species trophic ecology and Hg sources given by the ensemble of C, N, S and Hg stable isotopes (Layman and Allgeier, 2012). To limit calculation biases when comparing small and/or unbalanced samples, standard ellipses areas were corrected for small sample size (SEA_C) (Syväranta et al., 2013). Niche areas of each species were estimated via 10^6 Bayesian permutation runs (SEA_B) (Layman et al., 2012). Direct pairwise comparisons were performed and considered meaningful when probability of occurrence (e.g. number of model solutions where a given situation was found) exceeded 95 %. The geometric overlap among ellipses and differences between SEA_C was also measured and compared between species (Ryan et al., 2013).

Descriptive statistical analysis was conducted in GraphPad Prism version 8.4.2 for Windows (GraphPad Software, San Diego, California USA, www.graphpad.com). Multivariate and SIBER analysis was instead run in R version 4.0.5 (R Development Core Team, 2011).

2.4. Data interpretation

Each response variable was used to interpret all the different aspects of seals ecology and Hg accumulation (Table 5.2). To interpret the PC ordination, we applied the type I scaling system (Legendre and Legendre, 2012; ter Braak, 1994):

1. Distances between object points approximate the Euclidean distances between objects. Objects ordinated closer together can be expected to have similar variable values;
2. The length of the arrow indicate the importance of the variable along a PC;
3. The angle of such arrow with PC1 and PC2 estimates the correlation of the variable to one PC or the other ($<90^\circ$ = strong correlation);

4. The distribution of each data point with respect to the arrow reflect the position of such point within the measured range for that variables: points closer to the points would reflect higher values of the variable than points close to the base of the arrow.

Table 5.2. Ecological Interpretation of response variables in hooded, harp and ringed seals.

Variables	Interpretation	Definition
THg	Levels of Hg exposure	THg concentrations
$\delta^{13}\text{C}$ and $\delta^{34}\text{S}$	Habitat use: Offshore vs. coastal Benthic/Pelagic vs. sympagic	Trophic tracers
$\delta^{15}\text{N}$	Trophic position	
$\Delta^{199}\text{Hg}$ and $\delta^{202}\text{Hg}$	Habitat use: Offshore vs. coastal Hg reservoirs: Seawater vs. freshwater/ice	Marine Hg tracers
$\Delta^{200}\text{Hg}$ and $\Delta^{204}\text{Hg}$	Hg reservoirs: Precipitations vs. atmosphere	Atmospheric Hg tracers
Hg isotope slopes	Hg environmental formation and pathways	Hg sources

In this study, we interpreted and discussed Hg stable isotope data as (1) simple delta values, (2) isotopic slopes and (3) extent of MDF and MIF. In the last case, the term “Hg MDF” will refer to variation of $\delta^{202}\text{Hg}$ values. “Hg odd MIF” will refer to variation of $\Delta^{199}\text{Hg}$ and $\Delta^{201}\text{Hg}$ values, while “Hg even MIF” will refer to variation of $\Delta^{200}\text{Hg}$ and $\Delta^{204}\text{Hg}$ values.

In this study we did not quantify Hg species. Therefore, in our discussion we refer to MeHg as the ensemble of methylated Hg forms (monomethyl and dimethyl-Hg).

3. RESULTS

3.1. Multivariate analysis

The RDA analysis and the ANOVA post-hoc permutation test showed that the selected input factors explained around 60 % of the variability of our response variables (adjusted $R^2 = 0.616$, $F = 3.69$, $p < 0.0001$). RDA1 and RDA2 explained 83 % of the total variance of our dataset (Table A5.2). The eigenvalue loadings showed that, along RDA1, $\delta^{34}\text{S}$ value was the variable influencing the most the distribution of the data (score = -2.81). Along RDA2, most of the variability was explained by $\delta^{13}\text{C}$ and $\delta^{15}\text{N}$ values (score = -0.88 and -0.99; respectively). The most important factors explaining the variability of our dataset were the sampling area (adjusted $R^2 = 0.372$, $F = 14.81$, $p = 0.001$) and the species (adjusted $R^2 = 0.363$, $F = 14.42$, $p = 0.001$), explaining 37 % and 36 % of the total variance, respectively (Table A5.3).

With regard to the PCA, PC1 and PC2 explained 58 % of all the analyzed variables (Table A5.3). The eigenvalue loadings showed that along PC1 $\Delta^{200}\text{Hg}$ explained most of the variability (score = -1.20), followed by $\delta^{34}\text{S}$ (score = -1.10), $\Delta^{204}\text{Hg}$ (score = 1.08) and $\Delta^{199}\text{Hg}$ values (score = 1.01). Along PC2 $\delta^{13}\text{C}$ explained most of the variability (score = 0.98), followed by $\delta^{202}\text{Hg}$ (score = 0.92) and $\delta^{15}\text{N}$ values (score = 0.88) (Table A5.3).

3.2. SIBER

Hooded seals presented the largest SEA_B (Mode, 95 % CI: 0.93, 0.60 – 1.41), followed by harp seals (Mode, 95 % CI: 0.31, 0.14 – 0.68) and ringed seals (Mode, 95 % CI: 0.22, 0.14 – 0.37). Hooded seal SEA_B was larger than those of harp and ringed seals in 99 and 100 % of model's runs. Harp seals' SEA_B was larger than that of ringed seals only in 81.2 % of model's runs. Therefore, these two SEAs were not considered significantly different. No overlap was found between hooded and ringed seals multivariate niches. Only a small overlap resulted between harp and hooded seals, involving 7 % of harp seals' niche and 3 % of hooded seals' niche. The measurement of Layman metrics did not add any significant information to data interpretation, therefore we won't discuss them further. All measured values are summarized in Table A5.4.

3.3. Stable isotope ratios

$\delta^{13}\text{C}$ values differed significantly between species ($KW = 97.1$, $p < 0.0001$), with hooded seals being the most enriched in ^{13}C , followed by harp and ringed seals (Table 5.3). Hooded seal presented

significantly higher $\delta^{34}\text{S}$ values than the other 2 species ($KW = 50.1$, $p = 0.0003$), which did not differ between each other. No difference was found for $\delta^{15}\text{N}$ between the 3 species ($KW = 1.51$, $p = 0.469$). In hooded seals, $\delta^{13}\text{C}$ values differed only between adult males, and the other age groups ($KW = 13.4$, $p = 0.004$). Adult males and yearlings presented significantly higher $\delta^{15}\text{N}$ values than adult females and subadults ($KW = 33.8$, $p < 0.0001$). No difference was found between the $\delta^{34}\text{S}$ values of all age groups ($KW = 9.75$, $p = 0.02$). In harp seals, no difference was found for $\delta^{13}\text{C}$ and $\delta^{34}\text{S}$ values ($KW = 5.62$, $p = 0.13$, $KW = 6.32$, $p = 0.10$; respectively). Conversely, yearlings resulted significantly more enriched in ^{15}N with respect to adult females ($KW = 25.2$, $p < 0.0001$). In ringed seals, no difference was found between $\delta^{13}\text{C}$, $\delta^{15}\text{N}$ and $\delta^{34}\text{S}$ values of all age groups ($KW = 4.37$, $p = 0.22$, $KW = 5.75$, $p = 0.12$ and $KW = 2.11$, $p = 0.55$; respectively).

Hg stable isotope ratios differed significantly between species (2w-ANOVA $F = 25.5$, $p < 0.0001$; Table 5.3). Hooded and harp seals presented significantly higher $\delta^{202}\text{Hg}$ values compared to ringed seals ($p < 0.0001$ on both cases). Hooded seals presented also significantly higher $\Delta^{200}\text{Hg}$ and $\Delta^{201}\text{Hg}$ values than ringed seals ($p = 0.001$ and $p = 0.003$, respectively). No differences were found for $\Delta^{199}\text{Hg}$ and $\Delta^{204}\text{Hg}$. The $\Delta^{199}\text{Hg}/\Delta^{201}\text{Hg}$ slope ranged from 1.09 ± 0.05 and 1.09 ± 0.06 in harp and hooded seals, to 1.25 ± 0.06 in ringed seals. All slopes showed a significant correlation between the isotopes ($p < 0.0001$, $R^2 = 0.977$, $R^2 = 0.902$ and $R^2 = 0.947$, respectively). The $\Delta^{199}\text{Hg}/\delta^{202}\text{Hg}$ slope ranged from 0.6 ± 0.09 and 0.91 ± 0.07 in harp and hooded seals, to 1.41 ± 0.33 in ringed seals. All slopes showed a significant correlation between the isotopes when fitted to zero ($p < 0.0001$, $R^2 = 0.325$, $R^2 = 0.380$ and $R^2 = 0.648$, respectively). The $\Delta^{200}\text{Hg}/\Delta^{204}\text{Hg}$ slope ranged from -0.16 ± 0.09 in hooded seals, -0.10 ± 0.18 in harp seals to -0.06 ± 0.07 in ringed seals. None of these slopes were significant. The $\Delta^{200}\text{Hg}/\delta^{202}\text{Hg}$ slope ranged from 0.00 ± 0.01 in harp seals, 0.00 ± 0.01 in ringed seals, to 0.03 ± 0.005 in hooded seals. The slope showed a significant correlation only for hooded seals ($p < 0.0001$, $R^2 = 0.03$). Because of the large variability in Hg even MIF values, the interpretation of $\Delta^{200}\text{Hg}/\Delta^{204}\text{Hg}$ and $\Delta^{200}\text{Hg}/\delta^{202}\text{Hg}$ slopes might be misleading. As such, these slopes were not interpreted, but only presented in Figure A5.1.

3.4. Mercury levels

THg concentrations differed significantly between species ($KW = 90.1$, $p < 0.0001$), with ringed seals presenting the highest values, followed by hooded and harp seals (Figure 5.4). For hooded seals, adult males were significantly more contaminated than subadults and yearlings ($p = 0.0001$ and $p = 0.0009$, respectively), but did not differ from adult females (Table 5.4). For harp seals, the only difference was found between yearlings and all other age groups ($KW = 14.9$, $p = 0.0008$). For ringed seals, no difference was observed between age groups ($KW = 6.46$, $p = 0.09$).

Table 5.3. Carbon, nitrogen, sulphur and Hg stable isotope values measured in muscle tissue of hooded, harp and ringed seals from the East coast of Greenland from 2008 and 2019. Data are expressed in delta notation, in per mill (‰). Mass-dependent fractionation (MDF) is shown as δ , mass-independent fractionation (MIF) is shown as Δ . Results are presented as Mean \pm SD, (Min – Max) *n*. N_{tot} = Number or analyzed seals.

	Hooded seal <i>Cystophora cristata</i> Cc (N_{tot} = 52)	Harp seal <i>Pagophilus groenlandicus</i> Pg (N_{tot} = 42)	Ringed seal <i>Pusa hispida</i> Ph (N_{tot} = 134)
$\delta^{13}\text{C}$	-20.2 \pm 0.48 (-20.9 to -18.9) 52	-20.8 \pm 0.59 (-22.0 to -19.3) 28	-21.3 \pm 0.49 (-23.3 to -20.5) 116
$\delta^{15}\text{N}$	14.1 \pm 0.99 (12.3 - 16.6) 52	13.9 \pm 1.0 (11.6 - 15.9) 39	14.2 \pm 0.93 (11.7 - 15.9) 118
$\delta^{34}\text{S}$	18.8 \pm 2.47 (12.0 - 21.8) 51	17.1 \pm 0.97 (14.5 - 17.9) 39	16.5 \pm 1.25 (14.0 - 19.0) 117
$\delta^{202}\text{Hg}$	0.86 \pm 0.36 (0.15 - 1.64) 35	0.99 \pm 0.37 (0.34 - 1.56) 12	0.21 \pm 0.31 (-0.44 to 1.32) 28
$\Delta^{199}\text{Hg}$	0.91 \pm 0.18 (0.36 - 1.22) 35	0.74 \pm 0.19 (0.51 - 1.16) 12	0.80 \pm 0.21 (0.43 - 1.43) 28
$\Delta^{200}\text{Hg}$	0.03 \pm 0.03 (-0.03 to 0.09) 35	0.00 \pm 0.03 (-0.03 to 0.08) 12	-0.00 \pm 0.02 (-0.04 to 0.05) 28
$\Delta^{201}\text{Hg}$	0.75 \pm 0.15 (0.29 - 1.03) 35	0.60 \pm 0.17 (0.45 - 0.99) 12	0.61 \pm 0.17 (0.34 - 1.10) 28
$\Delta^{204}\text{Hg}$	-0.03 \pm 0.07 (-0.19 to 0.10) 35	0.01 \pm 0.05 (-0.10 to 0.08) 12	0.00 \pm 0.02 (-0.16 to 0.11) 28

Table 5.4. THg concentrations (as ng g⁻¹ dw) in the muscle of hooded, harp and ringed seals sampled between 2008 and 2019 in along the East coast of Greenland. Data are presented by age group as Mean (Median) \pm SD, (Min – Max). *n* : Number of analyzed samples. N_{tot} = Number or analyzed seals.

	Hooded seal <i>Cystophora cristata</i> Cc (N_{tot} = 52)	Harp seal <i>Pagophilus groenlandicus</i> Pg (N_{tot} = 42)	Ringed seal <i>Pusa hispida</i> Ph (N_{tot} = 134)
Adult Males	2237 (1489) \pm 1753 (613 - 4907) <i>n</i> : 8	461 <i>n</i> : 1	1219 (1237) \pm 447 (249 - 2174) <i>n</i> : 35
Adult Females	773 (629) \pm 340 (365 - 1443) <i>n</i> : 12	498 (413) \pm 297 (256 - 1163) <i>n</i> : 15	1043 (905) \pm 442 (381 - 2207) <i>n</i> : 32
Subadults	442 (402) \pm 228 (92 - 762) <i>n</i> : 20	720 (795) \pm 220 (472 - 892) <i>n</i> : 3	1265 (1251) \pm 530 (441 - 3508) <i>n</i> : 60
Yearlings	454 (410) \pm 233 (152 - 933) <i>n</i> : 12	283 (225) \pm 240 (55.5 - 1145) <i>n</i> : 19	1048 (967) \pm 422 (602 - 1215) <i>n</i> : 6

4. DISCUSSION

4.1. Habitat use is the most important factor influencing the multi-isotopic composition of Arctic true seals

The RDA analysis shows that the most important factors to significantly explain the isotopic variance of hooded, harp and ringed seals are the sampling location (37 % of variability) and the species (36 % of variability). However, in this particular case we should not consider these 2 factors as separated. In this study, each species was sampled from a different sampling location: the hooded seal from the “West ice” (offshore, open water, pack-ice), the harp seal from the “Denmark Strait” (offshore, continental shelf, pack-ice) and the ringed seal from the Scoresby Sound (inshore, fjord, land fast ice) (Figure 5.1). Since the sampling location and the species overlap, they should influence in the same way the variability of our dataset. This is confirmed by the similar percentage of variability they explain in the RDA. The hooded seal is an oceanic subarctic species, which uses the drifting pack-ice of the Greenland Sea during winter for breeding and mating (Andersen et al., 2013). Afterwards, they undertake long migrations all around the North Atlantic Ocean, from the southernmost coasts of Europe to Svalbard (Bellido et al., 2009; Stenson, 2014). Hooded seals were never observed in coastal waters of the Greenland Sea (Vacquie-Garcia et al., 2017). This species remains strongly associated with the continental shelf edge and deep ocean (Tucker et al., 2009). The harp seal is also an offshore species which relies on the drifting pack-ice for breeding and mating. However, this species undergoes shorter annual migrations – often limited to the northern waters of the Atlantic Ocean – and remains mostly associated with the continental shelf (Tucker et al., 2009). The eastern Greenland subpopulation of ringed seal adventures only rarely offshore, remaining year-round along the coast and within fjords (e.g. King Oscar Fjord, Scoresby Sound) (Born et al., 2004; Teilmann and Kapel, 2014). Looking at the sampling map, we can also observe how the 3 sampling zones of this study not only overlap with the 3 species, but also reflect the 3 different habitat uses. **This first finding indicates that the habitat use is the most important factor influencing the isotopic variability of true seals in the Greenland Sea.**

The RDA loadings show how, along both RDA1 and RDA2, most of the variability was expressed by $\delta^{34}\text{S} > \delta^{13}\text{C} \gg \delta^{15}\text{N}$ (Table A5.3). This second finding indicates that hooded, harp and ringed seals differ mostly in their C, N and S stable isotope ratios. While $\delta^{15}\text{N}$ values are usually used a proxy of species trophic position, $\delta^{13}\text{C}$ and $\delta^{34}\text{S}$ values have been used to trace marine mammals' habitat use (coastal vs. offshore, benthic vs. pelagic) (Giménez et al., 2018). The fact that $\delta^{13}\text{C}$ and $\delta^{34}\text{S}$ are more important than $\delta^{15}\text{N}$ in differentiating the 3 species, confirms again the importance of habitat use with regards to seal isotopic separation.

Nevertheless, the ANOVA permutation test shows that these variables explain only 60 % of the total variance between our species. This suggests that other variables (e.g. Hg stable isotopes) are

contributing in differentiating the 3 species within the PC space, and explaining the 40 % of variance not expressed by $\delta^{15}\text{N}$, $\delta^{13}\text{C}$ and $\delta^{34}\text{S}$ values. To test this hypothesis, we conducted a multivariate PCA/SEA analysis combining all trophic and Hg isotopic tracers. The PCA assesses which isotopic tracer is the most important variable to describe the variance between our 3 species. Then, the calculation of species multivariate niches (SEA_B) allows to quantitatively measure species-specific differences.

Harp and ringed seals' SEAs are homogeneously distributed on the central and right side of the graph respectively (Figure 5.3). Hooded seals present the largest SEA, widely distributed over the left side of PC1 and all along PC2. No significant overlap occurs between the multivariate niches of hooded, harp and ringed seals (blue, red and green SEA, respectively).

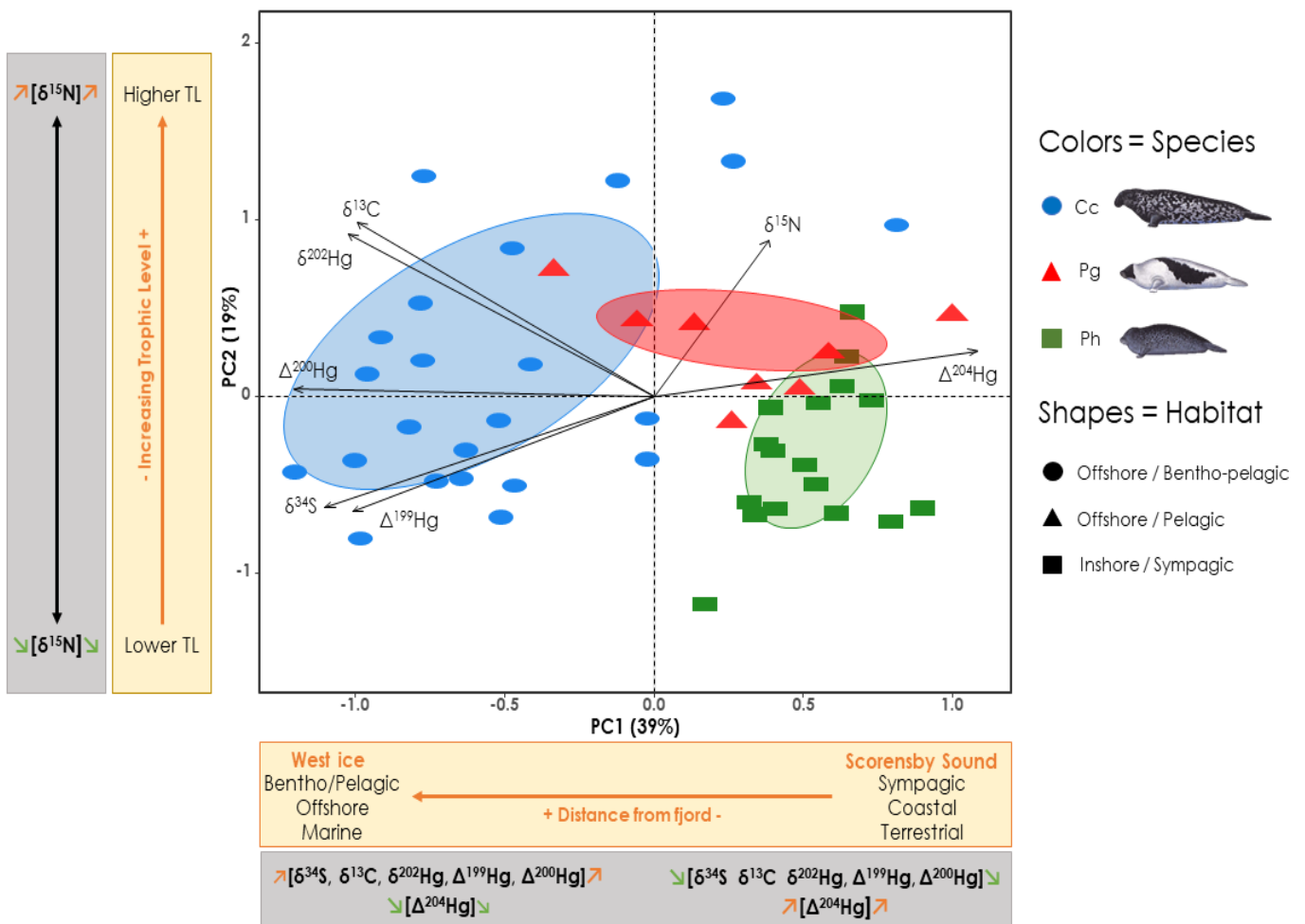


Figure 5.3. PCA scores biplot for hooded seals (Cc), harp seals (Pg) and ringed seals (Ph) sampled between 2008 and 2019 in the Greenland Sea. The response variables are shown as black arrows. Species are shown by colors as presented in the biplot. Multivariate niches are represented by the SIBER modelled SEA_B (40 % of total data points of each species). The variance of response variables along PC1 and PC2 is shown in the grey boxes. Orange arrows indicate an increase in the δ (or Δ) value, green arrows indicate a decrease. The ecological interpretation of the multivariate niches is shown in the orange boxes. The percentage explained by each PC is shown between brackets for each axis.

The distribution of seals' SEAs along PC1 reflect the 3 different habitats use: inshore, within the Scoresby Sound for ringed seals, on the continental shelf of the Denmark Strait for harp seals and the offshore west ice for hooded seals (Figure A5.2). **This shows that habitat use is also the most important factor to influence Hg isotopic composition of Arctic true seals.** The PCA loadings show that along PC1 the most important variables for species SEAs distribution are: $\Delta^{200}\text{Hg} > \delta^{34}\text{S} > \Delta^{204}\text{Hg} > \delta^{202}\text{Hg} > \Delta^{199}\text{Hg} > \delta^{13}\text{C}$ (Table A5.2). This confirms that Hg stable isotopes are as important as C, N and S ones in differentiating hooded, harp and ringed seals.

The distribution of SEAs along PC1 indicate that:

- Hooded seal niche is characterized by higher values of $\delta^{34}\text{S}$ and $\delta^{13}\text{C}$, $\delta^{202}\text{Hg}$ and $\Delta^{199}\text{Hg}$, $\Delta^{200}\text{Hg}$, and negative values of $\Delta^{204}\text{Hg}$;
- Ringed seal niche is characterized by lower values of $\delta^{34}\text{S}$ and $\delta^{13}\text{C}$, $\delta^{202}\text{Hg}$ and $\Delta^{199}\text{Hg}$, $\Delta^{200}\text{Hg}$, and positive values of $\Delta^{204}\text{Hg}$;
- Harp seal niche is characterized by intermediate values of $\delta^{34}\text{S}$ and $\delta^{13}\text{C}$, $\delta^{202}\text{Hg}$ and $\Delta^{199}\text{Hg}$, but presented values of $\Delta^{200}\text{Hg}$ and $\Delta^{204}\text{Hg}$ similar to hooded seals.

As seen in previous literature, each of these variables can act as proxies of several aspects of the trophic ecology of marine predators (Table 5.2) (Das et al., 2017; Li et al., 2020; Pinzone et al., 2019; Renedo et al., 2018). In the case of Hg stable isotopes, they could additionally trace possible difference in Hg sourcing as a consequence of seal habitat use (Cransveld et al., 2017; Le Croizier et al., 2020; Pinzone et al., 2021a).

The PCA loadings show how the most important variables for species SEAs distribution along PC2 are: $\delta^{15}\text{N}$ and $\delta^{202}\text{Hg}$ (Table A5.2). The analysis of data suggests that the large spread of hooded seal SEA along PC2 could be linked with shifts in diet and habitat use between age groups. To study this hypothesis, we conducted a second PCA and RDA for hooded seals only (Figure A5.3). Since the main focus of this chapter are Hg sources, we do not discuss this part here. A more detailed explication can be found in Annex to Chapter 5 (page [230](#)).

4.2. Offshore *versus* coastal habitat use

$\delta^{34}\text{S}$ values in marine biota respond to changes in the abundance and isotopic composition of sulfates (SO_4^{2-}) in the water column (Böttcher et al., 2007). Several factors may modify sulfate cycling such as salinity gradients, concentration of organic matter (OM), proximity of freshwater inputs or, in coastal areas, anoxic reactions in sea bottom sediments (Böttcher et al., 2000). The $\delta^{34}\text{S}$ of modern ocean sulfate is spatially homogeneous (20.9 to 21.1 ‰), reflecting the sources and sinks of sulfate to the ocean (Tostevin et al., 2014). Marine biota living in coastal or freshwater ecosystems are usually depleted in ^{34}S ($\delta^{34}\text{S}$ from 5‰ to 15‰) as a result of the higher proportion of isotopically depleted

sulfide relative to enriched aqueous sulfates typical of these zones, and the strong oxidation and processing of riverine OM (Fry and Chumchal, 2011; Tostevin et al., 2014). For this reason stable S isotopes can help defining the habitat use (e.g. hunting and distribution) of a species (Connolly et al., 2004; Gomes and Hurtgen, 2013). Hooded seals present physiological adaptations (Geiseler et al., 2013) that allow them to dive down to mesopelagic waters (>700m of depth since their first months of life; Folkow et al., 2010) and hunt for a large variety of benthic-pelagic species such as cephalopods (*Gonatus fabricii*) and gadidae (*Gadus morhua* and *Boreogadus saida*) (Haug et al., 2004; Potelev et al., 2014). Therefore, **the higher $\delta^{34}\text{S}$ values of hooded seals (19 to 21 ‰) might reflect the general deep oceanic hunting behavior of this species.**

Harp and ringed seals present $\delta^{34}\text{S}$ values ranging from 14 to 19 ‰. Harp seals are generalist pelagic hunters, remaining within the first 50m of the water column in most of their dives. Also, they are found in strong association with pack-ice for the bigger part of the year (Folkow et al., 2004; Nordøy et al., 2008). $\delta^{34}\text{S}$ values ranging from 16 to 18 ‰ agree with values found in sulfate from subsurface offshore waters near pack-ice, where S cycling can be influenced by several processes (Tostevin et al., 2014). **Harp seal $\delta^{34}\text{S}$ values might be related to the higher reliance on ^{34}S depleted sulfides typical of S and OM processing under the ice** (Carnat et al., 2018; Vancoppenolle et al., 2013). The ringed seal is a very territorial species, relying on the fjords land fast and pack-ice all year round (Born et al., 2004; Siegstad et al., 2014). $\delta^{34}\text{S}$ values ranging from 14 to 17 ‰ are in agreement with ice-S compounds and marine biota associated with Antarctic sea-ice (Carnat et al., 2018; Michel et al., 2019), as well as anadromous fish living in coastal waters (Fry and Chumchal, 2011). Therefore, **ringed seal $\delta^{34}\text{S}$ values could reflect their reliance on ^{34}S depleted sulfides typical of S and OM from sea-ice and terrestrial watersheds, typical of coastal zones like fjords.**

Such interpretation is confirmed by the gradient of $\delta^{13}\text{C}$ values that are the highest in hooded seals, followed by harp seals and ringed seals. Ringed seal low $\delta^{13}\text{C}$ values are most likely related to the influence of freshwater input in the Scoresby Sound from rivers and melting ice (Cottier et al., 2010; de la Vega et al., 2019). In offshore water, increasing $\delta^{13}\text{C}$ values are found going from surface to mesopelagic waters (Le Croizier et al., 2019; Pinzone et al., 2019; Tucker et al., 2013). This results from the influence of organic C (OC) remineralization and processing in the anoxic deeper layers of the water column (Çoban-Yildiz et al., 2006; Woodland et al., 2012). Therefore, **the higher $\delta^{13}\text{C}$ values of hooded seals compared to harp seals might reflect their difference in deep versus shallow hunting behavior.**

4.3. Habitat use influences mercury sources

4.3.1. Tracers of Hg atmospheric sources

$\Delta^{200}\text{Hg}$ values have been used to describe Hg cycling in the atmospheric reservoir. The values found in our species are in the range described for marine biota and for Arctic marine mammals (Demers et al., 2013; Masbou et al., 2018). Masbou et al. (2018) hypothesized that the near-zero $\Delta^{200}\text{Hg}$ of Arctic Ocean biota is linked to the small size of the Arctic basin, strong continental influence via river runoff and the presence of ice cover that limits atmospheric Hg wet deposition. The range of $\Delta^{204}\text{Hg}$ values found in hooded, harp and ringed seals from Eastern Greenland was large and slightly overlapping between species (Table 5.3). It shows the opposite pattern of $\Delta^{200}\text{Hg}$ values. Higher and positive $\Delta^{200}\text{Hg}$ values (with negative $\Delta^{204}\text{Hg}$), as those showed by the offshore hooded and harp seals (on average 0.03 ‰ and 0.00 ‰, respectively), are usually found in atmospheric Hg^{2+} from wet and dry precipitations (Lepak et al., 2015). On the other hand, small negative $\Delta^{200}\text{Hg}$ values (with positive $\Delta^{204}\text{Hg}$) like those found in the coastal ringed seal (on average -0.03 ‰), are usually found in gaseous Hg^0 in the atmosphere (Sun et al., 2019). Moreover, the negative $\Delta^{200}\text{Hg}$ found in ringed seals resembles more closely the low values found in boreal soils (-0.02 ± 0.03 ‰; Obrist et al., 2017) than those found in Arctic Ocean sediments (0.00 ± 0.03 ‰; Gleason et al., 2017). This indicates that **Hg in muscle of ringed seal might derive from terrestrial atmospheric Hg inputs**. On the other hand, **Hg in muscle of hooded and harp seals might derive from precipitation particulate-bound Hg inputs** through direct exchange between the atmosphere and sea surface (Chen et al., 2012; Gratz et al., 2010).

4.3.2. Tracers of Hg marine sources

$\delta^{202}\text{Hg}$ and $\Delta^{199}\text{Hg}$ values found in our 3 species are in the range of previous reported data for seabirds, ringed seals, polar bears and narwhals living in regions above the 70°N latitude (Masbou et al., 2018, 2015a; Renedo et al., 2020). $\delta^{202}\text{Hg}$ and $\Delta^{199}\text{Hg}$ values are the highest in hooded seals, followed by harp seals and ringed seals (Table 5.3). Several studies have shown how the extent of Hg MDF (mostly represented by $\delta^{202}\text{Hg}$) and Hg odd MIF (mostly represented by $\Delta^{199}\text{Hg}$) increases going from coastal to offshore ecosystems (Li et al., 2016a; Perrot et al., 2019). Indeed, negative and near-zero MDF values of ringed seals were in accordance with values found in estuarine fish from the Northeastern coast of the U.S. and the Gulf of Mexico (Kwon et al., 2014; Senn et al., 2010), denoting a coastal habitat use. In these areas, the presence of more suspended particle loads and dissolve OM (DOM) reduces light penetration, generally leading to lower rates of Hg MDF (Li et al., 2016b). As such, MeHg bioaccumulated in coastal food webs is strongly depleted in ^{202}Hg and presents low $\delta^{202}\text{Hg}$ values (Le Croizier et al., 2020; Pinzone et al., 2021a). On the other hand, the more oligotrophic character of marine offshore waters leads to deeper light influx in the water column on

one side, and slower Hg redistribution between water layers on the other (Bowman et al., 2020). This relates to longer photochemical MeHg processing, higher rates of Hg MDF and consequently higher $\delta^{202}\text{Hg}$ and values in pelagic food webs (Kwon et al., 2020). The same processes affect also odd MIF values. Egg shelves $\Delta^{199}\text{Hg}$ values of Arctic seabirds like murre, terns and gulls were found to decrease with a more inshore distribution of nests, reflecting the higher input of Hg terrestrial geogenic reservoirs (Day et al., 2012; Hebert, 2019).

Another aspect that might contribute to the lower $\delta^{202}\text{Hg}$ and $\Delta^{199}\text{Hg}$ values in ringed seals, is their reliance on sea-ice. Point et al. (2011) proposed that the presence of sea-ice might impart negative Hg odd MIF in murre eggs. They discussed how higher concentrations of sea-ice could behave like a barrier to Hg exchanges between the oceanic and atmospheric reservoirs and limit radiation fluxes (Point et al., 2011). This would have a negative feedback on net photochemical degradation of MeHg in surface waters and result in lower rates of Hg MDF and odd MIF, with respect to open offshore waters (Point et al., 2011). These findings indicate that **in ringed seals Hg originates mostly from the marine coastal ecosystem, while in hooded and harp seals Hg originates mostly from the marine offshore ecosystem.**

4.4. Habitat use influences mercury pathways

Photochemical reactions such as Hg^{2+} reduction to Hg^0 , or MeHg photodegradation in the environment, result in specific $\Delta^{199}\text{Hg}/\Delta^{201}\text{Hg}$ and $\Delta^{199}\text{Hg}/\delta^{202}\text{Hg}$ regression lines with a precise slope value (Blum, 2011). The comparison between reference slopes and those found in biological samples are used to identify the pathways of Hg processing in the environment (Bergquist and Blum, 2009). Hg slopes differ a lot between offshore and coastal species (Figure 5.4). While hooded and harp seals present a similar $\Delta^{199}\text{Hg}/\Delta^{201}\text{Hg}$ in the line of 1.09 ± 0.05 , ringed seals present a slope of 1.25 ± 0.06 (Figure 5.4A). In the same way, while hooded and harp seals present $\Delta^{199}\text{Hg}/\delta^{202}\text{Hg}$ slopes of 0.91 ± 0.07 and 0.06 ± 0.09 respectively, ringed seals fall in the line of 1.41 ± 0.33 (Figure 5.4B). The comparison of our findings with reference slopes shows how **Hg accumulated in ringed seals seem to derive from MeHg photochemical processes** (Bergquist and Blum, 2007b), while **Hg accumulated in the other 2 species would originate from a mix of Hg^{2+} photoreduction** in both snow (slope value ~ 1.07) and seawater (slope value ~ 1.00) (Kwon et al., 2014; Sherman et al., 2010). These slopes confirm our previous interpretation of Hg atmospheric tracers ([§4.3.1](#)).

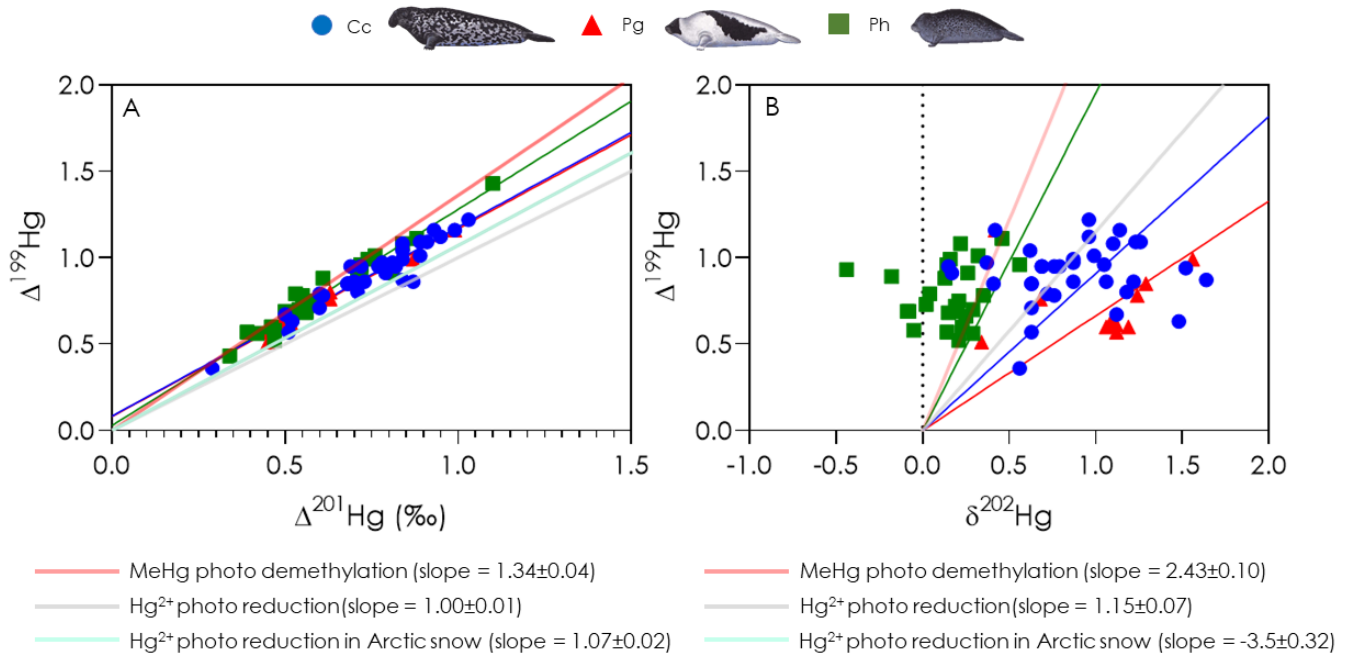


Figure 5.4. $\Delta^{199}\text{Hg}/\Delta^{201}\text{Hg}$ (A) and $\Delta^{199}\text{Hg}/\delta^{202}\text{Hg}$ (B) slopes measured in hooded (Cc, blue line), harp (Pg, red line) and ringed seals (Ph, green lines). MeHg photo-demethylation and Hg^{2+} photo-reduction slopes were extracted from (Blum et al., 2014). MeHg photo-demethylation and Hg^{2+} photo-reduction slopes in Arctic snow were extracted from (Sherman et al., 2010). Slopes are represented as mean ± SE (Standard Error). In Figure B, the $\Delta^{199}\text{Hg}/\delta^{202}\text{Hg}$ slope for Arctic snow is not figured since is not representative of our results.

4.5. Habitat use influences levels of mercury exposure

Our initial hypothesis was that preying on larger and higher trophic level benthic-pelagic prey, as in the case of hooded seals, would determine higher rates of exposure to Hg and consequently higher concentrations in seal tissues (Blévin et al., 2020; Bustamante et al., 2003; Cardona-Marek et al., 2009; Mcmeans et al., 2014a; Peterson et al., 2015; Pinzone et al., 2019). This is not confirmed by our results that instead suggest habitat use as the main driver of higher THg in muscle of Arctic seals. THg concentrations differ significantly between species with ringed seals being the most contaminated, followed by hooded and harp seals (Figure 5.5).

Previous studies demonstrated how based on the areas and food webs they exploit, marine predators might be exposed to different sources or processing of Hg, or more specifically MeHg (Mieiro et al., 2009; Pinzone et al., 2021a). The comparison of our isotopic data with THg concentrations confirms that this might be valid also for Greenland Sea seals. **The strong territoriality of ringed seal within the Scoresby Sound area leads to higher Hg exposure.** This results in higher THg bioaccumulation in this species compared to offshore pelagic and benthic-pelagic species like the harp and hooded seals. Inland anthropogenic activities such as extensive agriculture and industrial production can be important sources of Hg to the coastal marine environment, via their connection through rivers (Monperrus et al., 2007; Soerensen et al., 2016b).

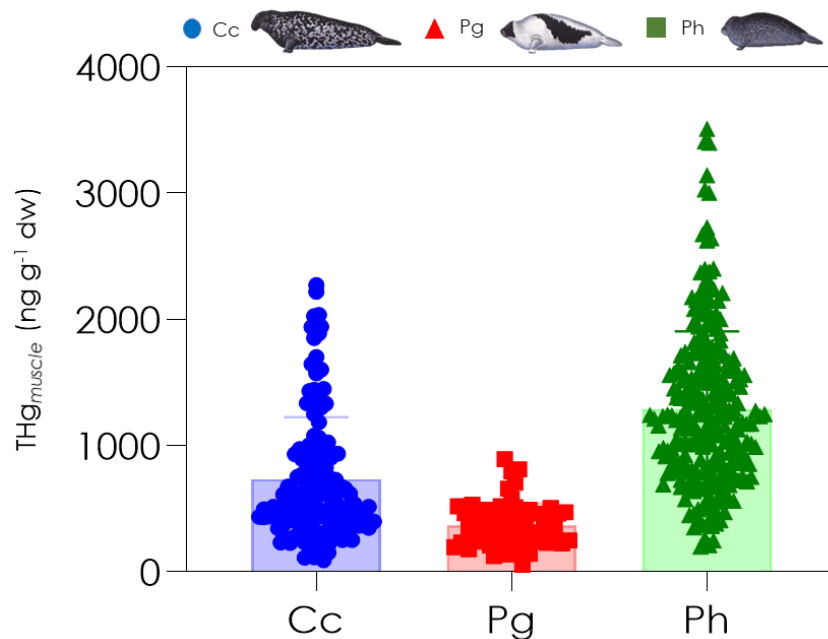


Figure 5.5. THg concentrations in muscle of hooded (Cc, blue), harp (Pg, red) and ringed seals (Ph, green) sampled between 2008 and 2019 along the Eastern coast of Greenland. Data are represented as bars (mean \pm SD) and single data points. Habitat use is represented by shapes: circle for offshore/benthopelagic/oceanic, triangle for offshore/pelagic, square for coastal/sympagic. Data are presented as $\text{ng g}^{-1} \text{ dw}$.

In the Scoresby Sound the only large human settlement is Ittoqqortoormiit, with a population of 468 in 2017 (Crump et al., 2017). This is considered one of the most pristine and remote areas of the Arctic. Therefore, higher **THg concentrations** in ringed seals are most likely **related with the pathways of Hg processing in the marine environment, rather than levels of anthropogenic pollution.**

One of the largest MeHg source in the oceans is believed to be production by **heterotrophic bacteria** in oxic surface seawaters (Blum et al., 2013). Water-column methylation is amplified in stratified waters, rich in nutrients and organic carbon (OC) like the river mouths and shallow coastal areas (Schartup et al., 2015a, 2013).

Riverine run-offs is considered as a major source of MeHg into Arctic fjords and ocean basins (Dastoor and Durnford, 2013; Schartup et al., 2015a). Arctic rivers are recognized as seasonal carriers of terrestrial Hg and OM from **vegetation, permafrost and glaciers** during spring thawing (Charette et al., 2020; Obrist et al., 2017; Seifert et al., 2019). Hg deposits onto the permafrost surface from the atmosphere, where it bonds with organic matter in the active layer (Schuster et al., 2018). Once frozen, microbial decay effectively ceases, blocking the reemission of Hg, which will be permanently store in permafrost until the warmer period (Schuster et al., 2018; Smith-Downey et al., 2010). This causes seasonal peaks of Hg export to rivers during permafrost thawing, enhancing Hg methylation in estuarine areas (Lim et al., 2019).

Increasing evidences are arising on the importance of **marginal sea-ice** as a zone of a substantial production of MeHg in the Arctic (Heimbürger et al., 2015; Soerensen et al., 2016a). Previous studies on Antarctic land fast ice confirmed the simultaneous presence of microbial communities responsible for both Hg²⁺ methylation and reduction in polar sea-ice (Gionfriddo et al., 2016; Schartup et al., 2019). In addition to the potential for *in situ* methylation, ice cover suppresses Hg⁰ evasion from marine surface waters, thereby increasing the pool of Hg²⁺ available to methylating bacteria (DiMento et al., 2019; Schartup et al., 2019). The mechanism of sea-ice production and melting creates a highly stratified surface water column that has been proposed to enhance MeHg production (Baya et al., 2015). Beattie et al. (2014) have also shown the occurrence of biologically mediated MeHg production within the sea-ice itself, as well as at the ice-water interface. This was confirmed by other studies that showed a positive correlation between chlorophyll a (a proxy for primary production) and MeHg concentration in arctic and Antarctic sea ice (Cossa et al., 2011a). **Arctic sea-ice algae and sub-ice phytoplankton** account for 57 % of the total annual primary production in the Arctic Ocean (Boetius et al., 2013; Gosselin et al., 1997). Moreover, the rates of Hg uptake in marine organisms are the highest at the base of the food web, where Hg concentrations increase between 10³ and 10⁶ times during uptake by primary producers (Schartup et al., 2018; Zhang et al., 2019). This implies that MeHg produced in sea-ice and bioaccumulated by sea ice algae may contribute disproportionately to Arctic biota MeHg exposure (Schartup et al., 2020).

The $\Delta^{199}\text{Hg}/\Delta^{201}\text{Hg}$ and $\Delta^{199}\text{Hg}/\delta^{202}\text{Hg}$ slopes calculated in this study indicate that Hg accumulated by ringed seals derives from MeHg processing rather than Hg²⁺ photodegradation processes. Seemingly, Hg stable isotope values support the importance of terrigenous Hg inputs.

Stomach content analysis have reported that the diet of ringed seals in the Scoresby Sound is mainly composed by polar cod *Boreogadus saida* and Arctic cod *Arctogadus glacialis*, and invertebrates like *Parathemisto spp.*, *Eusirus cuspidatus* and Mysidae (Siegstad et al., 2014). These are believed to be the key species of Arctic sympagic food webs (Kohlbach et al., 2019, 2017; Steiner et al., 2019). These findings confirm that **terrestrial, riverine and sea-ice inputs are all important sources of Hg to ringed seals, whilst hooded and harp seals rely on offshore marine sources** (Figure 5.6). **Hg cycling characteristic of polar coastal areas exposes ringed seals to higher levels of THg, leading to large bioaccumulation in their muscle.**

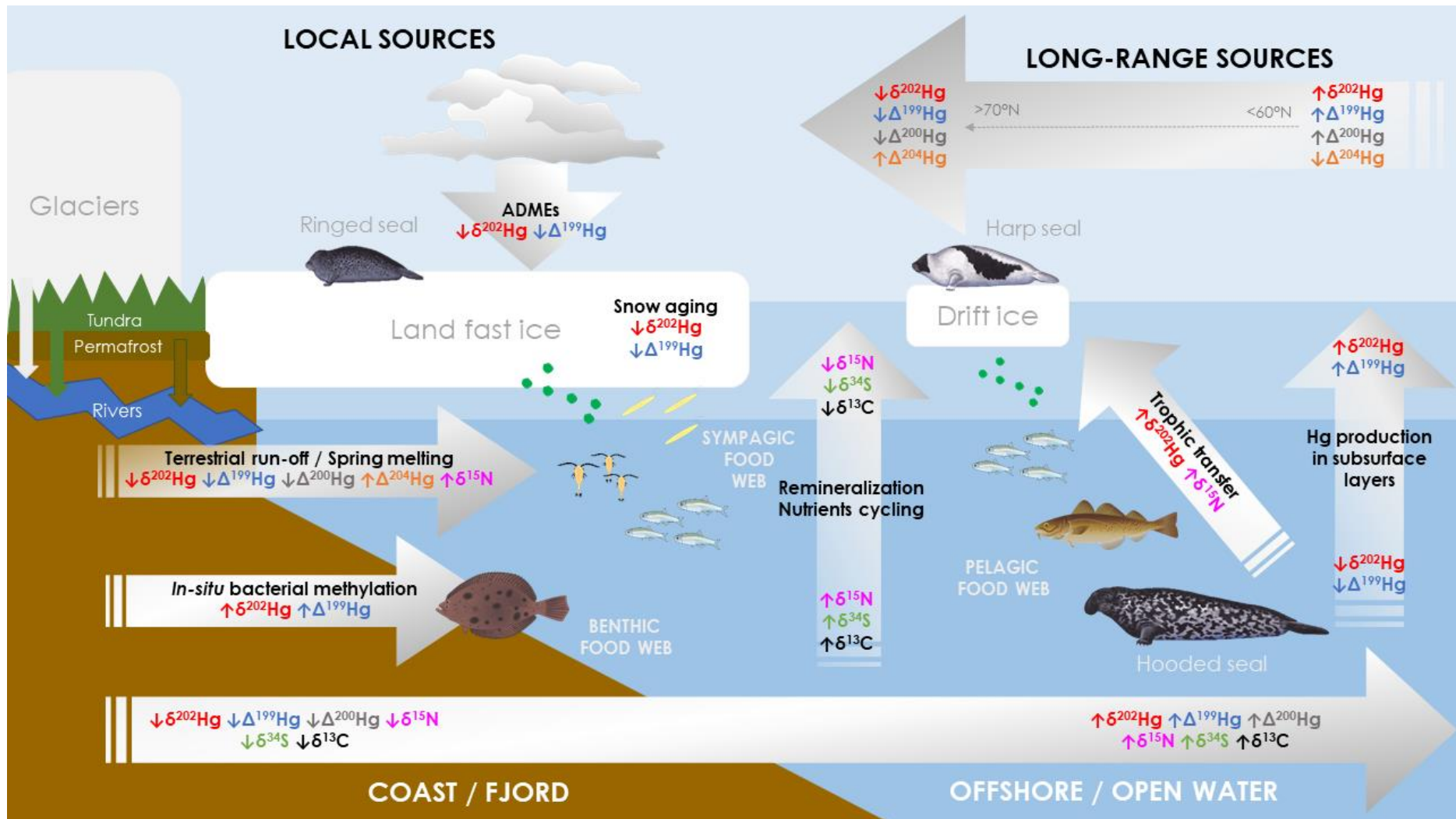


Figure 5.6. Conceptual representation of the influence of habitat use on Hg stable isotopes of ringed seal *Pusa hispida*, hooded seal *Cystophora cristata* and harp seal *Pagophilus groenlandicus* living in the Greenland Sea. Each isotope ratio is represented by a different color. \downarrow indicates a decrease in delta values, \uparrow indicates an increase in delta values. Grey arrow indicate the direction of change. In black are represented the processing causing changes in stable isotope values.

5. CONCLUSIONS

In this chapter we applied a multi-isotopic approach to assess the main factor influencing the levels of Hg exposure to Arctic seals living in the Greenland Sea. **Our main conclusions** can be summarized as follow:

1. The application of C, N, S and Hg stable isotopes together was essential to differentiate seal multi-isotopic niches;
2. Habitat use is the most important factor in determining the levels of Hg exposure to true seals in the Greenland Sea;
3. Hg stable isotope ratios and slopes discriminated between marine *versus* terrestrial sources of Hg pollution;
4. Ringed seals, which have a coastal and sympagic habitat use, are directly influenced by the higher rates of MeHg production typical of estuarine and sea-ice ecosystems, and consequently accumulate higher levels of Hg in their muscle with respect to offshore hooded and harp seals.

To our best knowledge this work represents the **first assessment of Hg sources in Greenland Sea seals**. It shows that also at small scale, marine predators like seals might be exposed to different Hg sources. This seems to be a more important driver of Hg bioaccumulation in Arctic marine predators than the levels of Hg in the environment.

These findings raise attention about refocusing the directions of Arctic marine mammals' conservation. For example, **when considering the potential impacts of climate change on Hg pollution, higher attention should be put on “where” marine mammals eat, rather than “what” they eat.**

Chapter 6

Impact of environmental changes on Hg temporal trends in Arctic true seals

ABSTRACT

Rationale: Several observations exist about the impact of climate change on the trophic ecology of marine predators. As a consequence, exposure to pollutants like mercury (Hg) has changed in time, with the greatest changes observed in Arctic marine mammals. The combination of C, N, S and Hg stable isotope ratios with THg concentrations allowed in the previous chapter to trace Hg sources in Greenland Sea seals, showing that sympagic species are potentially exposed to higher contamination levels, with respect to offshore benthic-pelagic ones. No species-specific data are available yet about the potential shift of Hg sources on a temporal scale, as a consequence of climate change.

Main question: Which are the main factors influencing trends of Hg sources and bioaccumulation in Greenland Sea seals over time?

Methods: We measured C, N, S, Hg stable isotopes and total-Hg (THg) concentrations in muscle of hooded seal *Cystophora cristata* and ringed seal *Pusa hispida* sampled in the Greenland Sea between 1985 and 2019. We compiled a suite of weather and climate time series, as well as broad-scale teleconnection indices such as the Arctic Oscillation (AO) and North Atlantic Oscillation (NAO). We followed a step-by-step approach to construct linear mixing models (LMMs), combining all variables with THg concentrations, to identify possible key predictors and assess any main effects on temporal contamination trends.

Results: For ringed seals, the top selected models indicated $\delta^{15}\text{N}$ values as the best descriptor of THg concentrations in time. Subsequent correlation of $\delta^{15}\text{N}$ with NAO, surface air temperature, sea-ice, $\delta^{202}\text{Hg}$ and $\Delta^{199}\text{Hg}$ values showed that in this species THg trends are mostly explained by shifts in Hg sources, linked with general ecosystemic changes. For hooded seals, the top selected models indicated $\delta^{13}\text{C}$ values, biomass of Atlantic cod and Greenland halibut as the best descriptors of THg concentrations in time. In this species, THg trends showed a significant decrease (1.5 % / year), mostly linked to changes in prey availability.

Keywords: Hg sources, climate change, temporal trend, Hg stable isotopes, Arctic Atlantification

1. INTRODUCTION

Until the 80s, Hg increase in Arctic biota was in line with the increase in the environment. In the last 3 decades however, scientists have observed a mismatch between concentrations in marine biota and the atmosphere (UNEP, 2013). The worsening of climatic change in the Arctic Ocean is adding up to this mismatch, complicating the comprehension of Hg temporal in Arctic marine biota (Chen et al., 2018; Dietz et al., 2013).

While some species show no temporal shift (e.g. Arctic char, black guillemot) and others show a decrease in THg concentrations since the past (e.g. Caribous and moose), marine mammals show significant increasing trends (up to 5 % / year in narwhals from Baffin Bay) (Braune et al., 2011). Such trends are not spatially consistent. In ringed seals, studies report increasing THg in Northwestern Greenland and Hudson Strait and decreasing THg in Resolute Bay (Houde et al., 2020; Rigét et al., 2011). In the same way, polar bears' hepatic THg are increasing in Canada, but decreasing in Central East Greenland (Routti et al., 2011; Yurkowski et al., 2020).

From the combination of several datasets and studies, a set of protocols was established in order to conduct Hg temporal trend analysis in Arctic wildlife (Bignert et al., 2004; Braune et al., 2011). These protocols foreseen the use of linear mixing models, where temporal trends in THg concentrations are assessed in response of a series of descriptor (climatic or ecological) variables at the same time (Foster et al., 2019a, 2019b). Since the last Hg assessment report (AMAP, 2011), there has been an increasing interest in understanding Hg trends in Arctic wildlife. However, the high complexity of (1) polar climatic processes, (2) Arctic Hg cycling and (3) trophic ecology of Arctic marine predators, strongly limit the interpretation of the impact of climate change on temporal trends of pollution.

The Greenland Sea is one of the regions more impacted by climate change (Laidre et al., 2015). Yet, because of its remoteness, it's one of the least studied areas. Indigenous people living in Itoqqortoormiit report important changes in the number and type of catches during traditional hunting of polar bears and ice seals (Laidre et al., 2018). Additionally, strong shifts in cetaceans abundances and distribution are recorded, as consequence of increased competition for resources and habitat change (Moore et al., 2019). In chapter 5 we demonstrated how habitat use influence Hg sources and levels in hooded, harp and ringed seals living in the Greenland Sea. Starting from these results, questions arise about the effect of environmental changes on Hg sources and seal trophic ecology and the consequence it might bring about the rates of Hg bioaccumulation.

In chapter 5, we demonstrated how the combination of C, N, S and Hg stable isotopes is a powerful tool for the discrimination of Arctic seals' trophic ecology and Hg sources at spatial scale. More specifically, we showed how:

- $\delta^{13}\text{C}$ and $\delta^{34}\text{S}$ are optimal tracers of seal habitat use (Chapter 5, §4.2);
- $\delta^{202}\text{Hg}$ and $\Delta^{199}\text{Hg}$ are optimal tracers of marine Hg sources (Chapter 5, §4.3.2), and

- $\Delta^{200}\text{Hg}$ and $\Delta^{204}\text{Hg}$ are optimal tracers of terrestrial Hg sources (Chapter 5, §4.3.1).

As such, they can be added to Hg temporal analysis of Arctic wildlife and refine the understanding of shifts in Hg exposure as a consequence of Arctic climate change.

The **main objective** of this chapter is to assess temporal variation of Hg bioaccumulation ringed seal *Pusa hispida* and the hooded seal *Cystophora cristata*, sampled in the Greenland Sea between 1985 and 2019.

Using muscle as monitoring tissue, we run multiple linear mixing models to integrate data of Hg stable isotopes into the temporal analysis of THg concentrations, in combination with C, N and S stable isotopes and climatic variables.

We did so to answer 3 **specific questions**:

1. Is Hg increasing or decreasing in Greenland Sea marine mammals?
2. Which are the main factors explaining Hg trends among trophic ecology, climate change and Hg sourcing?
3. Which species of marine mammal is the most affected by climate change?

2. MATERIAL AND METHODS

2.1. Sampling

This study was conducted on muscle tissue of 155 hooded seal *Cystophora cristata* and 252 ringed seal *Pusa hispida*, collected in the Greenland Sea from 1985 to 2019 (Figure 2.4, §2.2). Samples derive from tissue banks and *in-situ* harvesting (Chapter 2, §4.1). Seals' harvesting was conducted after obtainment of permits for scientific hunting by the Government of the Environment of Greenland, Norway and Denarmk, as explained in the ethical statement (Chapter 2, §3.2). For each animal information about geographical coordinates of sampling, weight, standard length and sex was recorded. Samples of muscle tissues were stored at -20°C in a three layer packaging.

2.2. Analysis

We measured THg levels (expressed in ng g⁻¹ dw), using atomic absorption spectroscopy (AAS) on a Tri-cell Direct Mercury Analyzer 80 (DMA-80 evo, Milestone, Italy) (Chapter 2, §7.1). We measured C, N and S and Hg stable isotopes (expressed in δ notation, in per mill ‰) using an IRMS (IsoPrime 100, Isoprime, U.K.) coupled in continuous flow to an elemental analyzer (EA, Vario MICRO cube, Elementar, Germany) (Chapter 2, §7.2). THg concentrations, $\delta^{13}\text{C}$ and $\delta^{15}\text{N}$ values were measured on the totality of samples. Hg stable isotopes (expressed in δ notation, in per mill ‰) were measured in a subsample of individuals, due to time and budget constrains (Table A6.1 and Table A6.2). Hg isotopic analyses were performed in a Nu Plasma HR MC-ICPMS (Nu Instruments, UK using a continuous flow Cold Vapor Generation (CVG) after Hot block (HB) pre-digestion (Chapter 2, §7.4).

2.3. Correction of $\delta^{13}\text{C}$ values

Enhanced atmospheric CO₂ since the industrial period is causing an increase in ¹³C-depleted anthropogenic CO₂ transfer into the oceans. This has resulted in a decline in the $\delta^{13}\text{C}$ values of Dissolved Inorganic Carbon ($\delta^{13}\text{C}$ -DIC), known as the Suess effect (-0.017‰ per year, globally) (Tagliabue and Bopp, 2008). A recent work calculated for the Arctic region a decline in $\delta^{13}\text{C}$ -DIC values of -0.011 ± 0.001 ‰ per year, from 1977 to 2014 (de la Vega et al., 2019). In order to eliminate the confounding effect of the CO₂-related temporal trend, we corrected $\delta^{13}\text{C}$ values measured in muscle of hooded and ringed seals, using the Suess effect value measured specifically for the Arctic.

2.4. Extraction of biological and climatic variables

Satellite-based and model-based climatic, biological and nutrient data from 1978 to 2019 was compiled for two locations (Northeast Atlantic and Scoresby Sound) to enable comparisons with THg tissue concentrations (Table 6.1). Scoresby Sound was bounded by coordinates 68°N/30°W to 73°N/20°W, but for the Northeast Atlantic, data was collected from two areas (71°N/28°W to 86°N/30°E for the first polygon and 60°N/44°W to 70.99°N/15°E for the second polygon) before being averaged. Greenland Sea and Arctic sea-ice extent were used as regional and large scale climate indices respectively. Ice extent is calculated as the surface of each pixel with >15 % of ice cover. Monthly values from each year were averaged to obtain an annual ice area index. The number of sea-ice free days was calculated considering days with less than 50 % of sea-ice coverage. For the data extracted from the GIOVANNI database, land data was excluded. Ice extent for the Northeast Atlantic was represented by the Greenland Sea dataset from the Arctic ROOS website. The data of Halibut *Reinhardtius hippoglossoides*, Atlantic Cod *Gadus morhua* and Polar Cod *Boreogadus saida* biomasses were acquired from the ICES library and the Demersal Fish Institute of Marine Research in Norway. We used the AOI (Atlantic Oscillation Index) as a large-scale climate index and calculated an AO winter index as the monthly means of November–May prior to the collection of samples.

2.5. Statistics analysis

We used multi-variate linear mixed-effect models (LMMs) to investigate the influence of biological, ecological and environmental drivers on THg concentrations, as previously published (Dietz et al., 2021a). Following well established protocols we log₁₀-transformed THg concentrations and standard length data (Braune et al., 2011). We selected time series for which most of the sampling years (1985 to 2019) were available. THg trends were found to lag with weather/climate by at least 3 years owing to trophic exchange of THg from prey to predator alone (Foster et al., 2019b). For this reason, correlation matrices between SL-corrected THg concentration residuals and weather/climate/diet variables lagged -1, 0, 3, 5, 7 and 10 years were constructed for both hooded and ringed seals. For each weather/climate variable, the time lag that yielded the maximum correlation (*r*, Pearson correlation of pairwise comparisons) was identified. Optimal time lagged variables were selected specifically for each species and used in the construction of the subsequent LMMs.

Because of the restricted number of Hg stable isotope analysis, we could not run LMMs, which are sensible to small *n* size. Thus, we studied temporal trends and variance of these variables separately, using simple linear regressions. Hg stable isotope values presented a normal distribution in both species. We used 1way-ANOVA for multi-year analysis of variance and Pearson correlation for temporal trend analysis.

Table 6.1. Time series data for atmospheric teleconnections, climate and fish catches collected for the Northeast Atlantic and the Scoresby Sound. Time periods differ between variables due to availability of data.

Category	Variable	Abbreviation	Unit	Time Period	Data Type and Treatment*	Source
Teleconnections	North Atlantic Oscillation (NAO)	NAO	Index	1975-2019	Annual means computed from the monthly NAO index data.	NOAA, National Centers for Environmental Informations. https://www.ncdc.noaa.gov/teleconnections/nao/
	Winter Atlantic Oscillation (AO)	AOw	Index	1975-2019	Annual means computed from the monthly AO index data.	NOAA National Weather Service, Climate prediction center. https://www.cpc.ncep.noaa.gov/products/precip/
Climatic	Number of sea-ice free days	SIFD	Days	1981-2021	Annual means calculated from percentage of sea-ice cover (<50 % considered sea-ice free)	GIOVANNI. Online environment for the display and analysis of geophysical parameters (NASA). https://giovanni.gsfc.nasa.gov/giovanni/
	Greenland Sea Sea-Ice Extent *	GSSIE	Km ²	1978-2019	Annual means computed from NERSC satellite monthly means	ARCTIC ROOS. Arctic Regional Ocean Observing System https://arctic.roos.org/node/99
	Arctic Sea-Ice extent	ASIE	Km ²	1975-2019	Annual means computed from satellite monthly means	NOAA, National Centers for Environmental Informations. Data provided by the National Snow and Ice Data Center. https://www.ncdc.noaa.gov/snow:and:ice:extent/
	Summer Arctic Sea-Ice Extent	SASIE	Km ²	1975-2019	Mean of pan-Arctic sea-ice extent for the month of September	NOAA, National Centers for Environmental Informations. Data provided by the National Snow and Ice Data Center. https://www.ncdc.noaa.gov/snow:and:ice:extent/
	Surface Air Temperature	SAT	°C	1985-2019	Annual means computed from MERRA-2 Model monthly means with 4 km resolution	GIOVANNI. Online environment for the display and analysis of geophysical parameters (NASA). https://giovanni.gsfc.nasa.gov/giovanni/
Biological	Greenland Halibut Biomass	Rh (from <i>Reinhardtius hippoglossoides</i>)	Tonnes	1995-2019	Annual means acquired from ICES database. Data for Stocks and Fishing Pressures	ICES. Advice on fishing opportunities, catch, and effort (2019). https://www.ices.dk/publications/library/Pages/default.aspx#k=Reinhardtius%20hippoglossoides
	Atlantic Cod Biomass	Gm (from <i>Gadus morhua</i>)	Tonnes	1995-2019	Annual means acquired from ICES database	ICES. Advice on fishing opportunities, catch, and effort (2019). https://www.ices.dk/publications/library/Pages/default.aspx#k=Gadus%20morhua
	Barent Sea Capelin Biomass	Mv (from <i>Mallotus villosus</i>)	Tonnes	1973 - 2019	Annual means acquired from MOSJ database	Data accessed from the environmental Monitoring of Svalbard and Jan Mayen (MOSJ) webpage: https://www.mosj.no/en/fauna/marine/capelin.html . Data provided by the Insititute of Marine Research (IMR, www.imr.no).
	Polar Cod Biomass	Bs (from <i>Boreogadus saida</i>)	Tonnes	1986-2019	Annual means acquired from the Demersal Fish Institute of Marine Research in Norway	Personal communication by Harald Gjørseter from the Demersal Fish Institute of Marine Research (Norway) included in the integrated assessment in the Barent Sea (2019)

* No specific ice extent data available for the Scoresby Sound

We followed a step-by-step established protocol to generate an a priori list of candidate models containing all appropriate iterations of predictor variables (including a null model with intercept only) (Foster et al., 2019a). We used an information-theoretic approach based on Akaike's information criterion corrected for small sample size (AICc) for the selection of most parsimonious models (Table A6.3 and Table A6.4). We started with a list of base models (as detailed afterwards) and then added to the best (most parsimonious) resulting model other variables:

1. Base models: including predictor variables such as year and $\delta^{15}\text{N}$ values, to test the effect of Hg historical production and trophic level (inferred by $\delta^{15}\text{N}$) on THg accumulation;
2. Ecological models: including $\delta^{13}\text{C}$ and $\delta^{34}\text{S}$ values, to test the influence of seal habitat use;
3. Teleconnection models: including optimally time-lagged indices of atmospheric weather patterns like the North Atlantic Oscillation (NAO) and winter Arctic Oscillation (AO);
4. Climatic models: including optimally time-lagged climatic variables like sea-ice extent (at regional and panarctic scale), surface air temperature and so on;
5. Diet models: including optimally time-lagged data of fish spawning stock biomass (in tonnes). The most parsimonious of these models was selected as the final LMM to be interpreted (Table A6.5).

All predictor variables were centered and scaled to further reduce collinearity (i.e., VIFs), especially among interaction terms, and facilitate comparison of effect sizes (Dietz et al., 2021a). The final selected model set was chosen conservatively by including all models within $\text{DAICc} < 10$.

Conditional model averaging using the final top-selected models was conducted to generate averaged regression coefficient estimates for all predictors, weighted by AIC weight. Calculated 85 % confidence intervals (CI) for averaged parameter estimates were used to determine meaningful predictor variables, assuming that variables with 85 % CIs that do not overlap zero significantly affect the response variable (Dietz et al., 2021a). Model assumptions were verified by plotting residuals versus fitted values, residuals versus each covariate in the model, and normal quantile-quantile plots for residual normality.

LMMs were run with the 'stats' package, model selection and condition averaging were performed using the 'MuMIn' package, in the software R version 4.0.5 (R Development Core Team, 2011).

3. RESULTS

3.1. Linear Mixing Models (LMMs)

For both hooded and ringed seals, \log_{10} -transformed THg correlated positively with \log_{10} -transformed standard length ($r = 0.26$, $p = 0.0001$, adjusted $R^2 = 0.06$ and $r = 0.43$, $p < 0.0001$, adjusted $R^2 = 0.18$, respectively). We extracted the residuals from this model to correct for the effect of age. SL-corrected THg residuals were moderately correlated with year for hooded seals ($r = -0.26$, $p = 0.0001$, adjusted $R^2 = 0.10$), going from 1388 ng g⁻¹ in 1985 to 644 ng g⁻¹ in 2019 (1.5 % decrease / year). For ringed seals, SL-corrected THg residuals increased from 1987 to 2000 and started decreasing thereafter. No significant temporal trend was observed in this species ($r = -0.76$, $p = 0.663$, adjusted $R^2 = -0.003$). Because of the correlation with hooded seal THg, time was viewed as a confounding factor and included as a predictor variable in the following LMM models (Foster et al., 2019a). This was done for both species.

SL-corrected THg residuals correlated with candidate predictor variables at different time lags. In general, teleconnection data moderately correlated at time lags of :1–0yr (e.g. for 1yr-lagged NAO, $r = 0.22$), while fish catches and climatic variables strongly correlated at the time lag of 5yr (e.g. for 5yr-lagged Atlantic cod, $r = 2.45$; for 5y-lagged Arctic sea-ice extent, $r = 3.28$).

Model-averaged regression estimates from top selected LMMs indicated $\delta^{15}\text{N}$, year, NAO, $\delta^{13}\text{C}_{\text{corr}}$, catches of Atlantic cod, polar cod and surface air temperature as predictors of THg trends in ringed seals (Table 6.2). $\delta^{15}\text{N}$, polar cod and NAO contributed positively to THg levels, while all other variables contributed negatively. $\delta^{15}\text{N}$ resulted as the only significant predictor ($p < 0.0001$).

Model-averaged regression estimates from top selected LMMs indicated $\delta^{15}\text{N}$, year, $\delta^{13}\text{C}_{\text{corr}}$, winter AO, Greenland Sea sea-ice extent, surface air temperature and catches of Greenland halibut and Atlantic cod as predictors of THg trends in hooded seals (Table 6.3). $\delta^{15}\text{N}$, $\delta^{13}\text{C}_{\text{corr}}$, surface air temperature and halibut biomass contributed positively to THg levels, while Greenland Sea sea-ice extent year and winter AO contributed negatively. $\delta^{13}\text{C}_{\text{corr}}$, Greenland halibut and Atlantic cod biomasses resulted as significant predictors ($p < 0.0001$, $p = 0.01$ and $p = 0.003$, respectively).

3.2. Hg stable isotopes' trends

For hooded seals, $\delta^{202}\text{Hg}$ differed between years ($F = 2.66$, $p = 0.04$), as well as $\Delta^{199}\text{Hg}$ ($F = 2.93$, $p = 0.03$). $\Delta^{200}\text{Hg}$ values did not vary in time ($F = 0.47$, $p = 0.79$). For ringed seals, $\delta^{202}\text{Hg}$ varied between years ($F = 3.20$, $p = 0.03$) as well as $\Delta^{199}\text{Hg}$ ($F = 5.96$, $p = 0.002$) and $\Delta^{200}\text{Hg}$ values ($F = 6.78$, $p = 0.001$). A negative correlation was found between ringed seal $\Delta^{200}\text{Hg}$ values and sampling year ($r = -0.94$, $R^2 = 0.89$, $p = 0.02$). No other correlation were found.

Table 6.2. Estimated regression parameters, adjusted standard errors (SE), z-values and p-values for the linear mixed-effect models (LMM) predicting **ringed seals** THg concentrations in time. Presented are conditional model averaged estimates for the top selected models based on $\Delta\text{AICc} < 10$. All parameters were centered and scaled prior to LMM, thus estimates are also scaled.

	Estimate	adjusted SE	z	p value
Intercept	0.00	0.06	0.00	1.00
Year	-0.16	0.19	0.84	0.40
$\delta^{15}\text{N}$	0.42	0.07	5.79	<0.0001
$\delta^{13}\text{C}_{\text{corr}}$	-0.10	0.13	0.82	0.41
NAO	0.15	0.10	1.58	0.12
Surface Air Temperature	-0.10	0.10	0.99	0.32
Atlantic cod	-0.19	0.12	1.55	0.12
Polar cod	0.09	0.09	1.04	0.30

* NAO = 1yr lag; Surface Air Temperature = 1yr lag; Fish catches = 5yr lag.

Table 6.3. Estimated regression parameters, adjusted standard errors (SE), z-values and p-values for the linear mixed-effect models (LMM) predicting **hooded seals** THg concentrations. Presented are conditional model averaged estimates for the top selected models based on $\Delta\text{AICc} < 10$. All parameters were centered and scaled prior to LMM, thus estimates are also scaled.

	Estimate	adjusted SE	z	p value
Intercept	-0.02	0.08	0.26	0.80
Year	-0.68	0.35	1.97	0.05
$\delta^{15}\text{N}$	0.14	0.12	1.17	0.24
$\delta^{13}\text{C}_{\text{corr}}$	0.50	0.15	3.34	0.001
Winter AO	-0.14	0.15	0.98	0.33
Greenland Sea sea-ice extent	-0.33	0.34	0.99	0.32
Surface air temperature	0.06	0.12	0.47	0.64
Greenland Halibut	0.37	0.15	2.56	0.01
Atlantic cod	-0.55	0.19	2.93	0.003

* Winter AO = 1yr lag; Surface Air Temperature = 1yr lag; Greenland Sea-Ice extent = 5yr lag; Fish catches = 5yr lag.

4. DISCUSSION

4.1. Mercury trends in ringed seals

For ringed seals, model-averaged regression estimates from top selected LMMs indicated that $\delta^{15}\text{N}$ was the strongest predictor, showing a positive correlation with THg concentrations. This means that, **in time, when $\delta^{15}\text{N}$ increases, also THg concentrations does** (Figure 6.1A). THg temporal trend show an increase from 1990 until 2000, followed by a decrease until 2010 and a plateau thereafter. $\delta^{15}\text{N}$ temporal trend show an increase until 2000, a decrease between 2000 and 2010, and a step increase thereafter (Figure 6.1B).

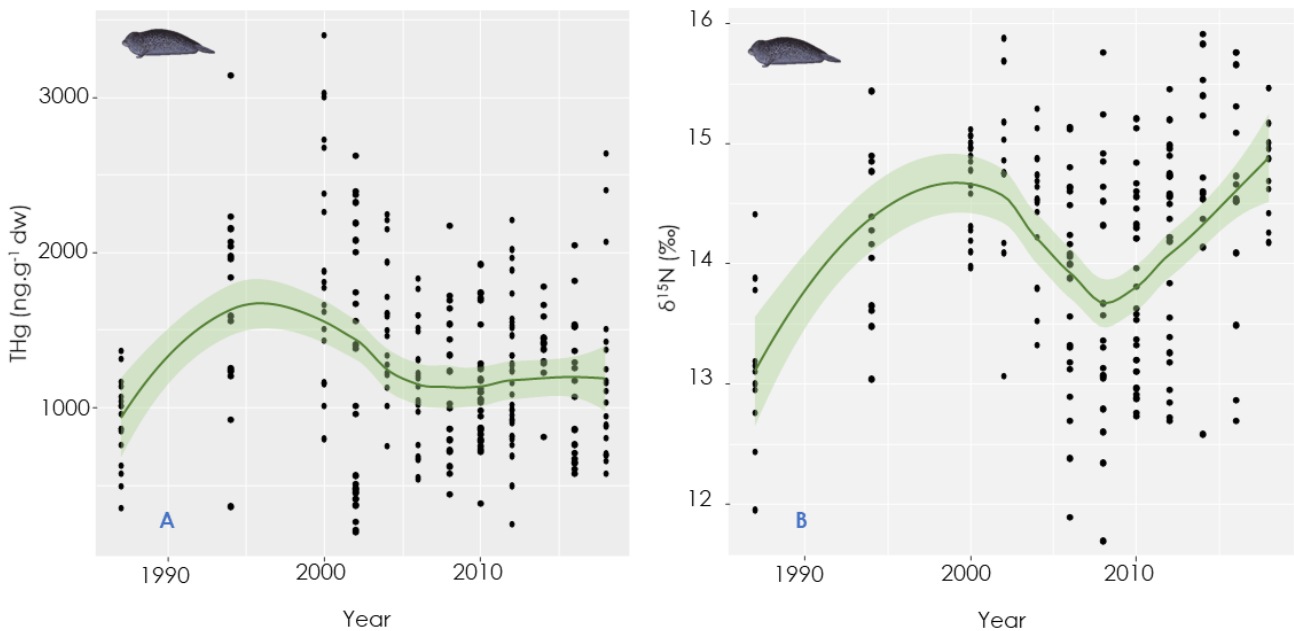


Figure 6.1. (A) Time trend of THg concentrations ($\text{ng g}^{-1} \text{ dw}$) measured in muscle of **ringed seals** sampled from 1987 and 2018. (B) Time trend of the $\delta^{15}\text{N}$ values (per mill, ‰), indicated by the conditional averaging as the strongest indicator of ringed seal THg concentrations. Indicated are the raw values (black dots). A smoothed conditional mean curve (and 85 % C.I.) is fitted using loess functions (green line).

These trends might result from:

- a change in trophic position of ringed seal prey (Dietz et al., 2021a);
- a shift in habitat use by ringed seals (Houde et al., 2020); or
- a shift in $\delta^{15}\text{N}$ at the base of the marine food web (Woodland et al., 2012).

However, the sole interpretation of $\delta^{15}\text{N}$ and THg values do not allow to go further in discussing contamination trends in ringed seals. Model-averaged regression estimates from top selected LMMs indicated $\delta^{15}\text{N}$ as the only factor to significantly explain THg trends. However, looking separately into the trends of other variables like fish biomass or climatic variables, we observe clear correlations with

THg concentrations over time. The strong codependency between $\delta^{15}\text{N}$ and THg might mask the influence of these other variables as a consequence of LMMs limitations (Annex to chapter 6, §1). As such, we do not valid the results of model-averaging in ringed seals and discuss also other variables indicated by the most parsimonious model which we believe are important drivers of THg concentrations (Table 6.2).

4.1.1. The Atlantification of the Arctic as mercury and $\delta^{15}\text{N}$ descriptor

After $\delta^{15}\text{N}$, the top selected models indicate biomass of the Atlantic cod as second best THg predictor in ringed seals (Figure 6.2). If the trophic position of prey species was the best predictor of ringed seal THg levels, we would expect a positive correlation between Atlantic cod biomass and THg concentrations. Instead, the averaging analysis indicate that the biomass of Atlantic cod influenced negatively THg concentrations (Table 6.2).

The spawning stock biomass of the Atlantic cod strongly decrease after 1990 reaching a minimum between 1995 to 2005 (Figure 6.2A). After 2005 a steep increase is observed. When cod biomass is the highest, THg and $\delta^{15}\text{N}$ values are the lowest. This suggests that other factors (beside prey trophic position) influence ringed seal THg between 1990 and 2005.

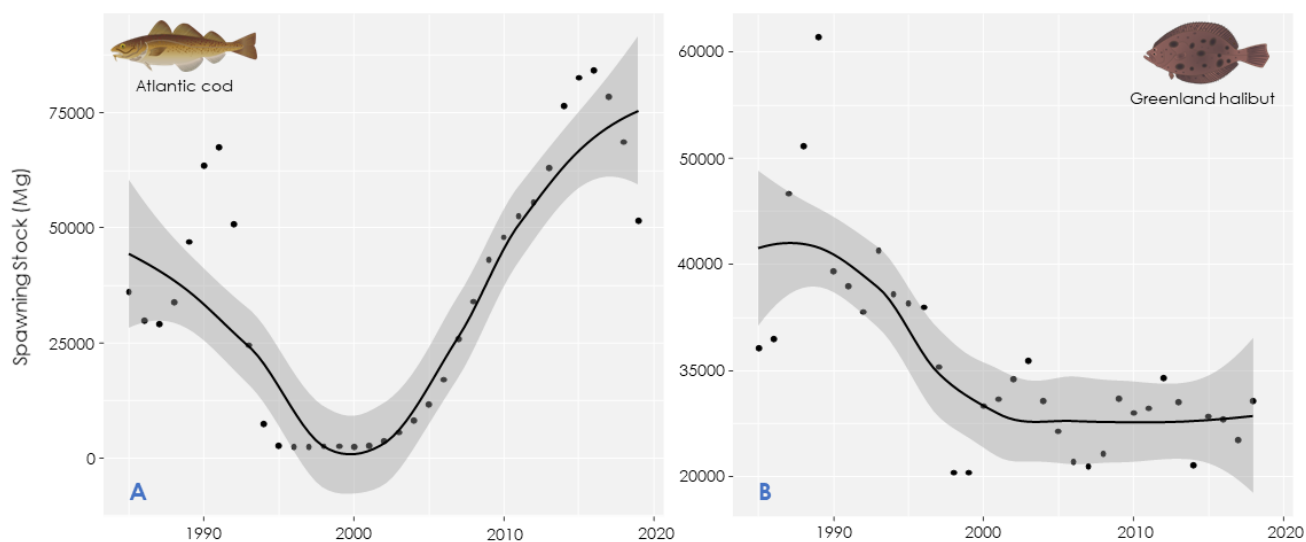


Figure 6.2. Time trend of Atlantic cod *Gadus morhua* (A) and Greenland halibut *Reinhardtius hippoglossoides* (B) spawning stock biomass (in tonnes or Mg). Annual means are represented by the black dots. A smoothed conditional mean curve (and 85 % C.I.) is fitted using loess functions (gray line).

Since 1990, the Arctic Ocean has been subjected to a period of great environmental change, commonly known as “Borealization” (Krause-Jensen et al., 2020). In the Eurasian sector of the Arctic, such process is mostly linked with an increasing inflow of North Atlantic waters into the Arctic, referred to as “Atlantification” (Polyakov et al., 2017). One of the main consequences is the Northward shift

of Atlantic species (e.g. Atlantic cod or mackerel), while species like polar cod have become rare (Kovacs et al., 2011). This has caused an increase in pelagic biomass in Arctic waters (6 to 30 million) in the last 3 decades (Laidre et al., 2015; Moore et al., 2019) and transformed the Arctic from a system dominated by ice-associated and benthic fish, to a more pelagic-fish dominated one (**“pelagification” of the Arctic**; Krause-Jensen et al., 2020).

Pelagic food webs are characterized by lower THg concentrations and $\delta^{15}\text{N}$ values than sympagic and benthic and sympagic ones (Chapter 5, [§4.3](#) and [§4.5](#)) (Søreide et al., 2006; Yunda-Guarin et al., 2020). As a consequence of the pelagification, the entire Greenland Sea marine food web would acquire a more “pelagic” behavior with regards to the rates of uptake by primary producers of N and C isotopes, as well as environmental Hg recycling between water layers (Ceia et al., 2018; Perry et al., 1999). This would result in lower $\delta^{15}\text{N}$, $\delta^{13}\text{C}$ and THg values in consumers for all trophic levels (Blévin et al., 2020).

An increase of boreal species like the Atlantic cod at the expense of Arctic species in conjunction with decreasing $\delta^{15}\text{N}$, $\delta^{13}\text{C}$ and THg trends were already observed in the diet of ringed seals from the Canadian and Norwegian Arctic (Bengtsson et al., 2020; Houde et al., 2020; Lowther et al., 2017). However, the questions remain about wheater this shift in diet ocured through a shift in predators’ habitat use (especially hunting behaviour) from sympagic to pelagic, or to a shift in the composition and structure of the food web they rely on.

In the previous chapter, we observed how $\delta^{34}\text{S}$ values are perfect tracers of Arctic seals’ habitat use. They indeed separated the sympagic ringed seal (~15 – 17 ‰) from the offshore benthic-pelagic hooded seal (~19 – 21 ‰) (Chapter 5, [§4.2](#)). The LMMs analysis conducted in this chapter shows how $\delta^{34}\text{S}$ values of ringed seals do not change in time and do not correlate with $\delta^{15}\text{N}$, $\delta^{13}\text{C}$ and THg trends. This confirms that **habitat use of ringed seals did not change in time**. Our findings suggest that **THg trends of ringed seals** have been affected by a bottom-up shift of the entire food web (Ceia et al., 2018), rather than a change in prey trophic position.

4.1.2. Climatic variables as mercury descriptors

Although climatic variables like NAO and surface air temperature are not considered as significant predictors by the LMMs analysis, their temporal trends strongly associate with ringed seal THg. The top selected models indicate how surface air temperature influences negatively ringed seal THg concentrations, while NAO influences them positively (Table 6.2). This means that during periods of low surface air temperature, THg concentrations in ringed seals increase. Viceversa during periods of high surface air temperature. During periods of positive NAO, THg concentrations in ringed seals increase. Viceversa during periods of negative NAO.

The opposite correlation between THg, surface air temperature and NAO fits well with the current understanding of weather and climate effects on Hg cycling in the Arctic (Macdonald et al., 2005). A positive NAO circulation is associated with increased atmospheric advection into Arctic regions from Europe, Asia and eastern North America (Ma et al., 2016; Macdonald et al., 2005) and strong cyclonic wind fields over the Arctic, which transport more ice through Fram Strait (Chapter 1, [Figure 1.7](#)) (Mckinney et al., 2013). This results in lower temperatures and increased sea-ice extent. Opposite patterns are seen during negative NAO periods, characterized by elevated temperatures and lower sea-ice extent.

Warmer spring temperatures and reduced sea-ice cover are associated with increased THg concentrations in the atmosphere, but decreased THg concentrations in oceanic surface water (Chen et al., 2015; Fisher et al., 2013).

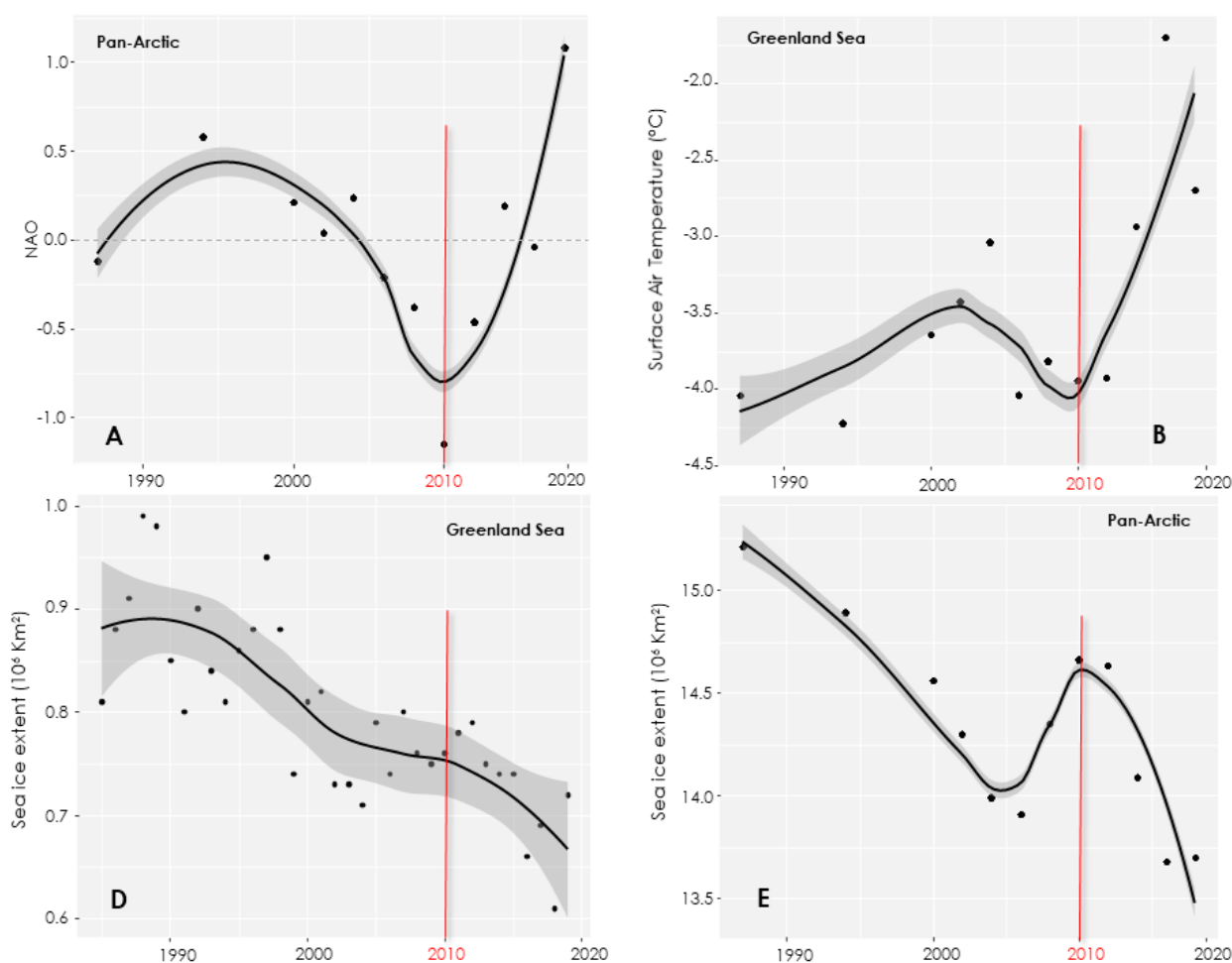


Figure 6.3. Time trend of the NAO (North Atlantic Oscillation) (A), Greenland Sea sea surface air temperature (B), Greenland Sea sea ice extent (C) and Arctic sea ice extent (D). Annual means are represented by the black dots. A smoothed conditional mean curve (and 85 % C.I.) is fitted using loess functions (gray line). Sea ice extent data are represented in 10^6 km^2 , while surface air temperature in degrees Celsius ($^{\circ}\text{C}$). Data were extracted as explained in Table 6.1. Greenland Sea sea ice extent from ARCTIC ROOS (Arctic Regional Ocean Observing System); Arctic sea ice extent and NAO from NASA : National Snow and Ice Data Center; Surface Air temperature from NASA – GIOVANNI, Online environment for the display and analysis of geophysical parameters.

Hg stable isotopes analysis showed how the higher influx of light into surface waters in ice-free areas enhance MeHg photodegradation, potentially reducing its bioavailability to marine food webs (Point et al., 2011). Additionally, higher wind speeds are thought to increase Hg deposition to sea-ice *versus* surface oceanic waters (Fisher et al., 2013). Therefore, the decrease in ringed seal THg concentrations observed between 2000 and 2010 might relate with the strong negative NAO characteristic of that decade (Figure 6.3A).

4.2. Mercury trends in hooded seals

Model-averaged regression estimates from top selected LMMs indicate that $\delta^{13}\text{C}$ (corrected for the Suess effect: $-0.01\text{‰} / \text{year}$, Figure 6.4), Atlantic cod and Greenland halibut biomass are the strongest predictors of hooded seal THg concentrations (Figure 6.2). $\delta^{13}\text{C}$ and Greenland halibut correlate positively with hooded seal THg concentrations, while Atlantic cod correlate negatively (Table 6.3). Age-corrected THg concentrations in Greenland Sea hooded seals show a continuous decreasing trend ($1.5\% / \text{year}$), resulting in modern levels being nearly the half (on average) of those measured in 1985 (Figure 6.4A). This is in accordance with the declining Hg trends observed in the Arctic ecosystem (Chen et al., 2015).

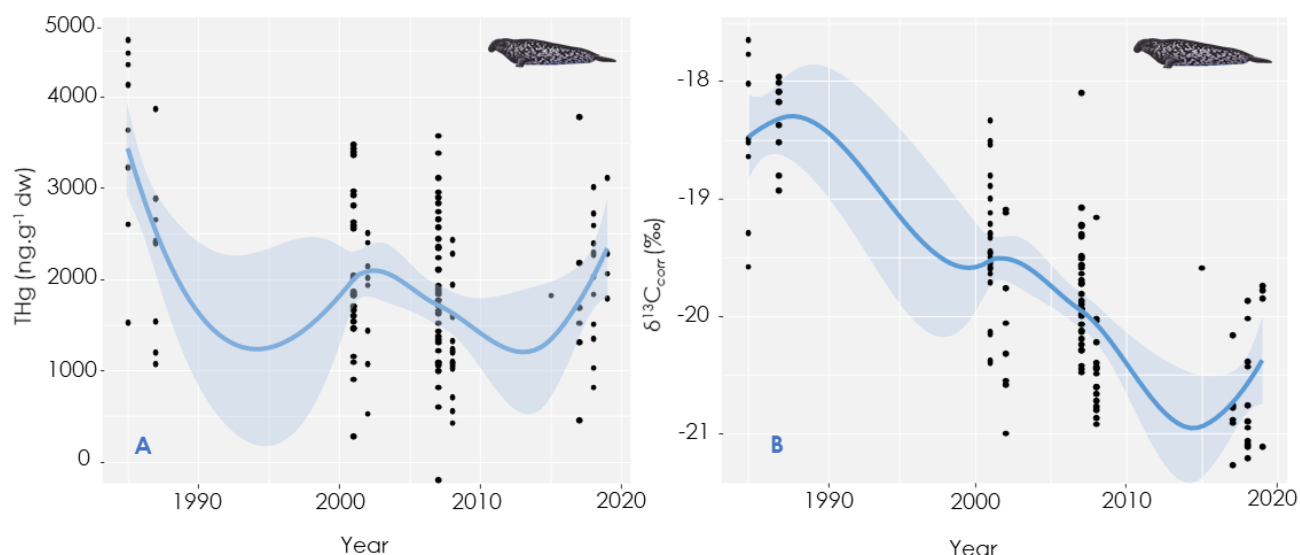


Figure 6.4. (A) Time trend of THg concentrations ($\text{ng g}^{-1} \text{dw}$) measured in muscle of **hooded seals** sampled from 1985 and 2019. (B) Time trend of the $\delta^{13}\text{C}$ values (per mill, ‰), indicated by the conditional averaging as the strongest indicators of hooded seals' THg concentrations. Raw values are indicated by black dots. A smoothed conditional mean curve (and 85 % C.I.) is fitted using loess functions (blue line).

4.2.1. Prey choice as descriptor of mercury and $\delta^{13}\text{C}$ values

Hooded seal THg negative trend strongly associates with $\delta^{13}\text{C}$ change in time. Hooded seal $\delta^{13}\text{C}$ values (corrected for the Suess effect) decrease at a rate of $-0.07 \pm 0.005 \text{ ‰}$, between 1985 and 2019 (Figure 6.4B). This is in the same range of previous observations on bowhead whales from the Pacific Arctic and other marine mammals (de la Vega et al., 2019). These findings suggest that other processes, in addition to the global changes in CO_2 cycling, might be affecting $\delta^{13}\text{C}$ of subarctic seal species.

The consequences brought by the Atlantification are vast across the Eurasian Arctic (Laidre et al., 2015). In the Greenland Sea, scientists observe:

1. 10 – 12 days longer sea-ice free season;
2. A sea ice edge retreat of 250 – 375km;
3. A 15 % decrease in the net primary production (Moore et al., 2019).

In addition, we observe in this work around 30 % decrease of mean annual extent of the Greenland Sea sea-ice between 1985 and 2019 (Figure 6.3C). The combined effect of sea-ice loss with increased energy demand from higher temperatures lead to lower biomass of benthic and demersal fish species (Petrik et al., 2020). Hooded seal THg and $\delta^{13}\text{C}$ values strongly correlate with the increase of Atlantic cod biomass and the drastic decrease of the Greenland halibut stock (Figure 6.3). This supports the idea that the **THg decrease observed in hooded seals is related to a change in hooded seals' prey**: from benthic Arctic species like the Greenland halibut, to pelagic species like the Atlantic cod.

As for ringed seals, no difference is found in $\delta^{34}\text{S}$ values values between 1985 and 2019, confirming that habitat use of hooded seals did not change in time. The temporal decrease in hooded seal THg concentrations, associated with an increasing biomass of pelagic *versus* benthic prey confirm that **shifting to a pelagic-dominated diet as a consequence of climate change is leading to lower Hg accumulation in large subarctic predators**.

4.3. Temporal trends of mercury sources

4.3.1. $\delta^{202}\text{Hg}$ traces the higher abundance of subarctic versus arctic prey

$\delta^{202}\text{Hg}$ values of hooded seals increase constantly in time, with $\delta^{202}\text{Hg}$ values significantly higher in 2019 than 1985 (Figure 6.5). In chapter 5, we observed lower $\delta^{202}\text{Hg}$ values for sympagic species with respect to pelagic ones. This was consistent with the difference in prey biodiversity and Hg cycling between marine food webs (Chapter 5, §4.3). Moreover, $\delta^{202}\text{Hg}$ values were found to decrease with increasing latitude (Chapter 5, Figure 5.6). Thus, the **increase of $\delta^{202}\text{Hg}$ values of hooded seals is**

consistent with the shift in diet from the Arctic and benthic Greenland halibut to subarctic and pelagic Atlantic cod.

$\delta^{202}\text{Hg}$ values of ringed seals significantly decrease from the 80s to 2008, to increase again thereafter. No difference is found between the 80s and today. This pattern strongly associates with $\delta^{15}\text{N}$ trends and only partly with THg concentrations. This suggests that several factors are affecting Hg sourcing in this species year by year, resulting in no clear temporal trend. This confirms our hypothesis that **ringed seal THg concentrations are directly linked with climate-driven baseline changes**, rather than prey trophic position (This chapter, §4.1.2).

4.3.2. $\Delta^{199}\text{Hg}$ traces higher competition between ringed and hooded seals

$\Delta^{199}\text{Hg}$ of ringed seals are significantly higher in the 80s than today, while for hooded seals $\Delta^{199}\text{Hg}$ decreases significantly only in the recent years (Figure 6.5). Inter-annual differences in $\Delta^{199}\text{Hg}$ of both species are much weaker and difficult to interpret. However, what can be underlined is that in recent years, $\Delta^{199}\text{Hg}$ values of hooded and ringed seals overlap much more than in the past. This could well be a result of the **increasing overlap of ringed and hooded seals hunting strategies and competition for the same resource** (e.g. Atlantic cod).

4.3.3. $\Delta^{200}\text{Hg}$ traces higher input of low-latitude Hg in the Arctic ringed seals

For ringed seals, $\Delta^{200}\text{Hg}$ values decrease significantly between 1987 and 2018 (Figure 6.5). Conversely, no differences are found for hooded seals. As shown in chapter 5 (§4.3), $\Delta^{200}\text{Hg}$ is an efficient tracer of Hg origin in Arctic marine predators at both local and global scale (Masbou et al., 2018). Hooded seals present a large distribution, ranging from the Fram Strait and Svalbard down to the European coastline, with exceptional sightings in the Mediterranean Sea (Bellido et al., 2009). The absence of $\Delta^{200}\text{Hg}$ temporal change in this species is expected, since they reflect the homogenization of Hg sources all across hooded seal hunting range.

On the other hand, **the important $\Delta^{200}\text{Hg}$ decrease observed in ringed seals most probably reflect a change in Hg sources**. $\Delta^{200}\text{Hg}$ shows a positive Southward gradient, resulting in polar ecosystem being depleted in ^{200}Hg compared to lower latitudes (Masbou et al., 2018). At the same time, coastal Arctic seal species demonstrate to have lower $\Delta^{200}\text{Hg}$ values than offshore ones, as a result of the higher importance of terrestrial Hg reservoirs (e.g. rivers, land fast ice, atmospheric Hg^0) as sources of Hg to sympagic food webs (chapter 5, §4.4 and §4.5).

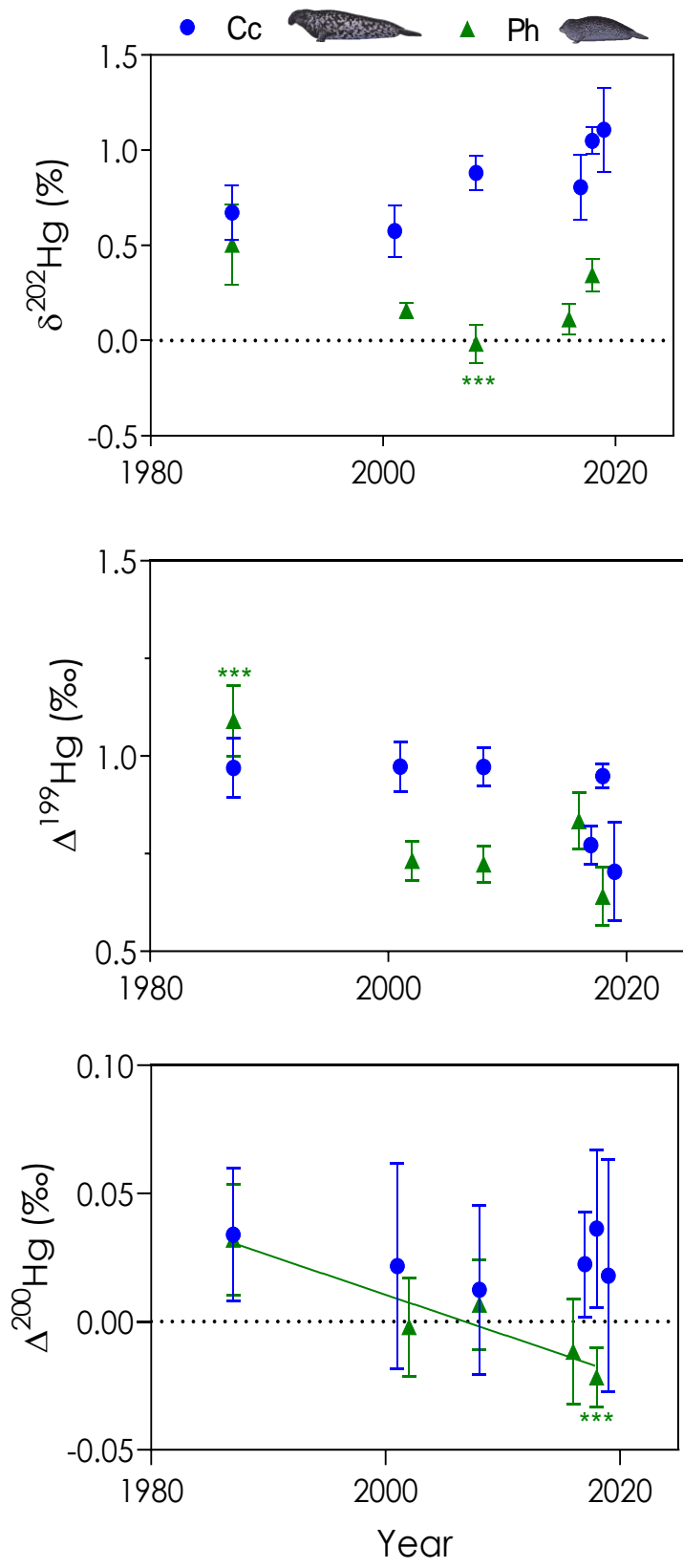


Figure 6.5. $\delta^{202}\text{Hg}$, $\Delta^{199}\text{Hg}$ and $\Delta^{200}\text{Hg}$ values in muscle of **hooded seal** *C. cristata* (blue dots) and **ringed seals** *P. hispida*, sampled in the Greenland Sea between 1985 and 2019. Data are shown as average \pm SD. Significant temporal linear regression of ringed seals' $\Delta^{200}\text{Hg}$ values in time is shown by a straight green line. Asterisks represent significant variance between groups (1-way ANOVA test, $\alpha = 0.05$).

Therefore, the decreasing trends of Greenland Sea ringed seal $\Delta^{200}\text{Hg}$ observed in this study might reflect two processes:

1. THg transport from lower latitudes to the Greenland Sea is decreasing in time.

Around 30 % of Hg accumulated in the Arctic Ocean originates from anthropogenic activities at lower latitudes (~15 % East Asia, ~3 % Europe, ~2 % North America) (UNEP, 2018). $\Delta^{200}\text{Hg}$ decreasing trends in Greenland Sea ringed seals might reflect the decreasing inputs of Hg from other countries. This is supported by the decrease in atmospheric THg concentrations measured in the Arctic Ocean (Chen et al., 2015).

2. THg inputs from terrestrial reservoirs are increasing in time.

Recent studies, as well as results presented in chapter 5, have shown how **Arctic terrestrial reservoirs of Hg** (e.g. permafrost, tundra and glaciers) are important sources of Hg to marine food webs, as a consequence of climate change (French et al., 2014; Obrist et al., 2017; Schuster et al., 2018). Boreal soils and vegetations are characterized by negative $\Delta^{200}\text{Hg}$ values compared to Arctic Ocean sediments (Chapter 5, §4.5). Therefore, the decrease in ringed seal $\Delta^{200}\text{Hg}$ values over time might represent a larger importance of terrestrial Hg sources in Hg bioaccumulation today with respect to the past. This hypothesis is further supported by the divergence of THg and $\delta^{15}\text{N}$ trends we observe in ringed seals after 2010 (Figure 6.1). While THg seems to reach a plateau, $\delta^{15}\text{N}$ values start to strongly increase again (Figure 6.1). The seasonal fluctuation of freshwater run-offs results in seasonal shifts in Arctic biota $\delta^{15}\text{N}$. For example, body feathers (representing the summer period) of little auks from Kap Høeg present higher $\delta^{15}\text{N}$ values compared to head feathers (representing the winter period; Renedo 2020).

In polar ecosystems, N is sequestered in different forms into sea-ice from air and surface waters. With time, the effect of nitrate consumption leads to an ^{15}N enrichment of the N pool in sea-ice (Fripiat et al., 2014). In spring, during ice melting in terrestrial and marine ecosystems, this results in seasonal peaks of high- $\delta^{15}\text{N}$ particulate N inputs into the marine ecosystem, which become available for processing by the base of the food web (Fripiat et al., 2014; Tuerena et al., 2020). In addition, thawing of permafrost and tundra enrich rivers in organic matter (OM) and nutrients, leading to spring freshwater run-offs, which have higher $\delta^{15}\text{N}$ than marine ecosystems (Yunda-Guarin et al., 2020).

The year 2010 is considered as a tipping point for the Arctic Ocean, after which irreversible environmental changes started to occur (Figure 6.3) (Krause-Jensen et al., 2020). Starting from that year, we observe:

- a 1.5°C increase in the last 10 years of the annual mean of surface air temperature of the Greenland Sea region (-4°C in 2010 and -2.5°C in 2019) (Figure 6.3B);
- higher terrestrial inputs during melt seasons (Fortier et al., 2015; McClelland et al., 2012).
- an irreversible decreasing trend of sea-ice loss on a panarctic scale (Figure 6.3).

Even if Arctic sea-ice extent does not correlate with THg concentrations, its trend is strongly associated with $\delta^{15}\text{N}$ values ($r = -0.27$, $p < 0.0001$, adjusted $R^2 = 0.08$; Figure 6.3D). Therefore, the **higher rates of sea-ice, permafrost and glaciers' loss observed since 2010, might be leading to higher uptake of ^{15}N enriched OM by sympagic primary producers.**

The concurrent increase in $\delta^{15}\text{N}$ values and decrease in $\Delta^{200}\text{Hg}$ is observed in ringed seals but not hooded seals. This strongly supports the hypothesis that **climate change has been affecting more directly coastal marine food webs than offshore ones (Figure 6.6).**

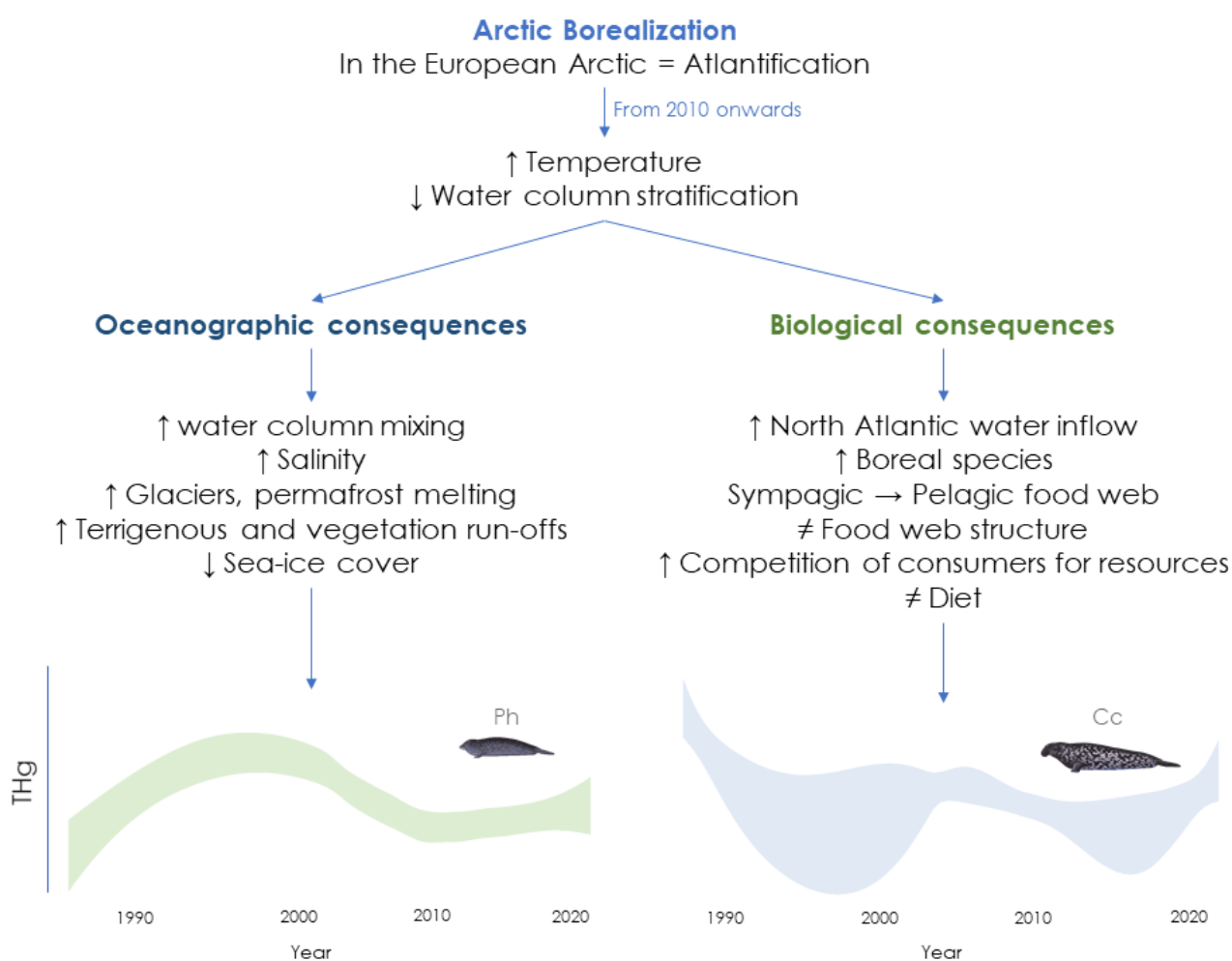


Figure 6.6. Conceptual summary of the main oceanographic and biological processes governing temporal trends of THg concentrations in muscle of hooded seal *Cystophora cristata* (Cc, blue) and ringed seal *Pusa hispida* (Ph, green) from the Greenland Sea.

5. CONCLUSIONS

The main objective of this chapter was to assess the main factors influencing temporal trends of THg concentrations and sources (inferred by Hg stable isotopes) in ringed seal *Pusa hispida* and hooded seal *Cystophora cristata* from the Greenland Sea.

Our **main findings** can be summarized as follows:

1. Although in different ways, both species of true seals show **decreasing trends of THg** concentrations between the 80s and today;
2. In ringed seals, THg trends result from a complex interplay of environmental and climatic processes like the **Atlantification of Arctic marine food webs**, and reflect a shift of the entire ecosystem;
3. In hooded seals, THg trends are related to a shift between benthic-dominated *versus* pelagic-dominated diet, as a result of the **pelagification of Arctic marine food webs**;
4. Hg stable isotopes trends show a **shift in Hg sourcing to Arctic marine predators**, as a result of: **(1)** Increased abundance of North Atlantic pelagic prey; **(2)** increased competition of exploitable resources; **(3)** decreased Hg atmospheric influx from northern midlatitudes; and **(4)** increase importance of Hg terrestrial reservoirs to Hg sourcing in sympagic foodwebs.

Chapter 7

General Discussion

1. THE ARCTIC: A HOTSPOT FOR Hg POLLUTION STUDIES

Over the past 30 years, the Arctic has been warming faster than any other region on Earth (Post, 2013). This process is commonly referred to as **Arctic amplification** (Stjern et al., 2019). Sea-ice loss and surface warming are believed to be 2 of the main mechanisms exacerbating such process (Dai et al., 2019). A long series of climatic, physio-chemical and biological consequences are observed (Chapter 1, §2.4). Snow cover over land in the Arctic is decreasing, notably in spring, and glaciers are retreating across all regions (AMAP, 2017). In addition, Arctic permafrost is warming up, thawing and releasing gasses (e.g. methane) and pollutants (e.g. Hg²⁺) accumulated in the past (Schaefer et al., 2020; Stjern et al., 2019). Scientists first started to see evidence of changes in Arctic climate in the 1980s (Krause-Jensen et al., 2020). Since then, the changes have become much more pronounced.

Understanding the **consequences that environmental changes have on Hg pollution** is more urgent in the Arctic than any other regions of the world. The Arctic region acts as both sink and source of the global Hg cycle (Chapter 1, §2). Several evidences about the influence of climate-driven environmental changes on Hg bioaccumulation in marine biota have been published (Sundseth et al., 2015; Yurkowski et al., 2020). However, **no clear causality has been established** yet, especially at the higher trophic levels of the food web. Marine predators like Arctic true seals present complex physiologies and ecologies, leading to difficult tracing of bottom-up processes (Leroux and Loreau, 2015; Macdonald et al., 2005). Due to differences in demographic pressure, scientific efforts concentrated only on few regions of the Arctic (e.g. Canadian Arctic, Northwestern Greenland) (Dietz et al., 2019). The **remote position of the Greenland Sea** and scattered human settlements along the Eastern coast of Greenland, brought to much less scientific attention in this area. THg temporal and spatial trends in marine and terrestrial predators living in the Greenland Sea are wildly missing. Few exceptions are seabirds (Fort et al., *Pers. Comm.*), ringed seals (Rigét et al., 2011) and polar bears (Routti et al., 2011).

Species like the hooded seal *Cystophora cristata*, harp seal *Pagophilus groenlandicus* and the ringed seal *Pusa hispida* are the most common marine mammals inhabiting the eastern coast of Greenland (Rosing-Asvid, 2010). As such, they represent the main food source of local apex predators like polar bears and humans. The consumption of **traditional food** varies a lot between regions, based on the proximity to international imports (Deutch et al., 2007). Total energy intake from traditional food amounts to 12 to 15 % in South Greenland, and around 26 % in North Greenland (Qaanaaq) (Rigét et al., 2019). Within the Arctic, Canadian and Greenland Inuit populations present blood Hg concentrations 5 to 50 times higher than in other regions (Adlard et al., 2021), exceeding suggested thresholds of weekly THg intakes (4 µg kg⁻¹ body mass, WHO 2011) (Abass et al., 2016; AMAP, 2015). More effective hunting methods are being implemented, including larger and faster boats and fishing vessels, riffles and gillnets (Sonne et al., 2017). This, in addition to potential shifts in hunting

procedures related to climate change (Huntington et al., 2017, 2016; Laidre et al., 2018; Lovvorn et al., 2018), might lead to higher Hg exposure and dietary intake in hunting communities. **Forecast of future Hg trends** in the Greenland Sea, is therefore necessary not only to manage the general health of seals populations, but also that of local human communities (AMAP, 2021a; Sonne et al., 2017).

2. SPATIAL HG TRENDS IN ARCTIC SEALS: WHAT ARE WE MISSING?

THg concentrations of muscle of hooded, harp and ringed seals from the Greenland seals are in the same range as in previous studies (Table 7.1). The highest concentrations are found in the Canadian Arctic, followed by western Greenland and North Atlantic. The lowest concentrations are found in Greenland Sea subpopulations. This finding is in accordance with spatial trends observed also in other predators from the Arctic and North Atlantic Ocean (Dietz et al., 2021b, 2000; Renedo et al., 2020; Routti et al., 2011). **Geographical patterns of THg concentrations of Arctic marine biota were related to several factors:**

- Trophic level (Lehnherr, 2014);
- Food web structure (Braune et al., 2014; Horton et al., 2009; Mcmeans et al., 2014b; Young et al., 2010);
- Physiological changes during nursing periods (Habran et al., 2019);
- Habitat use and feeding behavior (Loseto et al., 2008a, 2008b; Renedo et al., 2020);
- Levels of environmental Hg pollution (Amos et al., 2013; Brown et al., 2017);
- Type of Hg sources (Jonsson et al., 2014a).

Until now, the sole measurement of THg (and rarely methylated-Hg, MeHg), **failed to concretely connect the complex interplay between these factors, Hg bioaccumulation and climate change**. The recent boom in Hg stable isotopes studies shows that the importance of **Hg sources** to marine biota has been **underestimated** (Pućko et al., 2014). As we will discuss later on, such works focus on primary producers and consumers, suggesting that the dynamic of Hg sourcing might differ in higher trophic level predators (Lavoie et al., 2013).

To overcome the limitations given by the analysis of one (or few) parameters (e.g. THg levels, $\delta^{13}\text{C}$ or $\delta^{15}\text{N}$), we developed in this thesis **multivariate models** that integrate ecological, environmental and contamination variables to:

1. Study **the influence** of seal metabolism (Chapter 3 and 4), trophic ecology (Chapter 5) and environmental change (Chapter 6) on levels of Hg bioaccumulation, and
2. Assess **Hg sources** in Arctic true seals living in the Greenland Sea (This chapter).

Table 7.1. THg concentrations measured in muscle of hooded seal *C. Cristata*, harp seal *P. Groenlandicus* and ringed seal *P. Hispidus* from several areas of the Arctic. Concentrations are presented as $\mu\text{g}\cdot\text{g}^{-1}$ dw. Literature concentrations that were expressed in ww, were transformed using the ww/dw ratio calculated in our samples: 3.4 ± 0.5 for hooded seal ($n = 135$), 3.1 ± 0.5 for ringed seals ($n = 125$) and 3.6 ± 0.2 for harp seals ($n = 23$) (Table A2.1). When possible, data are presented as Average \pm Standard Deviation, (Min – Max), n . NA = Data not available for this area. Out of range = area outside the distribution range of the species.

Area	Sampling site	Year	Arctic seal species			Reference
			Hooded seal	Harp seal	Ringed seal	
Western Greenland	Upernavik	1973 - 1976	0.68 (0.54 - 0.82) 10	0.86 (0.40 - 0.82) 11	0.71 (0.15 - 1.58) 10	(Johansen et al., 1980)
	Umanak	1973 - 1976	Out of range	0.72 (0.40 - 0.94) 12	Out of range	(Johansen et al., 1980)
Eastern Greenland	Greenland Sea	1985	(0.14 - 0.95) 22	(0.29 - 1.91) 29	NA	(Julshamn and Grahl-Nielsen, 2000)
	Greenland Sea	1999	0.54 ± 0.20 (0.27 - 1.05) 25	0.50 ± 0.29 (0.14 - 1.12) 25	NA	(Brunborg et al., 2006)
	Greenland Sea	1985 - 2019	0.32 ± 0.40 (0.05 - 3.93) 155	0.12 ± 0.08 (0.17 - 0.43) 61	0.40 ± 0.21 (0.06 - 1.68) 235	This study
Norway	Svalbard	1996	NA	NA	0.1 17	(Fant et al., 2001)
Western Canadian Arctic	North Baffin Island	1976	Out of range	Out of range	0.96 ± 0.25 36	(Smith and Armstrong, 1978)
	Beaufort Sea	2017	Out of range	Out of range	0.71 ± 0.37 15	(Houde et al., 2020)
	Resolute Bay	2017	Out of range	Out of range	1.58 ± 0.59 10	(Houde et al., 2020)
	West	1987 - 1993	Out of range	Out of range	1.27 ± 0.90	(Wagemann et al., 1996)
	East	1989 - 1993	Out of range	Out of range	1.21 ± 0.53	(Wagemann et al., 1996)
	Eureka	1994	Out of range	Out of range	2.05 ± 1.30	(Wagemann et al., 1996)
Eastern Canadian Arctic	Hudson Bay	1999 - 2006	Out of range	Out of range	0.68 ± 0.22	(Young et al., 2010)
	Hudson Bay Arviat, Nunavut	2003 - 2015	Out of range	Out of range	(0.8 - 6.9)	(Yurkowski et al., 2020)
	Hudson Bay	2017	Out of range	Out of range	0.65 ± 3.07 38	(Houde et al., 2020)
	Ungava/Nunatsiavut	2017	Out of range	Out of range	0.5 ± 0.46 17	(Houde et al., 2020)
	Eastern Baffin Island	2011	Out of range	Out of range	0.77 ± 0.34 14	(Houde et al., 2020)
Southeast Canada (North Atlantic Ocean)	Gulf St. Lawrence	1984	Out of range	1.32 ± 0.81 20	Out of range	(Wagemann et al., 1988)

3. TROPHIC LEVEL, METABOLISM OR HABITAT USE?

3.1. Higher trophic level does not mean higher mercury

THg levels were found to increase with trophic level in marine food webs at global scale (“biomagnification”) (Lavoie et al., 2013). Prey species and trophic position were considered as the main factors governing the rates of THg biomagnification (Dehn et al., 2006). As such, our initial hypothesis was that a seal species feeding on large and high trophic level prey, like the hooded seal, would be exposed to higher levels of THg than the harp and the ringed seals, feeding mostly on shoaling fish. $\delta^{202}\text{Hg}$ and $\delta^{15}\text{N}$ values are commonly used to trace Hg trophic transfer and trophic position in marine predators, because of the many biotic processes N and Hg undergo during assimilation from prey to predator (Cantalapiedra-Hijar et al., 2015; Tsui et al., 2019). As for N, several studies have shown how consumers’ tissues are enriched in ^{202}Hg compared to their prey, as a consequence of Hg metabolism throughout the food web (Meng et al., 2020; Perrot et al., 2012). This hypothesis was confirmed in some high trophic level animals like marine mammals but rejected in others (Kwon et al., 2012).

The calculation of trophic enrichment factors (TEFs) conducted in chapter 4 showed how there was no significant difference between $\delta^{202}\text{Hg}$ of hooded seal muscle and their prey, the herring (Chapter 4, §4.3). A positive significant TEF was observed only for hair (Chapter 4, §4.3). This suggests that $\delta^{202}\text{Hg}$ trophic enrichment is influenced by metabolic processes that are tissue-specific. Thus, depending on the selected tissue, $\delta^{202}\text{Hg}$ might reflect trophic enrichment or not at all. Since we measured Hg stable isotopes in seal muscle, we should interpret the $\delta^{202}\text{Hg}$ range of Greenland Sea seals more as a result of environmental Hg processing, before uptake into the animal (Chapter 4, §4.3). This is supported by the PCA results obtained in chapter 5 which showed that, among all tested factors, trophic position (represented by $\delta^{202}\text{Hg}$ and $\delta^{15}\text{N}$) was the least important at explaining the isotopic variability of Greenland Sea seals (Chapter 5, §4.2). This explains why **ringed seals present higher THg concentrations than hooded seals, even with similar trophic position** (Chapter 5, §3.4 and §4.5).

This confirms that, in the Greenland Sea, the **trophic position** of seals and their prey **does not govern the levels of Hg bioaccumulation**.

3.2. Specialized nursing does not put seals at risk

Arctic true seals have developed several **physiological adaptations** to increase the chance of survival of newborns in the cold and unstable Arctic environment (Blix, 2016). These adaptations regard mostly key-periods of life like gestation, lactation and postweaning fast (Lydersen et al., 1997;

Tucker et al., 2013). Our initial hypothesis was that such specialized nursing strategies might exacerbate Hg processing within the organisms and make Arctic marine mammals more sensitive to Hg bioaccumulation.

The hooded seal is one of the most specialized species of Arctic true seals, presenting the shortest period of lactation among all mammals (Lydersen et al., 1997). During 3 to 4 days, both hooded seal mothers and pups undergo extreme metabolic changes (Chapter 2, §1.1). Mothers lose half of their biomass, while pups reach almost the double of their weight at birth. After weaning, hooded seals pups will need only 2 weeks to be able to hunt (Chapter 2, §1.1). This is much shorter than for other species like the harp seal (4 weeks) and ringed seals (5 to 6 weeks) (Chapter 2, Table 2.1). We expected that the intense growing rates of hooded seals pups could make this species more sensitive to changes in Hg exposure as a consequence of global change, in comparison to other species. The analysis conducted in chapter 3 and 4 showed that the patterns of **C, N, S, and Hg isotopy** observed in hooded seals are more related with **ontogenetic shifts in seals' metabolism**, rather than specific physiological adaptations.

This confirms that species-specific **differences in nursing strategies do not govern Hg bioaccumulation**. As such, **we should not expect highly specialized species like the hooded seal to be more impacted** by shifts in Hg exposure caused by climate change.

3.3. Different habitat use, different mercury sources

Our multi-isotopic analysis indicated **habitat use as the strongest driver of both THg concentrations and sources** in Greenland Sea true seals (Chapter 5, §4.1). A coastal and sympagic behavior determines in ringed seal higher THg concentrations than the offshore pelagic harp and hooded seals (Chapter 5 and 6). These findings disagree with global trends where Hg bioaccumulation (mostly as MeHg) is typically higher in meso- and oligotrophic offshore ecosystems compared to eutrophic coastal ones (Wu et al., 2019).

Marine phytoplankton is the entrance door of Hg to marine food webs. Previous measurements suggest that seawater concentrations of MeHg, cell size and diversity are the main drivers of phytoplankton MeHg uptake rates across ecosystems (Schartup et al., 2018). When ecosystems are less productive (e.g. open ocean), smaller phytoplankton with greater surface area-to-volume ratios are more abundant to maximize nutrient uptake efficiency, which effectively increases MeHg uptake (Schartup et al., 2018). Conversely, higher nutrient status in coastal areas can lead to a greater abundance of larger cells, reducing nutrient uptake at the base of the food web and potentially also MeHg uptake (Wang, 2002). This process is called **Hg biodilution** (Driscoll et al., 2012). The type and amount of **natural organic matter** (OM) adds up to these processes, acting as a competitor in

scavenging seawater Hg and reducing its uptake by primary producers (Graham et al., 2012). Accordingly, in the OM-poor waters of the Northwest Atlantic margin and shelves, phytoplankton MeHg concentrations are found to be 4 times higher than OM-rich estuarine locations (Schartup et al., 2018).

If Hg biodilution and OM availability were the only factors affecting Hg levels in marine food webs, we should observe the same patterns also at higher trophic levels. This should be especially true in Arctic coastal areas, where the seasonal shifts in nutrients and Hg load from terrestrial systems are very strong (Carmack et al., 2015; Soerensen et al., 2017). However, recent evidences point out that Hg bioaccumulation in marine predators does not depend exclusively on baseline Hg levels and primary producers' activity (Jonsson et al., 2017; Thingstad et al., 2008). Scientists observed that the most critical drivers of Hg reactivity and bioavailability are:

- The **source and form of OM** present in the water (Schartup et al., 2018, 2015b);
- The diversity of **Hg pools** (Jonsson et al., 2014b); and
- The **composition of food web** (Jonsson et al., 2017).

Schartup et al. (2015) found that in **northern coastal and estuarine ecosystems**, the majority of dissolved OM in seawater was of terrestrial origin. Successive studies confirmed how an higher proportion of terrestrial *versus* marine OM, enhances MeHg production and bioaccumulation (Soerensen et al., 2017, 2016b). The large abundance of terrigenous OM heavily reduces light penetration, enhancing heterotrophic *versus* photosynthetic primary production in terrestrial run-offs. Bacterial activity is more efficient in producing MeHg than phytoplankton (Fisher et al., 2012). Most of the terrigenous MeHg is absorbed by pelagic zooplankton once reached the marine environment. Benthic invertebrates instead accumulate mostly marine MeHg, produced *in-situ* by bacteria in the bottom sediments (Jonsson et al., 2017). This results in the same pattern we observe in hooded, harp and ringed seals: biota exposed to terrigenous sources presents higher THg concentrations than organisms exposed to MeHg from bottom sediments (Jonsson et al., 2017).

On the other hand, on **the Northwest Atlantic shelf and margin**, scientists found that dissolved OM in seawater is predominantly of marine origin (Schartup et al., 2015b). Here, higher levels of marine dissolved OM are found to lower MeHg production and uptake, following the global trends (Lavoie et al., 2013; Schartup et al., 2015b).

These findings demonstrate that:

1. It is **not the abundance of Hg and nutrients in the environment** *per se* to dictate uptake rates in coastal *versus* offshore marine food webs; rather
2. **The source of Hg and nutrients is the dominant driver of transformation pathways** in the environment and ultimately rates of **Hg bioaccumulation in Arctic marine predators**.

4. HG SOURCES IN SEALS FROM THE GREENLAND SEA

The comparison of THg levels in hard tissues of humans and marine mammals between the pre-industrial era and modern days shows that around 92 % of the present-day Hg in Arctic wildlife is of man-made origin (Dietz et al., 2009). Despite the absence of major Hg point sources in the region, anthropogenic Hg enters the Arctic marine environment through:

- **Long-range inputs:** atmospheric and water masses circulations from midlatitudes;
- Local inputs: local marine production and terrestrial run-offs (e.g. glaciers, rivers).

The Arctic Ocean surface water has a residence time of about 10 years (Brown et al., 2017). Moreover, using stable Hg isotopes, Lehnherr et al. (2011) showed that reactions producing or demethylating MeHg are rapid, which implies that MeHg cannot be transported over long distances in the water (Lehnherr et al., 2011; Wang et al., 2012). On the other hand, the latest estimates propose that **118 ± 20 Mg of Hg emitted yearly in the atmosphere is transported to the Arctic**. Circa 65 ± 20 Mg year⁻¹ are deposited in surface Arctic waters (AMAP, 2021b). Based on these data, it could be easily proposed that Hg bioaccumulation in Arctic marine predators results from differences in the past and modern history of Hg production by northern midlatitude countries. In this regard, the higher biotic Hg concentrations in the western Canadian Arctic could be related to the elevated atmospheric deposition of anthropogenic Hg from Asian sources (Brown et al., 2018). However, recent Hg budgets show how emissions of Hg in the atmosphere are decreasing globally (AMAP, 2021b; Chen et al., 2015).

If long-range atmospheric inputs were the only factor controlling THg trends in Arctic biota, we should not observe large spatial differences (Table 7.1), but a steady decrease across all regions of the Arctic. In chapter 6 we saw how this is not occurring, as different species of true seals can show opposite temporal trends even at the small scale of the Greenland Sea (Chapter 6, §4).

Many hypotheses propose **local sources** as strong controllers of marine biotic Hg concentrations in the Arctic ocean (Soerensen et al., 2016a):

- **Rivers** contribute disproportionately to Hg input and biological uptake in marine food webs at a panarctic scale (Fisher et al., 2013; Soerensen et al., 2016a). Thus, the higher concentrations of Hg in the Canadian Arctic might relate to the larger freshwater input in the area, through the Mackenzie River (Routti et al., 2011).
- The Western Arctic Ocean presents naturally high geological background of Hg, constituting an important **reservoir of legacy Hg** which supplies almost all of the ocean water transiting its passages (Brown et al., 2017).
- The longitudinal biotic THg gradient reflects the **THg gradient measured in the oceanic water masses**: North Pacific > Arctic > North Atlantic Ocean (Brown et al., 2017).

These studies base their interpretation solely on THg levels, while it is MeHg which is readily bioaccumulated by marine food webs. Wang et al. (2018) recently linked the **distribution of the subsurface MeHg peak** to the spatial variability in biotic uptake. They showed that in the Western Arctic Ocean the MeHg maximum occurs at shallower depths than the eastern part, just below the surface productive layer (Wang et al., 2018). As such, in this area MeHg availability to organisms at the base of the marine food webs is enhanced (Wang et al., 2018).

These first considerations suggest that:

1. Although generally relevant, **long-range Hg sources** might **not be the main drivers of THg** in Arctic marine biota;
2. **Local Hg sources primarily govern Hg bioaccumulation in Arctic marine food webs**. This would explain why we observe a large spatial and temporal variability of Hg trends even at small scale, namely in true seals from the Greenland Sea ([Chapter 5](#) and [6](#)).

However, **no direct evidence exists yet** validating all these hypotheses in marine mammals.

4.1. Local or global?

Hg stable isotopes can be used to trace Hg sources in marine wildlife (Tsui et al., 2019). As such they can help answer the question about the origin of Hg bioaccumulated in Arctic marine predators at local and global scale.

4.1.1. Arctic or non Arctic?

Hg even MIF (here represented by $\Delta^{200}\text{Hg}$) has been increasingly used as tracer of Hg atmospheric reservoirs (Chapter 5, [§4.3](#); Cai and Chen, 2015). When compared to the literature, $\Delta^{200}\text{Hg}$ values show a **remarkable latitudinal gradient** (Figure 7.1). $\Delta^{200}\text{Hg}$ are the highest in sharks from the Indian Ocean, followed by fish from the Pacific Ocean, ringed seals from the Baikal Lake, human hair from the Faroe Islands, pilot whales from the North Atlantic Ocean, marine mammals and seabirds from Alaska, and finally Greenland Sea seals and seabirds (Figure 7.1). **The near-zero $\Delta^{200}\text{Hg}$ of $>60^\circ\text{N}$ latitudes** was previously linked to the small size of the Arctic basin, strong continental influence via river runoff, and the limited Hg^0 uptake by the Arctic Ocean because of ice cover and saturation of surface waters in dissolved Hg (Masbou et al., 2018; Renedo et al., 2020).

At first sight, $\Delta^{200}\text{Hg}$ in muscle of Greenland Sea seals seems to confirm that the bioaccumulated Hg by hooded, harp and ringed seals is locally assimilated.

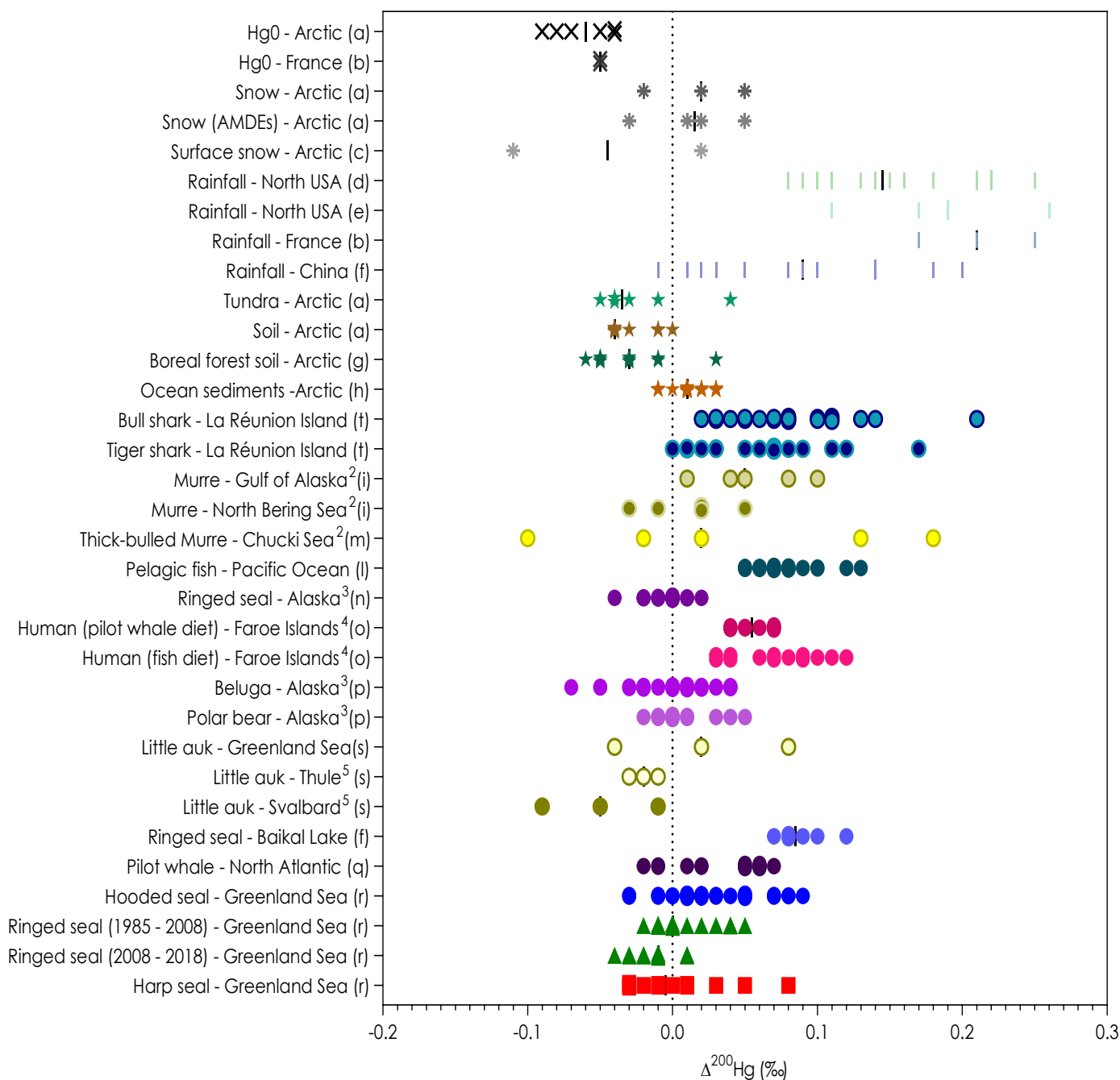


Figure 7.1. $\Delta^{200}\text{Hg}$ range in marine, freshwater and terrestrial ecosystems, with special attention to the Arctic region. Each point represents an individual data, the black vertical line represents the mean. Data are represented in δ notation as ‰. Animals' $\Delta^{200}\text{Hg}$ values derive from a variety of tissues. Measurements on muscle were favored. When not possible, other tissues were used. Number 1 = blood, 2= eggs, 3= liver, 4=hair, 5=head feathers. Letters refer to the different papers we extracted the data from. (a) (Obrist et al., 2017); (b) (Enrico et al., 2016); (c) (Sherman et al., 2012); (d) (Gratz et al., 2010); (e) (Demers et al., 2013); (f) (Wang et al., 2015); (g) (Jiskra et al., 2017); (h) (Gleason et al., 2017); (i) (Day et al., 2012); (l) (Blum et al., 2013); (m) (Point et al., 2011); (n) (Masbou et al., 2015a); (o) (Li et al., 2014); (p) (Masbou et al., 2018); (q) (Li et al., 2020); (r) This study; (s) (Renedo et al., 2020); (t) (Le Croizier et al., 2020). Greenland Sea true seals are represented like previous chapters: hooded seals as blue dots, ringed seals as green triangles, harp seals as red squares.

A second look at $\Delta^{200}\text{Hg}$ values of other marine mammals and of wet and dry precipitation, shows a finer pattern (Figure 7.1). Ringed seals from Greenland Sea and Alaska, as well as polar bears and beluga from Alaska show $\Delta^{200}\text{Hg}$ values closer to those found in Arctic tundra and soils. On the other hand, $\Delta^{200}\text{Hg}$ of hooded and harp seals and North Atlantic pilot whales show intermediate values between Arctic Ocean sediments and rainfall from lower latitudes (e.g. China). This suggests that:

In the Greenland Sea, Hg accumulated by **sympagic, coastal** marine mammals derive from **local Hg sources (mostly terrigenous)**, while **offshore pelagic** marine mammals are exposed to a **mix of local Hg marine reservoirs and long-range atmospheric sources** (chapter 5, §4.2 and §4.3).

4.1.2. Near but far: Greenland Sea seals are exposed to different mercury sources

Once determined Hg sources at large scale, $\delta^{202}\text{Hg}$ and $\Delta^{199}\text{Hg}$ values can help refine local Hg sourcing in Greenland Sea seals. The **range of $\delta^{202}\text{Hg}$ values** measured in muscle of hooded, harp and ringed seals from the Greenland Sea is quite wide, in accordance with previous literature in marine wildlife (Figure 7.2). Hg MDF (represented by $\delta^{202}\text{Hg}$) varies between latitudes in consequence of different biotic and abiotic processes (Tsui et al., 2019). For example, $\delta^{202}\text{Hg}$ values of beluga livers were previously found to show a latitudinal southward gradient going from the Beaufort Sea to the Bering Sea (Masbou et al., 2018). However, when comparing with the literature, $\delta^{202}\text{Hg}$ of Greenland seals, as well as other organisms, does not seem to vary with latitude or longitude (Figure 7.2).

$\delta^{202}\text{Hg}$ of **hooded and harp seals** from the Greenland Sea resemble those of pelagic fish from the Pacific Ocean, the Gulf of Mexico, the bull and tiger sharks from La Réunion Island and pilot whales from the **North Atlantic Ocean** (Figure 7.2). $\delta^{202}\text{Hg}$ of **ringed seals** from the Greenland seals are instead closer to coastal fish from North America and Europe, as well as to Arctic marine mammals strongly associated to **land fast ice and coastal food webs** like the polar bear, beluga and ringed seals from Alaska (Figure 7.2).

$\Delta^{199}\text{Hg}$ range of Greenland Sea hooded, harp and ringed seals is much smaller than $\delta^{202}\text{Hg}$ (Figure 7.3). This in accordance with the absence of Hg MIF by organism's metabolism, as already published (Kwon et al., 2012; Tsui et al., 2019) and observed in chapter 4 (§4.3). $\Delta^{199}\text{Hg}$ values of Greenland Sea seals resemble little auks from Greenland (East and West) and Svalbard (Renedo et al., 2020). Near-zero $\Delta^{199}\text{Hg}$ are common of polar regions like the Arctic and are mostly related to:

- The **limited or absent iHg or methylated Hg (MeHg) photochemistry** in sea ice covered areas (Point et al., 2011; Renedo et al., 2020);
- The seasonal influence of extreme **negative AMDEs** (< -5‰) (Sherman et al., 2010).

However, when compared with the literature, $\Delta^{199}\text{Hg}$ values follow only weakly a latitudinal gradient. The higher values are found in seabirds from Antarctic, followed by fish from the Pacific Ocean, sharks from the Indian Ocean and biota from North America and Europe (Figure 7.3).

If latitude was the only factor influencing $\Delta^{199}\text{Hg}$ values, Greenland seals would present $\Delta^{199}\text{Hg}$ values closer to Baikal ringed seals than to Pacific or Indian fish (Figure 7.3). Instead, ringed seals from Lake Baikal have very distinct $\Delta^{199}\text{Hg}$ values with respect to all other regions. In the same way, Greenland Sea seals and seabirds present $\Delta^{199}\text{Hg}$ ranges identical to seabass from European estuaries (Cransveld et al., 2017; Renedo et al., 2020).

Researchers suggest that the variation of $\delta^{202}\text{Hg}$ and $\Delta^{199}\text{Hg}$ values among marine food webs is mostly led by animal habitat use (Gantner et al., 2009; Masbou et al., 2015a). This is also confirmed by our findings in chapter 5 (§4.3). The extent of Hg MDF depends on Hg processing at the base of marine food webs (Chapter 5, §4.5). At the same time, odd MIF is determined by photochemical Hg^{2+} photoreduction and MeHg breakdown (Zheng and Hintelmann, 2009). As such, a **decreasing offshore – inshore pattern** of $\delta^{202}\text{Hg}$ and $\Delta^{199}\text{Hg}$ is commonly observed in Arctic animals (as explained in chapter 5; §4.5). This is linked to:

- Upstream: higher concentrations of OM (particulate or dissolved), nutrients, and MeHg (Soerensen et al., 2017, 2016b);
- Estuary: shallower MeHg subsurface maximum, enhanced Hg scavenging by sinking OM, enhanced primary production (Li et al., 2016a; Schartup et al., 2013);
- Sea ice: surface-snow aging (bacteria or light induced), ice particles fallout, sea ice algae and pelagic algae blooms (Heimbürger et al., 2015, 2010; Schartup et al., 2020);
- Air: Spring AMDEs (Sherman et al., 2012, 2010).

This results in lower light penetration, slower Hg processing in the environment and lower rates of Hg MDF and MIF (Chapter 5, §4.5). Consequently, **coastal nutrient-rich ecosystems are characterized by lower $\delta^{202}\text{Hg}$ and $\Delta^{199}\text{Hg}$ values than offshore oligotrophic ones.**

To our best knowledge, these findings represent **the first assessment of Hg sources in Greenland seals**. The application of Hg stable isotopes confirms that:

1. Even **at a small spatial scale** (e.g. hundreds of km in the Greenland Sea), **true seals** are **subjected to different sources of Hg in the marine environment**, as a consequence of their different habitat use;
2. At local scale, **exposure and bioaccumulation of Hg** in Greenland Sea seals **is strongly dependent on local marine sourcing and processing related to sea-ice and freshwater run-offs**.

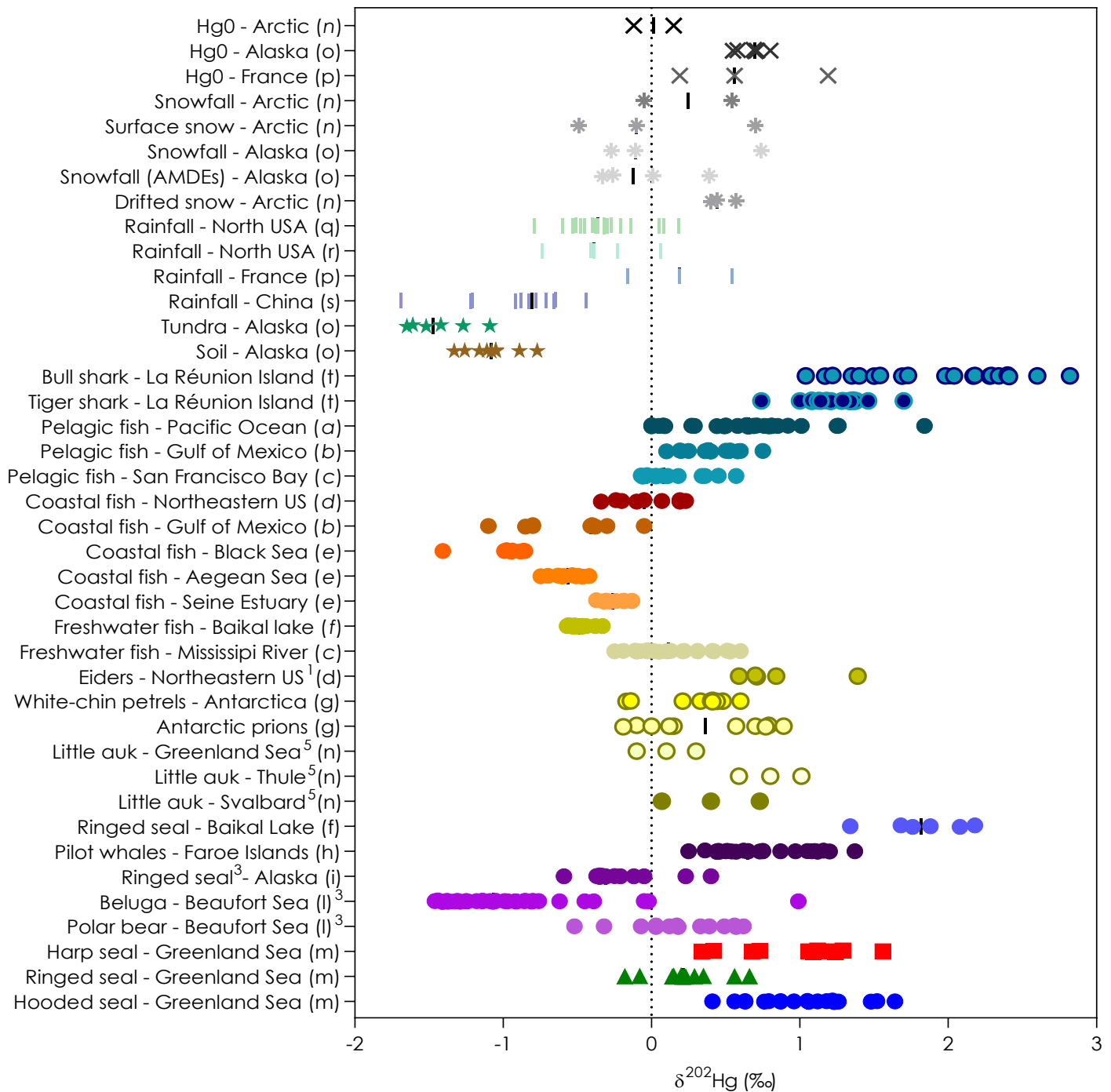


Figure 7.2. $\delta^{202}\text{Hg}$ range in marine, freshwater and terrestrial ecosystems, with special attention to the Arctic region. Each point represents an individual data, the black vertical line represents the mean. Data are represented in δ notation as ‰. Animals' $\delta^{202}\text{Hg}$ values derive from a variety of tissues. Measurements on muscle were favoured. When not possible other tissues were used. Number 1 = blood, 2= eggs, 3= liver, 4=hair, 5=head feathers. Letters refer to the different papers we extracted the data from. (a) (Blum et al., 2013); (b) (Senn et al., 2010); (c) (Gehrke and Blum, 2011); (d) (Kwon et al., 2014); (e) (Cransveld et al., 2017); (f) (Perrot et al., 2012); (g) (Renedo et al., 2018); (h) (Li et al., 2020); (i) (Masbou et al., 2015a); (l) (Masbou et al., 2018); (m) This study; (n) (Sherman et al., 2012); (o) (Obrist et al., 2017); (p) (Enrico et al., 2016); (q) (Gratz et al., 2010); (r) (Demers et al., 2013); (s) (Wang et al., 2015); (t) (Le Croizier et al., 2020). Greenland Sea true seals are represented like previous chapters: hooded seals as **blue dots**, ringed seals as **green triangles**, harp seals as **red squares**.

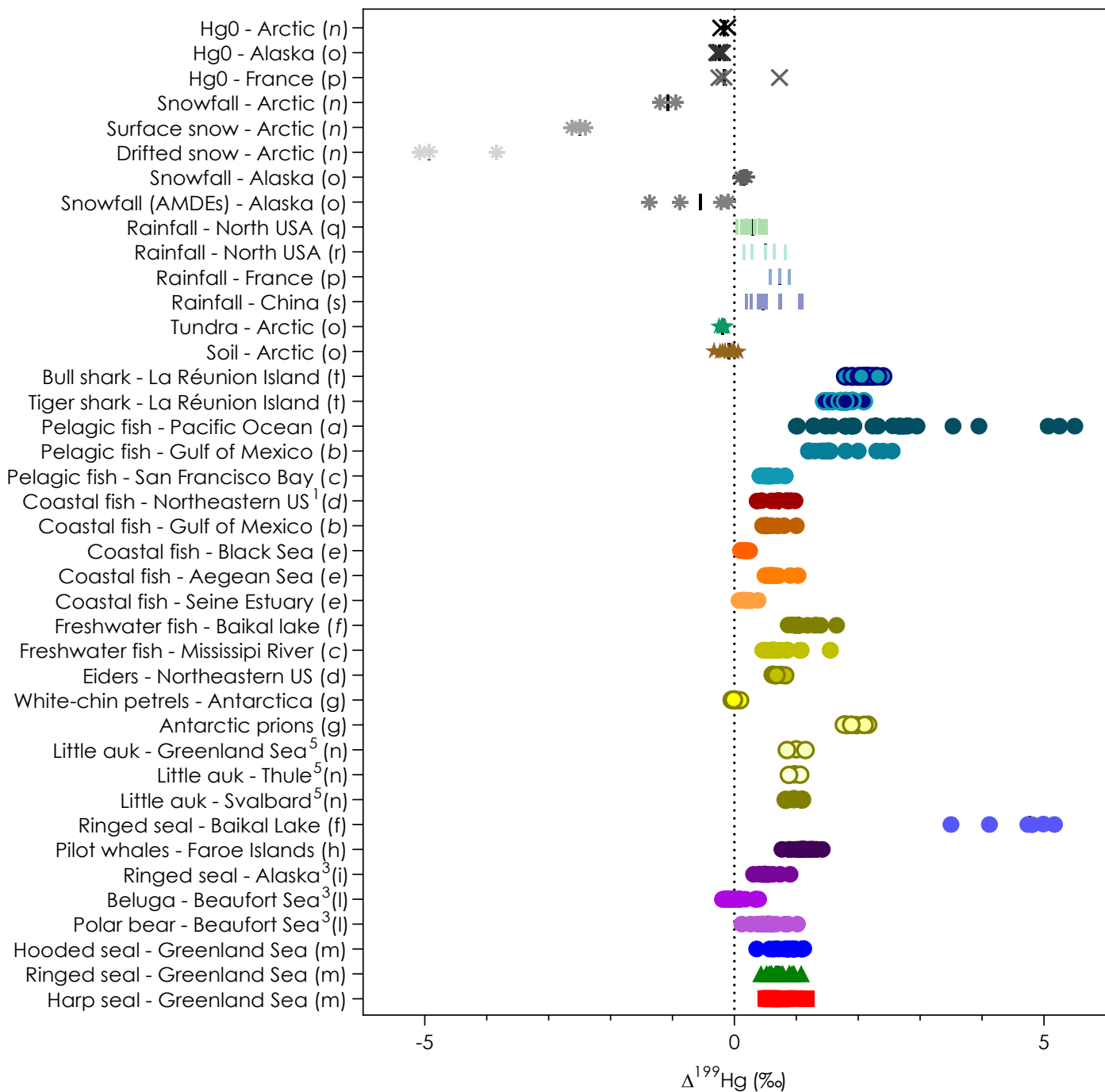


Figure 7.3. $\Delta^{199}\text{Hg}$ range in marine, freshwater and terrestrial ecosystems, with special attention to the Arctic region. Each point represents an individual data, the black vertical line represents the mean. Data are represented in δ notation as ‰. Animals' $\Delta^{199}\text{Hg}$ values derive from a variety of tissues. Measurements on muscle were favoured. When not possible other tissues were used. Number 1 = blood, 2= eggs, 3= liver, 4=hair, 5=head feathers. Letters refer to the different papers we extracted the data from. (a) (Blum et al., 2013); (b) (Senn et al., 2010); (c) (Gehrke and Blum, 2011); (d) (Kwon et al., 2014); (e) (Cransveld et al., 2017); (f) (Perrot et al., 2012); (g) (Renedo et al., 2018); (h) (Li et al., 2020); (i) (Masbou et al., 2015a); (l) (Masbou et al., 2018); (m) This study; (n) (Sherman et al., 2012); (o) (Obrist et al., 2017); (p) (Enrico et al., 2016); (q) (Gratz et al., 2010); (r) (Demers et al., 2013); (s) (Wang et al., 2015); (t) (Le Croizier et al., 2020). Greenland Sea true seals are represented like previous chapters: hooded seals as **blue dots**, ringed seals as **green triangles**, harp seals as **red squares**.

5. PRESENT AND FUTURE DYNAMIC OF MERCURY IN GREENLAND SEA MARINE PREDATORS

5.1. A changing Arctic

The largest change observed in **sea-ice** is in its summer extent (September). 2012 (Figure 7.4, red dotted line) consists in the lower record for Arctic sea-ice cover, with only 3.4 million km² of extent compared to the 6.3 million km² median for the 1981-2010 period (Figure 7.4, grey line). 2020 represents the second lowest minimum of summer sea ice extent: 3.8 million km² (Figure 7.4, green line). Sea-ice cover and structure are instrumental for both coastal and offshore marine food webs, governing food web complexity, energy transfer, and biomagnification of pollutants like Hg (Post, 2013). A decrease in sea-ice cover was linked to higher rates of MeHg breakdown and consequently declining THg trends in marine biota (Point et al., 2011). A decrease in sea-ice cover was linked to higher rates of MeHg breakdown and consequently declining THg trends in marine biota (Point et al., 2011).

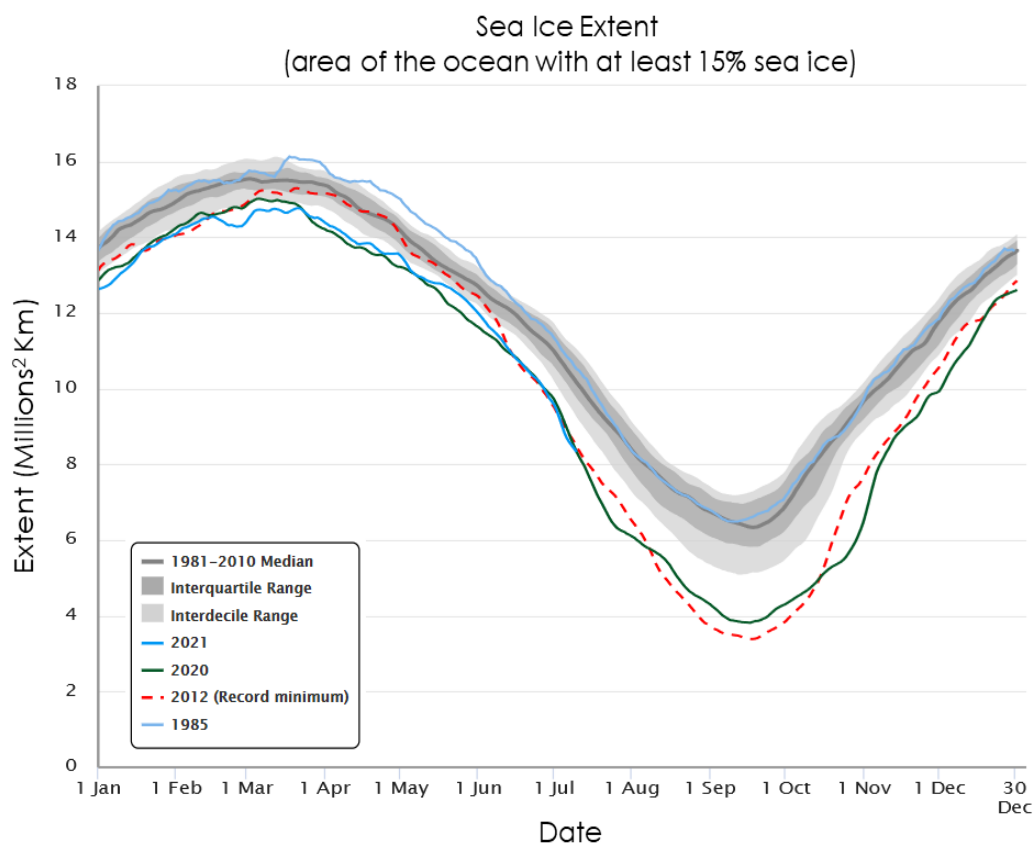


Figure 7.4. Annual variation of sea ice extent (in millions of square kilometers) in the Northern Hemisphere for the time period analyzed in this thesis: 1985 - 2021. The grey line represents the median for the 1981-2010 period. This graph was made with ChArctic v3.3.8, and extracted from [National Snow and Ice Data Center](#) (accessed on: 12/07/2021).

However, Schartup et al. (2020) found significantly higher concentrations of MeHg in FYI than in MYI, and suggested that the temporal shift in sea-ice age might enhance Hg exposure to marine biota (Schartup et al., 2020).

The Arctic has lost more than 50 % of its oldest multiyear ice (MYI) and is undergoing a regime shift from a system dominated by MYI (until 2011) to a **system dominated by seasonal ice (FYI)** (Miles et al., 2020). In March 1985, 4 years old sea-ice constituted 33 % of the sea-ice in the Arctic Ocean (Figure 7.5). In March 2019, 4 years old sea-ice made up 1.2 % of the pack (Perovich et al. 2019). In Eastern Greenland a decrease in sea-ice age was observed for both land fast and pack-ice. This might constitute a significant changing driver of Hg bioaccumulation in both offshore and coastal marine food webs.

Land fast ice forms along the coast from water or by accumulation of floating ice of any age and can extend from a few meters to several hundred kilometers from the coast (Trishchenko and Luo, 2021). Land fast ice consists in 12 % of the total sea-ice presents in the Northern hemisphere (Mahoney et al., 2014).

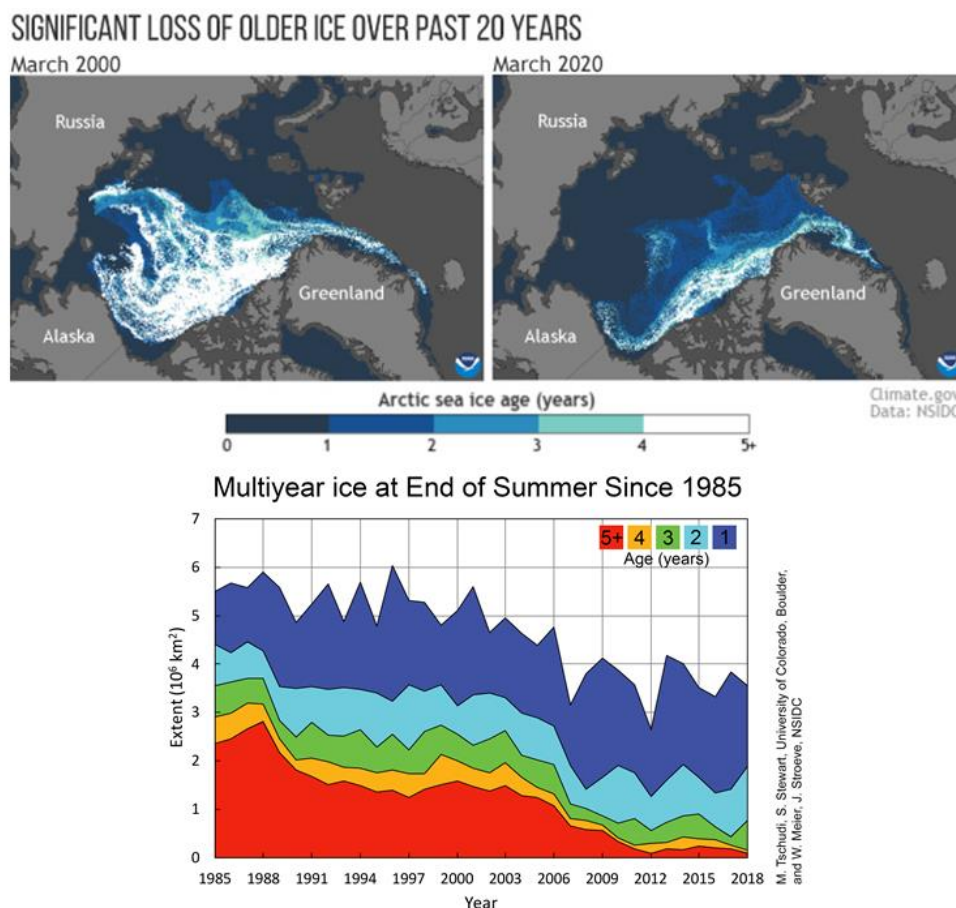


Figure 7.5. Temporal change in Arctic sea ice age: (A) distribution and (B) extent (in 10⁶ km²). (A) The age of sea ice in the Arctic at winter maximum in 2000 (left, week of March 18) and 2020 (right, week of March 21). Maps reproduced from [NOAA Climate.gov](https://climate.gov), based on data from the National Snow and Ice Data Center. (B) Graph reproduced by Tschudi et al. 2019, from [National Snow and Ice Data Center](https://www.nsidc.org) (accessed on: 12/07/2021).

In the Scoresby Sound, **land fast ice** provides an important substrate for the sustenance of humans and sympagic coastal food web (Post, 2013). Ringed seals depend on it for breeding, feeding and hiding from predators (Chapter 2, §1.3). A decrease of -0.53 % per decade (1976 – 2007) of land fast ice was observed In the Greenland Sea area (Yu et al., 2014).

Pack-ice (or drift ice) forms offshore after a characteristic formation processes including grease and pancakes, at seawater temperature of -1.8°C (Werner, 2005). It is not attached to the shoreline and drifts in response to winds and currents. At its maximum extent pack-ice can cover an area comprising 13 % of the Earth's surface, making it a biome that compares with those of the tundra and deserts (Mahoney et al., 2014). In offshore areas, pack-ice is the main driver of photosynthetic primary production and act as physical substrate for pagophilic pelagic seals like harp seals (Chapter 1, §2.2). The oceanic hooded seals instead depend on pack-ice mostly for breeding (Chapter 5, §4.2). Knowing that (1) local Hg sources are the main drivers of THg bioaccumulation in Arctic seals (Chapter 5), that (2) different trophic behaviors lead to different Hg sources and bioaccumulation in Greenland seals (Chapter 6) and that (3) sea-ice and freshwater inputs influence Hg cycling in fjordic marine food webs (This chapter, §4.1), raises the following questions:

1. Can **climate change significantly alter Hg cycling** in response to sea-ice loss and increased freshwater run-off?
2. Do **seal species respond similarly**?

In the next paragraphs we integrate the major outcomes of this work to depict **Hg dynamic in marine predators in a context of present and future Arctic climate change**.

5.2. Offshore foodwebs

The decrease in pack-ice extent along the Eastern coast of Greenland ranges between -0.1 to -0.5 % per decade in the Fram Strait, to -15 to -5 % per decade in the Greenland Sea (Dai et al., 2019). The decrease of sea-ice cover in offshore environment is believed to lead to:

- **Higher light penetration**, bringing to higher rates of MeHg breakdown (Point et al., 2011);
- **Higher influx of warm North Atlantic waters**, disrupting water stratification, enhancing Hg remobilization within the water column and lowering a build-up of MeHg concentrations in surface water layers (Bowman et al., 2020; Polyakov et al., 2017);
- **A shift in food web structure**, leading to higher reliance on pelagic prey *versus* sympagic ones by species like the harp seal and lower MeHg dietary intake (Petrik et al., 2020), and

- **Increased** intensity and area of **algal blooms** (Leu et al., 2015; Tedesco et al., 2019).

During spring of 2019, a ~1500 km long region along the edge of the Greenland Sea pack-ice showed on average ~18 times higher chlorophyll- α concentrations than during the same month of the previous years on record (2003-18; Frey et al., 2019; Tremblay et al., 2015). In this area, positive trends in primary productivity have been observed since 2003 (~20.5 % increase) (Barber et al., 2015; Leu et al., 2015). The increase in pelagic photosynthetic biomass along the Greenland Sea pack-ice margin could then be responsible for an increase of Hg biodilution. All of these factors might contribute to the decreasing trends in THg concentrations observed in marine predators like hooded seals as well as in their prey.

As discussed before, hooded seals are exposed to a mixture of Hg produced in the oceanic water column and long-range atmospheric inputs (via wet and dry deposition) (This chapter, §4.1.1). As such, **hooded seal THg trends reflect emissions at global scale and inputs to the North Atlantic Oceans** (Ceia et al., 2018). Because of their specialized hunting on demersal Greenland halibut and squids from the *Gonatus* genus, the hooded seal might be more **impacted by bottom-up shifts of food web structure** compared to more generalist species, namely the shift from a Greenland halibut dominated-diet to an Atlantic cod dominated-diet (Chapter 6, §4.2).

The combination of environmental changes expected for offshore food webs with the trophic behavior of oceanic seals suggests that a decrease in THg concentrations is expected in Greenland Sea oceanic predators like the hooded and harp seals (Figure 7.6). Accordingly, hooded seals present **decreasing THg concentrations (1.5 % / year)** (Chapter 6, §4.2), in agreement with decreasing THg levels observed in the Atlantic cod between the 70s and the 2000s in Norway, the Faroe Islands and Iceland (-0.8 / year, -2.4 / year and -4.9 to -7.4 / year respectively) (Braune et al., 2011).

5.3. Coastal food webs

Together with the loss of land fast ice, the latest climatic studies foreseen that the main change in Arctic coastal marine ecosystems will be:

- An **increase of terrestrial runoff** ranging between 15 and 50 % depending on the region of the Arctic (Oppenheimer et al., 2019). This would comprise higher coastal erosion, larger losses of Greenland ice sheet mass ($-263 \pm 21 \text{ Gt yr}^{-1}$) as well as coastal glaciers across all Arctic regions ($-212 \pm 29 \text{ Gt yr}^{-1}$) (Meredith et al., 2019).

Jonsson et al. (2017) predicted concentration of MeHg in zooplankton in the Bothnian Sea coastal areas to increase as much as a factor of 3 to 6, following the ecological and biogeochemical impacts of a 30 % increase in terrestrial runoff. This would occur as a consequence of increased bacterial respiration, eutrophication and hypoxia, **shifting primary production from autotrophic**

(phytoplankton) to heterotrophic (Jonsson et al., 2017). The microbial loop would become the most important driver of primary production and Hg uptake in the baseline.

- **Freshening of surface marine layers**, believed to **enhance water stratification** at local scale. The latest IPCC reports show a ~2.18 to 2.42 % increase of the upper 200m stratification in Arctic waters from 1970 and 2017 (Meredith et al., 2019).

Enhanced stratification has several potential serious consequences:

- **Disruption of sinking and redistribution** of both OM and nutrients like nitrate (Oppenheimer et al., 2019).
- **Reduction of phytoplankton size** (Li et al., 2009). Small-sized phytoplankton is known to play a key role in marine MeHg dynamics, because it sinks slower and boosts remineralization and MeHg production in the pycnocline waters (Heimbürger et al., 2010). In parallel, small-sized plankton blooms occur deeper in the photic zone, closer to the MeHg maximum, which may further enhance biological uptake of MeHg (Heimbürger et al., 2015).
- **Disruption of the benthic-pelagic coupling** characteristic of polar coastal areas. In winter, when light is limited by the thick sea-ice cover, the resuspension of sediments and lateral advection of bio-material from bottom sediments and freshwater run-offs are the main food sources of pelagic organisms. limiting energy flow and Hg transfer in the food web.

Coastal species like the ringed seal, are exposed to several sources of Hg: terrestrial freshwater runoff, sea-ice and local atmospheric inputs, and *in situ* production via bacterial activity in the sediments (This chapter, §4). As such, **ringed seals' THg trends reflect mostly the complex interplay of changes in the environment they live in** (Loseto et al., 2008b; Pinzone et al., 2021a). This determines a larger variability in Hg sources in time and consequently lead to the nonlinear THg accumulation trends observed in ringed seals (This chapter, Figure 7.7; Chapter 6, §4.1). This also supports the inconsistency of THg trends found in ringed seals from different areas of the Arctic: increasing THg trends in Northwestern Greenland, no trend in Western Canada and decreasing trends (-2.5 % / year) in Resolute (Houde et al., 2020; Rigét et al., 2012; Yurkowski et al., 2020), as well as in others Greenland Sea coastal predators, like the glaucous gull (Fort J., *pers. comm.*), the polar bear and the black guillemot (Braune et al., 2011).

These findings demonstrate that:

1. **Species response to climate change is governed by changes in Hg sources rather than Hg levels;**
2. **Coastal species are at higher risk** of increasing Hg exposure in the future, compared to offshore species.

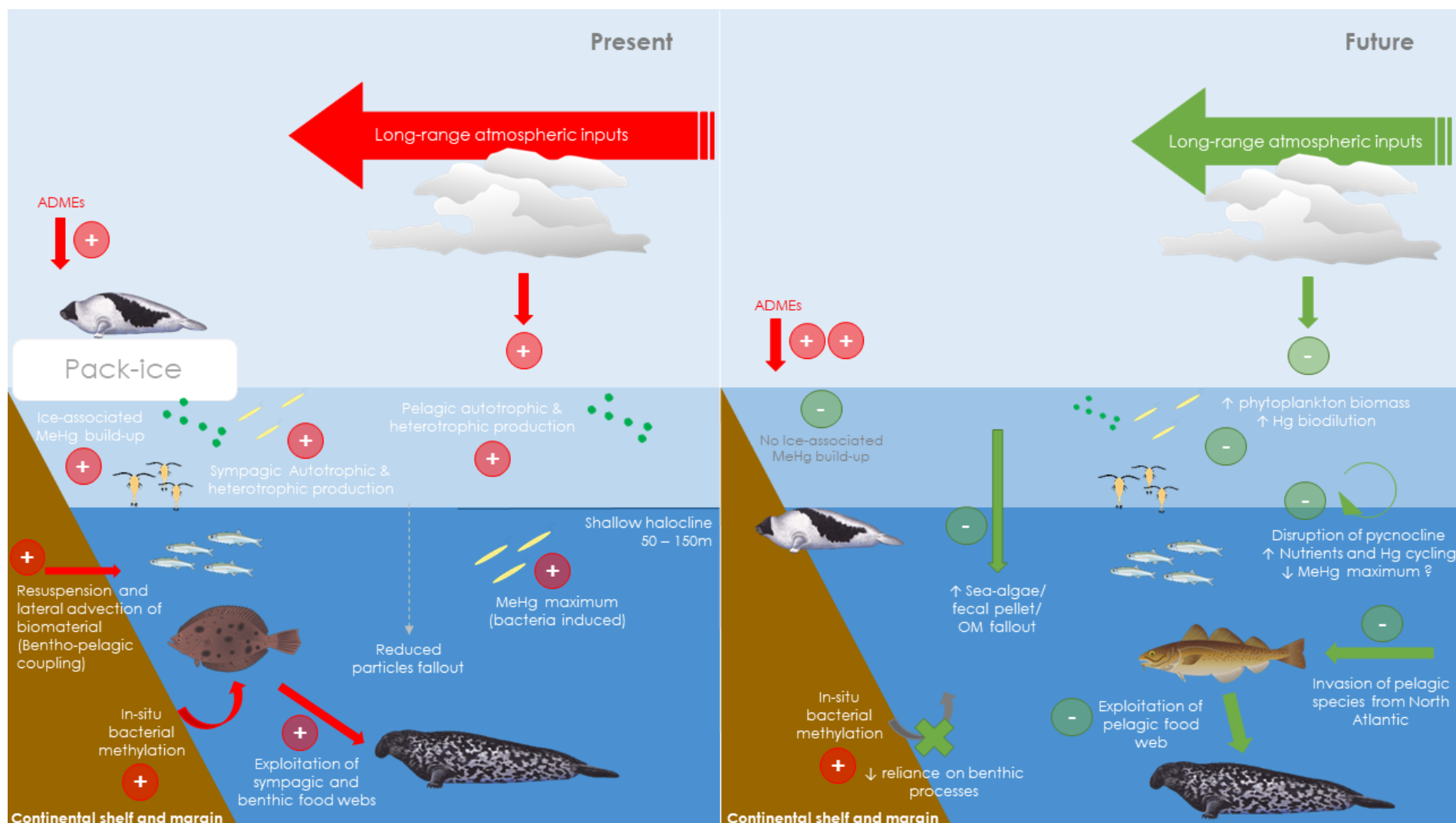


Figure 7.6. Conceptual Hg dynamic in the offshore marine predators hooded seal *Cystophora cristata* and harp seal *Pagophilus groenlandicus*, in a context of present and future climate change in the Greenland Sea (period 1985 – 2019). Red arrows represent processes which increase THg muscle concentrations. Green arrows represent processes which decrease THg muscle concentrations

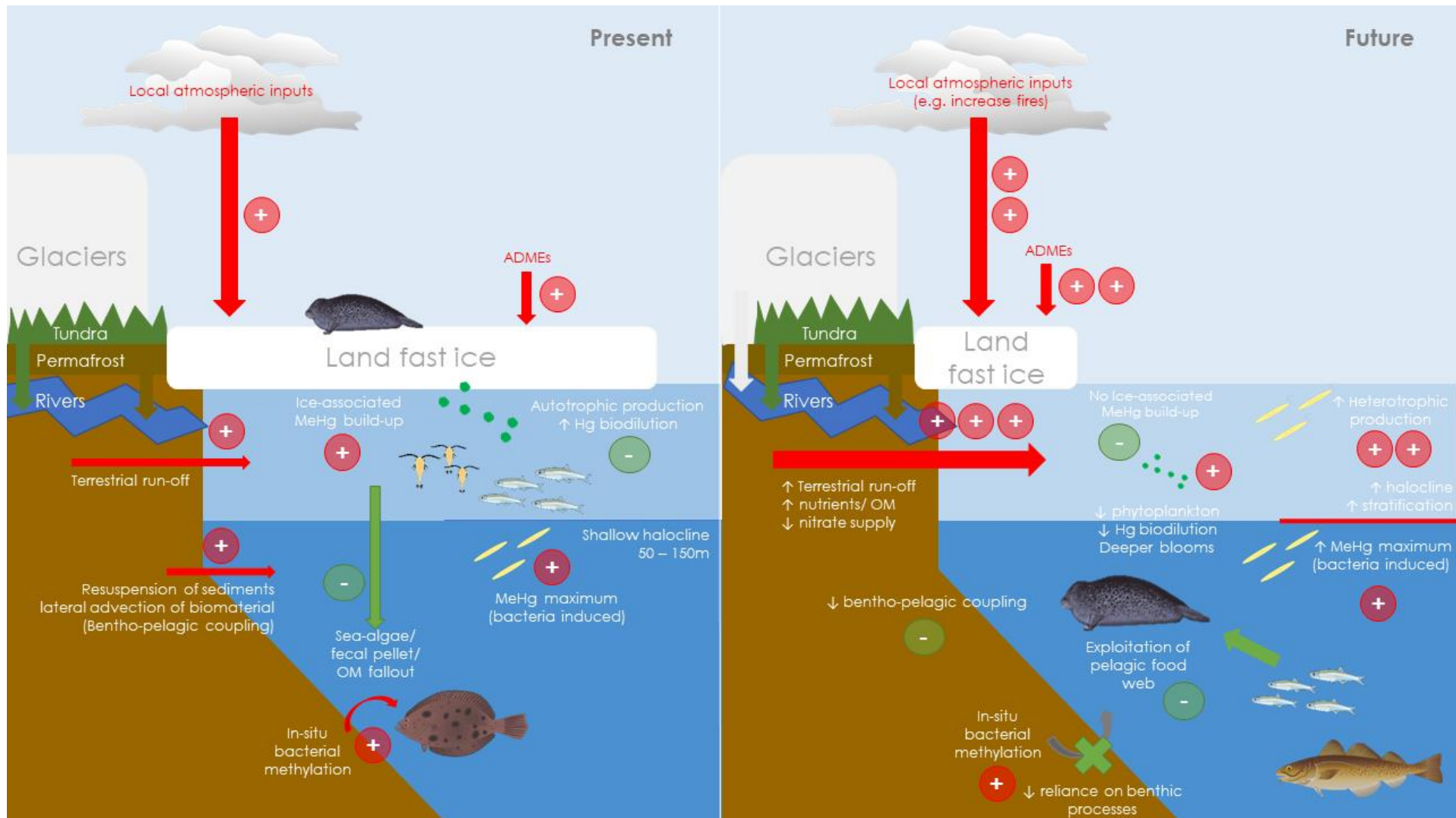


Figure 7.7. Conceptual Hg dynamic in the coastal marine predator ringed seal *Pusa hispida*, in a context of present and future climate change in the Greenland Sea (period 1985 – 2019). Red arrows represent processes which increase THg muscle concentrations. Green arrows represent processes which decrease THg muscle concentrations.

Take home message

To our best knowledge, this thesis represents **the first attempt at linking Hg sources in Greenland Sea true seals with climate change, using Hg stable isotopes**. Our findings add an important additional piece to the immense puzzle of Hg dynamics in Arctic marine food webs.

The major outcome is **that Hg accumulation in Arctic marine predators is strongly species-specific and depend on their habitat use**. This explains why responses to climate change have been vast and inconsistent not only between species, but also within the same species from different regions of the Arctic. **While Hg exposure to oceanic specialized species will be affected by global-scale ecological changes, Hg exposure to coastal generalist species will depend on specific bio-chemical processes at local scale**.

A recent paper demonstrated how the Greenland ice sheet is responsible for the influx of 521 to 3300 mmol km⁻² of Hg per year during melting. These quantities are 2 orders of magnitude higher than what was measured for Arctic rivers (4 to 20 mmol km⁻² year⁻¹) (Hawkings et al., 2021). These recent discoveries stress the importance of **pursuing research** about the impact of terrestrial Hg reservoirs on Arctic coastal marine ecosystems.

Our finding complicates further mitigation of Hg pollution in the Arctic region, pushing future scientific and management efforts to **incorporate a species-specific focus at both local and global scale**.

References

- Abass, K., Carlsen, A., Rautio, A., 2016. ARCTIC MONITORING AND ASSESSMENT PROGRAM New approaches in human health risk assessment. *Int. J. Circumpolar Health* 75, 1–7. <https://doi.org/10.3402/ijch.v75.33845>
- ACIA, 2005. Arctic Climate Impact Assessment. ACIA overview report, Cambridge University Press.
- Adams, T.S., Sterner, R.W., 2000. The Effect of Dietary Nitrogen Content on Trophic Level 15 N Enrichment. *Limnol. Oceanogr.* 45, 601–607. <https://doi.org/10.4319/lo.2000.45.3.0601>
- Adlard, B., Lemire, M., Bonefeld-Jørgensen, E.C., Long, M., Ólafsdóttir, K., Odland, J.O., Rautio, A., Myllynen, P., Sandanger, T.M., Dudarev, A.A., Bergdahl, I.A., Wennberg, M., Berner, J., Ayotte, P., 2021. MercuNorth—monitoring mercury in pregnant women from the Arctic as a baseline to assess the effectiveness of the Minamata Convention. *Int. J. Circumpolar Health* 80. <https://doi.org/10.1080/22423982.2021.1881345>
- Ajsuvakova, O.P., Tinkov, A.A., Aschner, M., Rocha, J.B.T., Michalke, B., Skalnaya, M.G., Skalny, A. V, Butnariu, M., Dadar, M., Sarac, I., Aaseth, J., Bjørklund, G., 2020. Sulfhydryl groups as targets of mercury toxicity The binding of Hg to Cys mediates multiple toxic effects. *Coord Chem Rev* 417. <https://doi.org/10.1016/j.ccr.2020.213343>
- Albert, C., Helgason, H.H., Brault-Favrou, M., Robertson, G.J., Descamps, S., Amélineau, F., Danielsen, J., Dietz, R., Elliott, K., Erikstad, K.E., Eulaers, I., Ezhov, A., Fitzsimmons, M.G., Gavriilo, M., Golubova, E., Grémillet, D., Hatch, S., Huffeldt, N.P., Jakubas, D., Kitaysky, A., Kolbeinsson, Y., Krasnov, Y., Lorentsen, S.-H., Lorentzen, E., Mallory, M.L., Merkel, B., Merkel, F.R., Montevecchi, W., Mosbech, A., Olsen, B., Orben, R.A., Patterson, A., Provencher, J., Plumejeaud, C., Pratte, I., Reiertsen, K., Renner, H., Rojek, N., Romano, M., Strøm, H., Systad, H., Takahashi, A., Thiebot, J.-B., Lindberg Thórarinnsson, T., Will, A.P., Wojczulanis-Jakubas, K., Bustamante, P., Fort, J., 2021. Seasonal variation of mercury contamination in Arctic seabirds: A pan-Arctic assessment. *Sci. Total Environ.* 750, 142201. <https://doi.org/10.1016/j.scitotenv.2020.142201>
- Alonso, J.C., Huecas, V., Alonso, J.A., Abelenda, M., Muñoz-Pulido, R., Puerta, M.L., 1991. Hematology and blood chemistry of adult white storks (*Ciconia ciconia*). *Comp. Biochem. Physiol.* 98, 395–397.
- Altunay, N., Elik, A., Gürkan, R., 2019. Food Additives & Contaminants : Part A Natural deep eutectic solvent-based ultrasound- assisted-microextraction for extraction , pre- concentration and analysis of methylmercury and total mercury in fish and environmental waters by spectrophotometry. *Food Addit. Contam. Part A* 36, 1079–1097. <https://doi.org/10.1080/19440049.2019.1619939>
- Alves, E.Q., Macario, K., Ascough, P., Bronk Ramsey, C., 2018. The Worldwide Marine Radiocarbon Reservoir Effect: Definitions, Mechanisms, and Prospects. *Rev. Geophys.* 56, 278–305. <https://doi.org/10.1002/2017RG000588>
- Alvira-Iraizoz, F., Nordøy, E.S., 2019. Evidence of seawater drinking in fasting subadult hooded seals (*Cystophora cristata*). *J. Anim. Behav. Biometeorol.* 7, 52–59. <https://doi.org/10.31893/2318-1265jabb.v7n2p52-59>
- AMAP, 2021a. Human Health in the Arctic 2021. Summary for Policy-makers. Tromsø, Norway.
- AMAP, 2021b. 2021 AMAP Mercury Assessment. Summary for Policy-makers. Oslo, Norway.
- AMAP, 2019. ARCTIC CLIMATE CHANGE UPDATE 2019.
- AMAP, 2017. Snow, water, ice and permafrost in the Arctic (SWIPA) 2017. Arctic monitoring and Assessment Programme (AMAP), Oslo, Norway.
- AMAP, 2015. AMAP assessment 2015: Human health in the Arctic, AMAP assessment report. AMAP, Oslo, Norway.

<https://doi.org/10.3402/ijch.v75.33949>

- AMAP, 2012. Arctic climate issues 2011: Changes in Arctic snow, water, ice and permafrost, SWIPA 2011 Overview Report. Arctic Monitoring and Assessment Programme (AMAP), Oslo. Arctic monitoring and Assessment Programme (AMAP), Oslo, Norway.
- AMAP, 2011. AMAP Assessment 2011: Mercury in the Arctic. Oslo, Norway.
- AMAP, 1997a. The Arctic, in: Arctic Pollution Issues: A State of the Arctic Environment Report. Oslo, Norway, pp. 4–19. [https://doi.org/ISBN 82-7655-060-6](https://doi.org/ISBN%2082-7655-060-6)
- AMAP, 1997b. Polar Ecology, in: Arctic Pollution Issues: A State of the Arctic Environment Report. Arctic monitoring and Assessment Programme (AMAP), Oslo, Norway, pp. 34–49.
- Ambrose, S.H., Norr, L., 1993. Carbon isotopic evidence for routing of dietary protein to bone collagen, and whole diet to bone apatite carbonate: purified diet growth experiments, in: Lambert, J., Grupe, G. (Eds.), Prehistoric Human Bone: Archaeology at the Molecular Level. Springer-Verlag, Berlin, pp. 1–37.
- Amos, H.M., Jacob, D.J., Streets, D.G., Sunderland, E.M., 2013. Legacy impacts of all-time anthropogenic emissions on the global mercury cycle. *Global Biogeochem. Cycles* 27, 410–421. <https://doi.org/10.1002/gbc.20040>
- Andersen, J.M., Wiersma, Y.F., Stenson, G., 2009. Movement Patterns of Hooded Seals (*Cystophora cristata*) in the Northwest Atlantic Ocean during the Post-Moult and Pre-Breed Seasons 42, 1–11. <https://doi.org/10.2960/J.v42.m649>
- Andersen, J.M., Wiersma, Y.F., Stenson, G.B., Hammill, M.O., Rosing-Asvid, A., Skern-Mauritzen, M., 2013. Habitat selection by hooded seals (*Cystophora cristata*) in the Northwest Atlantic Ocean. *ICES J. Mar. Sci.* 70, 173–185. <https://doi.org/10.1093/icesjms/fss133>
- Angot, H., Hoffman, N., Giang, A., Thackray, C.P., Hendricks, A.N., Urban, N.R., Selin, N.E., 2018. Global and Local Impacts of Delayed Mercury Mitigation Efforts. *Environ. Sci. Technol.* 52, 12968–12977. <https://doi.org/10.1021/acs.est.8b04542>
- Armitage, T.W.K., Manucharyan, G.E., Petty, A.A., Kwok, R., Thompson, A.F., 2020. Enhanced eddy activity in the Beaufort Gyre in response to sea ice loss. *Nat. Commun.* 761. <https://doi.org/10.1038/s41467-020-14449-z>
- Arnould, J.P.Y., Luque, S.P., Guinet, C., Costa, D.P., Kingston, J., Shaffer, S. a, 2003. The comparative energetics and growth strategies of sympatric Antarctic and subantarctic fur seal pups at Iles Crozet. *J. Exp. Biol.* 206, 4497–4506. <https://doi.org/10.1242/jeb.00703>
- Aspmo, K., Temme, C., Berg, T., Ferrari, C., Gauchard, P.-A., Fain, X., Wibetoe, G., 2006. Mercury in the Atmosphere, Snow and Melt Water Ponds in the North Atlantic Ocean during Arctic Summer. *Environ. Sci. Technol.* 40, 4083–4089. <https://doi.org/10.1021/es052117z>
- Atherton, P.J., Smith, K., 2012. Muscle protein synthesis in response to nutrition and exercise. *J. Physiol.* 590, 1049–57. <https://doi.org/10.1113/jphysiol.2011.225003>
- Atwell, L., Hobson, K.A., Welch, H.E., 1998. Biomagnification and bioaccumulation of mercury in an arctic food web: insights from stable nitrogen isotopes analysis. *Can. J. Fish. Aquac. Sci.* 55, 1114–1121.
- Aubail, A., Teilmann, J., Dietz, R., Rigét, F., Harkonen, T., Karlsson, O., Rosing-Asvid, A., Caurant, F., 2011. Investigation of mercury concentrations in fur of phocid seals using stable isotopes as tracers of trophic levels and geographical regions. *Polar Biol.* 34, 1411–1420. <https://doi.org/10.1007/s00300-011-0996-z>
- Bajzak, C.E., Cote, S.D., Hammill, M.O., Stenson, G., 2009. Intersexual differences in the postbreeding foraging

- behaviour of the Northwest Atlantic hooded seal. *Mar. Ecol. Prog. Ser.* 385, 285–294. <https://doi.org/10.3354/meps08015>
- Balcom, P.H., Schartup, A.T., Mason, R.P., Chen, C.Y., 2015. Sources of water column methylmercury across multiple estuaries in the Northeast U.S. *Mar. Chem.* 177, 721–730. <https://doi.org/10.1016/j.marchem.2015.10.012>
- Barber, D.G., Hop, H., Mundy, C.J., Else, B., Dmitrenko, I.A., Tremblay, J.-E., Ehn, J.K., Assmy, P., Daase, M., Candlish, L.M., Rysgaard, S., 2015. Selected physical, biological and biogeochemical implications of a rapidly changing Arctic Marginal Ice Zone. *Prog. Oceanogr.* 139, 122–150. <https://doi.org/10.1016/j.pocean.2015.09.003>
- Barkay, T., Poulain, A.J., 2007. Mercury (micro)biogeochemistry in polar environments. *FEMS Microbiol. Ecol.* 59, 232–241. <https://doi.org/10.1111/j.1574-6941.2006.00246.x>
- Basu, N., Scheuhammer, A.M., Rouvinen-Watt, K., Douglas Evans, R., Trudeau, V.L., Chan, L.H.M., 2010. In vitro and whole animal evidence that methylmercury disrupts GABAergic systems in discrete brain regions in captive mink. <https://doi.org/10.1016/j.cbpc.2010.01.001>
- Basu, N., Scheuhammer, A.M., Rouvinen-Watt, K., Grochowina, N., Douglas Evans, R., O'brien, M., Chan, H.M., 2006. Decreased N-methyl-D-aspartic acid (NMDA) receptor levels are associated with mercury exposure in wild and captive mink. <https://doi.org/10.1016/j.neuro.2006.12.007>
- Baya, P.A., 2015. Investigating the sources and fate of monomethylmercury and dimethylmercury in the Arctic marine boundary layer and waters. *Environ. Sci. Technol.* 49, 223–232.
- Baya, P.A., Gosselin, M., Lehnerr, I., St.Louis, V.L., Hintelmann, H., 2015. Determination of Monomethylmercury and Dimethylmercury in the Arctic Marine Boundary Layer. *Environ. Sci. Technol.* 49, 223–232. <https://doi.org/10.1021/es502601z>
- Bearhop, S., Waldron, S., Votier, S.C., Furness, R.W., 2002. Factors that influence assimilation rates and fractionation of nitrogen and carbon stable isotopes in avian blood and feathers. *Physiol. Biochem. Zool.* 75, 451–458. <https://doi.org/10.1086/342800>
- Beattie, S.A., Armstrong, D., Chaulk, A., Comte, J., Gosselin, M., Wang, F., 2014. Total and Methylated Mercury in Arctic Multiyear Sea Ice. *Environ. Sci. Technol.* 48, 5575–5582. <https://doi.org/10.1021/es5008033>
- Bellido, J.J., Castillo, J.J., Farfán, M. a., Martín, J.J., Mons, J.L., Real, R., 2009. First records of hooded seals (*Cystophora cristata*) in the Mediterranean Sea. *Mar. Biodivers. Rec.* 1, 2006–2007. <https://doi.org/10.1017/S1755267207007804>
- Beltran, R.S., Peterson, S.H., Mchuron, E.A., Reichmuth, C., Hückstädt, L.A., Costa, D.P., 2016. Seals and sea lions are what they eat, plus what? Determination of trophic discrimination factors for seven pinniped species. *Rapid Commun. Mass Spectrom.* 30, 1115–1122. <https://doi.org/10.1002/rcm.7539>.Seals
- Bengtsson, O., Lydersen, C., Kovacs, K.M., Lindström, U., 2020. Ringed seal (*Pusa hispida*) diet on the west coast of Spitsbergen, Svalbard, Norway: during a time of ecosystem change. *Polar Biol.* 43, 773–788. <https://doi.org/10.1007/s00300-020-02684-5>
- Bérail, S., Cavalheiro, J., Tessier, E., Barre, J.P.G., Pedrero, Z., Donard, O.F.X., Amouroux, D., 2017. Determination of total Hg isotopic composition at ultra-trace levels by on line cold vapor generation and dual gold-amalgamation coupled to MC-ICP-MS. *J. Anal. At. Spectrom.* 32, 373–384. <https://doi.org/10.1039/C6JA00375C>
- Bergquist, B.A., Blum, J.D., 2009. The odds and evens of mercury isotopes: Applications of mass-dependent and mass-independent isotope fractionation. *Elements* 5, 353–357. <https://doi.org/10.2113/gselements.5.6.353>

- Bergquist, B.A., Blum, J.D., 2007a. Mass-dependent and-independent fractionation of Hg isotopes by photoreduction in aquatic systems. *Science* (80-.). 318, 417–420.
- Bergquist, B.A., Blum, J.D., 2007b. Mass-dependent and -independent fractionation of Hg isotopes by photoreduction in aquatic systems. *Science* (80-.). 318, 417–421.
- Bignert, A., Rigét, F., Braune, B., Outridge, P., Wilson, S., 2004. Recent temporal trend monitoring of mercury in Arctic biota - How powerful are the existing data sets? *J. Environ. Monit.* 6, 351–355. <https://doi.org/10.1039/b312118f>
- Bintanja, R., 2018. The impact of Arctic warming on increased rainfall. *Sci. Rep.* 8, 6. <https://doi.org/10.1038/s41598-018-34450-3>
- Biuw, M., Nilssen, K.T., Haug, T., Stenson, G., 2018. Report From Surveys To Assess Harp And Hooded Seal Pup Production In The Greenland Sea Pack-Ice In 2018.
- Bjørklund, G., Chirumbolo, S., Dadar, M., Pivina, L., Lindh, U., Butnariu, M., Aaseth, J., 2019. Mercury exposure and its effects on fertility and pregnancy outcome. *Basic Clin. Pharmacol. Toxicol.* 125, 317–327. <https://doi.org/10.1111/bcpt.13264>
- Black, F.J., Conaway, C.H., Flegal, A.R., 2009. Stability of Dimethyl Mercury in Seawater and Its Conversion to Monomethyl Mercury. *Environ. Sci. Technol.* 43, 4056–4062. <https://doi.org/10.1021/es9001218>
- Blackstock, J.C., 1989. CHAPTER 16 - Nitrogen Metabolism, in: Blackstock, J.C.B.T.-G. to B. (Ed.), . Butterworth-Heinemann, pp. 196–207. <https://doi.org/https://doi.org/10.1016/B978-0-7236-1151-6.50022-4>
- Blévin, P., Aars, J., Andersen, M., Blanchet, M.A., Hanssen, L., Herzke, D., Jeffreys, R.M., Nordøy, E.S., Pinzone, M., De La Vega, C., Routti, H., 2020. Pelagic vs Coastal - Key Drivers of Pollutant Levels in Barents Sea Polar Bears with Contrasted Space-Use Strategies. *Environ. Sci. Technol.* 54, 985–995. <https://doi.org/10.1021/acs.est.9b04626>
- Blix, A.S., 2016. Adaptations to polar life in mammals and birds. *J. Exp. Biol.* 219, 1093–1105. <https://doi.org/10.1242/jeb.120477>
- Blix, A.S., 2005. Arctic animals and their adaptations of life on the edge, 1st ed. Tapir Academic Press, Trondheim.
- Blum, J.D., 2011. Applications of stable mercury isotopes to biogeochemistry, in: Baskaran, M. (Ed.), *Handbook of Environmental Isotope Geochemistry*. Springer, Berlin, pp. 229–245.
- Blum, J.D., Bergquist, B.A., 2007. Reporting of variations in the natural isotopic composition of mercury. *Anal. Bioanal. Chem.* 388, 353–359. <https://doi.org/10.1007/s00216-007-1236-9>
- Blum, J.D., Johnson, M.W., 2017. Recent developments in mercury stable isotope analysis. *Rev. Mineral. Geochemistry* 82, 733–757. <https://doi.org/10.2138/rmg.2017.82.17>
- Blum, J.D., Popp, B.N., Drazen, J.C., Anela Choy, C., Johnson, M.W., 2013. Methylmercury production below the mixed layer in the North Pacific Ocean. *Nat. Geosci.* 6, 879–884. <https://doi.org/10.1038/ngeo1918>
- Blum, J.D., Sherman, L.S., Johnson, M.W., 2014. Mercury Isotopes in Earth and Environmental Sciences. *Annu. Rev. Earth Planet. Sci.* 42, 249–269. <https://doi.org/10.1146/annurev-earth-050212-124107>
- Boecklen, W.J., Yarnes, C.T., Cook, B.A., James, A.C., 2011. On the Use of Stable Isotopes in Trophic Ecology. *Annu. Rev. Ecol. Evol. Syst.* 42, 411–440. <https://doi.org/doi:10.1146/annurev-ecolsys-102209-144726>
- Boetius, A., Albrecht, S., Bakker, K., Bienhold, C., Felden, J., Fernández-Méndez, M., Hendricks, S., Katlein, C., Lalande, C., Krumpfen, T., Nicolaus, M., Peeken, I., Rabe, B., Rogacheva, A., Rybakova, E., Somavilla, R., Wenzhöfer, F., Felden, J., 2013. Export of algal biomass from the melting arctic sea ice. *Science* (80-.). 339,

- 1430–1432. <https://doi.org/10.1126/science.1231346>
- Bolea-Fernandez, E., Rua-Ibarz, A., Krupp, E.M., Feldmann, J., Vanhaecke, F., 2019. High-precision isotopic analysis sheds new light on mercury metabolism in long-finned pilot whales (*Globicephala melas*). *Sci. Rep.* 9, 7262. <https://doi.org/10.1038/s41598-019-43825-z>
- Bond, A.L., Diamond, A.W., 2011. Recent Bayesian stable-isotope mixing models are highly sensitive to variation in discrimination factors. *Ecol. Appl.* 21, 1017–23. <https://doi.org/10.1644/13-mamm-a-014.1>
- Bond, A.L., Hobson, K.A., Branfireun, B.A., 2015. Rapidly increasing methyl mercury in endangered ivory gull (*Pagophila eburnea*) feathers over a 130 year record. *Proc. R. Soc. B Biol. Sci.* 282. <https://doi.org/10.1098/rspb.2015.0032>
- Born, E.W., Teilmann, J., Acquarone, M., Rigét, F., 2004. Habitat use of ringed seals (*Phoca hispida*) in the North Water area (North Baffin Bay). *Arctic* 57, 129–142. <https://doi.org/10.14430/arctic490>
- Born, E.W., Teilmann, J., Rigét, F., 1998. Abundance of ringed seals (*Phoca hispida*) in the Kong Oscars Fjord, Scoresby Sund and adjacent areas in eastern Greenland. *NAMMCO Sci. Publ.* 1, 152–166. <https://doi.org/10.7557/3.2985>
- Böttcher, M.E., Brumsack, H.J., Dürselen, C.D., 2007. The isotopic composition of modern seawater sulfate: I. Coastal waters with special regard to the North Sea. *J. Mar. Syst.* 67, 73–82. <https://doi.org/10.1016/j.jmarsys.2006.09.006>
- Böttcher, M.E., Schale, H., Schnetger, B., Wallmann, K., Brumsack, H.J., 2000. Stable sulfur isotopes indicate net sulfate reduction in near-surface sediments of the deep Arabian Sea. *Deep. Res. Part II Top. Stud. Oceanogr.* 47, 2769–2783. [https://doi.org/10.1016/S0967-0645\(00\)00048-5](https://doi.org/10.1016/S0967-0645(00)00048-5)
- Bowen, W.D., Iverson, S.J., 2013. Methods of estimating marine mammal diets: A review of validation experiments and sources of bias and uncertainty. *Mar. Mammal Sci.* 29, 719–754. <https://doi.org/10.1111/j.1748-7692.2012.00604.x>
- Bowman, K.L., Collins, R.E., Agather, A.M., Lamborg, C.H., Hammerschmidt, C.R., Kaul, D., Dupont, C.L., Christensen, G.A., Elias, D.A., 2019. Distribution of mercury-cycling genes in the Arctic and equatorial Pacific Oceans and their relationship to mercury speciation. *Limnol. Oceanogr.* 65, S310–S320. <https://doi.org/10.1002/lno.11310>
- Bowman, K.L., Lamborg, C.H., Agather, A.M., 2020. A global perspective on mercury cycling in the ocean. *Sci. Total Environ.* 710, 136166. <https://doi.org/10.1016/j.scitotenv.2019.136166>
- Boyd, E.S., Barkay, T., 2012. The mercury resistance operon: From an origin in a geothermal environment to an efficient detoxification machine. *Front. Microbiol.* 3, 1–13. <https://doi.org/10.3389/fmicb.2012.00349>
- Bragulla, H.H., Homberger, D.G., 2009. Structure and functions of keratin proteins in simple, stratified, keratinized and cornified epithelia. *J. Anat.* 214, 516–559. <https://doi.org/10.1111/j.1469-7580.2009.01066.x>
- Braune, B., Carrie, J., Dietz, R., Evans, M., Gaden, A., Gantner, N., Hedman, J., Hobson, K., Loseto, L., Muir, D., Outridge, P., Rigét, F., Rognerud, S., Stern, G., Verta, M., Wang, F., Wängberg, I., 2011. Are Mercury Levels in Arctic Biota Increasing or Decreasing, and Why? How much higher are current mercury levels in Arctic biota than in the pre-industrial period, and thus what is the anthropogenic contribution to mercury in modern biota?, in: *AMAP Assessment Report 2011: Mercury in the Arctic*. Arctic monitoring and Assessment Programme (AMAP), Oslo, Norway, pp. 85–112.
- Braune, B.M., Gaston, A.J., Hobson, K.A., Gilchrist, H.G., Mallory, M.L., 2014. Changes in food web structure alter trends of mercury uptake at two seabird colonies in the Canadian Arctic. *Environ. Sci. Technol.* 48, 13246–13252.

<https://doi.org/10.1021/es5036249>

- Bravo, A.G., Cosio, C., 2020. Biotic formation of methylmercury: A bio–physico–chemical conundrum. *Limnol. Oceanogr.* 65, 1010–1027. <https://doi.org/10.1002/lno.11366>
- Bridges, C.C., Zalups, R.K., 2017. Mechanisms involved in the transport of mercuric ions in target tissues. *Arch. Toxicol.* 91, 63–81. <https://doi.org/10.1007/s00204-016-1803-y>
- Bridges, C.C., Zalups, R.K., 2010. Transport of inorganic mercury and methylmercury in target tissues and organs. *J. Environ. Heal. B Crit. Rev.* 13, 385–410. <https://doi.org/10.1016/j.physbeh.2017.03.040>
- Bridou, R., Monperrus, M., Rodriguez Gonzalez, P., Guyoneaud, R., Amouroux, D., 2011. Simultaneous determination of mercury methylation and demethylation capacities of various sulfate-reducing bacteria using species-specific isotopic tracers. *Environ. Toxicol. Chem.* 30, 337–344.
- Brosnan, J., Brosnan, M., 2006. The Sulfur-Containing Amino Acids: An Overview. *J. Nutr.* 136, 16365–16405.
- Broussard, L.A., Hammett-stabler, C.A., Winecker, R.E., 2002. The Toxicology of Mercury. *Lab. Med.* 33.
- Brown, T.A., Chrystal, E., Ferguson, S.H., Yurkowski, D.J., Watt, C., Hussey, N.E., Kelley, T.C., Belt, S.T., 2017. Coupled changes between the H-Print biomarker and $\delta^{15}\text{N}$ indicates a variable sea ice carbon contribution to the diet of Cumberland Sound beluga whales. *Limnol. Oceanogr.* 62, 1606–1619. <https://doi.org/10.1002/lno.10520>
- Brown, T.A., Galicia, M.P., Thiemann, G.W., Belt, S.T., Yurkowski, D.J., Dyck, M.G., 2018. High contributions of sea ice derived carbon in polar bear (*Ursus maritimus*) tissue. *PLoS One* 13, 1–13. <https://doi.org/10.1371/journal.pone.0191631>
- Brown, T.M., Fisk, A.T., Wang, X., Ferguson, S.H., Young, B.G., Reimer, K.J., Muir, D.C.G., 2016. Mercury and cadmium in ringed seals in the Canadian Arctic: Influence of location and diet. *Sci. Total Environ.* 545–546, 503–511. <https://doi.org/10.1016/j.scitotenv.2015.12.030>
- Brown, T.M., Macdonald, R.W., Muir, D.C.G., Letcher, R.J., 2018. The distribution and trends of persistent organic pollutants and mercury in marine mammals from Canada’s Eastern Arctic. *Sci. Total Environ.* 618, 500–517. <https://doi.org/10.1016/j.scitotenv.2017.11.052>
- Brown, T.M., Macdonald, R.W., Muir, D.C.G., Letcher, R.J., 2017. The distribution and trends of persistent organic pollutants and mercury in marine mammals from Canada’s Eastern Arctic. *Sci. Total Environ.* 618, 500–517. <https://doi.org/10.1016/j.scitotenv.2017.11.052>
- Brunborg, L.A., Graff, I.E., Frøyland, L., Julshamn, K., 2006. Levels of non-essential elements in muscle from harp seal (*Phagophilus groenlandicus*) and hooded seal (*Cystophora cristata*) caught in the Greenland Sea area. *Sci. Total Environ.* 366, 784–798. <https://doi.org/10.1016/j.scitotenv.2005.10.020>
- Buchachenko, A.L., 2013. Mass-Independent Isotope Effects. *J. Phys. Chem. B* 117, 2231–2238. <https://doi.org/10.1021/jp308727w>
- Buchachenko, A.L., 2009. Mercury isotope effects in the environmental chemistry and biochemistry of mercury-containing compounds. *Russ. Chem. Rev.* 78, 319–328. <https://doi.org/10.1070/rc2009v078n04abeh003904>
- Buchachenko, A.L., 2001. Magnetic Isotope Effect: Nuclear Spin Control of Chemical Reactions. *J. Phys. Chem. A* 105, 9995–10011. <https://doi.org/10.1021/jp011261d>
- Buckman, K.L., Seelen, E.A., Mason, R.P., Balcom, P., Taylor, V.F., Ward, J.E., Chen, C.Y., 2019. Sediment organic carbon and temperature effects on methylmercury concentration : A mesocosm experiment. *Sci. Total Environ.* 666, 1316–1326. <https://doi.org/10.1016/j.scitotenv.2019.02.302>

- Budikova, D., 2009. Role of Arctic sea ice in global atmospheric circulation: A review. *Glob. Planet. Change.* <https://doi.org/10.1016/j.gloplacha.2009.04.001>
- Burn, C.R., 1995. Where does the polar night begin? *Can. Geogr.* 39, 68–74.
- Bustamante, P., Bocher, P., Chereil, Y., Miramand, P., Caurant, F., 2003. Distribution of trace elements in the tissues of benthic and pelagic fish from the Kerguelen Islands. *Sci. Total Environ.* 313, 25–39. [https://doi.org/10.1016/S0048-9697\(03\)00265-1](https://doi.org/10.1016/S0048-9697(03)00265-1)
- Buttigieg, P.L., Ramette, A., 2014. A guide to statistical analysis in microbial ecology: a community-focused, living review of multivariate data analyses. *FEMS Microbiol. Ecol.* 90, 543–550. <https://doi.org/10.1111/1574-6941.12437>
- Cai, H., Chen, J., 2015. Mass-independent fractionation of even mercury isotopes. <https://doi.org/10.1007/s11434-015-0968-8>
- Cantalapiedra-Hijar, G., Ortigues-Marty, I., Sepchat, B., Agabriel, J., Huneau, J.F., Fouillet, H., 2015. Diet–animal fractionation of nitrogen stable isotopes reflects the efficiency of nitrogen assimilation in ruminants. *Br. J. Nutr.* 113, 1158–1169. [https://doi.org/DOI: 10.1017/S0007114514004449](https://doi.org/DOI:10.1017/S0007114514004449)
- Capelli, R., Das, K., De Pellegrini, R., Drava, G., Lepoint, G., Miglio, C., Minganti, V., Poggi, R., 2008. Distribution of trace elements in organs of six species of cetaceans from the Ligurian Sea (Mediterranean), and the relationship with stable carbon and nitrogen ratios. *Sci. Total Environ.* 390–569.
- Cardona-Marek, T., Knott, K.K., Meyer, B.E., O’hara, T.M., 2009. Mercury concentrations in Souther Beaufort Sea polar bears: variation based on stable isotopes of carbon and nitrogen, *Environmental Toxicology and Chemistry.*
- Carlens, H., Lydersen, C., Krafft, B.A., Kovacs, K.M., 2006. Spring haul-out behavior of ringed seals (*Pusa hispida*) in Kongsfjorden, Svalbard. *Mar. Mammal Sci.* 22, 379–393. <https://doi.org/10.1111/j.1748-7692.2006.00034.x>
- Carmack, E., Winsor, P., Williams, W., 2015. The contiguous panarctic Riverine Coastal Domain: A unifying concept. *Prog. Oceanogr.* 139, 13–23. <https://doi.org/10.1016/j.pcean.2015.07.014>
- Carnat, G., Said-Ahmad, W., Fripiat, F., Wittek, B., Tison, J.L., Uhlig, C., Amrani, A., 2018. Variability in sulfur isotope composition suggests unique dimethylsulfoniopropionate cycling and microalgae metabolism in Antarctic sea ice. *Commun. Biol.* 1. <https://doi.org/10.1038/s42003-018-0228-y>
- Caut, S., Angulo, E., Courchamp, F., 2009. Variation in discrimination factors ($\Delta^{15}\text{N}$ and $\Delta^{13}\text{C}$): The effect of diet isotopic values and applications for diet reconstruction. *J. Appl. Ecol.* 46, 443–453. <https://doi.org/10.1111/j.1365-2664.2009.01620.x>
- Ceia, F.R., Chereil, Y., Paiva, V.H., Ramos, J.A., 2018. Stable Isotope Dynamics ($\delta^{13}\text{C}$ and $\delta^{15}\text{N}$) in Neritic and Oceanic Waters of the North Atlantic Inferred From GPS-Tracked Cory’s Shearwaters. *Front. Mar. Sci.* 5. <https://doi.org/10.3389/fmars.2018.00377>
- Chabot, D., Stenson, G.B., 2002. Growth and seasonal fluctuations in size and condition of male Northwest Atlantic harp seals *Phoca groenlandica*: An analysis using sequential growth curves. *Mar. Ecol. Prog. Ser.* 227, 25–42. <https://doi.org/10.3354/meps227025>
- Chakrabarti, Saroj K, Loua, Kovana M, Bai, Chengjiang, Durham, Heather, Panisset, J.-C., Chakrabarti, S K, Loua, K M, Bai, C, Durham, H, 1998. Modulation of Monoamine Oxidase Activity in Different Brain Regions and Platelets Following Exposure of Rats to Methylmercury, *Neurotoxicology and Teratology.*
- Chandan, P., Ghosh, S., Bergquist, B.A., 2015. Mercury Isotope Fractionation during Aqueous Photoreduction of

- Monomethylmercury in the Presence of Dissolved Organic Matter. *Environ. Sci. Technol.* 49, 259–267. <https://doi.org/10.1021/es5034553>
- Charette, M.A., Kipp, L.E., Jensen, L.T., Dabrowski, J.S., Whitmore, L.M., Fitzsimmons, J.N., Williford, T., Ulfso, A., Jones, E., Bundy, R.M., Vivancos, S.M., Pahnke, K., John, S.G., Xiang, Y., Hatta, M., Petrova, M. V., Heimbürger-Boavida, L.E., Bauch, D., Newton, R., Pasqualini, A., Agather, A.M., Amon, R.M.W., Anderson, R.F., Andersson, P.S., Benner, R., Bowman, K.L., Edwards, R.L., Gdaniec, S., Gerringa, L.J.A., González, A.G., Granskog, M., Haley, B., Hammerschmidt, C.R., Hansell, D.A., Henderson, P.B., Kadko, D.C., Kaiser, K., Laan, P., Lam, P.J., Lamborg, C.H., Levier, M., Li, X., Margolin, A.R., Measures, C., Middag, R., Millero, F.J., Moore, W.S., Paffrath, R., Planquette, H., Rabe, B., Reader, H., Rember, R., Rijkenberg, M.J.A., Roy-Barman, M., Rutgers van der Loeff, M., Saito, M., Schauer, U., Schlosser, P., Sherrell, R.M., Shiller, A.M., Slagter, H., Sonke, J.E., Stedmon, C., Woosley, R.J., Valk, O., van Ooijen, J., Zhang, R., 2020. The Transpolar Drift as a Source of Riverine and Shelf-Derived Trace Elements to the Central Arctic Ocean. *J. Geophys. Res. Ocean.* 125, 1–34. <https://doi.org/10.1029/2019JC015920>
- Chen, J. Bin, Hintelmann, H., Feng, X. Bin, Dimock, B., 2012. Unusual fractionation of both odd and even mercury isotopes in precipitation from Peterborough, ON, Canada. *Geochim. Cosmochim. Acta* 90, 33–46. <https://doi.org/10.1016/j.gca.2012.05.005>
- Chen, C.Y., Amirbahman, A., Fisher, N., Harding, G., Lamborg, C., Taylor, D., 2008. Methylmercury in Marine Ecosystems: Spatial Patterns and Processes of Production, Bioaccumulation, and Biomagnification. *Ecohealth* 5, 399–408. <https://doi.org/10.1007/s10393-008-0201-1.Methylmercury>
- Chen, C.Y., Driscoll, C.T., Eagles-Smith, C.A., Eckley, C.S., Gay, D.A., Hsu-Kim, H., Keane, S.E., Kirk, J.L., Mason, R.P., Obrist, D., Selin, H., Selin, N.E., Thompson, M.R., 2018. A Critical Time for Mercury Science to Inform Global Policy. *Environ. Sci. Technol.* 52, 9556–9561. <https://doi.org/10.1021/acs.est.8b02286>
- Chen, J., Pehkonen, S.O., Lin, C.-J., 2003. Degradation of monomethylmercury chloride by hydroxyl radicals in simulated natural waters. *Water Res.* 37, 2496–2504.
- Chen, L., Zhang, W., Zhang, Y., Tong, Y., Liu, M., Wang, H., Xie, H., Wang, X., 2018. Historical and future trends in global source-receptor relationships of mercury. *Sci. Total Environ.* 610, 24–31. <https://doi.org/10.1016/j.scitotenv.2017.07.182>
- Chen, L., Zhang, Y., Jacob, D.J., Soerensen, A.L., Fisher, J.A., Horowitz, H.M., Corbitt, E.S., Wang, X., 2015. A decline in Arctic Ocean mercury suggested by differences in decadal trends of atmospheric mercury between the Arctic and northern midlatitudes. *Geophys. Res. Lett.* 42. <https://doi.org/10.1002/2015GL064051>
- Cherel, Y., Hobson, K.A., Bailleul, F., Groscolas, R., 2005. Nutrition, physiology, and stable isotopes: New information from fasting and molting penguins. *Ecology* 86, 2881–2888. <https://doi.org/10.1890/05-0562>
- Cherel, Y., Hobson, K.A., Guinet, C., 2015. Milk isotopic values demonstrate that nursing fur seal pups are a full trophic level higher than their mothers. *Rapid Commun. Mass Spectrom.* 29, 1485–1490. <https://doi.org/10.1002/rcm.7243>
- Choi, J., Ishizuya-Oka, A., Buchholz, D.R., 2017. Growth, Development, and Intestinal Remodeling Occurs in the Absence of Thyroid Hormone Receptor α in Tadpoles of *Xenopus tropicalis*. *Endocrinology* 158, 1623–1633.
- Cizdziel, J., Hinnert, T., Cross, C., Pollard, J., 2003. Distribution of mercury in the tissues of five species of freshwater fish from Lake Mead, USA. *J. Environ. Monit.* 5, 802–807. <https://doi.org/10.1039/b307641p>

- Clarkson, T.W., 2007. Mechanisms of Mercury Disposition in the Body 764, 757–764. <https://doi.org/10.1002/ajim.20476>.
- Clarkson, T.W., Magos, L., 2006. The toxicology of mercury and its chemical compounds. *Crit. Rev. Toxicol.* 36, 609–662. <https://doi.org/10.1080/10408440600845619>
- Clarkson, T.W., Vyas, J.B., Ballatori, N., 2007. Mechanisms of mercury disposition in the body. *Am. J. Ind. Med.* 50, 757–764. <https://doi.org/10.1002/ajim.20476>
- Clémens, S., Monperrus, M., Donard, O.F.X., Amouroux, D., Guérin, T., 2012. Mercury speciation in seafood using isotope dilution analysis: A review. *Talanta* 89, 12–20. <https://doi.org/10.1016/j.talanta.2011.12.064>
- Çoban-Yildiz, Y., Altabet, M.A., Yilmaz, A., Tuğrul, S., 2006. Carbon and nitrogen isotopic ratios of suspended particulate organic matter (SPOM) in the Black Sea water column. *Deep. Res. Part II Top. Stud. Oceanogr.* 53, 1875–1892. <https://doi.org/10.1016/j.dsr2.2006.03.021>
- Coltman, D.W., Stenson, G., Hammill, M.O., Haug, T., Davis, C.S., Fulton, T.L., 2007. Panmictic population structure in the hooded seal (*Cystophora cristata*). *Mol. Ecol.* 16, 1639–1648. <https://doi.org/https://doi.org/10.1111/j.1365-294X.2007.03229.x>
- Connolly, R.M., Guest, M.A., Melville, A.J., Oakes, J.M., 2004. Sulfur stable isotopes separate producers in marine food-web analysis. *Oecologia* 138, 161–167. <https://doi.org/10.1007/s00442-003-1415-0>
- Coplen, T.B., 2011. Guidelines and recommended terms for expression of stable-isotope-ratio and gas-ratio measurement results. *Rapid Commun. Mass Spectrom.* 25, 2538–2560. <https://doi.org/10.1002/rcm.5129>
- Cossa, D., B., A., Pirrone, N., 2009. The origin of methylmercury in open Mediterranean waters. *Limnol. Oceanogr.* 54, 837–844.
- Cossa, D., Heimbürger, L.-E., Lannuzel, D., Rintoul, S.R., Butler, E.C. V, Bowie, A.R., Averty, B., Watson, R.J., Remenyi, T., 2011a. Mercury in the Southern Ocean. *Geochim. Cosmochim. Acta* 75, 4037–4052. <https://doi.org/https://doi.org/10.1016/j.gca.2011.05.001>
- Cossa, D., Rintoul, S.R., Cossa, D., Heimbü, L., Rintoul, S.R., Butler, E.C. V, Bowie, A.R., 2011b. Mercury in the Southern Ocean Mercury in the Southern Ocean. *Geochim. Cosmochim. Acta* 75, 4037–4052.
- Cottier, F.R., Nilsen, F., Skogseth, R., Tverberg, V., Skardhamar, J., Svendsen, H., 2010. Arctic fjords: A review of the oceanographic environment and dominant physical processes. *Geol. Soc. Spec. Publ.* 344, 35–50. <https://doi.org/10.1144/SP344.4>
- Cransveld, A., Amouroux, D., Tessier, E., Koutrakis, E., Ozturk, A.A., Bettoso, N., Mieiro, C.L., Bérail, S., Barre, J.P.G., Sturaro, N., Schnitzler, J., Das, K., 2017. Mercury Stable Isotopes Discriminate Different Populations of European Seabass and Trace Potential Hg Sources around Europe. *Environ. Sci. Technol.* 51, 12219–12228. <https://doi.org/10.1021/acs.est.7b01307>
- Croisetière, L., Hare, L., Tessier, A., Cabana, G., 2009. Sulphur stable isotopes can distinguish trophic dependence on sediments and plankton in boreal lakes. *Freshw. Biol.* 54, 1006–1015. <https://doi.org/https://doi.org/10.1111/j.1365-2427.2008.02147.x>
- Crump, J., Westerveld, L., Barnes, R., 2017. 20 years of Action - Indigenous people of the Arctic Council [WWW Document]. GRID-Arendal.
- Cucherousset, J., Villéger, S., 2015. Quantifying the multiple facets of isotopic diversity: New metrics for stable isotope ecology. *Ecol. Indic.* 56, 152–160. <https://doi.org/10.1016/j.ecolind.2015.03.032>

- Cumming, D.H.M., 2015. Seal Range State Policy and Management Review. Gland, Switzerland.
- Dai, A., Luo, D., Song, M., Liu, J., 2019. Arctic amplification is caused by sea-ice loss under increasing CO₂. *Nat. Clim. Chang.* 121, 13pp. <https://doi.org/10.1038/s41467-018-07954-9>
- Dalerum, F., Angerbjörn, A., 2005. Resolving temporal variation in vertebrate diets using naturally occurring stable isotopes. *Oecologia* 144, 647–658. <https://doi.org/10.1007/s00442-005-0118-0>
- Das, K., Debacker, V., Pillet, S., Bouquegneau, J.-M., 2003. Heavy metals in marine mammals, in: Vos, J.G., Bossart, G.D., Fournier, M., O’Shea, T. (Eds.), *Toxicology of Marine Mammals*. Taylor & Francis, London, pp. 135–167. <https://doi.org/10.1201/9780203165577.ch7>
- Das, K., Holleville, O., Ryan, C., Berrow, S., Gilles, A., Ody, D., Michel, L.N., 2017. Isotopic niches of fin whales from the Mediterranean Sea and the Celtic Sea (North Atlantic). *Mar. Environ. Res.* 127, 75–83. <https://doi.org/10.1016/j.marenvres.2017.03.009>
- Das, K., Siebert, U., Fontaine, M.M., Jauniaux, T., Holsbeek, L., Bouquegneau, J.-M.M.J., T., J., 2004. Ecological and pathological factors related to trace metal concentrations in harbour porpoises *Phocoena phocoena* from the North Sea and adjacent areas. *Mar. Ecol. Prog. Ser.* 281, 281–283. <https://doi.org/10.3354/meps281283>
- Das, K., Siebert, U., Gillet, A., Dupont, A., Di-Poi, C., Fonfara, S., Mazzucchelli, G., De Pauw, E., De Pauw-Gillet, M.C., 2008. Mercury immune toxicity in harbour seals: Links to in vitro toxicity. *Environ. Heal. A Glob. Access Sci. Source* 7, 1–17. <https://doi.org/10.1186/1476-069X-7-52>
- Dastoor, A.P., Durnford, D.A., 2013. Arctic Ocean : Is It a Sink or a Source of Atmospheric Mercury ? *Environ. Sci. Technol.* 48, 1707–1717. <https://doi.org/10.1021/es404473e>
- Dauwe, T., Bervoets, L., Pinxten, R., Blust, R., Eens, M., 2003. Variation of heavy metals within and among feathers of birds of prey: effects of molt and external contamination. *Environ. Pollut.* 124, 429–436. [https://doi.org/https://doi.org/10.1016/S0269-7491\(03\)00044-7](https://doi.org/https://doi.org/10.1016/S0269-7491(03)00044-7)
- Day, R.D., Roseneau, D.G., Berail, S., Hobson, K.A., Donard, O.F.X., Vander Pol, S.S., Pugh, R.S., Moors, A.J., Long, S.E., Becker, P.R., 2012. Mercury Stable Isotopes in Seabird Eggs Reflect a Gradient from Terrestrial Geogenic to Oceanic Mercury Reservoirs. *Environ. Sci. Technol.* 46, 5327–5335. <https://doi.org/10.1021/es2047156>
- de la Vega, C., Jeffreys, R.M., Tuerena, R., Ganeshram, R., Mahaffey, C., 2019. Temporal and spatial trends in marine carbon isotopes in the Arctic Ocean and implications for food web studies. *Glob. Chang. Biol.* 25, 4116–4130. <https://doi.org/10.1111/gcb.14832>
- de la Vega, C., Mahaffey, C., Tuerena, R.E., Yurkowski, D.J., Ferguson, S.H., Stenson, G.B., Nordøy, E.S., Haug, T., Biuw, M., Smout, S., Hopkins, J., Tagliabue, A., Jeffreys, R.M., 2020. Arctic seals as tracers of environmental and ecological change. *Limnol. Oceanogr. Lett.* <https://doi.org/10.1002/lol2.10176>
- Dehn, L., Follmann, E.H., Thomas, D.L., Sheffield, G.G., Rosa, C., Duffy, L.K., Hara, T.M.O., 2006. Trophic relationships in an Arctic food web and implications for trace metal transfer. *Sci. Total Environ.* 362, 103–123. <https://doi.org/10.1016/j.scitotenv.2005.11.012>
- Demers, J.D., Blum, J.D., Zak, D.R., 2013. Mercury isotopes in a forested ecosystem: Implications for air-surface exchange dynamics and the global mercury cycle. *Global Biogeochem. Cycles* 27, 222–238. <https://doi.org/10.1002/gbc.20021>
- DeNiro, M.J., Epstein, S., 1978. Influence of diet on the distribution of carbon isotopes in animals. *Geochim. Cosmochim. Acta* 42, 495–506. [https://doi.org/https://doi.org/10.1016/0016-7037\(78\)90199-0](https://doi.org/https://doi.org/10.1016/0016-7037(78)90199-0)

- Derous, D., ten Doeschate, M., Brownlow, A.C., Davison, N.J., Lusseau, D., 2020. Toward New Ecologically Relevant Markers of Health for Cetaceans. *Front. Mar. Sci.* 7, 1–8. <https://doi.org/10.3389/fmars.2020.00367>
- Desforages, J.-P., Marques, G.M., Beumer, L.T., Chimienti, M., Hansen, L.H., Pedersen, S.H., Schmidt, N.M., van Beest, F.M., 2021a. Environment and physiology shape Arctic ungulate population dynamics. *Glob. Chang. Biol.* 00, 1–17. <https://doi.org/10.1111/gcb.15484>
- Desforages, J.-P., Mikkelsen, B., Dam, M., Sveegaard, S., Sonne, C., Dietz, R., Basu, N., 2021b. Neurotoxicology Mercury and neurochemical biomarkers in multiple brain regions of five Arctic marine mammals 84, 136–145. <https://doi.org/10.1016/j.neuro.2021.03.006>
- Deutch, B., Dyerberg, J., Sloth Pedersen, H., Aschlund, E., Hansen, J.C., 2007. Traditional and modern Greenlandic food-Dietary composition, nutrients and contaminants. *Sci. Total Environ.* 384, 106–119. <https://doi.org/10.1016/j.scitotenv.2007.05.042>
- Dietz, R., Born, E.W., Rigét, F., Aubail, A., Sonne, C., Drimmie, R., Basu, N., 2011. Temporal Trends and Future Predictions of Mercury Concentrations in Northwest Greenland Polar Bear (*Ursus maritimus*) Hair. *Environ. Sci. Technol.* 45, 1458–1465. <https://doi.org/10.1021/es1028734>
- Dietz, R., Desforages, J.-P., Rigét, F.F., Aubail, A., Garde, E., Ambus, P., Drimmie, R., Heide-Jørgensen, M.P., Sonne, C., 2021a. Analysis of narwhal tusks reveals lifelong feeding ecology and mercury exposure. *Curr. Biol.* 31, 2012–2019.e2. <https://doi.org/10.1016/j.cub.2021.02.018>
- Dietz, R., Fort, J., Sonne, C., Albert, C., Bustnes, J.O., Christensen, T.K., Ciesielski, T.M., Danielsen, J., Dastnai, S., Eens, M., Erikstad, K.E., Galatius, A., Garbus, S.E., Gilg, O., Hanssen, S.A., Helander, B., Helberg, M., Jaspers, V.L.B., Jenssen, B.M., Jónsson, J.E., Kauhala, K., Kolbeinsson, Y., Kyhn, L.A., Labansen, A.L., Larsen, M.M., Lindstøm, U., Reiertsen, T.K., Rigét, F.F., Roos, A., Strand, J., Strøm, H., Sveegaard, S., Søndergaard, J., Sun, J., Teilmann, J., Therkildsen, O.R., Thórarinsson, T.L., Tjørnløv, R.S., Wilson, S., Eulaers, I., 2021b. A risk assessment of the effects of mercury on Baltic Sea, Greater North Sea and North Atlantic wildlife, fish and bivalves. *Environ. Int.* 146. <https://doi.org/10.1016/j.envint.2020.106178>
- Dietz, R., Heide-Jørgensen, M.P., Härkönen, T., Teilmann, J., Valentin, N., 1991. Age determination of european harbour seal, *Phoca Vitulina* L. *Sarsia* 76, 17–21. <https://doi.org/10.1080/00364827.1991.10413461>
- Dietz, R., Letcher, R.J., Desforages, J.-P., Eulaers, I., Sonne, C., Wilson, S., Andersen-Ranberg, E., Basu, N., Barst, B.D., Bustnes, J.O., Bytingsvik, J., Ciesielski, T.M., Drevnick, P.E., Gabrielsen, G.W., Haarr, A., Hylland, K., Jenssen, B.M., Levin, M., McKinney, M.A., Nørregaard, R.D., Pedersen, K.E., Provencher, J., Styrihave, B., Tartu, S., Aars, J., Ackerman, J.T., Rosing-Asvid, A., Barrett, R., Bignert, A., Born, E.W., Branigan, M., Braune, B., Bryan, C.E., Dam, M., Eagles-Smith, C.A., Evans, M., Evans, T.J., Fisk, A.T., Gamberg, M., Gustavson, K., Hartman, C.A., Helander, B., Herzog, M.P., Hoekstra, P.F., Houde, M., Hoydal, K., Jackson, A.K., Kucklick, J., Lie, E., Loseto, L., Mallory, M.L., Miljeteig, C., Mosbech, A., Muir, D.C.G., Nielsen, S.T., Peacock, E., Pedro, S., Peterson, S.H., Polder, A., Rigét, F., Roach, P., Saunes, H., Sinding, M.H.S., Skaare, J.U., Søndergaard, J., Stenson, G., Stern, G., Treu, G., Schuur, S.S., Víkingsson, G., 2019. Current state of knowledge on biological effects from contaminants on arctic wildlife and fish. *Sci. Total Environ.* 696, 133792. <https://doi.org/10.1016/j.scitotenv.2019.133792>
- Dietz, R., Outridge, P.M., Hobson, K.A., 2009. Anthropogenic contributions to mercury levels in present-day Arctic animals-A review. *Sci. Total Environ.* 407, 6120–6131. <https://doi.org/10.1016/j.scitotenv.2009.08.036>

- Dietz, R., Rigét, F., Born, E.W., 2000. Geographical differences of zinc, cadmium, mercury and selenium in polar bears (*Ursus maritimus*) from Greenland. *Sci. Total Environ.* 245, 25–47.
- Dietz, R., Sonne, C., Basu, N., Braune, B., O'Hara, T., Letcher, R.J., Scheuhammer, T., Andersen, M., Andreasen, C., Andriashek, D., Asmund, G., Aubail, A., Baagøe, H., Born, E.W., Chan, H.M., Derocher, A.E., Grandjean, P., Knott, K., Kirkegaard, M., Krey, A., Lunn, N., Messier, F., Obbard, M., Olsen, M.T., Ostertag, S., Peacock, E., Renzoni, A., Rigét, F., Skaare, J.U., Stern, G., Stirling, I., Taylor, M., Wiig, Ø., Wilson, S., Aars, J., 2013. What are the toxicological effects of mercury in Arctic biota? *Sci. Total Environ.* 443, 775–790. <https://doi.org/10.1016/j.scitotenv.2012.11.046>
- DiMento, B.P., Mason, R.P., Brooks, S., Moore, C., 2019. The impact of sea ice on the air-sea exchange of mercury in the Arctic Ocean. *Deep. Res. Part I Oceanogr. Res. Pap.* 144, 28–38. <https://doi.org/10.1016/j.dsr.2018.12.001>
- Doi, H., Akamatsu, F., González, A.L., 2017. Starvation effects on nitrogen and carbon stable isotopes of animals: An insight from meta-analysis of fasting experiments. *R. Soc. Open Sci.* 4. <https://doi.org/10.1098/rsos.170633>
- Doi, H., Kikuchi, E., Mizota, C., Satoh, N., Shikano, S., Yurlova, N., Yadrenkina, E., Zuykova, E., 2004. Carbon, nitrogen, and sulfur isotope changes and hydro-geological processes in a saline lake chain. *Hydrobiologia* 529, 225–235. <https://doi.org/10.1007/s10750-004-6418-2>
- Douglas, T.A., Blum, J.D., 2019. Mercury Isotopes Reveal Atmospheric Gaseous Mercury Deposition Directly to the Arctic Coastal Snowpack. *Environ. Sci. Technol. Lett.* 6, 235–242. <https://doi.org/10.1021/acs.estlett.9b00131>
- Douglas, T.A., Loseto, L.L., MacDonald, R.W., Outridge, P., Dommergue, A., Poulain, A., Amyot, M., Barkay, T., Berg, T., Chetelat, J., Constant, P., Evans, M., Ferrari, C., Gantner, N., Johnson, M.S., Kirk, J., Kroer, N., Larose, C., Lean, D., Nielsen, T.G., Poissant, L., Rognerud, S., Skov, H., Sørensen, S., Wang, F., Wilson, S., Zdanowicz, C.M., 2012. The fate of mercury in Arctic terrestrial and aquatic ecosystems, a review. *Environ. Chem.* 9, 321–355. <https://doi.org/10.1071/EN11140>
- Douglas, T.A., Sturm, M., Blum, J.D., Polashenski, C., Stuefer, S., Hiemstra, C., Steffen, A., Filhol, S., Prevost, R., 2017. A Pulse of Mercury and Major Ions in Snowmelt Runoff from a Small Arctic Alaska Watershed. *Environ. Sci. Technol.* 51, 11145–11155. <https://doi.org/10.1021/acs.est.7b03683>
- Driscoll, C.T., Chen, C.Y., Hammerschmidt, C.R., Mason, R.P., Gilmour, C.C., Sunderland, E.M., Greenfield, B.K., Buckman, K.L., Lamborg, C.H., 2012. Nutrient supply and mercury dynamics in marine ecosystems: A conceptual model. *Environ. Res.* 119, 118–131. <https://doi.org/10.1016/j.envres.2012.05.002>
- Du, H., Ma, M., Igarashi, Y., Wang, D., 2019. Biotic and Abiotic Degradation of Methylmercury in Aquatic Ecosystems: A Review. *Bull. Environ. Contam. Toxicol.* 102, 605–611. <https://doi.org/10.1007/s00128-018-2530-2>
- Durnford, D., Dastoor, A., Figueras-Nieto, D., Ryjkov, A., 2010. Long range transport of mercury to the Arctic and across Canada. *Atmos. Chem. Phys.* 10, 6063–6086. <https://doi.org/10.5194/acp-10-6063-2010>
- Eagles-Smith, C.A., Ackerman, J.T., Yee, J., Adelsbach, T.L., 2009. Mercury demethylation in waterbird livers: dose-response thresholds and differences among species. *Environ. Toxicol. Chem.* 28, 568–77. <https://doi.org/10.1897/08-245.1>
- Eagles-Smith, C.A., Silbergeld, E.K., Basu, N., Bustamante, P., Diaz-Barriga, F., Hopkins, W.A., Kidd, K.A., Nyland, J.F., 2018. Modulators of mercury risk to wildlife and humans in the context of rapid global change. *Ambio* 47, 170–197. <https://doi.org/10.1007/s13280-017-1011-x>
- Enrico, M., Roux, G. Le, Maruszczak, N., Heimbürger, L.-E., Claustres, A., Fu, X., Sun, R., Sonke, J.E., 2016.

- Atmospheric Mercury Transfer to Peat Bogs Dominated by Gaseous Elemental Mercury Dry Deposition. *Environ. Sci. Technol.* 50, 2405–2412. <https://doi.org/10.1021/acs.est.5b06058>
- Epov, V.N., Rodriguez-Gonzalez, P., Sonke, J.E., Tessier, E., Amouroux, D., Bourgoïn, L.M., Donard, O.F.X., 2008. Simultaneous Determination of Species-Specific Isotopic Composition of Hg by Gas Chromatography Coupled to Multicollector ICPMS. *Anal. Chem.* 80, 3530–3538. <https://doi.org/10.1021/ac800384b>
- EU Commission, 2020. EU Regulation N° 142. *Off. J. Eur. Union* 020.001, 357pp.
- EU Parliament, 2009. EU Regulation N°1069. *Off. J. Eur. Union* 300, 1–33.
- European Parliament and The Council, 2010. DIRECTIVE 2010/63/EU on the protection of animals used for scientific purposes. *Off. J. Eur. Union L* 276, 33–78.
- Ewald, J.D., Kirk, J.L., Li, M., Sunderland, E.M., 2019. Organ-specific differences in mercury speciation and accumulation across ringed seal (*Phoca hispida*) life stages. *Sci. Total Environ.* 650, 2013–2020. <https://doi.org/10.1016/j.scitotenv.2018.09.299>
- Faïn, X., Ferrari, C.P., Dommergue, A., Albert, M., Battle, M., Arnaud, L., Barnola, J.M., Cairns, W., Barbante, C., Boutron, C., 2008. Mercury in the snow and firn at Summit Station, Central Greenland, and implications for the study of past atmospheric mercury levels. *Atmos. Chem. Phys.* 8, 3441–3457. <https://doi.org/10.5194/acp-8-3441-2008>
- Fant, M.L., Nyman, M., Helle, E., Rudbäck, E., 2001. Mercury, cadmium, lead and selenium in ringed seals (*Phoca hispida*) from the Baltic Sea and from Svalbard. *Environ. Pollut.* 11, 493–501.
- FAO/WHO, 2003. Summary and conclusions, annex 4, Joint FAO/WHO Expert Committee on Food Additives, 61st Meeting.
- Feng, C., Pedrero, Z., Gentès, S., Barre, J., Renedo, M., Tessier, E., Berail, S., Maury-Brachet, R., Mesmer-Dudons, N., Baudrimont, M., Legeay, A., Maurice, L., Gonzalez, P., Amouroux, D., 2015. Specific Pathways of Dietary Methylmercury and Inorganic Mercury Determined by Mercury Speciation and Isotopic Composition in Zebrafish (*Danio rerio*). *Environ. Sci. Technol.* 49, 12984–12993. <https://doi.org/10.1021/acs.est.5b03587>
- Ferguson, S.H., Stirling, I., McLoughlin, P., 2005. Climate change and ringed seal (*Phoca hispida*) recruitment in Western Hudson Bay. *Mar. Mammal Sci.* 21, 121–135.
- Fisher, J.A., Jacob, D.J., Soerensen, A.L., Amos, H.M., Steffen, A., Sunderland, E.M., 2012. Riverine source of Arctic Ocean mercury inferred from atmospheric observations. *Nat. Geosci.* 5, 499–504. <https://doi.org/10.1038/ngeo1478>
- Fisher, J.A., Jacob, D.J., Wang, Q., Bahreini, R., Carouge, C.C., Cubison, M.J., Dibb, J.E., Diehl, T., Jimenez, J.L., Leibensperger, E.M., Lu, Z., Meinders, M.B.J., Pye, H.O.T., Quinn, P.K., Sharma, S., Streets, D.G., van Donkelaar, A., Yantosca, R.M., 2011. Sources, distribution, and acidity of sulfate-ammonium aerosol in the Arctic in winter-spring. *Atmos. Environ.* 45, 7301–7318. <https://doi.org/10.1016/j.atmosenv.2011.08.030>
- Fisher, J.A., Jacob, Daniel J, Soerensen, Anne L, Amos, Helen M, Corbitt, Elizabeth S, Streets, David G, Wang, Qiaoqiao, Yantosca, Robert M, Sunderland, Elsie M, Fisher, C., Jacob, D J, Soerensen, A L, Amos, H M, Corbitt, E S, Streets, D G, Wang, Q, Yantosca, R M, Sunderland, E M, 2013. Factors driving mercury variability in the Arctic atmosphere and ocean over the past 30 years. *Glob. Biogeochem. Cycles* 27, 1226–1235. <https://doi.org/10.1002/2013GB004689>
- Folkow, L.P., Blix, A.S., 1999. Diving behaviour of hooded seals (*Cystophora cristata*) in the Greenland and Norwegian

- Seas. *Polar Biol.* 22, 61–74. <https://doi.org/10.1007/s003000050391>
- Folkow, L.P., Mårtensson, P.E., Blix, A.S., 1996. Annual distribution of hooded seals (*Cystophora cristata*) in the Greenland and Norwegian seas. *Polar Biol.* 16, 179–189. <https://doi.org/10.1007/BF02329206>
- Folkow, L.P., Nordøy, E.S., Blix, A.S., 2010. Remarkable development of diving performance and migrations of hooded seals (*Cystophora cristata*) during their first year of life. *Polar Biol.* 33, 433–441. <https://doi.org/10.1007/s00300-009-0718-y>
- Folkow, L.P., Nordøy, E.S., Blix, A.S., 2004. Distribution and diving behaviour of harp seals (*Pagophilus groenlandicus*) from the Greenland Sea stock. *Polar Biol.* 27, 281–298. <https://doi.org/10.1007/s00300-004-0591-7>
- Fortier, L., Reist, J.D., Ferguson S H, Archambault, P., J. Matley, Macdonald, R.W., 2015. Arctic Change: Impacts on Marine Ecosystems and Contaminants. From Sci. to Policy West. Cent. Can. Arct. an Integr. Reg. Impact Study *Clim. Chang. Mod.* 432.
- Fossato da Silva, D.A., Teixeira, C.T., Scarano, W.R., Favareto, A.P.A., Fernandez, C.D.B., Grotto, D., Barbosa, F., Kempinas, W.D.G., 2011. Effects of methylmercury on male reproductive functions in Wistar rats. *Reprod. Toxicol.* 31, 431–439. <https://doi.org/10.1016/j.reprotox.2011.01.002>
- Fossi, M.C., Marsili, L., 1997. The use of non-destructive biomarkers in the study of marine mammals. *Biomarkers* 2, 205–216.
- Foster, K.L., Braune, B.M., Gaston, A.J., Mallory, M.L., 2019a. Climate influence on mercury in Arctic seabirds. *Sci. Total Environ.* 693, 133569. <https://doi.org/10.1016/j.scitotenv.2019.07.375>
- Foster, K.L., Braune, B.M., Gaston, A.J., Mallory, M.L., 2019b. Climate Influence on Legacy Organochlorine Pollutants in Arctic Seabirds. <https://doi.org/10.1021/acs.est.8b07106>
- Freitas, C., Kovacs, K.M., Ims, R.A., Fedak, M.A., Lydersen, C., 2008. Ringed seal post-moulting movement tactics and habitat selection. *Oecologia* 155, 193–204. <https://doi.org/10.1007/s00442-007-0894-9>
- French, T.D., Houben, A.J., Desforges, J.-P., Kimpe, L.E., Kokelj, S. V., Poulain, A.J., Smol, J.P., Wang, X., Blais, J.M., 2014. Dissolved organic carbon thresholds affect mercury bioaccumulation in Arctic lakes. *Environ. Sci. Technol.* 48, 3162–3168. <https://doi.org/10.1021/es403849d>
- Frey, K.E., Comiso, J.C., Cooper, L.W., Grebmeier, J.M., Stock, L. V., 2019. Arctic Ocean Primary Productivity: The Response of Marine Algae to Climate Warming and Sea Ice Decline.
- Friedlaender, A.S., Johnston, D.W., Fink, S.L., Lavigne, D.M., 2006. Variation in Ice Cover on the East Coast of Canada , Implications for harp and hooded seals. *Environment* 29, 1–8.
- Fripiat, F., Sigman, D.M., Fawcett, S.E., Rafter, P.A., Weigand, M.A., Tison, J.-L., 2014. New insights into sea ice nitrogen biogeochemical dynamics from the nitrogen isotopes. *Global Biogeochem. Cycles* 28, 115–130. <https://doi.org/10.1002/2013GB004729>
- Fry, B., 2006. Stable Isotope Ecology, 3rd ed, *Encyclopedia of Ecology*. Springer Science+Business Media, LCC. <https://doi.org/10.1016/b978-0-12-409548-9.10915-7>
- Fry, B., Chumchal, M.M., 2011. Sulfur stable isotope indicators of residency in estuarine fish. *Limnol. Oceanogr.* 56, 1563–1576. <https://doi.org/10.4319/lo.2011.56.5.1563>
- Gantner, N., Hintelmann, H., Zheng, W., Muir, D.C., 2009. Variations in stable isotope fractionation of Hg in food webs of Arctic lakes. *Environ. Sci. Technol.* 43, 9148–9154. <https://doi.org/10.1021/es901771r>

- Garde, E., 2013. Seals in Greenland: An important component of culture and economy. Copenhagen.
- Gaston, A.J., Gilchrist, H.G., Mallory, M.L., 2005. Variation in ice conditions has strong effects on the breeding of marine birds at Prince Leopold Island, Nunavut. *Ecography (Cop.)*. 28, 331–344. <https://doi.org/10.1111/j.0906-7590.2005.04179.x>
- Gaston, A.J., Woo, K., Hipfner, J.M., 2003. Trends in Forage Fish Populations in Northern Hudson Bay since 1981, as Determined from the Diet of Nestling Thick-Billed Murres *Uria lomvia*. *Arctic* 56, 227–233. <https://doi.org/10.14430/arctic618>
- Gehrke, G.E., Blum, J.D., 2011. Mercury Cycling in the Marine Environment: Insights from mercury stable isotopes. University of Michigan, United States -- Michigan.
- Gehrke, G.E., Blum, J.D., Slotton, D.G., Greenfield, B.K., 2011. Mercury Isotopes Link Mercury in San Francisco Bay Forage Fish to Surface Sediments. *Environ. Sci. Technol.* 45, 1264–1270. <https://doi.org/10.1021/es103053y>
- Geiseler, S.J., Blix, A.S., Burns, J.M., Folkow, L.P., 2013. Rapid postnatal development of myoglobin from large liver iron stores in hooded seals. *J. Exp. Biol.* 216, 1793–1798. <https://doi.org/10.1242/jeb.082099>
- Geiseler, S.J., Larson, J., Folkow, L.P., 2016. Synaptic transmission despite severe hypoxia in hippocampal slices of the deep-diving hooded seal. *Neuroscience* 334, 39–46. <https://doi.org/10.1016/j.neuroscience.2016.07.034>
- Gentès, S., Maury-Brachet, R., Feng, C., Pedrero, Z., Tessier, E., Legeay, A., Mesmer-Dudons, N., Baudrimont, M., Maurice, L., Amouroux, D., Gonzalez, P., 2015. Specific Effects of Dietary Methylmercury and Inorganic Mercury in Zebrafish (*Danio rerio*) Determined by Genetic, Histological, and Metallothionein Responses. *Environ. Sci. Technol.* 49, 14560–14569. <https://doi.org/10.1021/acs.est.5b03586>
- Gentry, R.L., Holt, J.R., 1982. Equipment and techniques for handling northern fur seals. NOAA Tech. Rep. NMFS SSRF-758 15.
- Germain, L.R., Koch, P.L., Harvey, J., McCarthy, M.D., 2013. Nitrogen isotope fractionation in amino acids from harbor seals: Implications for compound-specific trophic position calculations. *Mar. Ecol. Prog. Ser.* 482, 265–277. <https://doi.org/10.3354/meps10257>
- Germain, L.R., McCarthy, M.D., Koch, P.L., Harvey, J.T., 2012. Stable carbon and nitrogen isotopes in multiple tissues of wild and captive harbor seals (*Phoca vitulina*) off the California coast. *Mar. Mammal Sci.* 28, 542–560. <https://doi.org/10.1111/j.1748-7692.2011.00516.x>
- Gilmour, C.C., Elias, D.A., Kucken, A.M., Brown, S.D., Palumbo, A. V., Schadt, C.W., Wall, J.D., 2011. Sulfate-reducing bacterium *Desulfovibrio desulfuricans* ND132 as a model for understanding bacterial mercury methylation. *Appl. Environ. Microbiol.* 77, 3938–3951. <https://doi.org/10.1128/AEM.02993-10>
- Gilmour, C.C., Podar, M., Bullock, A.L., Graham, A.M., Brown, S.D., Somenahally, A.C., Johs, A., Hurt, R.A., Bailey, K.L., Elias, D.A., 2013. Mercury methylation by novel microorganisms from new environments. *Environ. Sci. Technol.* 47, 11810–11820. <https://doi.org/10.1021/es403075t>
- Giménez, J., Cañadas, A., Ramírez, F., Afán, I., García-Tiscar, S., Fernández-Maldonado, C., Castillo, J.J., de Stephanis, R., 2018. Living apart together: Niche partitioning among Alboran Sea cetaceans. *Ecol. Indic.* 95, 32–40. <https://doi.org/10.1016/j.ecolind.2018.07.020>
- Gionfriddo, C.M., Tate, M.T., Wick, R.R., Schultz, M.B., Zemla, A., Thelen, M.P., Schofield, R., Krabbenhoft, D.P., Holt, K.E., Moreau, J.W., 2016. Microbial mercury methylation in Antarctic sea ice. *Nat. Microbiol.* 1, 1–12. <https://doi.org/10.1038/nmicrobiol.2016.127>

- Gleason, J.D., Blum, J.D., Moore, T.C., Polyak, L., Jakobsson, M., Meyers, P.A., Biswas, A., 2017. Sources and cycling of mercury in the paleo Arctic Ocean from Hg stable isotope variations in Eocene and Quaternary sediments. *Geochim. Cosmochim. Acta* 197, 245–262. <https://doi.org/10.1016/j.gca.2016.10.033>
- Goix, S., Maurice, L., Laffont, L., Rinaldo, R., Lagane, C., Chmeleff, J., Menges, J., Heimbürger, L.E., Maury-Brachet, R., Sonke, J.E., 2019. Quantifying the impacts of artisanal gold mining on a tropical river system using mercury isotopes. *Chemosphere* 219, 684–694. <https://doi.org/10.1016/j.chemosphere.2018.12.036>
- Gomes, M.L., Hurtgen, M.T., 2013. Sulfur isotope systematics of a euxinic, low-sulfate lake: Evaluating the importance of the reservoir effect in modern and ancient oceans. *Geology* 41, 663–666. <https://doi.org/10.1130/G34187.1>
- Gosselin, M., Levasseur, M., Wheeler, P.A., Horner, R.A., Booth, B.C., 1997. New measurements of phytoplankton and ice algal production in the Arctic Ocean. *Deep Sea Res. Part II Top. Stud. Oceanogr.* 44, 1623–1644. [https://doi.org/https://doi.org/10.1016/S0967-0645\(97\)00054-4](https://doi.org/https://doi.org/10.1016/S0967-0645(97)00054-4)
- Graham, A.M., Aiken, G.R., Gilmour, C.C., 2012. Dissolved organic matter enhances microbial mercury methylation under sulfidic conditions. *Environ. Sci. Technol.* 46, 2715–2723. <https://doi.org/10.1021/es203658f>
- Grandjean, P., Satoh, H., Murata, K., Eto, K., 2010. Adverse effects of methylmercury: environmental health research implications. *Environ. Health Perspect.* 118, 1137–1145. <https://doi.org/10.1289/ehp.0901757>
- Gratz, L.E., Keeler, G.J., Blum, J.D., Sherman, L.S., 2010. Isotopic Composition and Fractionation of Mercury in Great Lakes Precipitation and Ambient Air. *Environ. Sci. Technol.* 44, 7764–7770. <https://doi.org/10.1021/es100383w>
- Gregoire, D., Poulain, A., 2014. A little bit of light goes a long way: The role of phototrophs on mercury cycling. *Metallomics* 6, 12.
- Habran, S., Damseaux, F., Pomeroy, P., Debier, C., Crocker, D., Lepoint, G., Das, K., 2019. Changes in stable isotope compositions during fasting in phocid seals. *Rapid Commun. Mass Spectrom.* 33, 176–184. <https://doi.org/10.1002/rcm.8308>
- Habran, S., Pomeroy, P.P., Debier, C., Das, K., 2013. Changes in trace elements during lactation in a marine top predator, the grey seal. *Aquat. Toxicol.* 126, 455–466. <https://doi.org/10.1016/j.aquatox.2012.08.011>
- Haitzer, M., Aiken, G.R., Ryan, J.N., 2002. Binding of mercury(II) to dissolved organic matter: The role of the mercury-to-DOM concentration ratio. *Environ. Sci. Technol.* 36, 3564–3570. <https://doi.org/10.1021/es025699i>
- Hammerschmidt, C., Fitzgerald, W.F., 2006. Bioaccumulation and Trophic Transfer of Methylmercury in Long Island Sound. *Arch. Environ. Contam. Toxicol.* 51, 416–424. <https://doi.org/10.1007/s00244-005-0265-7>
- Hammill, M.O., 2018. Ringed seal, *Pusa hispida*, in: Wursig, B., Thewissen, J.G.M., Kovacs, K.M. (Eds.), *Encyclopedia of Marine Mammals*. pp. 972–974.
- Hammill, M.O., Smith, T.G., 1991. THE ROLE OF PREDATION IN THE ECOLOGY OF THE RINGED SEAL IN BARROW STRAIT, NORTHWEST TERRITORIES, CANADA. *Mar. Mammal Sci.* 7, 123–135. <https://doi.org/https://doi.org/10.1111/j.1748-7692.1991.tb00559.x>
- Hansen, J.C., Van Oostdam, J., Gilman, A.P., Odland, J.Ø., Donaldson, S.G., Vaktskjold, A., Tikhonov, C., Dudarev, A.A., Ayotte, P., E., B.J., Bonefeld-Jørgensen, E.C., Carlsen, A., Ólafsdóttir, K., Pedersen, H.S., Weber, J.-P., Savolainen, M., Skinner, K., 2016. AMAP-IPY meeting in Iqaluk, Nunavut, Canada (June 2009), and AMAP human health assessment 2009, in: Kallenborn, R. (Ed.), *Implications and Consequences of Anthropogenic Pollution in Polar Environments*. Springer Berlin Heidelberg, p. xv + 259.
- Hansson, S., Hobbie, J.E., Elmgren, R., Larsson, U., Fry, B., Johansson, S., 1997. the Stable Nitrogen Isotope Ratio As

- a Marker of Food-Web. Ecology 78, 2249–2257. [https://doi.org/10.1890/0012-9658\(1997\)078\[2249:TSNIRA\]2.0.CO;2](https://doi.org/10.1890/0012-9658(1997)078[2249:TSNIRA]2.0.CO;2)
- Harada, M., 1995. Minamata Disease: Methylmercury Poisoning in Japan Caused by Environmental Pollution. *Crit. Rev. Toxicol.* 25, 1–24. <https://doi.org/10.3109/10408449509089885>
- Hare, P.E., Fogel, M.L., Stafford, T.W.J., Mitchelf, A.D., Hoeringa, T.C., 1991. The Isotopic Composition of Carbon and Nitrogen in Individual Amino Acids Isolated from Modern and Fossil Proteins. *J. Archaeol. Sci.* 18, 277–292.
- Haug, T., Bogstad, B., Chierici, M., Gjørseter, H., Hallfredsson, E.H., Høines, Å.S., Hoel, A.H., Ingvaldsen, R.B., Jørgensen, L.L., Knutsen, T., Loeng, H., Naustvoll, L.J., Røttingen, I., Sunnanå, K., 2017a. Future harvest of living resources in the Arctic Ocean north of the Nordic and Barents Seas: A review of possibilities and constraints. *Fish. Res.* 188, 38–57. <https://doi.org/10.1016/j.fishres.2016.12.002>
- Haug, T., Bogstad, B., Chierici, M., Gjørseter, H., Hallfredsson, E.H., Høines, Å.S., Hoel, A.H., Ingvaldsen, R.B., Jørgensen, L.L., Knutsen, T., Loeng, H., Naustvoll, L.J., Røttingen, I., Sunnanå, K., 2017b. Future harvest of living resources in the Arctic Ocean north of the Nordic and Barents Seas: A review of possibilities and constraints. *Fish. Res.* 188, 38–57. <https://doi.org/10.1016/j.fishres.2016.12.002>
- Haug, T., Nilssen, K.T., Lindblom, L., 2004. Feeding habits of harp and hooded seals in summer and winter. *Polar Res.* 23 23, 35–42.
- Haug, T., Smout, S., Nilssen, K., Lindstrøm, U., Øigård, T., 2013. Functional relationship between harp seal body condition and available prey in the Barents Sea. *Mar. Ecol. Prog. Ser.* 484, 287–301. <https://doi.org/10.3354/meps10272>
- Haug, T., Stenson, G.B., Corkeron, P.J., Nilssen, K.T., 2006. Estimation of harp seal (*Pagophilus groenlandicus*) pup production in the North Atlantic completed: Results from surveys in the Greenland Sea in 2002. *ICES J. Mar. Sci.* 63, 95–104. <https://doi.org/10.1016/j.icesjms.2005.07.005>
- Hawkings, J.R., Linhoff, B.S., Wadham, J.L., Stibal, M., Lamborg, C.H., Carling, G.T., Lamarche-Gagnon, G., Kohler, T.J., Ward, R., Hendry, K.R., Falteisek, L., Kellerman, A.M., Cameron, K.A., Hatton, J.E., Tingey, S., Holt, A.D., Vinšová, P., Hofer, S., Bulínová, M., Větrovský, T., Meire, L., Spencer, R.G.M., 2021. Large subglacial source of mercury from the southwestern margin of the Greenland Ice Sheet. *Nat. Geosci.* <https://doi.org/10.1038/s41561-021-00753-w>
- Hayes, J.M., 2001. Fractionation of the Isotopes of Carbon and Hydrogen in Biosynthetic Processes. *Rev. Mineral. Geochemistry* 43, 225–277. <https://doi.org/10.2138/gsrmg.43.1.225>
- Hazen, E.L., Abrahms, B., Brodie, S., Carroll, G., Jacox, M.G., Savoca, M.S., Scales, K.L., Sydeman, W.J., Bograd, S.J., 2019. Marine top predators as climate and ecosystem sentinels. *Front. Ecol. Environ.* 17, 565–574. <https://doi.org/10.1002/fee.2125>
- Healy, K., Kelly, S.B.A., Guillerme, T., Inger, R., Bearhop, S., L., J.A., 2016. Predicting trophic discrimination factor using Bayesian inference and phylogenetic, ecological and physiological data. *DEsIR:Discrimination Estimation in R. PeerJPreprints*.
- Healy, K., Kelly, S.B.A., Guillerme, T., Inger, R., Bearhop, S., L., J.A., Jackson, A.L., 2017. Predicting trophic discrimination factor using Bayesian inference and phylogenetic, ecological and physiological data. *DEsIR: Discrimination Estimation in R. PeerJPreprints* 5. <https://doi.org/https://doi.org/10.7287/peerj.preprints.1950v3>
- Hebert, C.E., 2019. The river runs through it: The Athabasca River delivers mercury to aquatic birds breeding far

- downstream. *PLoS One* 14, 19pp. <https://doi.org/10.1371/journal.pone.0206192>
- Heimbürger, L.-E., Cossa, D., Marty, J.-C., Migon, C., Averty, B., Dufour, A., Ras, J., 2010. Methyl mercury distributions in relation to the presence of nano- and picophytoplankton in an oceanic water column (Ligurian Sea, North-western Mediterranean). *Geochim. Cosmochim. Acta* 74, 5549–5559.
- Heimbürger, L.-E., Sonke, J.E., Cossa, D., Point, D., Lagane, C., Laffont, L., Galfond, B.T., Nicolaus, M., Rabe, B., van der Loeff, M.R., 2015. Shallow methylmercury production in the marginal sea ice zone of the central Arctic Ocean. *Sci. Rep.* 5, 10318. <https://doi.org/10.1038/srep10318>
- Hertz, E., Trudel, M., Cox, M.K., Mazumder, A., 2015. Effects of fasting and nutritional restriction on the isotopic ratios of nitrogen and carbon: A meta-analysis. *Ecol. Evol.* 5, 4829–4839. <https://doi.org/10.1002/ece3.1738>
- Hesslein, R.H., Hallard, K.A., Ramlal, P., 1993. Replacement of Sulfur, Carbon, and Nitrogen in Tissue of Growing Broad Whitefish (*Coregonus nasus*) in Response to a Change in Diet Traced by $\delta^{34}\text{S}$, $\delta^{13}\text{C}$, and $\delta^{15}\text{N}$. *Can. J. Fish. Aquat. Sci.* 50, 2071–2076.
- Hobson, K., Clark, R., 1992. Assessing avian diets using stable isotopes I: turnover of ^{13}C in tissues. *Condor* 94, 181–188. <https://doi.org/10.2307/1368807>
- Hobson, K.A., Clark, R.G., 1992. Assessing Avian Diets Using Stable Isotopes II: Factors Influencing Diet-Tissue Fractionation. *Condor* 94, 189–197. <https://doi.org/10.2307/1368808>
- Hobson, K.A., Schell, D.M., Renouf, D., Noseworthy, E., 1996. Stable carbon and nitrogen isotopic fractionation between diet and tissues of captive seals: implications for dietary reconstructions involving marine mammals. *Can. J. Fish. Aquat. Sci.* 53, 528–533. <https://doi.org/10.1139/f95-209>
- Hoff, M.L.M., Fabrizius, A., Czech-Damal, N.U., Folkow, L.P., Burmester, T., 2017. Transcriptome analysis identifies key metabolic changes in the hooded seal (*Cystophora cristata*) brain in response to hypoxia and reoxygenation. *PLoS One* 12, 1–21. <https://doi.org/10.1371/journal.pone.0169366>
- Hong, Y.-S., Kim, Y.-M., Lee, K.-E., 2012. Methylmercury exposure and health effects. *J. Prev. Med. public Heal.* 45, 353–363. <https://doi.org/10.3961/jpmph.2012.45.6.353>
- Horton, T.W., Blum, J.D., Xie, Z., Hren, M., Chamberlain, C.P., 2009. Stable isotope food-web analysis and mercury biomagnification in polar bears (*Ursus maritimus*). *Polar Res.* 28, 443–454. <https://doi.org/10.1111/j.1751-8369.2009.00114.x>
- Houde, M., Taranu, Z.E., Wang, X., Young, B., Gagnon, P., Ferguson, S.H., Kwan, M., Muir, D.C.G., 2020. Mercury in Ringed Seals (*Pusa hispida*) from the Canadian Arctic in Relation to Time and Climate Parameters. *Environ. Toxicol. Chem.* 00, 1–13. <https://doi.org/10.1002/etc.4865>
- Howland, M.R., Corr, L.T., Young, S.M.M., Jones, V., Jim, S., Van Der Merwe, N.J., Mitchell, A.D., Evershed, R.P., 2003. Expression of the dietary isotope signal in the compound-specific $\delta^{13}\text{C}$ values of pig bone lipids and amino acids. *Int. J. Osteoarchaeol.* 13, 54–65. <https://doi.org/10.1002/oa.658>
- Hsu-Kim, H., Eckley, C.S., Achá, D., Feng, X., Gilmour, C.C., Jonsson, S., Mitchell, C.P.J., 2018. Challenges and opportunities for managing aquatic mercury pollution in altered landscapes. *Ambio* 47, 141–169. <https://doi.org/10.1007/s13280-017-1006-7>
- Hsu-Kim, H., Kucharzyk, K.H., Zhang, T., Deshusses, M.A., 2013. Mechanisms regulating mercury bioavailability for methylating microorganisms in the aquatic environment: A critical review. *Environ. Sci. Technol.* 47, 2441–2456. <https://doi.org/10.1021/es304370g>

- Hückstädt, L.A., Burns, J.M., Koch, P.L., McDonald, B.I., Crocker, D.E., Costa, D.P., 2012. Diet of a specialist in a changing environment: the crabeater seal along the western Antarctic Peninsula. *Mar. Ecol. Prog. Ser.* 455, 287–301. <https://doi.org/10.3354/meps09601>
- Huntington, H.P., Quakenbush, L.T., Nelson, M., 2017. Evaluating the Effects of Climate Change on Indigenous Marine Mammal Hunting in Northern and Western Alaska Using Traditional Knowledge. *Front. Mar. Sci.* 4, 319. <https://doi.org/10.3389/fmars.2017.00319>
- Huntington, H.P., Quakenbush, L.T., Nelson, M., 2016. Effects of changing sea ice on marine mammals and subsistence hunters in northern Alaska from traditional knowledge interviews. *Biol. Lett.* 12, 20160198. <https://doi.org/10.1098/rsbl.2016.0198>
- Hurrell, J.W., Kushnir, Y., Ottersen, G., Visbeck, M., 2003. An overview of the north atlantic oscillation. *Geophys. Monogr. Ser.* 134, 1–35. <https://doi.org/10.1029/134GM01>
- ICC Canada, 2014. The sea ice never stops: Circumpolar Inuit Reflections on sea ice use and shipping in Inuit Nunaat. <https://doi.org/10.1007/s13398-014-0173-7.2>
- ICES, 2019. ICES / NAFO / NAMMCO WORKING GROUP ON HARP AND HOODED SEALS (WGHARP). ICES Sci. reports 1, 193pp.
- IJsseldijk, L.L., Brownlow, A.C., Mazzariol, S. (Eds), 2020. Best practice on cetacean post mortem investigation and tissue sampling. ACCOBAMS/ASCOBANS 74pp.
- Jackson, A.C., 2018. Chronic Neurological Disease Due to Methylmercury Poisoning. *Can. J. Neurol. Sci. Le J. Can. des Sci. Neurol.* 45, 620–623. <https://doi.org/10.1017/cjn.2018.323>
- Jackson, A.L., Inger, R., Parnell, A.C., Bearhop, S., 2011. Comparing isotopic niche widths among and within communities: SIBER - Stable Isotope Bayesian Ellipses in R. *J. Anim. Ecol.* 80, 595–602. <https://doi.org/10.1111/j.1365-2656.2011.01806.x>
- Jakobsson, M., 2002. Hypsometry and volume of the Arctic Ocean and its constituent seas. *Geochemistry, Geophys. Geosystems* 3, 1525–2027.
- Jakobsson, M., Mayer, L.A., Bringensparr, C., Castro, C.F., Mohammad, R., Johnson, P., Ketter, T., Accettella, D., Amblas, D., An, L., Arndt, J.E., Canals, M., Casamor, J.L., Chauché, N., Coakley, B., Danielson, S., Demarte, M., Dickson, M.L., Dorschel, B., Dowdeswell, J.A., Dreutter, S., Fremand, A.C., Gallant, D., Hall, J.K., Hehemann, L., Hodnesdal, H., Hong, J., Ivaldi, R., Kane, E., Klaucke, I., Krawczyk, D.W., Kristoffersen, Y., Kuipers, B.R., Millan, R., Masetti, G., Morlighem, M., Noormets, R., Prescott, M.M., Rebesco, M., Rignot, E., Semiletov, I., Tate, A.J., Travaglini, P., Velicogna, I., Weatherall, P., Weinrebe, W., Willis, J.K., Wood, M., Zarayskaya, Y., Zhang, T., Zimmermann, M., Zinglensen, K.B., 2020. The International Bathymetric Chart of the Arctic Ocean Version 4.0. *Sci. Data* 7, 1–14. <https://doi.org/10.1038/s41597-020-0520-9>
- Jardine, T., Kidd, K.A., Fisk, A.T., 2006. Critical Review Applications , Considerations , and Sources of Uncertainty When Using Stable Isotope Analysis in Ecotoxicology. *Crit. Rev.* 40, 7501–7511. <https://doi.org/10.1021/es061263h>
- Jaspers, V.L.B., Voorspoels, S., Covaci, A., Lepoint, G., Eens, M., 2007. Evaluation of the usefulness of bird feathers as a non-destructive biomonitoring tool for organic pollutants: A comparative and meta-analytical approach. *Environ. Int.* 33, 328–337. <https://doi.org/10.1016/j.envint.2006.11.011>
- Jauniaux, T., Garcia Hartmann, M., Haelters, J., Tavernier, J., Coignoul, F., 2002. Echouage de mammifères marins:

- Guide d'intervention et procédures d'autopsie. *Ann. Med. Vet.* 146, 261–276.
- Jiskra, M., Wiederhold, J.G., Bourdon, B., Kretzschmar, R., 2012. Solution speciation controls mercury isotope fractionation of Hg(II) sorption to goethite. *Environ. Sci. Technol.* 46, 6654–6662. <https://doi.org/10.1021/es3008112>
- Jiskra, M., Wiederhold, J.G., Skyllberg, U., Kronberg, R.-M., Kretzschmar, R., 2017. Source tracing of natural organic matter bound mercury in boreal forest runoff with mercury stable isotopes. *Environ. Sci. Process. Impacts* 19, 1235–1248. <https://doi.org/10.1039/C7EM00245A>
- Johansen, P., Kapel, F. o., Kraul, I., 1980. Heavy Metals and Organochlorines in Marine Mammals From Greenland. ICES 32.
- Jonsson, S., Andersson, A., Nilsson, M.B., Skyllberg, U., Lundberg, E., Schaefer, J.K., Åkerblom, S., Björn, E., 2017. Terrestrial discharges mediate trophic shifts and enhance methylmercury accumulation in estuarine biota. *Sci. Adv.* 3, e1601239. <https://doi.org/10.1126/sciadv.1601239>
- Jonsson, S., Mazrui, N.M., Mason, R.P., 2016. Dimethylmercury Formation Mediated by Inorganic and Organic Reduced Sulfur Surfaces. *Sci. Rep.* 6, 1–7. <https://doi.org/10.1038/srep27958>
- Jonsson, S., Skyllberg, U., Nilsson, M.B., Lundberg, E., Andersson, A., Björn, E., 2014a. Differentiated availability of geochemical mercury pools controls methylmercury levels in estuarine sediment and biota. *Nat. Commun.* 5. <https://doi.org/10.1038/ncomms5624>
- Jonsson, S., Skyllberg, U., Nilsson, M.B., Lundberg, E., Andersson, A., Björn, E., 2014b. Differentiated availability of geochemical mercury pools controls methylmercury levels in estuarine sediment and biota. *Nat. Commun.* <https://doi.org/10.1038/ncomms5624>
- Julshamn, K., Grahl-Nielsen, O., 2000. Trace element levels in harp seal (*Pagophilus groenlandicus*) and hooded seal (*Cystophora cristata*) from the Greenland Sea. A multivariate approach. *Sci. Total Environ.* 250, 123–133. [https://doi.org/10.1016/S0048-9697\(00\)00371-5](https://doi.org/10.1016/S0048-9697(00)00371-5)
- Kanatous, S.B., Hawke, T.J., Trumble, S.J., Pearson, L.E., Watson, R.R., Garry, D.J., Williams, T.M., Davis, R.W., 2008. The ontogeny of aerobic and diving capacity in the skeletal muscles of Weddell seals. *J. Exp. Biol.* 211, 2559–65. <https://doi.org/10.1242/jeb.018119>
- Karagas, M.R., Choi, A.L., Oken, E., Horvat, M., Schoeny, R., Kamai, E., Cowell, W., Grandjean, P., Korrick, S., 2012. Evidence on the human health effects of low-level methylmercury exposure. *Environ. Health Perspect.* 120, 799–806. <https://doi.org/10.1289/ehp.1104494>
- Katz, S.A., Chatt, A., 1988. Hair analysis : applications in the biomedical and environmental sciences. New York : VCH Publishers ; Weinheim : VCH verlagsgesllschafts, New York.
- Kauhala, K., Bergenius, M., Isomursu, M., Raitaniemi, J., 2019. Reproductive rate and nutritional status of Baltic ringed seals. *Mammal Res.* 64, 109–120. <https://doi.org/10.1007/s13364-018-0381-1>
- Kearney, K., Hermann, A., Cheng, W., Ortiz, I., Aydin, K., 2019. A coupled pelagic-benthic-sympagic biogeochemical model for the Bering Sea : documentation and validation of the BESTNPZ model (v2019 . 08 . 23) within a high-resolution regional ocean model 1–68.
- Kehrig, C., Vílchez, J.M., Pérez-Montero, E., Iglesias-Páramo, J., Brinchmann, J., Kunth, D., Durrett, F., Bayo, F.M., 2015. The extended He II λ 4686-emitting region in IZw 18 unveiled: Clues for peculiar ionizing sources. *Astrophys. J. Lett.* 801, L28. <https://doi.org/10.1088/2041-8205/801/2/L28>

- Kehrig, H.A., Hauser-Davis, R.A., Seixas, T.G., Pinheiro, A.B., Di Benedetto, A.P.M., 2016. Mercury species, selenium, metallothioneins and glutathione in two dolphins from the southeastern Brazilian coast: Mercury detoxification and physiological differences in diving capacity. *Environ. Pollut.* 213, 785–792. <https://doi.org/10.1016/j.envpol.2016.03.041>
- Kelly, B.P., Badajos, O.H., Kunnasranta, M., Moran, J.R., Martinez-Bakker, M., Wartzok, D., Boveng, P., 2010. Seasonal home ranges and fidelity to breeding sites among ringed seals. *Polar Biol.* 33, 1095–1109. <https://doi.org/10.1007/s00300-010-0796-x>
- Kelly, Jeffrey F., 2000. Stable isotopes of carbon and in the study of avian and mammalian trophic ecology. *Can. J. Zool.* 78, 1–27. <https://doi.org/10.1139/z99-165>
- Kelly, J. F., 2000. Stable isotopes of carbon and nitrogen in the study of avian and mammalian trophic ecology. *Can. J. Zool.* 78, 1–27.
- Kelly, L.J., Martinez, C., Rio, D., 2010. The Fate of Carbon in Growing Fish: An Experimental Study of Isotopic Routing. *Phy. ihgiciil und Biochem. Zool.* 83, 473–80. <https://doi.org/10.1086/649628>
- Kershaw, J.L., Hall, A.J., 2019. Mercury in cetaceans: Exposure, bioaccumulation and toxicity. *Sci. Total Environ.* 694, 133683. <https://doi.org/10.1016/j.scitotenv.2019.133683>
- Khan, A.T., Atkinson, A., Graham, T.C., Thompson, S.J., Ali, S., Shireen, K.F., 2004. Effects of inorganic mercury on reproductive performance of mice. *Food Chem. Toxicol.* 42, 571–577. <https://doi.org/10.1016/j.fct.2003.10.018>
- Kidd, K.A., Clayden, M., Jardine, T., 2012. Bioaccumulation and biomagnification of mercury through food webs, in: Liu, G., Cai, Y., O'Driscoll, N. (Eds.), *Environmental Chemistry and Toxicology of Mercury*. John Wiley & Sons, Inc., Hoboken, New Jersey, pp. 455–499.
- Kim, H., Yeh, S.W., An, S. Il, Song, S.Y., 2020. Changes in the role of Pacific decadal oscillation on sea ice extent variability across the mid-1990s. *Sci. Rep.* 10, 1–10. <https://doi.org/10.1038/s41598-020-74260-0>
- Kirk, J.L., Lehnher, I., Andersson, M., Braune, B.M., Chan, L., Dastoor, A.P., Durnford, D., Gleason, A.L., Loseto, L.L., Steffen, A., St, V.L., 2012. Mercury in Arctic marine ecosystems : Sources , pathways and exposure. *Environ. Res.* 119, 64–87. <https://doi.org/10.1016/j.envres.2012.08.012>
- Klapstein, S.J., Driscoll, N.J.O., 2018. Methylmercury Biogeochemistry in Freshwater Ecosystems : A Review Focusing on DOM and Photodemethylation. *Bull. Environ. Contam. Toxicol.* 100, 14–25. <https://doi.org/10.1007/s00128-017-2236-x>
- Kodaira, T., Waseda, T., Nose, T., Inoue, J., 2020. Record high Pacific Arctic seawater temperatures and delayed sea ice advance in response to episodic atmospheric blocking. *Sci. Rep.* 1–12. <https://doi.org/10.1038/s41598-020-77488-y>
- Kohlbach, D., Ferguson, S.H., Brown, T.A., Michel, C., 2019. Landfast sea ice–benthic coupling during spring and potential impacts of system changes on food web dynamics in Eclipse Sound, Canadian Arctic. *Mar. Ecol. Prog. Ser.* 627, 33–48. <https://doi.org/10.3354/meps13071>
- Kohlbach, D., Graeve, M., A. Lange, B., David, C., Peeken, I., Flores, H., 2016. The importance of ice algae-produced carbon in the central Arctic Ocean ecosystem: Food web relationships revealed by lipid and stable isotope analyses. *Limnol. Oceanogr.* 61, 2027–2044. <https://doi.org/10.1002/lno.10351>
- Kohlbach, D., Schaafsma, F.L., Graeve, M., Lebreton, B., Lange, B.A., David, C., Vortkamp, M., Flores, H., 2017. Strong linkage of polar cod (*Boreogadus saida*) to sea ice algae-produced carbon: Evidence from stomach content,

- fatty acid and stable isotope analyses. *Prog. Oceanogr.* 152, 62–74.
<https://doi.org/https://doi.org/10.1016/j.pocean.2017.02.003>
- Kovacs, K.M., 2018. Hooded seal, *Cystophora cristata*, in: Wursig, B., Thewissen, J.G.M., Kovacs, K.M. (Eds.), *Encyclopedia of Marine Mammals*. pp. 477–478.
- Kovacs, K.M., 2016. *Cystophora cristata*, Hooded seal. IUCN Red List Threat. Species 2016 e.T6204A45225150.
<https://doi.org/T6204A45225150>
- Kovacs, K.M., 2015. *Pagophilus groenlandicus*, Harp Seal. IUCN Red List Threat. Species 2015 e.T41671A45231087.
<https://doi.org/10.2305/IUCN.UK.2015-4.RLTS.T41671A45231087.en>
- Kovacs, K.M., Lavigne, D.M., 1986. Maternal Investment and Neonatal Growth in Phocid Seals. *J. Anim. Ecol.* 55, 1035–1051. <https://doi.org/10.2307/4432>
- Kovacs, K.M., Lydersen, C., Overland, J.E., Moore, S.E., 2011. Impacts of changing sea-ice conditions on Arctic marine mammals. *Mar. Biodivers.* 41, 181–194. <https://doi.org/10.1007/s12526-010-0061-0>
- Krause-Jensen, D., George, D., Bacon, S., Claude, J., Gascard, J., Polyakov, I. V, Alkire, M.B., Bluhm, B.A., Brown, K.A., Carmack, E.C., Chierici, M., Danielson, S.L., Ellingsen, I., Ershova, E.A., Gårdfeldt, K., Ingvaldsen, R.B., Pnyushkov, A. V, Slagstad, D., Wassmann, P., 2020. Borealization of the Arctic Ocean in Response to Anomalous Advection From Sub-Arctic Seas. *Front. Mar. Sci.* 7, 32pp. <https://doi.org/10.3389/fmars.2020.00491>
- Kritee, K., Barkay, T., Blum, J.D., 2009. Mass dependent stable isotope fractionation of mercury during mer mediated microbial degradation of monomethylmercury. *Geochim. Cosmochim. Acta* 73, 1285–1296.
<https://doi.org/10.1016/j.gca.2008.11.038>
- Kritee, K., Blum, J.D., Barkay, T., 2008. Mercury Stable Isotope Fractionation during Reduction of Hg(II) by Different Microbial Pathways. *Environ. Sci. Technol.* 42, 9171–9177. <https://doi.org/10.1021/es801591k>
- Kritee, K., Motta, L.C., Blum, J.D., Tsui, M.T.K., Reinfelder, J.R., 2018. Photomicrobial Visible Light-Induced Magnetic Mass Independent Fractionation of Mercury in a Marine Microalga. *ACS Earth Sp. Chem.* 2, 432–440.
<https://doi.org/10.1021/acsearthspacechem.7b00056>
- Kurle, C.M., 2002. Stable-isotope ratios of blood components from captive northern fur seals (*Callorhinus ursinus*) and their diet: applications for studying the foraging ecology of wild otariids. *Can. J. Zool.* 80, 902–909.
- Kwon, S.Y., Blum, J.D., Carvan, M.J., Basu, N., Head, J.A., Madenjian, C.P., David, S.R., 2012. Absence of Fractionation of Mercury Isotopes during Trophic Transfer of Methylmercury to Freshwater Fish in Captivity. *Environ. Sci. Technol.* 46, 7527–7534. <https://doi.org/10.1021/es300794q>
- Kwon, S.Y., Blum, J.D., Chen, C.Y., Meattay, D.E., Mason, R.P., 2014. Mercury isotope study of sources and exposure pathways of methylmercury in estuarine food webs in the northeastern U.S. *Environ. Sci. Technol.* 48, 10089–10097. <https://doi.org/10.1021/es5020554>
- Kwon, S.Y., Blum, J.D., Chirby, M.A., Chesney, E.J., 2013. Application of mercury isotopes for tracing trophic transfer and internal distribution of mercury in marine fish feeding experiments. *Environ. Toxicol. Chem.* 32, 2322–2330.
<https://doi.org/10.1002/etc.2313>
- Kwon, S.Y., Blum, J.D., Yin, R., Tsui, M.T.K., Yang, Y.H., Choi, J.W., 2020. Mercury stable isotopes for monitoring the effectiveness of the Minamata Convention on Mercury. *Earth-Science Rev.* 203, 103111.
<https://doi.org/10.1016/j.earscirev.2020.103111>
- Laidre, K.L., Northey, A.D., Ugarte, F., 2018. Traditional knowledge about polar bears (*Ursus maritimus*) in East

- Greenland: Changes in the catch and climate over two decades. *Front. Mar. Sci.* 5, 1–16. <https://doi.org/10.3389/fmars.2018.00135>
- Laidre, K.L., Stern, H., Kovacs, K.M., Lowry, L., Moore, S.E., Regehr, E. V., Ferguson, S.H., Wiig, Ø., Boveng, P., Angliss, R.P., Born, E.W., Litovka, D., Quakenbush, L., Lydersen, C., Vongraven, D., Ugarte, F., 2015. Arctic marine mammal population status, sea ice habitat loss, and conservation recommendations for the 21st century. *Conserv. Biol.* 29, 724–737. <https://doi.org/10.1111/cobi.12474>
- Lannuzel, D., Tedesco, L., van Leeuwe, M., Campbell, K., Flores, H., Delille, B., Miller, L., Stefels, J., Assmy, P., Bowman, J., Brown, K., Castellani, G., Chierici, M., Crabeck, O., Damm, E., Else, B., Fransson, A., Fripiat, F., Geilfus, N.X., Jacques, C., Jones, E., Kaartokallio, H., Kotovitch, M., Meiners, K., Moreau, S., Nomura, D., Peeken, I., Rintala, J.M., Steiner, N., Tison, J.L., Vancoppenolle, M., Van der Linden, F., Vichi, M., Wongpan, P., 2020. The future of Arctic sea-ice biogeochemistry and ice-associated ecosystems. *Nat. Clim. Chang.* 10, 983–992. <https://doi.org/10.1038/s41558-020-00940-4>
- Lavigne, D.M., 2018. Harp Seal, *Pagophilus groenlandicus*, in: Wursig, B., Thewissen, J.G.M., Kovacs, K.M. (Eds.), *Encyclopedia of Marine Mammals*. Elsevier Inc., pp. 455–457.
- Lavoie, R.A., Jardine, T., Chumchal, M.M., Kidd, K.A., Campbell, L.M., 2013. Biomagnification of mercury in aquatic food webs: A worldwide meta-analysis. *Environ. Sci. Technol.* 47, 13385–13394. <https://doi.org/10.1021/es403103t>
- Layman, C.A., Albrey, A.D., Montaña, C.G., Post, D.M., 2007. Can Stable Isotope ratios provide for community-wide measures of trophic structure? *Ecology* 88, 42–48.
- Layman, C.A., Allgeier, J.E., 2012. Characterizing trophic ecology of generalist consumers: A case study of the invasive lionfish in the Bahamas. *Mar. Ecol. Prog. Ser.* 448, 131–141. <https://doi.org/10.3354/meps09511>
- Layman, C.A., Araujo, M.S., Boucek, R., Hammerschlag-Peyer, C.M., Harrison, E., Jud, Z.R., Matich, P., Rosenblatt, A.E., Vaudo, J.J., Yeager, L.A., Post, D.M., Bearhop, S., 2012. Applying stable isotopes to examine food-web structure: An overview of analytical tools. *Biol. Rev.* 87, 545–562. <https://doi.org/10.1111/j.1469-185X.2011.00208.x>
- Lazic, S.E., 2016. Package ‘desiR 1.2.’
- Le Croizier, G., Lorrain, A., Sonke, J.E., Jaquemet, S., Schaal, G., Renedo, M., Besnard, L., Cherel, Y., Point, D., 2020. Mercury isotopes as tracers of ecology and metabolism in two sympatric shark species. *Environ. Pollut.* 265. <https://doi.org/10.1016/j.envpol.2020.114931>
- Le Croizier, G., Schaal, G., Point, D., Le Loc’h, F., Machu, E., Fall, M., Munaron, J.M., Boyé, A., Walter, P., Laë, R., Tito De Morais, L., 2019. Stable isotope analyses revealed the influence of foraging habitat on mercury accumulation in tropical coastal marine fish. *Sci. Total Environ.* 650, 2129–2140. <https://doi.org/10.1016/j.scitotenv.2018.09.330>
- Lee, C.-S., Fisher, N.S., 2017. Bioaccumulation of methylmercury in a marine diatom and the influence of dissolved organic matter. *Mar. Chem.* 197, 70–79. <https://doi.org/10.1016/j.marchem.2017.09.005>
- Lee, C.S., Fisher, N.S., 2016. Methylmercury uptake by diverse marine phytoplankton. *Limnol. Oceanogr.* 61, 1626–1639. <https://doi.org/10.1002/lno.10318>
- Legendre, L., Ackley, S.F., Dieckmann, G.S., Gulliksen, B., Horner, R., Hoshiai, T., Melnikov, I.A., Reeburgh, W.S., Spindler, M., W., S.C., 1992. Ecology of sea ice biota - 2. Global significance. *Polar Biol.* 12, 429–444.

<https://doi.org/10.1007/bf00243114>

- Legendre, P., Legendre, L., 2012. *Numerical Ecology*. Elsevier B.V., Oxford.
- Lehnert, K., Desforges, J.-P., Das, K., Siebert, U., 2018. Ecotoxicological biomarkers and accumulation of contaminants in Pinnipeds, *Marine Mammal Ecotoxicology: Impacts of Multiple Stressors on Population Health*. Elsevier Inc. <https://doi.org/10.1016/B978-0-12-812144-3.00010-3>
- Lehnerr, I., 2014. Methylmercury biogeochemistry: A review with special reference to Arctic aquatic ecosystems. *Environ. Rev.* 22, 229–243. <https://doi.org/10.1139/er-2013-0059>
- Lehnerr, I., St. Louis, V.L., 2009. Importance of ultraviolet radiation in the photodemethylation of methylmercury in freshwater ecosystems. *Environ. Sci. Technol.* 43, 5692–5698. <https://doi.org/10.1021/es9002923>
- Lehnerr, I., St. Louis, V.L., Hintelmann, H., Kirk, J.L., 2011. Methylation of inorganic mercury in polar marine waters. *Nat. Geosci.* 4, 298–302. <https://doi.org/10.1038/ngeo1134>
- Lepak, R.F., Yin, R., Krabbenhoft, D.P., Ogorek, J.M., Dewild, J.F., Holsen, T.M., Hurley, J.P., 2015. Use of Stable Isotope Signatures to Determine Mercury Sources in the Great Lakes. *Environ. Sci. Technol. Lett.* 2, 335–341. <https://doi.org/10.1021/acs.estlett.5b00277>
- Leroux, S.J., Loreau, M., 2015. Theoretical perspectives on bottom-up and top-down interactions across ecosystems. *Trophic Ecol. Bottom-Up Top-Down Interact. Across Aquat. Terr. Syst.* 3–28. <https://doi.org/10.1017/CBO9781139924856.002>
- Lesage, V., Hammill, M.O., Kovacs, K.M., 2002a. Diet-tissue fractionation of stable carbon and nitrogen isotopes in phocid seals. *Mar. Mammal Sci.* 18, 182–193. <https://doi.org/10.1111/j.1748-7692.2002.tb01027.x>
- Lesage, V., Hammill, M.O., Kovacs, K.M., 2002b. Diet-tissue fractionation of stable carbon and nitrogen isotopes in phocid seals. *Mar. Mammal Sci.* 18, 182–193.
- Leu, E., Mundy, C.J., Assmy, P., Campbell, K., Gabrielsen, T.M., Gosselin, M., Juul-Pedersen, T., Gradinger, R., 2015. Arctic spring awakening-Steering principles behind the phenology of vernal ice algal blooms. *Prog. Oceanogr.* 139, 151–170. <https://doi.org/10.1016/j.pocean.2015.07.012>
- Li, M., Juang, C.A., Ewald, J.D., Yin, R., Mikkelsen, B., Krabbenhoft, D.P., Balcom, P.H., Dassuncao, C., Sunderland, E.M., 2020. Selenium and stable mercury isotopes provide new insights into mercury toxicokinetics in pilot whales. *Sci. Total Environ.* 710, 136325. <https://doi.org/10.1016/j.scitotenv.2019.136325>
- Li, M., Schartup, A.T., Valberg, A.P., Ewald, J.D., Krabbenhoft, D.P., Yin, R., Balcom, P.H., Sunderland, E.M., 2016a. Environmental Origins of Methylmercury Accumulated in Subarctic Estuarine Fish Indicated by Mercury Stable Isotopes. *Environ. Sci. Technol.* 50, 11559–11568. <https://doi.org/10.1021/acs.est.6b03206>
- Li, M., Sherman, L.S., Blum, J.D., Grandjean, P., Mikkelsen, B., Weihe, P., Sunderland, E.M., Shine, J.P., 2014. Assessing Sources of Human Methylmercury Exposure Using Stable Mercury Isotopes. *Environ. Sci. Technol.* 48, 8800–8806. <https://doi.org/10.1021/es500340r>
- Li, M., Von Stackelberg, K., Rheinberger, C.M., Hammitt, J.K., Krabbenhoft, D.P., Yin, R., Sunderland, E.M., 2016b. Insights from mercury stable isotopes into factors affecting the internal body burden of Methylmercury in frequent fish consumers. *Elementa* 2016, 1–13. <https://doi.org/10.12952/journal.elementa.000103>
- Li, P., Feng, X., Qiu, G., 2010. Methylmercury Exposure and Health Effects from Rice and Fish Consumption: A Review 2666–2691. <https://doi.org/10.3390/ijerph7062666>
- Li, W.K.W., McLaughlin, F.A., Lovejoy, C., Carmack, E.C., 2009. Smallest algae thrive as the arctic ocean freshens.

- Science (80-.). 326, 539. <https://doi.org/10.1126/science.1179798>
- Li, Y., Cai, Y., 2013. Progress in the study of mercury methylation and demethylation in aquatic environments. *Chinese Sci. Bull.* 58, 177–185. <https://doi.org/10.1007/s11434-012-5416-4>
- Lide, D.R., 2007. Electrochemical Series, in: Lide, D.R. (Ed.), *CRC Handbook of Chemistry and Physics*, Internet Version. Taylor & Francis, Boca Raton.
- Liem-Nguyen, V., Skyllberg, U., Björn, E., 2017. Thermodynamic Modeling of the Solubility and Chemical Speciation of Mercury and Methylmercury Driven by Organic Thiols and Micromolar Sulfide Concentrations in Boreal Wetland Soils. *Environ. Sci. Technol.* 51, 3678–3686. <https://doi.org/10.1021/acs.est.6b04622>
- Lim, A.G., Sonke, J.E., Krickov, I. V., Manasypov, R.M., Loiko, S. V., Pokrovsky, O.S., 2019. Enhanced particulate Hg export at the permafrost boundary, western Siberia. *Environ. Pollut.* 254, 113083. <https://doi.org/10.1016/j.envpol.2019.113083>
- Lindstrøm, U., Nilssen, K.T., Pettersen, L.M.S., Haug, T., 2013. Harp seal foraging behaviour during summer around Svalbard in the northern Barents Sea: Diet composition and the selection of prey. *Polar Biol.* 36, 305–320. <https://doi.org/10.1007/s00300-012-1260-x>
- Liu, G., Cai, Y., O’Driscoll, N., Feng, X., Jiang, G., 2012. Overview of mercury in the environment, in: Liu, G., Cai, Y., O’Driscoll, N. (Eds.), *Environmental Chemistry and Toxicology of Mercury*. John Wiley & Sons, Inc., Hoboken, New Jersey, p. 574.
- Liu, L., Mu, C., Schaefer, T., Roth, D.A., Zhang, T., Hugelius, G., Antweiler, R.C., Jafarov, E., Wickland, K.P., Gryziec, J.D., Krabbenhoft, D.P., Aiken, G.R., Dewild, J.F., Gusmeroli, A., Schuster, P.F., Herman-Mercer, N., Striegl, R.G., Schaefer, K.M., 2018. Permafrost Stores a Globally Significant Amount of Mercury. *Geophys. Res. Lett.* 45, 1463–1471. <https://doi.org/10.1002/2017gl075571>
- López-Berenguer, G., Peñalver, J., Martínez-López, E., 2020. A critical review about neurotoxic effects in marine mammals of mercury and other trace elements. *Chemosphere* 246. <https://doi.org/10.1016/j.chemosphere.2019.125688>
- Loseto, L.L., Stern, G.A., Deibel, D., Connelly, T.L., Prokopowicz, A., Lean, D.R.S., Fortier, L., Ferguson, S.H., 2008a. Linking mercury exposure to habitat and feeding behaviour in Beaufort Sea beluga whales. *J. Mar. Syst.* 74, 1012–1024. <https://doi.org/10.1016/j.jmarsys.2007.10.004>
- Loseto, L.L., Stern, G.A., Ferguson, S.H., 2008b. Size and biomagnification: How habitat selection explains beluga mercury levels. *Environ. Sci. Technol.* 42, 3982–3988. <https://doi.org/10.1021/es7024388>
- Lovvorn, J.R., Rocha, A.R., Mahoney, A.H., Jewett, S.C., 2018. Sustaining ecological and subsistence functions in conservation areas: Eider habitat and access by Native hunters along landfast ice. *Environ. Conserv.* 45, 361–369. <https://doi.org/10.1017/S0376892918000103>
- Lowry, L. 2016., 2016. *Pusa hispida*, Ringed seal. IUCN Red List Threat. Species 2016 e.T41672A45231341.
- Lowther, A.D., Fisk, A., Kovacs, K.M., Lydersen, C., 2017. Interdecadal changes in the marine food web along the west Spitsbergen coast detected in the stable isotope composition of ringed seal (*Pusa hispida*) whiskers. *Polar Biol.* 40, 2027–2033. <https://doi.org/10.1007/s00300-017-2122-3>
- Lozier, M.S., 2010. Deconstructing the conveyor belt. *Science* (80-.). 328, 1507–1511. <https://doi.org/10.1126/science.1189250>
- Lu, X., Liu, Y., Johs, A., Zhao, L., Wang, T., Yang, Z., Lin, H., Elias, D.A., Pierce, E.M., Liang, L., Barkay, T., Gu, B.,

2016. Anaerobic Mercury Methylation and Demethylation by *Geobacter bemidjiensis* Bem. *Environ. Sci. Technol.* 50, 4366–4373. <https://doi.org/10.1021/acs.est.6b00401>
- Lübcker, N., Whiteman, J.P., Millar, R.P., de Bruyn, P.J.N., Newsome, S.D., 2020. Fasting affects amino acid nitrogen isotope values: a new tool for identifying nitrogen balance of free-ranging mammals. *Oecologia*. <https://doi.org/10.1007/s00442-020-04645-5>
- Luo, H., Cheng, Q., Pan, X., 2020. Photochemical behaviors of mercury (Hg) species in aquatic systems: A systematic review on reaction process, mechanism, and influencing factor. *Sci. Total Environ.* 720, 137540. <https://doi.org/10.1016/j.scitotenv.2020.137540>
- Lydersen, C., Kovacs, K.M., Hammill, M.O., 1997. Energetics during nursing and early postweaning fasting in hooded seal (*Cystophora cristata*) pups from the Gulf of St Lawrence, Canada. *J. Comp. Physiol. B Biochem. Syst. Environ. Physiol.* 167, 81–88.
- Lyytikäinen, M., Pätynen, J., Hyvärinen, H., Sipilä, T., Kunasranta, M., 2015. Mercury and Selenium Balance in Endangered Saimaa Ringed Seal Depend on Age and Sex. *Environ. Sci. Technol.* 49, 11808–11816. <https://doi.org/10.1021/acs.est.5b01555>
- Ma, J., Hung, H., Macdonald, R.W., 2016. The influence of global climate change on the environmental fate of persistent organic pollutants: A review with emphasis on the Northern Hemisphere and the Arctic as a receptor. *Glob. Planet. Change* 146, 89–108. <https://doi.org/10.1016/j.gloplacha.2016.09.011>
- Ma, M., Du, H., Wang, D., 2019. Mercury methylation by anaerobic microorganisms: A review. *Crit. Rev. Environ. Sci. Technol.* 49, 1893–1936. <https://doi.org/10.1080/10643389.2019.1594517>
- Macdonald, R.W., Harner, T., Fyfe, J., 2005. Recent climate change in the Arctic and its impact on contaminant pathways and interpretation of temporal trend data. *Sci. Total Environ.* 342, 5–86. <https://doi.org/10.1016/j.scitotenv.2004.12.059>
- Magos, L., Clarkson, T.W., 2008. The assessment of the contribution of hair to methyl mercury excretion. *Toxicol. Lett.* 182, 48–49. <https://doi.org/10.1016/j.toxlet.2008.08.010>
- Mahoney, A.R., Eicken, H., Gaylord, A.G., Gens, R., 2014. Landfast sea ice extent in the Chukchi and Beaufort Seas: The annual cycle and decadal variability. *Cold Reg. Sci. Technol.* 103, 41–56. <https://doi.org/10.1016/j.coldregions.2014.03.003>
- Malde, A., 2019. Development of diving capacity and behaviour in harp seal (*Pagophilus groenlandicus*) weanlings from the Greenland Sea Stock (Master thesis). UiT - The Arctic University of Norway.
- Man, Y., Yin, R., Cai, K., Qin, C., Wang, J., Yan, H., Li, M., 2019. Primary amino acids affect the distribution of methylmercury rather than inorganic mercury among tissues of two farmed-raised fish species. *Chemosphere* 225, 320–328. <https://doi.org/10.1016/j.chemosphere.2019.03.058>
- Martínez-López, E., Peñalver, J., Lara, L., García-Fernández, A.J., 2019. Hg and Se in Organs of Three Cetacean Species from the Murcia Coastline (Mediterranean Sea). *Bull. Environ. Contam. Toxicol.* 103, 521–527. <https://doi.org/10.1007/s00128-019-02697-9>
- Martínez del Rio, C., Carleton, S.A., 2012. How fast and how faithful: the dynamics of isotopic incorporation into animal tissues. *J. Mammal.* 93, 353–359. <https://doi.org/10.1644/11-MAMM-S-165.1>
- Martínez Del Rio, C., Wolf, N., Carleton, S.A., Gannes, L.Z., 2009. Isotopic ecology ten years after a call for more laboratory experiments. *Biol. Rev.* 84, 91–111. <https://doi.org/10.1111/j.1469-185X.2008.00064.x>

- Marvin-Dipasquale, M., Agee, J., McGowan, C., Oremland, R.S., Thomas, M., Krabbenhoft, D., Gilmour, C.C., 2000. Methyl-mercury degradation pathways: A comparison among three mercury impacted ecosystems. *Environ. Sci. Technol.* 34, 4908–4916. <https://doi.org/10.1021/es0013125>
- Masbou, J., Point, D., Sonke, J.E., Frappart, F., Perrot, V., Amouroux, D., Richard, P., Becker, P.R., 2015a. Hg Stable Isotope Time Trend in Ringed Seals Registers Decreasing Sea Ice Cover in the Alaskan Arctic. *Environ. Sci. Technol.* 49, 8977–8985. <https://doi.org/10.1021/es5048446>
- Masbou, J., Sonke, J.E., Amouroux, D., Guillou, G., Becker, P.R., Point, D., 2018. Hg-Stable Isotope Variations in Marine Top Predators of the Western Arctic Ocean. *ACS Earth Sp. Chem.* 2, 479–490. <https://doi.org/10.1021/acsearthspacechem.8b00017>
- Masbou, Jérémy, Point, D., Guillou, G., Sonke, J., Lebreton, B., Masbou, Jeremy, Point, D., Guillou, G., Sonke, J., Lebreton, B., 2015b. Carbon stable isotope analysis of methylmercury toxin in biological materials by gas chromatography isotope ratio mass spectrometry. *Anal. Chem.* 87, 11732–11738. <https://doi.org/10.1021/acs.analchem.5b02918>
- Mason, R.P., Choi, A.L., Fitzgerald, W.F., Hammerschmidt, C.R., Lamborg, C.H., Soerensen, A.L., Sunderland, E.M., 2012. Mercury biogeochemical cycling in the ocean and policy implications. *Environ. Res.* 119, 101–117. <https://doi.org/10.1016/j.envres.2012.03.013>
- Mason, R.P., Sheu, G.R., 2002. Role of the ocean in the global mercury cycle. *Global Biogeochem. Cycles* 16, 40-1-40–14. <https://doi.org/10.1029/2001gb001440>
- Matley, J.K., Fisk, A.T., Dick, T.A., 2015. Foraging ecology of ringed seals (*Pusa hispida*), beluga whales (*Delphinapterus leucas*) and narwhals (*Monodon monoceros*) in the Canadian High Arctic determined by stomach content and stable isotope analysis. *Polar Res.* 34. <https://doi.org/10.3402/polar.v34.24295>
- Maury-Brachet, R., Durrieu, G., Dominique, Y., Boudou, A., 2006. Mercury distribution in fish organs and food regimes: Significant relationships from twelve species collected in French Guiana (Amazonian basin). *Sci. Total Environ.* 368, 262–270. <https://doi.org/http://dx.doi.org/10.1016/j.scitotenv.2005.09.077>
- Mawson, C.A., 1955. Meaning of “Turnover” in Biochemistry. *Nature* 176, 317.
- McClelland, J.W., Holmes, R.M., Dunton, K.H., Macdonald, R.W., 2012. The Arctic Ocean Estuary. *Estuaries and Coasts* 35, 353–368. <https://doi.org/10.1007/s12237-010-9357-3>
- McConnaughey, T., McRoy, C.P., 1979. Food-Web structure and the fractionation of Carbon isotopes in the bering sea. *Mar. Biol.* 53, 257–262. <https://doi.org/10.1007/bf00952434>
- McCutchan, J.H., Lewis Jr, W.M., Kendall, C., McGrath, C.C., 2003. Variation in trophic shift for stable isotope ratios of carbon, nitrogen, and sulfur. *Oikos* 102, 378–390. <https://doi.org/10.1034/j.1600-0706.2003.12098.x>
- McHuron, E.A., Holser, R.R., Costa, D.P., 2019. What’s in a whisker? Disentangling ecological and physiological isotopic signals. *Rapid Commun. Mass Spectrom.* 33, 57–66. <https://doi.org/10.1002/rcm.8312>
- McKinney, M.A., Iverson, S.J., Fisk, A.T., Sonne, C., Rigét, F., Letcher, R.J., Arts, M.T., Born, E.W., Rosing-Asvid, A., Dietz, R., 2013. Global change effects on the long-term feeding ecology and contaminant exposures of East Greenland polar bears. *Glob. Chang. Biol.* 19, 2360–2372. <https://doi.org/10.1111/gcb.12241>
- McKinney, M.A., Pedro, S., Dietz, R., Sonne, C., Fisk, A.T., Roy, D., Jenssen, B.M., Letcher, R.J., 2015. A review of ecological impacts of global climate change on persistent organic pollutant and mercury pathways and exposures in arctic marine ecosystems. *Curr. Zool.* 61, 617–628. <https://doi.org/10.1093/czoolo/61.4.617>

- McMahon, K.W., Hamady, L.L., Thorrold, S.R., 2013a. Ocean ecogeochemistry: a review. *Oceanogr. Mar. Biol. Annu. Rev.* 51, 327–374. <https://doi.org/doi:10.1201/b15406-6r10.1201/b15406-6>
- McMahon, K.W., Hamady, L.L., Thorrold, S.R., 2013b. A review of ecogeochemistry approaches to estimating movements of marine animals. *Limnol. Oceanogr.* 58, 697–714. <https://doi.org/10.4319/lo.2013.58.2.0697>
- Mcmeans, B.C., Arts, M.T., Fisk, A.T., 2014a. Impacts of food web structure and feeding behavior on mercury exposure in Greenland Sharks (*Somniosus microcephalus*). <https://doi.org/10.1016/j.scitotenv.2014.01.128>
- Mcmeans, B.C., Arts, M.T., Fisk, A.T., 2014b. Impacts of food web structure and feeding behavior on mercury exposure in Greenland Sharks (*Somniosus microcephalus*). <https://doi.org/10.1016/j.scitotenv.2014.01.128>
- McNaught, A.D., Wilkinson, A., 1997. IUPAC. Compendium of Chemical Terminology, 2nd ed. Blackwell Scientific Publications, Oxford. <https://doi.org/10.1351/goldbook>
- Mead, C., Lyons, J.R., Johnson, T.M., Anbar, A.D., 2013. Unique Hg Stable Isotope Signatures of Compact Fluorescent Lamp-Sourced Hg. *Environ. Sci. Technol.* 47, 2542–2547. <https://doi.org/10.1021/es303940p>
- Melnick, J.G., Yurkerwich, K., Parking, G., 2010. On the Chalcogenophilicity of Mercury: Evidence for a Strong Hg–Se Bond in [TmBut]HgSePh and its Relevance to the Toxicity of Mercury. *J. Am. Chem. Soc.* 132, 647–655. <https://doi.org/10.1021/ja907523x>
- Meng, M., Sun, R. yu, Liu, H. wei, Yu, B., Yin, Y. guang, Hu, L. gang, Chen, J. bin, Shi, J. bo, Jiang, G. bin, 2020. Mercury isotope variations within the marine food web of Chinese Bohai Sea: Implications for mercury sources and biogeochemical cycling. *J. Hazard. Mater.* 384, 121379. <https://doi.org/10.1016/j.jhazmat.2019.121379>
- Meredith, M., Sommerkorn, M., Cassotta, S., Derksen, C., Ekaykin, A., Hollowed, A., Kofinas, G., Mackintosh, A., Melbourne-Thomas, J., Muelbert, M.M.C., Ottersen, G., Pritchard, H., E.A.G. Schuur, 2019. Polar regions, in: Pörtner, H.-O., Roberts, D.C., Masson-Delmotte, V., Zhai, P., Tignor, M., Poloczanska, E., Mintenbeck, K., Alegría, A., Nicolai, M., Okem, A., Petzold, J., Rama, B., Weyer, N.M. (Eds.), IPCC Special Report on the Ocean and Cryosphere in a Changing Climate. pp. 203–320.
- Mergler, D., Anderson, H.A., Chan, L.H.M., Mahaffey, K.R., Murray, M., Sakamoto, M., Stern, A.H., 2007. Methylmercury exposure and health effects in humans: A worldwide concern. *Ambio* 36, 3–11. [https://doi.org/10.1579/0044-7447\(2007\)36\[3:MEAHEI\]2.0.CO;2](https://doi.org/10.1579/0044-7447(2007)36[3:MEAHEI]2.0.CO;2)
- Michel, L.N., Danis, B., Dubois, P., Eleaume, M., Fournier, J., Gallut, C., Jane, P., Lepoint, G., 2019. Increased sea ice cover alters food web structure in East Antarctica. *Sci. Rep.* 9, 1–11. <https://doi.org/10.1038/s41598-019-44605-5>
- Middelburg, J.J., 2014. Stable isotopes dissect aquatic food webs from the top to the bottom. *Biogeosciences* 11, 2357–2371. <https://doi.org/10.5194/bg-11-2357-2014>
- Mieiro, C.L., Pacheco, M., Pereira, M.E., Duarte, A.C., 2009. Mercury distribution in key tissues of fish (*Liza aurata*) inhabiting a contaminated estuary - Implications for human and ecosystem health risk assessment. *J. Environ. Monit.* 11, 1004–1012. <https://doi.org/10.1039/b821253h>
- Miles, M.W., Andresen, C.S., Dylmer, C. V., 2020. Evidence for extreme export of Arctic sea ice leading the abrupt onset of the Little Ice Age, *Sci. Adv.*
- Monperrus, M., Tessier, E., Amouroux, D., Leynaert, A., Huonnic, P., Donard, O.F.X., 2007. Mercury methylation, demethylation and reduction rates in coastal and marine surface waters of the Mediterranean Sea. *Mar. Chem.* 107, 49–63. <https://doi.org/10.1016/j.marchem.2007.01.018>
- Moore, C.W., Obrist, D., Steffen, A., Staebler, R.M., Douglas, T.A., Richter, A., Nghiem, S. V., 2014. Convective

- forcing of mercury and ozone in the Arctic boundary layer induced by leads in sea ice. *Nature* 506, 81–84. <https://doi.org/10.1038/nature12924>
- Moore, S.E., Haug, T., Víkingsson, G.A., Stenson, G.B., 2019. Baleen whale ecology in arctic and subarctic seas in an era of rapid habitat alteration. *Prog. Oceanogr.* 176, 102118. <https://doi.org/10.1016/j.pocean.2019.05.010>
- Morel, F.M.M., Kraepiel, A.M.L., Amyot, M., 1998. The chemical cycle and bioaccumulation of mercury. *Annu. Rev. Ecol. Evol. Syst.* 29, 543–66.
- Motta, L.C., Blum, J.D., Johnson, M.W., Umhau, B.P., Popp, B.N., Washburn, S.J., Drazen, J.C., Benitez-Nelson, C.R., Hannides, C.C.S., Close, H.G., Lamborg, C.H., 2019. Mercury Cycling in the North Pacific Subtropical Gyre as Revealed by Mercury Stable Isotope Ratios. *Global Biogeochem. Cycles* 33, 777–794. <https://doi.org/10.1029/2018GB006057>
- Motulsky, H.J., Brown, R.E., 2006. Detecting outliers when fitting data with nonlinear regression - A new method based on robust nonlinear regression and the false discovery rate. *BMC Bioinformatics* 7, 1–20. <https://doi.org/10.1186/1471-2105-7-123>
- Mu, C., Schuster, P.F., Abbott, B.W., Kang, S., Guo, J., Sun, S., Wu, Q., Zhang, T., 2020. Permafrost degradation enhances the risk of mercury release on Qinghai-Tibetan Plateau. *Sci. Total Environ.* 708. <https://doi.org/10.1016/j.scitotenv.2019.135127>
- Munson, K.M., Lamborg, C.H., Boiteau, R.M., Saito, M.A., 2018. Dynamic mercury methylation and demethylation in oligotrophic marine water. *Biogeosciences* 15, 6451–6460. <https://doi.org/10.5194/bg-15-6451-2018>
- Najbjerg, L., Sonne, C., Eulaers, I., Holm, P., Dietz, R., 2017. Are temporal changes in ringed seal (*Pusa hispida*) blubber thickness related to climate change and hunting ? Aarhus University.
- Nakazawa, E., Ikemoto, T., Hokura, A., Terada, Y., Kunito, T., Tanabe, S., Nakai, I., 2011. The presence of mercury selenide in various tissues of the striped dolphin: Evidence from μ -XRF-XRD and XAFS analyses. *Metallomics* 3, 719–725. <https://doi.org/10.1039/c0mt00106f>
- National legislation - NORWAY, 2017. Module 1: Norwegian Regulations for use of animals in experiments 12.
- National Research Council, 2000a. *Toxicological Effects of Methylmercury*, 1st ed. National Academy Press, Washington DC.
- National Research Council, 2000b. Chemistry, exposure, toxicokinetics and toxicodynamics, in: National Research Council (Ed.), *Toxicological Effects of Methylmercury*. National Academy Press, Washington DC, pp. 31–71.
- Ndu, U., Mason, R.P., Zhang, H., Lin, S., Visscher, P.T., 2012. Effect of inorganic and organic ligands on the bioavailability of methylmercury as determined by using a mer-lux bioreporter. *Appl. Environ. Microbiol.* 78, 7276–7282. <https://doi.org/10.1128/AEM.00362-12>
- Newsome, S.D., Clementz, M.T., Koch, P.L., 2010. Using stable isotope biogeochemistry to study marine mammal ecology. *Mar. Mammal Sci.* 26, 509–572. <https://doi.org/10.1111/j.1748-7692.2009.00354.x>
- Newsome, S.D., Erlenbach, J., Nicassio, N., Brooks, M., Jensen, S., Cutting, A., Stenhouse, G., Robbins, C.T., Cherry, S.G., Hash, A., Stricker, C.A., Rode, K.D., 2016. Isotopic Incorporation and the Effects of Fasting and Dietary Lipid Content on Isotopic Discrimination in Large Carnivorous Mammals. *Physiol. Biochem. Zool.* 89, 182–197. <https://doi.org/10.1086/686490>
- Newsome, S.D., Martinez del Rio, C., Bearhop, S., Phillips, D.L., 2007. A niche for isotopic ecology. *Front. Ecol. Environ.* 5, 429–436. <https://doi.org/10.1890/060150.01>

- Nielsen, C.O., Dietz, R., 1990. Distributional pattern of zinc, cadmium, mercury, and selenium in livers of Hooded Seal (*Cystophora cristata*). *Biol. Trace Elem. Res.* 24, 61–71. <https://doi.org/10.1007/BF02789141>
- Nordberg, G.F., Fowler, B.A., 2019. Examples of Risk Assessments of Human Metal Exposures and the Need for Mode of Action (MOA), Toxicokinetic-Toxicodynamic (TKTD) Modeling, and Adverse Outcome Pathways (AOPs), in: *Risk Assessment for Human Metal Exposures*. Elsevier, pp. 227–310. <https://doi.org/10.1016/b978-0-12-804227-4.00008-x>
- Nordøy, E.S., Folkow, L.P., Potelov, V., Prischemikhin, V., Blix, A.S., 2008. Seasonal distribution and dive behaviour of harp seals (*Pagophilus groenlandicus*) of the White Sea-Barents Sea stock. *Polar Biol.* 31, 1119–1135. <https://doi.org/10.1007/s00300-008-0453-9>
- Norici, A., Hell, R., Giordano, M., 2005. Sulfur and primary production in aquatic environments: An ecological perspective. *Photosynth. Res.* 86, 409–417. <https://doi.org/10.1007/s11120-005-3250-0>
- Norwegian Ministry of Agriculture and Food, 2009. Animal Welfare Act. LOV-2018-06-15-38, §12.
- Norwegian Ministry of Trade and Industry, 2003. Forskrift om utøvelse av selfangst i Vesterisen og Østisen. FOR-2003-02-11-151.
- Obrist, D., Agnan, Y., Jiskra, M., Olson, C.L., Colegrove, D.P., Hueber, J., Moore, C.W., Sonke, J.E., Helmig, D., 2017. Tundra uptake of atmospheric elemental mercury drives Arctic mercury pollution. *Nature* 547, 201–204. <https://doi.org/10.1038/nature22997>
- Obrist, D., Kirk, J.L., Zhang, L., Sunderland, E.M., Jiskra, M., Selin, N.E., 2018. A review of global environmental mercury processes in response to human and natural perturbations: Changes of emissions, climate, and land use. *Ambio* 47, 116–140. <https://doi.org/10.1007/s13280-017-1004-9>
- Oftedal, O.T., Bowen, W.D., Boness, D.J., 1996. Lactation performance and nutrient deposition in pups of the harp seal, *Phoca groenlandica*, on ice floes off Southeast Labrador. *Physiol. Zool.* 69, 635–657.
- Øigård, T.A., Haug, T., Nilssen, K.T., 2014. Current status of hooded seals in the Greenland Sea. Victims of climate change and predation? *Biol. Conserv.* 172, 29–36. <https://doi.org/10.1016/j.biocon.2014.02.007>
- Øigård, T.A., Haug, T., Nilssen, K.T., Salberg, A.B., 2009. Estimation of pup production of hooded and harp seals in the Greenland Sea in 2007: Reducing uncertainty using generalized additive models. *J. Northwest Atl. Fish. Sci.* 42, 103–123. <https://doi.org/10.2960/J.v42.m642>
- Oppenheimer, M., Glavovic, B.C., Hinkel, J., Wal, R. van de, Magnan, A.K., Abd-Elgawad, A., Cai, R., Cifuentes-Jara, M., DeConto, R.M., Ghosh, T., Hay, J., Isla, F., Marzeion, B., Meyssignac, B., Sebesvar, Z., 2019. Sea Level Rise and Implications for Low-Lying Islands, Coasts and Communities, in: Pörtner, H.-O., Roberts, D.C., Masson-Delmotte, V., Zhai, P., Tignor, M., Poloczanska, E., Mintenbeck, K., Alegría, A., Nicolai, M., Okem, A., Petzold, J., Rama, B., Weyer, N.M. (Eds.), *IPCC Special Report on the Ocean and Cryosphere in a Changing Climate*. pp. 321–444.
- Ostertag, S.K., Shaw, A.C., Basu, N., Chan, H.M., 2014. Molecular and Neurochemical Biomarkers in Arctic Beluga Whales (*Delphinapterus leucas*) Were Correlated to Brain Mercury and Selenium Concentrations. *Environ. Sci. Technol.* 48, 11551–11559. <https://doi.org/10.1021/es501369b>
- Outridge, P.M., MacDonald, R.W., Wang, F., Stern, G.A., Dastoor, A.P., 2008. A mass balance inventory of mercury in the Arctic Ocean. *Environ. Chem.* 5, 89–111. <https://doi.org/10.1071/EN08002>
- Outridge, P.M., Mason, R.P., Wang, F., Guerrero, S., Heimbürger-Boavida, L.E., 2018. Updated Global and Oceanic

- Mercury Budgets for the United Nations Global Mercury Assessment 2018. *Environ. Sci. Technol.* 52, 11466–11477. <https://doi.org/10.1021/acs.est.8b01246>
- Overland, J., Dunlea, E., Box, J.E., Corell, R., Forsius, M., Kattsov, V., Olsen, M.S., Pawlak, J., Reiersen, L.O., Wang, M., 2019. The urgency of Arctic change. *Polar Sci.* 21, 6–13. <https://doi.org/10.1016/j.polar.2018.11.008>
- Paranjape, A.R., Hall, B.D., 2017. Recent advances in the study of mercury methylation in aquatic systems. *Facets* 2, 85–119. <https://doi.org/10.1139/facets-2016-0027>
- Parcell, S., Cand, N.D., 2002. Sulfur in human nutrition applications in medicine . *Sulfur in Human Nutrition and Applications in Medicine. Altern. Med. Rev.* 7, 22–44.
- Park, J.D., Zheng, W., 2012. Human exposure and health effects of inorganic and elemental mercury. *J. Prev. Med. Public Heal.* 45, 344–352. <https://doi.org/10.3961/jpmph.2012.45.6.344>
- Parks, J.M., Johs, A., Podar, M., Bridou, R., Hurt, R.A., Smith, S.D., Tomanicek, S.J., Qian, Y., Brown, S.D., Brandt, C.C., Palumbo, A. V., Smith, J.C., Wall, J.D., Elias, D.A., Liang, L., 2013. The genetic basis for bacterial mercury methylation. *Science (80-)*. 339, 1332–1335. <https://doi.org/10.1126/science.1230667>
- Parnell, A.C., Phillips, D.L., Bearhop, S., Semmens, B.X., Ward, E.J., Moore, J.W., Jackson, A.L., Grey, J., Kelly, D.J., Inger, R., 2013. Bayesian stable isotope mixing models. *Environmetrics* 24, 387–399. <https://doi.org/10.1002/env.2221>
- Pearson, S.F., Levey, D.J., Greenberg, C.H., Martínez Del Rio, C., 2003. Effects of elemental composition on the incorporation of dietary nitrogen and carbon isotopic signatures in an omnivorous songbird. *Oecologia* 135, 516–23. <https://doi.org/10.1007/s00442-003-1221-8>
- Pedrero, Z., Bridou, R., Mounicou, S., Guyoneaud, R., Monperrus, M., Amouroux, D., 2012. Transformation, localization, and biomolecular binding of Hg species at subcellular level in methylating and nonmethylating sulfate-reducing bacteria. *Environ. Sci. Technol.* 46, 11744–11751. <https://doi.org/10.1021/es302412q>
- Pereira, P., Korbas, M., Pereira, V., Cappello, T., Maisano, M., Canário, J., Almeida, A., Pacheco, M., 2019. A multidimensional concept for mercury neuronal and sensory toxicity in fish-From toxicokinetics and biochemistry to morphometry and behavior. <https://doi.org/10.1016/j.bbagen.2019.01.020>
- Perrot, V., Epov, V.N., Pastukhov, M. V, Grebenshchikova, V.I., Zouiten, C., Sonke, J.E., Husted, S., Donard, O.F.X., Amouroux, D., 2010. Tracing Sources and Bioaccumulation of Mercury in Fish of Lake Baikal– Angara River Using Hg Isotopic Composition. *Environ. Sci. Technol.* 44, 8030–8037. <https://doi.org/10.1021/es101898e>
- Perrot, V., Landing, W.M., Grubbs, R.D., Salters, V.J.M., 2019. Mercury bioaccumulation in tile fish from the northeastern Gulf of Mexico 2 years after the Deepwater Horizon oil spill : Insights from Hg , C , N and S stable isotopes. *Sci. Total Environ.* 666, 828–838. <https://doi.org/10.1016/j.scitotenv.2019.02.295>
- Perrot, V., Masbou, J., Pastukhov, M. V., Epov, V.N., Point, D., Bérail, S., Becker, P.R., Sonke, J.E., Amouroux, D., 2015. Natural Hg isotopic composition of different Hg compounds in mammal tissues as a proxy for in vivo breakdown of toxic methylmercury. *Metallomics* 8, 170–178. <https://doi.org/10.1039/C5MT00286A>
- Perrot, V., Pastukhov, M. V, Epov, V.N., Husted, S., Donard, O.F.X., Amouroux, D., 2012. Higher Mass-Independent Isotope Fractionation of Methylmercury in the Pelagic Food Web of Lake Baikal (Russia). *Environ. Sci. Technol.* 46, 5902–5911. <https://doi.org/10.1021/es204572g>
- Perry, R.I., Thompson, P.A., Mackas, D.L., Harrison, P.J., Yelland, D.R., 1999. Stable carbon isotopes as pelagic food web tracers in adjacent shelf and slope regions off British Columbia, Canada. *Can. J. Fish. Aquat. Sci.* 56, 2477–

2486. <https://doi.org/10.1139/cjfas-56-12-2477>
- Peterson, B.J., Fry, B., 1987. Stable isotopes in Ecological studies. *Annu. Rev. Ecol. Syst.* 18, 293–320. <https://doi.org/10.1146/annurev.es.18.110187.001453>
- Peterson, S.H., Ackerman, J.T., Costa, D.P., 2016a. Mercury correlations among blood, muscle, and hair of northern elephant seals during the breeding and molting fasts. *Environ. Toxicol. Chem.* 35, 2103–2110. <https://doi.org/https://doi.org/10.1002/etc.3365>
- Peterson, S.H., Ackerman, J.T., Costa, D.P., 2015. Marine foraging ecology influences mercury bioaccumulation in deep-diving northern elephant seals. *Proc. R. Soc. B Biol. Sci.* 282. <https://doi.org/10.1098/rspb.2015.0710>
- Peterson, S.H., McHuron, E.A., Kennedy, S.N., Ackerman, J.T., Rea, L.D., Castellini, J.M., O’Hara, T.M., Costa, D.P., 2016b. Evaluating Hair as a Predictor of Blood Mercury: The Influence of Ontogenetic Phase and Life History in Pinnipeds. *Arch. Environ. Contam. Toxicol.* 70, 28–45. <https://doi.org/10.1007/s00244-015-0174-3>
- Petrik, C.M., Stock, C.A., Andersen, K.H., Daniël Van Denderen, P., Watson, J.R., 2020. Large Pelagic Fish Are Most Sensitive to Climate Change Despite Pelagification of Ocean Food Webs. *Front. Mar. Sci.* 7. <https://doi.org/10.3389/fmars.2020.588482>
- Petrova, M. V., 2020. Sources et processus qui gouvernent le cycle du mercure dans un contexte d’Océan Arctique changeant. University of Aix-Marseille.
- Petzke, K.J., Feist, T., Fleig, W.E., Metges, C.C., 2006. Nitrogen isotopic composition in hair protein is different in liver cirrhotic patients. *Rapid Commun. Mass Spectrom.* 20, 2973–2978. <https://doi.org/10.1002/rcm>
- Phillips, D.L., Inger, R., Bearhop, S., Jackson, A.L., Moore, J.W., Parnell, A.C., Semmens, B.X., Ward, E.J., 2014. Best practices for use of stable isotope mixing models in food web studies. *Can. J. Fish. Aquat. Sci.* 835, 823–835. <https://doi.org/10.1139/cjz-2014-0127>
- Pickhardt, P.C., Folt, C.L., Chen, C.Y., Klaue, B., Blum, J.D., 2018. Impacts of Zooplankton Composition and Algal Enrichment on the Accumulation of Mercury in an Experimental Freshwater Food Web Impacts of zooplankton composition and algal enrichment on the accumulation of mercury in an experimental freshwater food web. <https://doi.org/10.1016/j.scitotenv.2004.07.025>
- Pickhardt, P.C., Folt, C.L., Chen, C.Y., Klaue, B., Blum, J.D., 2002. Algal blooms reduce the uptake of toxic methylmercury in freshwater food webs 99, 4419–4423.
- Pinzone, M., Acquarone, M., Huyghebaert, L., Sturaro, N., Michel, L.N., Siebert, U., Das, K., 2017. Carbon, nitrogen and sulphur isotopic fractionation in captive juvenile hooded seal (*Cystophora cristata*): Application for diet analysis. *Rapid Commun. Mass Spectrom.* 31. <https://doi.org/10.1002/rcm.7955>
- Pinzone, M., Budzinski, H., Tasciotti, A., Ody, D., Lepoint, G., Schnitzler, J., Scholl, G., Thomé, J.-P.P., Tapie, N., Eppe, G., Das, K., 2015. POPs in free-ranging pilot whales, sperm whales and fin whales from the Mediterranean Sea: influence of biological and ecological factors. *Env. Res Submitted*, 185–196. <https://doi.org/10.1016/j.envres.2015.06.021>
- Pinzone, M., Cransveld, A., Tessier, E., Bérail, S., Schnitzler, J., Das, K., Amouroux, D., 2021a. Contamination levels and habitat use influence Hg stable isotopes and accumulation in the European seabass *Dicentrarchus labrax*. *Environ. Pollut.* 281. <https://doi.org/117008>
- Pinzone, M., Damseaux, F., Michel, L.N., Das, K., 2019. Stable isotope ratios of carbon, nitrogen and sulphur and mercury concentrations as descriptors of trophic ecology and contamination sources of Mediterranean whales.

- Chemosphere 237, 11 pp. <https://doi.org/10.1016/j.chemosphere.2019.124448>
- Pinzone, M., Nordøy, E.S., Eppe, G., Malherbe, C., Das, K., Collard, F., 2021b. First record of plastic debris in the stomach of a hooded seal pup from the Greenland Sea. *Mar. Pollut. Bull.* 167, 112350. <https://doi.org/10.1016/j.marpolbul.2021.112350>
- Pirrone, N., Cinnirella, S., Feng, X., Finkelman, R.B., Friedli, H.R., Leaner, J., Mason, R., Mukherjee, A.B., Stracher, G.B., Streets, D.G., Telmer, K., 2010. Global mercury emissions to the atmosphere from anthropogenic and natural sources. *Atmos. Chem. Phys.* 10, 5951–5964. <https://doi.org/10.5194/acp-10-5951-2010>
- Pirrone, N., Mason, R., 2009. Mercury fate and transport in the global atmosphere: Emissions, measurements and models, 1st ed, *Mercury Fate and Transport in the Global Atmosphere: Emissions, Measurements and Models*. Springer Science+Business Media, New York. <https://doi.org/10.1007/978-0-387-93958-2>
- Pizzochero, A.C., Michel, L.N., Chenery, S.R., McCarthy, I.D., Vianna, M., Malm, O., Lepoint, G., Das, K., Dorneles, P.R., 2018. Use of multielement stable isotope ratios to investigate ontogenetic movements of *Micropogonias furnieri* in a tropical Brazilian estuary. *Can. J. Fish. Aquat. Sci.* 75, 977–986. <https://doi.org/10.1139/cjfas-2017-0148>
- Podar, M., Gilmour, C.C., Brandt, C.C., Soren, A., Brown, S.D., Crable, B.R., Palumbo, A. V., Somenahally, A.C., Elias, D.A., 2015. Global prevalence and distribution of genes and microorganisms involved in mercury methylation. *Sci. Adv.* 1, 1–13. <https://doi.org/10.1126/sciadv.1500675>
- Point, D., Sonke, J.E., Day, R.D., Roseneau, D.G., Hobson, K.A., Pol, S.S. Vander, Moors, A.J., Pugh, R.S., Donard, O.F.X., Becker, P.R., 2011. Methylmercury photodegradation influenced by sea-ice cover in Arctic marine ecosystems. *Nat. Geosci.* 4, 188–194. <https://doi.org/10.1038/ngeo1049>
- Pollman, C.D., Engstrom, D.R., 2020. Legacy Mercury, in: Pollman, C.D., Axelrad, D.M., D.G., R. (Eds.), *Mercury and the Everglades. A Synthesis and Model for the Complex Ecosystem Restoration*. Springer, Cham, pp. 51–71. https://doi.org/10.1007/978-3-030-55635-8_3
- Polyakov, I. V., Pnyushkov, A. V., Alkire, M.B., Ashik, I.M., Baumann, T.M., Carmack, E.C., Goszczko, I., Guthrie, J., Ivanov, V. V., Kanzow, T., Krishfield, R., Kwok, R., Sundfjord, A., Morison, J., Rember, R., Yulin, A., 2017. Greater role for Atlantic inflows on sea-ice loss in the Eurasian Basin of the Arctic Ocean. *Science* (80-). 356, 285–291.
- Post, D.M., 2002. Using Stable Isotopes to Estimate Trophic Position: Models, Methods, and Assumptions. *Ecology* 83, 703. <https://doi.org/10.2307/3071875>
- Post, D.M., Layman, C.A., Arrington, D.A., Takimoto, G., Quattrochi, J., Montaña, C.G., 2007. Getting to the fat of the matter: models, methods and assumptions for dealing with lipids in stable isotope analyses. *Oecologia* 152, 179–89. <https://doi.org/10.1007/s00442-006-0630-x>
- Post, E., 2013. Ecological Consequences of sea-ice decline. *Science* (80-). 341, 519–524. <https://doi.org/10.1126/science.1235225>
- Potelev, V., Nilssen, K.T., Svetochev, V., Haug, T., 2014. Feeding habits of harp (*Phoca groenlandica*) and hooded seals (*Cystophora cristata*) during late winter, spring and early summer in the Greenland Sea. *NAMMCO Sci. Publ.* 2, 40. <https://doi.org/10.7557/3.2970>
- Poulain, A., Dastoor, A., Ryjkov, A., Subir, M., Semeniuk, K., Deeds, D., Ariya, P.A., Amyot, M., Kos, G., Toyota, K., Feinberg, A., 2015. Mercury Physicochemical and Biogeochemical Transformation in the Atmosphere and at

- Atmospheric Interfaces: A Review and Future Directions. *Chem. Rev.* 115, 3760–3802. <https://doi.org/10.1021/cr500667e>
- Pučko, M., Burt, A., Walkusz, W., Wang, F., Macdonald, R.W., Rysgaard, S., Barber, D.G., Tremblay, J.É., Stern, G.A., 2014. Transformation of mercury at the bottom of the arctic food web: An overlooked puzzle in the mercury exposure narrative. *Environ. Sci. Technol.* 48, 7280–7288. <https://doi.org/10.1021/es404851b>
- Qian, Y., Yin, X., Lin, H., Rao, B., Brooks, S.C., Liang, L., Gu, B., 2014. Why Dissolved Organic Matter Enhances Photodegradation of Methylmercury. <https://doi.org/10.1021/ez500254z>
- Ramette, A., 2007. Multivariate analyses in microbial ecology. *FEMS Microbiol. Ecol.* 62, 142–160. <https://doi.org/10.1111/j.1574-6941.2007.00375.x>
- Ramos, R., Gonzalez-Solis, J., 2012. Trace me if you can: the use of intrinsic biogeochemical markers in marine top predators. *Front. Ecol. Environ.* 10, 258–266.
- Reeves, R.R., 2014. Distribution, abundance and biology of ringed seals (*Phoca hispida*): an overview. *NAMMCO Sci. Publ.* 1, 9–45.
- Reitsema, L.J., 2013. Beyond diet reconstruction: Stable isotope applications to human physiology, health, and nutrition. *Am. J. Hum. Biol.* 25, 445–456. <https://doi.org/10.1002/ajhb.22398>
- Renedo, M., 2017. Sources and fate of methylmercury in the Southern Ocean: use of model seabirds and mercury stable isotopes. University of La Rochelle.
- Renedo, M., Amouroux, D., Albert, C., Bérail, S., Bråthen, V.S., Gavrilov, M., Grémillet, D., Helgason, H.H., Jakubas, D., Mosbech, A., Strøm, H., Tessier, E., Wojczulanis-Jakubas, K., Bustamante, P., Fort, J., 2020. Contrasting Spatial and Seasonal Trends of Methylmercury Exposure Pathways of Arctic Seabirds: Combination of Large-Scale Tracking and Stable Isotopic Approaches. *Environ. Sci. Technol.* 54, 13619–13629. <https://doi.org/10.1021/acs.est.0c03285>
- Renedo, M., Amouroux, D., Duval, B., Carravieri, A., Tessier, E., Barre, J., Bérail, S., Pedrero, Z., Cherel, Y., Bustamante, P., 2018. Seabird Tissues As Efficient Biomonitoring Tools for Hg Isotopic Investigations: Implications of Using Blood and Feathers from Chicks and Adults. *Environ. Sci. Technol.* 52, 4227–4234. <https://doi.org/10.1021/acs.est.8b00422>
- Renedo, M., Bustamante, P., Tessier, E., Pedrero, Z., Cherel, Y., Amouroux, D., 2017a. Assessment of mercury speciation in feathers using species-specific isotope dilution analysis. *Talanta* 174, 100–110. <https://doi.org/10.1016/j.talanta.2017.05.081>
- Renedo, M., Bustamante, P., Tessier, E., Pedrero, Z., Cherel, Y., Amouroux, D., 2017b. Assessment of mercury speciation in feathers using species-specific isotope dilution analysis. <https://doi.org/10.1016/j.talanta.2017.05.081>
- Renedo, M., Pedrero, Z., Amouroux, D., Cherel, Y., Bustamante, P., 2021. Mercury isotopes of key tissues document mercury metabolic processes in seabirds. *Chemosphere* 263, 127777. <https://doi.org/10.1016/j.chemosphere.2020.127777>
- Rice, K.M., Walker, E.M., Wu, M., Gillette, C., Blough, E.R., 2014. Environmental mercury and its toxic effects. *J. Am. Geriatr. Soc.* 47, 74–83. <https://doi.org/10.3961/jpmph.2014.47.2.74>
- Rigét, F., Braune, B., Bignert, A., Wilson, S., Aars, J., Born, E., Dam, M., Dietz, R., Evans, M., Evans, T., Gamberg, M., Gantner, N., Green, N., Gunnlaugsdóttir, H., Kannan, K., Letcher, R., Muir, D., Roach, P., Sonne, C., Stern, G., Wiig, Ø., 2011. Temporal trends of Hg in Arctic biota, an update. *Sci. Total Environ.* 409, 3520–3526.

- <https://doi.org/10.1016/j.scitotenv.2011.05.002>
- Rigét, F., Dietz, R., Hobson, K.A., 2012. Temporal trends of mercury in Greenland ringed seal populations in a warming climate. *J. Environ. Monit.* 14, 3249–3256. <https://doi.org/10.1039/c2em30687e>
- Rigét, F., Mosbech, A., Boertmann, D., Wegeberg, S., Merkel, F., Aastrup, P., Christensen, T., Ugarte, F., Hedeholm, R., Fritt-Rasmussen, J., 2019. The seas around greenland: An environmental status and future perspective, in: *World Seas: An Environmental Evaluation. Europe, the Americas and West Africa*. Academic Press, pp. 45–68. <https://doi.org/10.1016/B978-0-12-805068-2.00001-2>
- Rigét, F., Muir, D., Kwan, M., Savinova, T., Nyman, M., Woshner, V., O'Hara, T., 2005. Circumpolar pattern of mercury and cadmium in ringed seals. *Sci. Total Environ.* 351–352, 312–322. <https://doi.org/10.1016/j.scitotenv.2004.05.032>
- Robbins, C.T., Felicetti, L.A., Sponheimer, M., 2005. The effect of dietary protein quality on nitrogen isotope discrimination in mammals and birds. *Oecologia* 144, 534–540. <https://doi.org/10.1007/s00442-005-0021-8>
- Rodríguez-González, P., Epov, V.N., Bridou, R., Tessier, E., Guyoneaud, R., Monperrus, M., Amouroux, D., 2009. Species-Specific Stable Isotope Fractionation of Mercury during Hg(II) Methylation by an Anaerobic Bacteria (*Desulfobulbus propionicus*) under Dark Conditions. *Environ. Sci. Technol.* 43, 9183–9188. <https://doi.org/10.1021/es902206j>
- Rodríguez-González, P., Manuel Marchante-Gayón, J., Ignacio García Alonso, J.T., Sanz-Medel, A., 2005. Isotope dilution analysis for elemental speciation: A tutorial review. *Spectrochim. Acta Part B* 60, 151–207. <https://doi.org/10.1016/j.sab.2005.01.005>
- Ronald, K., Tessaro, S. V., Uthe, J.F., Freeman, H.C., Frank, R., 1977. Methylmercury poisoning in the harp seal (*Pagophilus groenlandicus*). *Sci. Total Environ.* 8, 1–11. [https://doi.org/https://doi.org/10.1016/0048-9697\(77\)90057-2](https://doi.org/https://doi.org/10.1016/0048-9697(77)90057-2)
- Rosati, G., Heimbürger, L.E., Melaku Canu, D., Lagane, C., Laffont, L., Rijkenberg, M.J.A., Gerringa, L.J.A., Solidoro, C., Gencarelli, C.N., Hedgecock, I.M., De Baar, H.J.W., Sonke, J.E., 2018. Mercury in the Black Sea: New Insights From Measurements and Numerical Modeling. *Global Biogeochem. Cycles* 32, 529–550. <https://doi.org/10.1002/2017GB005700>
- Rosing-Asvid, A., 2010. *Seals of Greenland*, 1st ed. Narayana Press, Gylling, Oqartussat, Greenland.
- Roth, J.D., Hobson, K.A., 2000. Stable carbon and nitrogen isotopic fractionation between diet and tissue of captive red fox: implications for dietary reconstruction. *Can. J. Zool.* 78, 848–852.
- Roth, J.D., Hobson, K.A., 1996. Stable carbon and nitrogen isotopic fractionation between diet and tissue of captive seals: implications for dietary reconstruction. *Can. J. Zool.* 78, 848–852. <https://doi.org/10.1139/z00-008>
- Routti, H., Atwood, T.C., Bechshoft, T., Boltunov, A., Ciesielski, T.M., Desforges, J.-P., Dietz, R., Gabrielsen, G.W., Jenssen, B.M., Letcher, R.J., McKinney, M.A., Morris, A.D., Rigét, F., Sonne, C., Styriehave, B., Tartu, S., 2019. State of knowledge on current exposure, fate and potential health effects of contaminants in polar bears from the circumpolar Arctic. *Sci. Total Environ.* 664, 1063–1083. <https://doi.org/10.1016/j.scitotenv.2019.02.030>
- Routti, H., Jenssen, B.M., Tartu, S., 2018. Ecotoxicologic stress in Arctic marine mammals, with particular focus on polar bears, *Marine Mammal Ecotoxicology: Impacts of Multiple Stressors on Population Health*. Elsevier Inc. <https://doi.org/10.1016/B978-0-12-812144-3.00013-9>
- Routti, H., Letcher, R.J., Born, E.W., Branigan, M., Dietz, R., Evans, T.J., Fisk, A.T., Peacock, E., Sonne, C., 2011.

- Spatial and temporal trends of selected trace elements in liver tissue from polar bears (*Ursus maritimus*) from Alaska, Canada and Greenland. *J. Environ. Monit.* 13, 2260–2267. <https://doi.org/10.1039/c1em10088b>
- Rudels, B., 2012. Arctic Ocean circulation and variability – Advection and external forcing encounter constraints and local processes. *Ocean Sci.* 8, 261–286. <https://doi.org/10.5194/os-8-261-2012>
- Rudels, B., 2009. Arctic Ocean Circulation, in: Steele, J.H., Thorpe, S.A., Turekian, K.K. (Eds.), *Encyclopedia of Ocean Sciences*. Academic Press, Boston, pp. 211–225.
- Ruiz-Cooley, R.I., Garcia, K.Y., Hetherington, E.D., 2011. Effects of lipid removal and preservatives on carbon and nitrogen stable isotope ratios of squid tissues: Implications for ecological studies. *J. Exp. Mar. Bio. Ecol.* 407, 101–107. <https://doi.org/https://doi.org/10.1016/j.jembe.2011.07.002>
- Ryan, C., Berrow, S.D., Mchugh, B., O'Donnell, C., Trueman, C.N., O'Connor, I., 2014. Prey preferences of sympatric fin (*Balaenoptera physalus*) and humpback (*Megaptera novaeangliae*) whales revealed by stable isotope mixing models. *Mar. Mammal Sci.* 30, 242–258. <https://doi.org/10.1111/mms.12034>
- Ryan, C., McHugh, B., CN, T., Sabin, R., Deaville, R., Harrod, C., SD, B., O'Connor, I., 2013. Stable isotope analysis of baleen reveals resource partitioning among sympatric rorquals and population structure in fin whales. *Mar. Ecol. Prog. Ser.* 479, 251–261. <https://doi.org/10.3354/meps10231>
- Savery, L.C., Evers, D.C., Wise, S.S., Falank, C., Wise, J., Gianios, C.J., Jerr, I., Thompson, W.D., Perkins, C., Zheng, T., Benedict, L., Wise, J.P.S., 2013. Global mercury and selenium concentrations in skin from free-ranging sperm whales (*Physeter macrocephalus*). *Sci Total Env.* 450, 59–71. <https://doi.org/10.1016/j.scitotenv.2013.01.070>
- Schaefer, J.K., Rocks, S.S., Zheng, W., Liang, L., Gu, B., Morel, F.M.M., 2011. Active transport, substrate specificity, and methylation of Hg(II) in anaerobic bacteria. *Proc. Natl. Acad. Sci. U. S. A.* 108, 8714–8719. <https://doi.org/10.1073/pnas.1105781108>
- Schaefer, K., Elshorbany, Y., Jafarov, E., Schuster, P.F., Striegl, R.G., Wickland, K.P., Sunderland, E.M., 2020. Potential impacts of mercury released from thawing permafrost. *Nat. Commun.* 11, 1–6. <https://doi.org/10.1038/s41467-020-18398-5>
- Schartup, A.T., 2016. Impacts of environmental change on methylmercury bioaccumulation in marine ecosystems, in: *Proceedings of the 18th International Conference on Heavy Metals in the Environment*. Ghent, Belgium.
- Schartup, A.T., Balcom, P.H., Soerensen, A.L., Gosnell, K.J., Calder, R.S.D., Mason, R.P., Sunderland, E.M., St. Louis, V.L., 2015a. Freshwater discharges drive high levels of methylmercury in Arctic marine biota. *Proc. Natl. Acad. Sci. U. S. A.* 112, 11789–11794. <https://doi.org/10.1073/pnas.1505541112>
- Schartup, A.T., Mason, R.P., Balcom, P.H., Hollweg, T.A., Chen, C.Y., 2013. Methylmercury production in estuarine sediments: Role of organic matter. *Environ. Sci. Technol.* 47, 695–700. <https://doi.org/10.1021/es302566w>
- Schartup, A.T., Ndu, U., Balcom, P.H., Mason, R.P., Sunderland, E.M., 2015b. Contrasting effects of marine and terrestrially derived dissolved organic matter on mercury speciation and bioavailability in seawater. *Environ. Sci. Technol.* 49, 5965–5972. <https://doi.org/10.1021/es506274x>
- Schartup, A.T., Qureshi, A., Dassuncao, C., Thackray, C.P., Harding, G., Sunderland, E.M., 2018. A Model for Methylmercury Uptake and Trophic Transfer by Marine Plankton. *Environ. Sci. Technol.* 52, 654–662. <https://doi.org/10.1021/acs.est.7b03821>
- Schartup, A.T., Soerensen, A.L., Heimbürger-Boavida, L.-E., 2020. Influence of the Arctic Sea-Ice Regime Shift on Sea-Ice Methylated Mercury Trends. *Environ. Sci. Technol. Lett.* 7, 708–713.

<https://doi.org/10.1021/acs.estlett.0c00465>

- Schartup, A.T., Thackray, C.P., Qureshi, A., Dassuncao, C., Gillespie, K., Hanke, A., Sunderland, E.M., 2019. Climate change and overfishing increase neurotoxicant in marine predators. *Nature* 572, 648–650. <https://doi.org/10.1038/s41586-019-1468-9>
- Schots, P.C., Bue, M.E., Nordøy, E.S., 2017. Hooded seal (*Cystophora cristata*) pups ingest snow and seawater during their post-weaning fast. *J. Comp. Physiol. B Biochem. Syst. Environ. Physiol.* 187, 493–502. <https://doi.org/10.1007/s00360-016-1048-3>
- Schuster, P.F., Schaefer, K.M., Aiken, G.R., Antweiler, R.C., Dewild, J.F., Gryziec, J.D., Gusmeroli, A., Hugelius, G., Jafarov, E., Krabbenhoft, D.P., Liu, L., Herman-Mercer, N., Mu, C., Roth, D.A., Schaefer, T., Striegl, R.G., Wickland, K.P., Zhang, T., 2018. Permafrost Stores a Globally Significant Amount of Mercury. *Geophys. Res. Lett.* 45, 1463–1471. <https://doi.org/10.1002/2017GL075571>
- Seifert, M., Hoppema, M., Burau, C., Elmer, C., Friedrichs, A., Geuer, J.K., John, U., Kanzow, T., Koch, B.P., Konrad, C., Van Der Jagt, H., Zielinski, O., 2019. Influence of Glacial Meltwater on Summer Biogeochemical Cycles in Scoresby Sund, East Greenland. *Front. Mar. Sci.* | www.frontiersin.org 1, 412. <https://doi.org/10.3389/fmars.2019.00412>
- Selin, N.E., 2009. Global Biogeochemical Cycling of Mercury: A Review. *Annu. Rev. Environ. Resour.* 34, 43–63. <https://doi.org/10.1146/annurev.environ.051308.084314>
- Senn, D.B., Chesney, E.J., Blum, J.D., Bank, M.S., Maage, A., Shine, J.P., 2010. Stable isotope (N, C, Hg) study of methylmercury sources and trophic transfer in the Northern Gulf of Mexico. *Environ. Sci. Technol.* 44, 1630–1637.
- Sharp, Z., 2007. *Principles of stable isotope geochemistry*, 2nd ed. Prentice Hall.
- Sherman, L.S., Blum, J.D., 2013. Mercury stable isotopes in sediments and largemouth bass from Florida lakes, USA. *Sci. Total Environ.* 448, 163–175. <https://doi.org/10.1016/j.scitotenv.2012.09.038>
- Sherman, L.S., Blum, J.D., Douglas, T.A., Steffen, A., 2012. Frost flowers growing in the Arctic ocean-atmosphere-sea ice-snow interface: 2. Mercury exchange between the atmosphere, snow, and frost flowers. *J. Geophys. Res. Atmos.* 117, 1–10. <https://doi.org/10.1029/2011JD016186>
- Sherman, L.S., Blum, J.D., Johnson, K.P., Keeler, G.J., Barres, J.A., Douglas, T.A., 2010. Mass-independent fractionation of mercury isotopes in Arctic snow driven by sunlight. *Nat. Geosci.* 3, 173–177. <https://doi.org/10.1038/ngeo758>
- Siegstad, H., Neve, P.B., Heide-Jørgensen, M.P., Härkönen, T., 2014. Diet of the ringed seal (*Phoca hispida*) in Greenland. *NAMMCO Sci. Publ.* 1, 229. <https://doi.org/10.7557/3.2991>
- Smith-Downey, N. V., Sunderland, E.M., Jacob, D.J., 2010. Anthropogenic impacts on global storage and emissions of mercury from terrestrial soils: Insights from a new global model. *J. Geophys. Res. Biogeosciences* 115. <https://doi.org/10.1029/2009JG001124>
- Smith, T.G., Armstrong, F.A.J., 1978. Mercury and Selenium in Ringed and Bearded Seal Tissues From Arctic Canada. *Arctic* 31. <https://doi.org/10.14430/arctic2643>
- Smylie, M.S., McDonough, C.J., Ann, L., Shervette, V.R., 2016. Mercury bioaccumulation in an estuarine predator: Biotic factors, abiotic factors, and assessments of fish health*. *Environ. Pollut.* 214, 169–176. <https://doi.org/10.1016/j.envpol.2016.04.007>

- Soerensen, A.L., Jacob, D.J., Schartup, A.T., Fisher, J.A., Lehnher, I., St Louis, V.L., Heimbürger, L.E., Sonke, J.E., Krabbenhoft, D.P., Sunderland, E.M., 2016a. A mass budget for mercury and methylmercury in the Arctic Ocean. *Global Biogeochem. Cycles* 30, 560–575. <https://doi.org/10.1002/2015GB005280>
- Soerensen, A.L., Schartup, A.T., Gustafsson, E., Gustafsson, B.G., Undeman, E., Björn, E., 2016b. Eutrophication Increases Phytoplankton Methylmercury Concentrations in a Coastal Sea - A Baltic Sea Case Study. *Environ. Sci. Technol.* 50, 11787–11796. <https://doi.org/10.1021/acs.est.6b02717>
- Soerensen, A.L., Schartup, A.T., Skrobonja, A., Björn, E., 2017. Organic matter drives high interannual variability in methylmercury concentrations in a subarctic coastal sea. *Environ. Pollut.* 229, 531–538. <https://doi.org/10.1016/j.envpol.2017.06.008>
- Sonne, C., Andersen-Ranberg, E., Rajala, E.L., Agerholm, J.S., Bonefeld-Jørgensen, E., Desforges, J.-P., Eulaers, I., Jenssen, B.M., Koch, A., Rosing-Asvid, A., Siebert, U., Tryland, M., Mulvad, G., Härkönen, T., Acquarone, M., Nordøy, E.S., Dietz, R., Magnusson, U., 2018. Seroprevalence for *Brucella* spp. in Baltic ringed seals (*Phoca hispida*) and East Greenland harp (*Pagophilus groenlandicus*) and hooded (*Cystophora cristata*) seals. *Vet. Immunol. Immunopathol.* 198, 14–18. <https://doi.org/10.1016/j.vetimm.2018.02.005>
- Sonne, C., Aspholm, O., Dietz, R., Andersen, S., Berntssen, M.H.G., Hylland, K., 2009a. A study of metal concentrations and metallothionein binding capacity in liver, kidney and brain tissues of three Arctic seal species. *Sci. Total Environ.* 407, 6166–6172. <https://doi.org/10.1016/j.scitotenv.2009.08.029>
- Sonne, C., Aspholm, O., Dietz, R., Andersen, S., Berntssen, M.H.G., Hylland, K., 2009b. A study of metal concentrations and metallothionein binding capacity in liver, kidney and brain tissues of three Arctic seal species. *Sci. Total Environ.* 407, 6166–6172. <https://doi.org/10.1016/j.scitotenv.2009.08.029>
- Sonne, C., Letcher, R.J., Jenssen, B.M., Desforges, J.-P., Eulaers, I., Andersen-Ranberg, E., Gustavson, K., Styriehave, B., Dietz, R., 2017. A veterinary perspective on One Health in the Arctic. *Acta Vet. Scand.* 59. <https://doi.org/10.1186/s13028-017-0353-5>
- Søreide, J.E., Hop, H., Carroll, M.L., Falk-Petersen, S., Hegseth, E.N., 2006. Seasonal food web structures and sympagic-pelagic coupling in the European Arctic revealed by stable isotopes and a two-source food web model. *Prog. Oceanogr.* 71, 59–87. <https://doi.org/10.1016/j.pocean.2006.06.001>
- Spiller, H.A., 2018. Rethinking mercury: the role of selenium in the pathophysiology of mercury toxicity. *Clin. Toxicol.* 56, 313–326. <https://doi.org/10.1080/15563650.2017.1400555>
- Steffen, A., Douglas, T., Amyot, M., Ariya, P., Aspmo, K., Berg, T., Bottenheim, J., Brooks, S., Cobbett, F., Dastoor, A., Dommergue, A., Ebinghaus, R., Ferrari, C., Gardfeldt, K., Goodsite, M.E., Lean, D., Poulain, A., Scherz, C., Skov, H., Sommar, J., Temme, C., 2007. A synthesis of atmospheric mercury depletion event chemistry linking atmosphere, snow and water, *Atmospheric Chemistry and Physics Discussions*. <https://doi.org/10.5194/acpd-7-10837-2007>
- Steiner, N.S., Bowman, J., Campbell, K., Chierici, M., Eronen-Rasimus, E., Falardeau, M., Flores, H., Fansson, A., Herr, H., Insley, S.J., Kauko, H.M., Lannuzel, D., Loseto, L., Lynnes, A., MAjewski, A., Meiners, K.M., Miller, L.A., Michel, L.N., Moreau, S., Nacke, M., Nomura, D., Tedesco, L., van Franeker, J.A., van Leeuwe, M.A., Wongpan, P., n.d. Climate Change Impacts on sea-ice ecosystems and associated ecosystem services. Submitted.
- Steiner, N.S., Cheung, W.W.L., Cisneros-Montemayor, A.M., Drost, H., Hayashida, H., Hoover, C., Lam, J., Sou, T., Sumaila, U.R., Suprenand, P., Tai, T.C., VanderZwaag, D.L., 2019. Impacts of the changing ocean-sea ice system

- on the key forage fish arctic cod (*Boreogadus saida*) and subsistence fisheries in the Western Canadian arctic-evaluating linked climate, ecosystem and economic (CEE) models. *Front. Mar. Sci.* 6. <https://doi.org/10.3389/fmars.2019.00179>
- Stenson, G., 2014. The Status of Harp and Hooded Seals in the North Atlantic 16.
- Stern, G.A., 2010. Mercury in Beluga, Narwhal and Walrus from the Canadian Arctic: status in 2010, in: *Synopsis of Research Conducted Under the 2009–2010 Northern Contaminants Program*. Indian and Northern Affairs Canada, pp. 126–134.
- Stern, G.A., Outridge, P.M., Wilson, S., Cole, A., Steffen, A., Macdonald, R.W., Zdanowicz, C., Hintelmann, H., Chételat, J., Wang, F., Loseto, L.L., 2011. How does climate change influence arctic mercury? *Sci. Total Environ.* 414, 22–42. <https://doi.org/10.1016/j.scitotenv.2011.10.039>
- Stevick, P.T., McConnell, B.J., Hammond, P.S., 2002. Patterns of movement, in: Hoelzel, A.R. (Ed.), *Marine Mammal Biology: An Evolutionary Approach*. Blackwell Scientific Publications, Oxford, pp. 185–216.
- Stewart, H.A., Jamieson, A.J., 2019. The five deeps: The location and depth of the deepest place in each of the world's oceans. *Earth-Science Rev.* 197. <https://doi.org/10.1016/j.earscirev.2019.102896>
- Stirling, I., Heide-Jørgensen, M.P., Lowry, L.F., Ferguson, S.H., Laidre, K.L., Wiig, Ø., 2008. Quantifying the Sensitivity of Arctic Marine Mammals To Climate-Induced Habitat Change. *Ecol. Appl.* 18, S97–S125. <https://doi.org/10.1890/06-0546.1>
- Stirling, I.A.N., Smith, T.G., 2004. Implications of Warm Temperatures and an Unusual Rain Event for the Survival of Ringed Seals on the Coast of Southeastern Baffin Island 57, 59–67.
- Stjern, C.W., Lund, M.T., Samset, B.H., Myhre, G., Forster, P.M., Andrews, T., Boucher, O., Faluvegi, G., Fläschner, D., Iversen, T., Kasoar, M., Kharin, V., Kirkevåg, A., Lamarque, J.-F., Olivie, D., Richardson, T., Sand, M., Shawki, D., Shindell, D., Smith, C.J., Takemura, T., Voulgarakis, A., 2019. Arctic Amplification Response to Individual Climate Drivers. *J. Geophys. Res. Atmos.* 124, 6698–6717. <https://doi.org/10.1029/2018JD029726>
- Storeheier, P. V., Nordøy, E.S., 2001. Physiological effects of seawater intake in adult harp seals during phase I of fasting. *Comp. Biochem. Physiol. - A Mol. Integr. Physiol.* 128, 307–315. [https://doi.org/10.1016/S1095-6433\(00\)00311-1](https://doi.org/10.1016/S1095-6433(00)00311-1)
- Sun, G., Sommar, J., Feng, X., Lin, C.-J., Ge, M., Wang, W., Yin, R., Fu, X., Shang, L., 2016. Mass-Dependent and -Independent Fractionation of Mercury Isotope during Gas-Phase Oxidation of Elemental Mercury Vapor by Atomic Cl and Br. *Environ. Sci. Technol.* 50, 9232–9241. <https://doi.org/10.1021/acs.est.6b01668>
- Sun, R., Jiskra, M., Amos, H.M., Zhang, Y., Sunderland, E.M., Sonke, J.E., 2019. Modelling the mercury stable isotope distribution of Earth surface reservoirs: Implications for global Hg cycling. *Geochim. Cosmochim. Acta* 246, 156–173. <https://doi.org/10.1016/j.gca.2018.11.036>
- Sunderland, E.M., Schartup, A.T., 2016. Biogeochemistry: Mercury methylation on ice. *Nat. Microbiol.* 1. <https://doi.org/10.1038/nmicrobiol.2016.165>
- Sundseth, K., Pacyna, J.M., Banel, A., Pacyna, E.G., Rautio, A., 2015. Climate change impacts on environmental and human exposure to mercury in the arctic. *Int. J. Environ. Res. Public Health* 12, 3579–3599. <https://doi.org/10.3390/ijerph120403579>
- Symon, C., 2011. Climate Change in the Arctic – A Hot Topic!
- Syväranta, J., Lensu, A., Marjomäki, T.J., Oksanen, S., Jones, R.I., 2013. An Empirical Evaluation of the Utility of

- Convex Hull and Standard Ellipse Areas for Assessing Population Niche Widths from Stable Isotope Data. *PLoS One* 8, 1–8. <https://doi.org/10.1371/journal.pone.0056094>
- Tagliabue, A., Bopp, L., 2008. Towards understanding global variability in ocean carbon‐13. *Glob. Biogeochem. Cycles* 22, 1025. <https://doi.org/10.1029/2007GB003037>
- Tai, C., Li, Y., Yin, Y., Scinto, L.J., Jiang, G., Cai, Y., 2014. Methylmercury Photodegradation in Surface Water of the Florida Everglades: Importance of Dissolved Organic Matter-Methylmercury Complexation. <https://doi.org/10.1021/es500316d>
- Tai, C., Wu, H., Li, Y., Yin, Y., Mao, Y., Cai, Y., Jiang, G., 2017. Photodegradation mechanism of methyl mercury in environmental waters. *Chinese Sci. Bull.* 62, 70–78. <https://doi.org/https://doi.org/10.1360/N972016-01011>
- Takaoka, S., Fujino, T., Kawakami, Y., Shigeoka, S., 2017. Prolonged and extensive health effects of methylmercury poisoning (Minamata disease) around the Shiranui sea. *J. Neurol. Sci.* 381, 376. <https://doi.org/10.1016/j.jns.2017.08.3276>
- Tedesco, L., Vichi, M., Scoccimarro, E., 2019. Sea-ice algal phenology in a warmer Arctic. *Sci. Adv.* 5, 12.
- Teilmann, J., Born, E.W., Acquarone, M., 1999. Behaviour of ringed seals tagged with satellite transmitters in the North Water polynya during fast-ice formation. *Can. J. Zool.* 77, 1934–1946. <https://doi.org/10.1139/cjz-77-12-1934>
- Teilmann, J., Kapel, F.O., 2014. Exploitation of ringed seals (*Phoca hispida*) in Greenland. *NAMMCO Sci. Publ.* 1, 130. <https://doi.org/10.7557/3.2984>
- ter Braak, C.J.F., 1994. Canonical community ordination. Part I: Basic theory and linear methods. *Cajo. Ecoscience* 1, 127–140.
- Thingstad, T.F., Bellerby, R.G.J., Bratbak, G., Børsheim, K.Y., Egge, J.K., Heldal, M., Larsen, A., Neill, C., Nejtgaard, J., Norland, S., Sandaa, R.-A., Skjoldal, E.F., Tanaka, T., Thyraug, R., Töpper, & B., 2008. Counterintuitive carbon-to-nutrient coupling in an Arctic pelagic ecosystem. *Nature* 455, 387–390. <https://doi.org/10.1038/nature07235>
- Tieszen, L.L., Boutton, T.W., Tesdahl, K.G., Slade, N.A., 1983. Fractionation and turnover of stable carbon isotopes in animal tissues: Implications for $\delta^{13}\text{C}$ analysis of diet. *Oecologia* 57, 32–37. <https://doi.org/10.1007/BF00379558>
- Tostevin, R., Turchyn, A. V., Farquhar, J., Johnston, D.T., Eldridge, D.L., Bishop, J.K.B., McIlvin, M., 2014. Multiple sulfur isotope constraints on the modern sulfur cycle. *Earth Planet. Sci. Lett.* 396, 14–21. <https://doi.org/10.1016/j.epsl.2014.03.057>
- Tremblay, J.É., Anderson, L.G., Matrai, P., Coupel, P., Bélangier, S., Michel, C., Reigstad, M., 2015. Global and regional drivers of nutrient supply, primary production and CO₂ drawdown in the changing Arctic Ocean. *Prog. Oceanogr.* 139, 171–196. <https://doi.org/10.1016/j.pocean.2015.08.009>
- Trishchenko, A.P., Luo, Y., 2021. Landfast Ice Mapping Using MODIS Clear-Sky Composites: Application for the Banks Island Coastline in Beaufort Sea and Comparison with Canadian Ice Service Data. *Can. J. Remote Sens.* 47, 143–158. <https://doi.org/10.1080/07038992.2021.1909466>
- Trueman, C.N., McGill, R.A.R., Guyard, P.H., 2005. The effect of growth rate on tissue-diet isotopic spacing in rapidly growing animals. An experimental study with Atlantic salmon (*Salmo salar*). *Rapid Commun. Mass Spectrom.* 19, 3239–3247. <https://doi.org/10.1002/rcm.2199>
- Trukhin, A.M., Simokon, M. V., 2018. Mercury in organs of Pacific walruses (*Odobenus rosmarus divergens*) from the Bering Sea. *Environ. Sci. Pollut. Res.* 25, 3360–3367. <https://doi.org/10.1007/s11356-017-0566-1>

- Trust, B.A., Fry, B., 1992. Stable sulphur isotopes in plants: a review. *Plant. Cell Environ.* 15, 1105–1110. <https://doi.org/10.1111/j.1365-3040.1992.tb01661.x>
- Tsui, M.T.K., Adams, E.M., Jackson, A.K., Evers, D.C., Blum, J.D., Balogh, S.J., 2018. Understanding sources of methylmercury in songbirds with stable mercury isotopes: Challenges and future directions. *Environ. Toxicol. Chem.* 37, 166–174. <https://doi.org/10.1002/etc.3941>
- Tsui, M.T.K., Blum, J.D., Kwon, S.Y., 2019. Review of stable mercury isotopes in ecology and biogeochemistry. *Sci. Total Environ.* 135386. <https://doi.org/10.1016/j.scitotenv.2019.135386>
- Tucker, S., Bowen, W.D., Iverson, S.J., Stenson, G.B., 2009. Intrinsic and extrinsic sources of variation in the diets of harp and hooded seals revealed by fatty acid profiles. *Can. J. Zool.* 87, 139–151. <https://doi.org/10.1139/Z08-145>
- Tucker, S., Stenson, G.B., Don Bowen, W., Iverson, S.J., 2013. Fueling phocids: Divergent exploitation of primary energy sources and parallel ontogenetic diet switches among three species of subarctic seals. *Mar. Mammal Sci.* 29, 428–447. <https://doi.org/10.1111/mms.12009>
- Tuerena, R., Hopkins, J., Ganeshram, R., Norman, L., de la Vega, C., Jeffreys, R., Mahaffey, C., 2020. Nitrate assimilation and regeneration in the Barents Sea: insights from nitrogen isotopes. *Biogeosciences Discuss.* 1–26. <https://doi.org/10.5194/bg-2020-293>
- UN Environment, 2017. Minamata Convention on Mercury - Text and Annexes [WWW Document]. United Nations Environ. <https://doi.org/10.5305/intelegamate.55.3.0582>
- UNECE, 2015. Model regulations on the transport of dangerous goods, 19th ed. United Nation Publication. <https://doi.org/10.18356/731c21b8-en>
- UNEP, 2018. Global Mercury Assessment 2018 270.
- UNEP, 2013. Global Mercury Assessment 2013: Sources, emissions, releases and environmental transport. United Nation Environment Programme Chemical Branch, Geneva, Switzerland.
- Vacque-Garcia, J., Lydersen, C., Biuw, M., Haug, T., Fedak, M.A., Kovacs, K.M., 2017. Hooded seal *Cystophora cristata* foraging areas in the Northeast Atlantic Ocean—Investigated using three complementary methods. *PLoS One* 12, 1–23. <https://doi.org/10.1371/journal.pone.0187889>
- Vancoppenolle, M., Meiners, K.M., Michel, C., Bopp, L., Brabant, F., Carnat, G., Delille, B., Lannuzel, D., Madec, G., Moreau, S., Tison, J., Merwe, P. Van Der, 2013. Role of sea ice in global biogeochemical cycles : emerging views and challenges.
- Vander Zanden, M.J., Clayton, M.K., Moody, E.K., Solomon, C.T., Weidel, B.C., 2015. Stable isotope turnover and half-life in animal tissues: A literature synthesis. *PLoS One* 10, 1–16. <https://doi.org/10.1371/journal.pone.0116182>
- Vanderklift, M.A., Ponsard, S., 2003. Sources of variation in consumer-diet $\delta^{15}\text{N}$ enrichment: A meta-analysis. *Oecologia* 136, 169–182. <https://doi.org/10.1007/s00442-003-1270-z>
- Vázquez-Medina, J.P., Zenteno-Savín, T., Elsner, R., 2007. Glutathione protection against dive-associated ischemia/reperfusion in ringed seal tissues. *J. Exp. Mar. Bio. Ecol.* 345, 110–118. <https://doi.org/10.1016/j.jembe.2007.02.003>
- Villar, E., Cabrol, L., Heimbürger-Boavida, L.E., 2020. Widespread microbial mercury methylation genes in the global ocean. *Environ. Microbiol. Rep.* 12, 277–287. <https://doi.org/10.1111/1758-2229.12829>
- Vost, E.E., Amyot, M., O'Driscoll, N.J., 2012. Photoreactions of mercury in aquatic systems, in: Liu, G., Cai, Y.,

- O'Driscoll, N. (Eds.), *Environmental Chemistry and Toxicology of Mercury*. John Wiley & Sons, Inc., Hoboken, New Jersey, pp. 193–218.
- Wagemann, R., Innes, S., Richard, P.R., 1996. Overview and regional and temporal differences of heavy metals in Arctic whales and ringed seals in the Canadian Arctic 186, 41–66.
- Wagemann, R., Stewart, R.E.A., Lockhart, W.L., Stewart, B.E., 1988. Trace metals and methyl-mercury: associations and transfer in harp seal (*Phoca groenlandica*) mothers and their pups. *Mar. Mammal Sci.* 4, 339–355.
- Wagemann, R., Trebacz, E., Boila, G., Lockhart, W.L., 1998. Methylmercury and total mercury in tissues of arctic marine mammals. *Sci. Total Environ.* 218, 19–31.
- Wang, F., MacDonald, R.W., Armstrong, D.A., Stern, G.A., 2012. Total and methylated mercury in the beaufort sea: The role of local and recent organic remineralization. *Environ. Sci. Technol.* 46, 11821–11828. <https://doi.org/10.1021/es302882d>
- Wang, K., Munson, K.M., Beaupré-Laperrière, A., Mucci, A., Macdonald, R.W., Wang, F., 2018. Subsurface seawater methylmercury maximum explains biotic mercury concentrations in the Canadian Arctic. *Sci. Rep.* 8, 1–5. <https://doi.org/10.1038/s41598-018-32760-0>
- Wang, R., Feng, X. Bin, Wang, W.X., 2013. In vivo mercury methylation and demethylation in freshwater tilapia quantified by mercury stable isotopes. *Environ. Sci. Technol.* 47, 7949–7957. <https://doi.org/10.1021/es3043774>
- Wang, S., McNamara, S.M., Moore, C.W., Obrist, D., Steffen, A., Shepson, P.B., Staebler, R.M., Raso, A.R.W., Pratt, K.A., 2019. Direct detection of atmospheric atomic bromine leading to mercury and ozone depletion. *Proc. Natl. Acad. Sci. U. S. A.* 116, 14479–14484. <https://doi.org/10.1073/pnas.1900613116>
- Wang, W.X., 2002. Interactions of trace metals and different marine food chains. *Mar. Ecol. Prog. Ser.* 243, 295–309. <https://doi.org/10.3354/meps243295>
- Wang, W.X., Tan, Q.G., 2019. Applications of dynamic models in predicting the bioaccumulation, transport and toxicity of trace metals in aquatic organisms. *Environ. Pollut.* 252, 1561–1573. <https://doi.org/10.1016/j.envpol.2019.06.043>
- Wang, X., Wang, W.X., 2017. Selenium induces the demethylation of mercury in marine fish. *Environ. Pollut.* 231, 1543–1551. <https://doi.org/10.1016/j.envpol.2017.09.014>
- Wang, Z., Chen, J., Feng, X., Hintelmann, H., Yuan, S., Cai, H., Huang, Q., Wang, S., Wang, F., 2015. Mass-dependent and mass-independent fractionation of mercury isotopes in precipitation from Guiyang, SW China. *Comptes Rendus - Geosci.* 347, 358–367. <https://doi.org/10.1016/j.crte.2015.02.006>
- Wassmann, P., Duarte, C.M., Agustí, S., Sejr, M.K., 2011. Footprints of climate change in the Arctic marine ecosystem. *Glob. Chang. Biol.* 17, 1235–1249. <https://doi.org/10.1111/j.1365-2486.2010.02311.x>
- Weihe, P., Grandjean, P., Jørgensen, P.J., 2005. Application of hair-mercury analysis to determine the impact of a seafood advisory. *Environ. Res.* 97, 201–208. <https://doi.org/10.1016/j.envres.2004.01.006>
- Weijts, L., Covaci, A., Yang, R.S.H., Das, K., Blust, R., 2011. A non-invasive approach to study lifetime exposure and bioaccumulation of PCBs in protected marine mammals: PBPK modeling in harbor porpoises. *Toxicol. Appl. Pharmacol.* 256, 136–145. <https://doi.org/10.1016/j.taap.2011.07.020>
- Werner, I., 2005. Seasonal dynamics, cryo-pelagic interactions and metabolic rates of arctic pack-ice and under-ice fauna - A review. *Polarforschung* 75, 1–19.
- Whalin, L., Kim, E., Mason, R., 2007. Factors influencing the oxidation, reduction, methylation and demethylation of

- mercury species in coastal waters 107, 278–294. <https://doi.org/10.1016/j.marchem.2007.04.002>
- WHO, 2015. Guidance on regulations for the Transport of Infectious Substances the Transport of Infectious Substances. WHO/HSE/GCR/2015.2.
- Wiederhold, J.G., 2015. Metal stable isotope signatures as tracers in environmental geochemistry. *Environ. Sci. Technol.* 49, 2606–2624. <https://doi.org/10.1021/es504683e>
- Wiederhold, J.G., Cramer, C.J., Daniel, K., Infante, I., Bourdon, B., Kretzschmar, R., 2010. Equilibrium Mercury Isotope Fractionation between Dissolved Hg(II) Species and Thiol-Bound Hg. *Environ. Sci. Technol.* 44, 4191–4197. <https://doi.org/10.1021/es100205t>
- Wiederhold, J.G., Skyllberg, U., Drott, A., Jiskra, M., Jonsson, S., Björn, E., Bourdon, B., Kretzschmar, R., 2015. Mercury Isotope Signatures in Contaminated Sediments as a Tracer for Local Industrial Pollution Sources. *Environ. Sci. Technol.* 49, 177–185. <https://doi.org/10.1021/es5044358>
- Wiig, Ø., 1985. Morphometric variation in the Hooded seal (*Cystophora cristata*). *J. Zool.* 206, 497–508. <https://doi.org/https://doi.org/10.1111/j.1469-7998.1985.tb03554.x>
- Włodarska-Kowalczyk, M., Aune, M., Michel, L.N., Zaborska, A., Legeżyńska, J., 2019. Is the trophic diversity of marine benthic consumers decoupled from taxonomic and functional trait diversity? Isotopic niches of Arctic communities. *Limnol. Oceanogr.* 64, 2140–2151. <https://doi.org/10.1002/lno.11174>
- Wolf, N., Carleton, S.A., Martínez del Rio, C., 2009a. Ten years of experimental animal isotopes ecology. *Funct. Ecol.* 23, 17–26. <https://doi.org/10.1111/j.1365-2435.2008.01529.x>
- Wolf, N., Carleton, S.A., Martínez Del Rio, C., 2009b. Ten years of experimental animal isotopic ecology. *Funct. Ecol.* 23, 17–26. <https://doi.org/10.1111/j.1365-2435.2008.01529.x>
- Woodgate, R., 2013. Arctic Ocean Circulation: Going Around At the Top Of the World. *Nat. Educ. Knowl.* 4, 8pp.
- Woodland, R.J., Rodríguez, M.A., Magnan, P., Glémet, H., Cabana, G., 2012. Incorporating temporally dynamic baselines in isotopic mixing models. *Ecology* 93, 131–144. <https://doi.org/10.1890/11-0505.1>
- Wu, P., Kainz, M.J., Bravo, A.G., Åkerblom, S., Sonesten, L., Bishop, K., 2019. The importance of bioconcentration into the pelagic food web base for methylmercury biomagnification: A meta-analysis. *Sci. Total Environ.* 646, 357–367. <https://doi.org/10.1016/j.scitotenv.2018.07.328>
- Yamakawa, A., Takeuchi, A., Shibata, Y., Berail, S., Donard, O.F.X., 2016. Determination of Hg isotopic compositions in certified reference material NIES No. 13 Human Hair by cold vapor generation multi-collector inductively coupled plasma mass spectrometry. *Accredit. Qual. Assur.* 21, 197–202. <https://doi.org/10.1007/s00769-016-1196-x>
- Yang, S., Liu, Y., 2016. Nuclear field shift effects on stable isotope fractionation: a review. *Acta Geochim.* 35, 227–239. <https://doi.org/10.1007/s11631-016-0109-3>
- Yee, S., Choi, B.H., 1996. Oxidative stress in neurotoxic effects of methylmercury poisoning. *Neurotoxicology* 17, 17–26.
- Yin, R., Feng, X., Li, X., Yu, B., Du, B., 2014. Trends and advances in mercury stable isotopes as a geochemical tracer. *Trends Environ. Anal. Chem.* 2, 1–10. <https://doi.org/10.1016/j.teac.2014.03.001>
- Yin, R., Feng, X., Shi, W., 2010. Applied Geochemistry Application of the stable-isotope system to the study of sources and fate of Hg in the environment: A review. *Appl. Geochemistry* 25, 1467–1477. <https://doi.org/10.1016/j.apgeochem.2010.07.007>

- Yorifuji, T., Tsuda, T., 2014. Minamata, in: *Encyclopedia of Toxicology: Third Edition*. Elsevier, pp. 340–344. <https://doi.org/10.1016/B978-0-12-386454-3.00038-5>
- Yoshida, M., 2002. Placental to fetal transfer of mercury and fetotoxicity. *Tohoku J. Exp. Med.* 196, 79–88. <https://doi.org/10.1620/tjem.196.79>
- Young, B.G., Loseto, L.L., Ferguson, S.H., 2010. Diet differences among age classes of Arctic seals: Evidence from stable isotope and mercury biomarkers. *Polar Biol.* 33, 153–162. <https://doi.org/10.1007/s00300-009-0693-3>
- Yu, B., Fu, X., Yin, R., Zhang, H., Wang, X., Lin, C.J., Wu, C., Zhang, Y., He, N., Fu, P., Wang, Z., Shang, L., Sommar, J., Sonke, J.E., Maurice, L., Guinot, B., Feng, X., 2016. Isotopic composition of atmospheric mercury in China: New evidence for sources and transformation processes in air and in vegetation. *Environ. Sci. Technol.* 50, 9362–9369. <https://doi.org/10.1021/acs.est.6b01782>
- Yu, Y., Stern, H., Fowler, C., Fetterer, F., Maslanik, J., 2014. Interannual variability of arctic landfast ice between 1976 and 2007. *J. Clim.* 27, 227–243. <https://doi.org/10.1175/JCLI-D-13-00178.1>
- Yunda-Guarin, G., Brown, T.A., Michel, L.N., Saint-Béat, B., Amiriaux, R., Nozais, C., Archambault, P., 2020. Reliance of deep-sea benthic macrofauna on ice-derived organic matter highlighted by multiple trophic markers during spring in Baffin Bay, Canadian Arctic. *Elem. Sci. Anthr.* 8, 1–18. <https://doi.org/10.1525/elementa.2020.047>
- Yurkowski, D.J., Richardson, E.S., Lunn, N.J., Muir, D.C.G., Johnson, A.C., Derocher, A.E., Ehrman, A.D., Houde, M., Young, B.G., Debets, C.D., Sciallo, L., Thiemann, G.W., Ferguson, S.H., 2020. Contrasting Temporal Patterns of Mercury, Niche Dynamics, and Body Fat Indices of Polar Bears and Ringed Seals in a Melting Icescape. *Environ. Sci. Technol.* 54, 2780–2789. <https://doi.org/10.1021/acs.est.9b06656>
- Zalups, R.K., 2000. Molecular interactions with mercury in the kidney. *Pharmacol. Rev.* 52, 113–143.
- Zanden, M.J. Vander, Rasmussen, J.B., 2001. Variation in $\delta^{15}\text{N}$ and $\delta^{13}\text{C}$ trophic fractionation: Implications for aquatic food web studies. *Limnol. Oceanogr.* 46, 2061–2066. <https://doi.org/10.4319/lo.2001.46.8.2061>
- Zhang, T., Hsu-kim, H., 2010. Photolytic degradation of methylmercury enhanced by binding to natural organic ligands. *Nat. Geosci.* 3, 473–476. <https://doi.org/10.1038/ngeo892>. Photolytic
- Zhang, Y., Soerensen, A.L., Schartup, A.T., Sunderland, E.M., 2019. A global model for methylmercury formation and uptake at the base of marine food webs. *Global Biogeochem. Cycles* in Press., 1–44. <https://doi.org/10.1029/2019GB006348>
- Zhao, H.-L., Zhu, X., Sui, Y., 2006. The short-lived Chinese emperors. *J. Am. Geriatr. Soc.* <https://doi.org/10.1111/j.1532-5415.2006.00821.x>
- Zheng, W., Demers, J.D., Lu, X., Bergquist, B.A., Anbar, A.D., Blum, J.D., Gu, B., 2019. Mercury Stable Isotope Fractionation during Abiotic Dark Oxidation in the Presence of Thiols and Natural Organic Matter. *Environ. Sci. Technol.* 53, 1853–1862. <https://doi.org/10.1021/acs.est.8b05047>
- Zheng, W., Gilleaudeau, G.J., Kah, L.C., Anbar, A.D., 2018. Mercury isotope signatures record photic zone euxinia in the Mesoproterozoic ocean. *Proc. Natl. Acad. Sci. U. S. A.* 115, 10594–10599. <https://doi.org/10.1073/pnas.1721733115>
- Zheng, W., Hintelmann, H., 2010. Isotope Fractionation of Mercury during Its Photochemical Reduction by Low-Molecular-Weight Organic Compounds. *J. Phys. Chem. A* 114, 4246–4253. <https://doi.org/10.1021/jp9111348>
- Zheng, W., Hintelmann, H., 2009. Mercury isotope fractionation during photoreduction in natural water is controlled by its Hg/DOC ratio. *Geochim. Cosmochim. Acta* 73, 6704–6715. <https://doi.org/10.1016/j.gca.2009.08.016>

Zhou, J., Smith, M.D., Cooper, S.J., Cheng, X., Smith, J.C., Parks, J.M., 2017. Modeling of the Passive Permeation of Mercury and Methylmercury Complexes Through a Bacterial Cytoplasmic Membrane. *Environ. Sci. Technol.* 51, 10595–10604. <https://doi.org/10.1021/acs.est.7b02204>

ANNEX

ANNEX to Chapter 1

1. BIOTIC DEMETHYLATION PROCESSES

Reductive demethylation is carried out by bacteria possessing the *mer* operon, occurring mostly in the aerobic zone (Boyd and Barkay, 2012; Du et al., 2019). It seems to be a direct method for Hg detoxification. The *mer* operon includes genes that encode several proteins responsive to Hg^{2+} or MMHg: (1) an activator/repressor (*MerR*), (2) a periplasmic scavenging protein (*MerP*) responsive to Hg^{2+} , (3) transport proteins to shuttle Hg^{2+} (*MerT*, *MerC*, *MerF*, *MerG*) or (4) MMHg (*MerE*) into bacterial cytoplasm, (5) mercuric reductase (*MerA*) to reduce Hg^{2+} to Hg^0 , and (6) organomercury-lyase (*MerB*) to de-methylate MMHg to Hg^{2+} (Brown et al. 2003; Busenlehner et al. 2003; Boyd and Barkay 2012). Briefly, this process consists on a first demethylation of MeHg by an enzyme (*merB*, organomercurial lyase) resulting in Hg^{2+} that is then degraded inside the bacterial cell by another enzyme (*merA*) and then evacuated from the cell as Hg^0 (Boyd and Barkay, 2012). The ensemble of the *mer* system is represented in Figure A1.1.

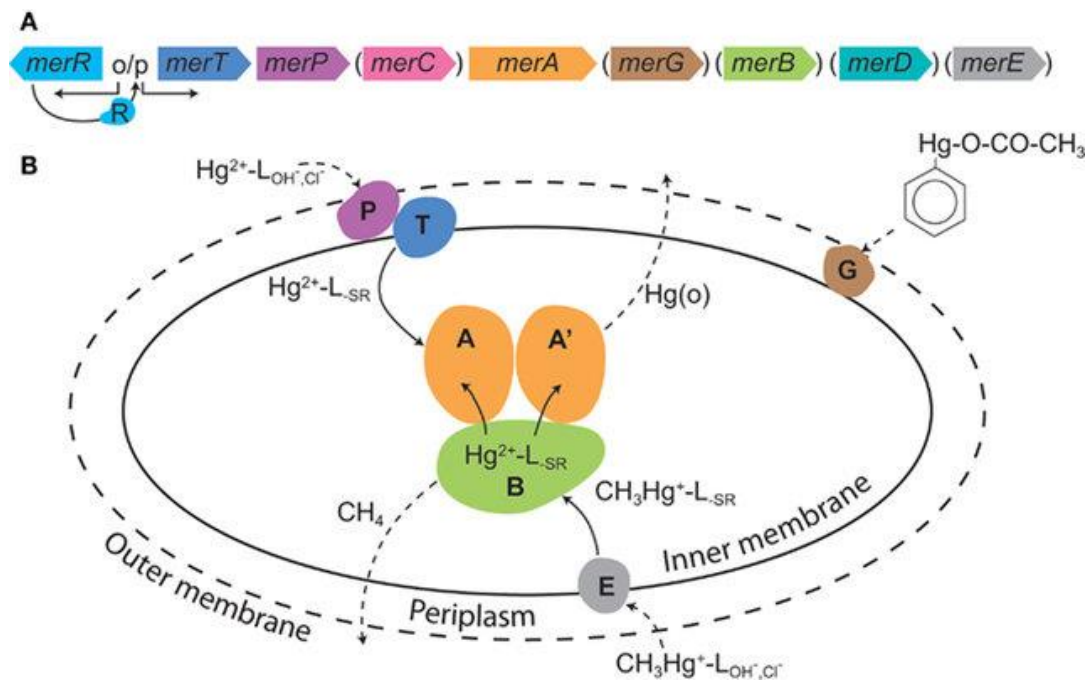
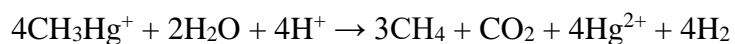
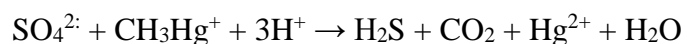


Figure A1.1. The *mer* system. **(A)** A generic *mer* operon with genes. Parentheses depict genes that are only rarely present in operons. **(B)** The cellular *mer*-encoded mercury detoxification mechanism. The outer cell wall is depicted by a broken line illustrating that not all microbes have an outer membrane; broken line arrows depict diffusion; solid line arrows indicate transport or transformations; L = ligand with subscripts denoting the ligand type. The colors of various *Mer* proteins correspond with the colors of the genes that encode for these proteins in (A). Reproduced from (Boyd and Barkay, 2012).

Oxidative demethylation instead is mostly operated by anaerobic bacteria in anoxic conditions (Lu et al., 2016). This process is still poorly understood but it possibly occurs as a by-product of bacterial metabolism (Marvin-Dipasquale et al., 2000). In methanogens Hg demethylation supposedly occurs during consumption of monomethylamines:



Whereas in SRB, MMHg is degraded by pathways related to acetate oxidation:



In contrast to reductive demethylation, catalyzed by the enzymatic system encoded by the operon *mer*, the oxidative demethylation does not appear to be a process for MeHg detoxification (Marvin-Dipasquale et al., 2000). Experimental studies have indicated that most part of methylating SRB are also capable of demethylating MeHg, however not all the bacteria that demethylate do necessarily methylate (Bridou et al., 2011). As well as for methylation, demethylation rates appear to be largely influenced by environmental parameters such as pH, redox conditions and salinity. However, while biological methylation is supposedly controlled by the bioavailability of Hg^{2+} , demethylation seems to not depend on environmental pollution levels (Bridou et al., 2011).

ANNEX to Chapter 2

TABLES

Table A2.1. Dry weight / Wet Weight (DW / WW) ratio and water content percentage (%) for hooded, harp and ringed seals from the Greenland Sea. Values are represented as mean \pm standard deviation (*n*) and were used to transform THg concentrations from dw to ww for those animals whose water content was not possible to measure.

Tissue	Species					
	Hooded seal		Harp seal		Ringed seal	
	DW / WW Ratio	Water content (%)	DW / WW Ratio	Water content (%)	DW / WW Ratio	Water content (%)
Muscle	3.4 \pm 0.5 (135)	70.5 \pm 2.9 (135)	3.6 \pm 0.2 (23)	71.9 \pm 2.0 (23)	3.1 \pm 0.5 (123)	67.8 \pm 6.7 (123)
Liver	3.2 \pm 0.4 (125)	68.1 \pm 4.0 (125)	3.4 \pm 0.2 (23)	70.6 \pm 2.2 (23)	3.2 \pm 1.8 (123)	66.7 \pm 4.3 (123)
Hair	Only DW	Only DW	Only DW	Only DW	Only DW	Only DW
Kidney	4.4 \pm 0.3 (14)	77.1 \pm 1.7 (14)	4.5 \pm 0.2 (23)	77.9 \pm 2.1 (23)	-	-
whole blood	3.6 \pm 0.3 (12)	72.2 \pm 2.0 (12)	4.2 \pm 0.4 (23)	75.8 \pm 2.3 (23)	-	-
Red Blood Cells	3.0 \pm 0.1 (6)	67.0 \pm 1.7 (6)	3.4 \pm 0.6 (14)	70.3 \pm 3.8 (14)	-	-
Heart	4.4 \pm 0.2 (12)	77.1 \pm 1.1 (12)	4.7 \pm 0.3 (23)	78.6 \pm 2.4 (23)	-	-
Lung	4.4 \pm 0.5 (14)	77.1 \pm 2.5 (14)	4.7 \pm 0.5 (23)	78.6 \pm 2.4 (23)	-	-
Brain	4.9 \pm 0.6 (12)	79.3 \pm 2.4 (12)	4.9 \pm 0.7 (21)	79.1 \pm 3.2 (21)	-	-
Spleen	4.2 \pm 0.2 (12)	76.2 \pm 1.0 (12)	4.1 \pm 0.3 (23)	75.7 \pm 2.5 (23)	-	-
Mammalian Gland	2.5 \pm 0.1 (3)	59.9 \pm 1.6 (3)	2.8 \pm 0.5 (8)	62.3 \pm 1.0 (8)	-	-
Umbilical cord	5.2 \pm 0.7 (3)	80.6 \pm 2.8 (3)	4.2 \pm 1.3 (5)	74.3 \pm 7.6 (5)	-	-
Gonads	4.7 \pm 0.4 (4)	78.7 \pm 1.7 (4)	6.3 \pm 1.0 (7)	83.6 \pm 27 (7)	-	-
Milk	Only WW	Only WW	Only WW	Only WW	Only WW	Only WW

Table A2.2. Measured $\delta^{13}\text{C}$, $\delta^{15}\text{N}$, $\delta^{34}\text{S}$ and C/N ratio of the primary and secondary standards analysed in this work. As = sulfanilic acid, Repl = seabass muscle, C6 = IAEA-C6, N1 = IAEA-N1, S1 = IAEA-S1. AVG = Average, SD = Standard Deviation.

Batch name and content	C/N	$\delta^{15}\text{N}$	$\delta^{13}\text{C}$	$\delta^{34}\text{S}$	
Liz 1 Muscle	As AVG	4.92	As AVG -0.26	As AVG -25.42	As AVG 6.19
	As SD	0.09	As SD 0.49	As SD 0.06	As SD 0.16
	Repl AVG	3.18	N1 AVG 0.40	C6 AVG -10.45	S1 AVG -0.82
	Repl SD	0.00	N1 SD 0.26	C6 SD 0.00	S1 SD 0.34
			Repl AVG 13.98	Repl AVG -19.13	Repl AVG 12.57
			Repl SD 0.27	Repl SD 0.06	Repl SD 0.15
Liz 2 Muscle	AS AVG	5.09	AS AVG -0.26	AS AVG -25.91	AS AVG 6.70
	AS SD	0.11	AS SD 0.19	AS SD 0.04	AS SD 0.34
	Repl AVG	3.19	Repl AVG 13.87	Repl AVG -19.44	Repl AVG 13.89
	Repl SD	0.01	Repl SD 0.04	Repl SD 0.06	Repl SD 0.38
			N1 AVG 0.39	C6 AVG -10.91	S1 AVG -0.11
			N1 SD 0.02	C6 SD 0.15	S1 SD 0.19
Liz 3 Muscle	AS AVG	4.95	AS AVG -0.36	AS AVG -26.03	AS AVG 6.61
	AS SD	0.14	AS SD 0.17	AS SD 0.04	AS SD 0.00
	Repl AVG	3.18	Repl AVG 13.81	Repl AVG -19.58	Repl AVG 14.04
	Repl SD	0.00	Repl SD 0.14	Repl SD 0.09	Repl SD 0.47
			N1 AVG 0.40	C6 AVG -10.94	S1 AVG -0.05
			N1 SD 0.00	C6 SD 0.04	S1 SD 0.19
Liz 4 Hair	AS AVG	5.02	AS AVG -0.17	AS AVG -25.93	AS AVG 6.35
	AS SD	0.12	AS SD 0.28	AS SD 0.04	AS SD 0.10
	Repl AVG	3.19	Repl AVG 14.08	Repl AVG -19.52	Repl AVG 13.85
	Repl SD	0.01	Repl SD 0.08	Repl SD 0.02	Repl SD 0.18
			N1 AVG 0.47	C6 AVG -10.85	S1 AVG -0.30
			N1 SD 0.10	C6 SD 0.01	S1 SD 0.00
Liz 5 Hair	AS AVG	5.09	AS AVG -0.36	AS AVG -26.05	AS AVG 5.92
	AS SD	0.07	AS SD 0.23	AS SD 0.07	AS SD 0.13
	Repl AVG	3.21	Repl AVG 13.72	Repl AVG -19.66	Repl AVG 13.43
	Repl SD	0.00	Repl SD 0.02	Repl SD 0.02	Repl SD 0.23
			N1 AVG 0.19	C6 AVG -11.01	S1 AVG -0.81
			N1 SD 0.08	C6 SD 0.07	S1 SD 0.33
Liz 6 Muscle	AS AVG	4.97	AS AVG -0.12	AS AVG -25.88	AS AVG 6.45
	AS SD	0.09	AS SD 0.17	AS SD 0.04	AS SD 0.09
	Repl AVG	3.19	Repl AVG 13.85	Repl AVG -19.48	Repl AVG 13.88
	Repl SD	0.01	Repl SD 0.08	Repl SD 0.05	Repl SD 0.20
			N1 AVG 0.43	C6 AVG -10.76	S1 AVG -0.41
			N1 SD 0.02	C6 SD 0.04	S1 SD 0.19
Liz 7 Hair	AS AVG	5.05	AS AVG -0.25	AS AVG -25.98	AS AVG 6.77
	AS SD	0.16	AS SD 0.30	AS SD 0.04	AS SD 0.10
	Repl AVG	3.19	Repl AVG 13.89	Repl AVG -19.58	Repl AVG 13.89
	Repl SD	0.00	Repl AS 0.06	Repl SD 0.04	Repl SD 0.27
			N1 AVG 0.30	C6 AVG -10.83	S1 AVG -0.27
			N1 SD 0.14	C6 SD 0.02	S1 SD 0.14
Liz 8 Muscle	AS AVG	5.09	AS AVG 0.15	AS AVG -25.86	AS AVG 6.76
	AS SD	0.10	AS SD 0.44	AS SD 0.11	AS SD 0.05

	Repl AVG	3.19	Repl AVG	12.77	Repl AVG	-19.52	Repl AVG	13.79
	Repl SD	0.00	Repl SD	0.09	Repl SD	0.08	Repl SD	0.41
			N1 AVG	0.40	C6 AVG	-10.83	S1 AVG	0.11
			N1 SD	0.00	C6 SD	0.04	S1 SD	0.27
Liz 9 Muscle Hair	AS AVG	4.99	AS AVG	-0.82	AS AVG	-28.35	AS AVG	-1.34
	AS SD	0.09	AS SD	0.25	AS SD	0.08	AS SD	0.16
	Repl AVG	3.18	Repl AVG	13.39	Repl AVG	-19.37	Repl AVG	12.69
	Repl Sd	0.02	Repl SD	0.12	Repl SD	0.07	Repl SD	0.98
			N1 AVG	0.49	C6 AVG	-10.73	S1 AVG	-0.16
			N1 SD	0.12	C6 SD	0.05	S1 SD	0.24
Alexis 1 Muscle	AS AVG	5.00	AS AVG	-0.71	AS AVG	-25.67	AS AVG	5.85
	AS SD	0.14	AS SD	1.47	AS SD	0.26	AS SD	0.39
	Repl AVG	3.64	Repl AVG	15.67	Repl AVG	-19.95	Repl AVG	18.28
	Repl SD	0.01	Repl SD	-	Repl SD	0.12	Repl SD	0.69
			N1 AVG	0.40	C6 AVG	-10.55	S1 AVG	0.84
			N1 SD	-	C6 SD	0.36	S1 SD	0.06
Alexis 2 Muscle	AS AVG	5.06	AS AVG	-0.90	AS AVG	-25.70	AS AVG	4.51
	AS SD	0.11	AS SD	0.96	AS SD	0.22	AS SD	0.33
	Repl AVG	3.32	Repl AVG	13.56	Repl AVG	-20.73	Repl AVG	19.37
	Repl Sd	0.01	Repl SD	0.13	Repl SD	0.08	Repl SD	0.52
			N1 AVG	0.32	C6 AVG	-10.85	S1 AVG	-0.27
			N1 SD	0.11	C6 SD	0.06	S1 SD	0.16
Alexis 3 Muscle	AS AVG	4.53	AS AVG	-1.78	AS AVG	-25.77	AS AVG	5.00
	AS SD	0.07	AS SD	0.43	AS SD	0.12	AS SD	0.35
	Repl AVG	3.40	Repl AVG	12.45	Repl AVG	-20.07	Repl AVG	18.77
	Repl SD	0.01	Repl SD	0.15	Repl SD	0.07	Repl SD	0.72
			N1 AVG	0.33	C6 AVG	-10.76	S1 AVG	-0.38
			N1 SD	0.09	C6 SD	0.05	S1 SD	0.10
Alexis 4 Hair	AS AVG	5.04	AS AVG	-1.23	AS AVG	-25.75	AS AVG	5.75
	AS SD	0.10	AS SD	0.56	AS SD	0.14	AS SD	0.52
	Repl AVG	3.17	Repl AVG	14.64	Repl AVG	-19.77	Repl AVG	13.84
	Repl Sd	0.01	Repl SD	0.04	Repl SD	0.07	Repl SD	0.34
			N1 AVG	0.49	C6 AVG	-10.81	S1 AVG	1.10
			N1 SD	0.12	C6 SD	0.02	S1 SD	0.21
Alexis 5 Hair	AS AVG	NA	AS AVG	-0.62	AS AVG	-25.56	AS AVG	5.19
	AS SD	NA	AS SD	0.11	AS SD	0.17	AS SD	0.40
	Repl AVG	NA	Repl AVG	14.38	Repl AVG	-	Repl AVG	13.51
	Repl SD	NA	Repl SD	0.20	Repl SD	-	Repl SD	0.42
			N1 AVG	0.40	C6 AVG	-10.86	S1 AVG	-0.40
			N1 SD	0.00	C6 SD	0.09	S1 SD	0.17
Alexis 6 Hair	AS AVG	NA	AS AVG	-0.59	AS AVG	-25.70	AS AVG	-
	AS SD	NA	AS SD	0.31	AS SD	0.07	AS SD	-
	Repl AVG	NA	Repl AVG	14.22	Repl AVG	-19.79	Repl AVG	13.57
	Repl Sd	NA	Repl SD	0.10	Repl SD	0.21	Repl SD	1.30
			N1 AVG	0.40	C6 AVG	-10.78	S1 AVG	-0.35
			N1 SD	0.01	C6 SD	0.04	S1 SD	0.11
	AS AVG	5.18	AS AVG	-0.49	AS AVG	-25.96	AS AVG	5.36

Alexis 7 Hair	AS SD	0.13	AS SD	0.25	AS SD	0.21	AS SD	0.36
	Repl AVG	3.18	Repl AVG	13.78	Repl AVG	-19.70	Repl AVG	13.03
	Repl SD	0.01	Repl SD	0.10	Repl SD	0.14	Repl SD	0.41
			N1 AVG	0.29	C6 AVG	-10.72	S1 AVG	-0.31
			N1 SD	0.16	C6 SD	0.11	S1 SD	0.03
Mar 1 Muscle RBC	AS AVG	5.22	AS AVG	-0.53	AS AVG	-25.35	AS AVG	5.62
	AS SD	0.14	AS SD	0.30	AS SD	0.39	AS SD	0.41
	Repl AVG	3.25	Repl AVG	13.84	Repl AVG	-19.56	Repl AVG	12.97
	Repl Sd	0.01	Repl SD	0.17	Repl SD	0.08	Repl SD	0.23
			N1 AVG	0.40	C6 AVG	-10.80	S1 AVG	-0.75
Mar 2 RBC Whole blood Lung	AS AVG	4.86	AS AVG	-0.28	AS AVG	-25.78	AS AVG	5.84
	AS SD	0.08	AS SD	0.38	AS SD	0.13	AS SD	0.12
	Repl AVG	3.17	Repl AVG	14.20	Repl AVG	-19.77	Repl AVG	13.65
	Repl SD	0.01	Repl SD	0.07	Repl SD	0.04	Repl SD	0.96
			N1 AVG	0.48	C6 AVG	-10.80	S1 AVG	0.41
Mar 3 Lung Kidney	AS AVG	5.13	AS AVG	-0.62	AS AVG	-25.69	AS AVG	6.01
	AS SD	0.16	AS SD	0.23	AS SD	0.18	AS SD	0.38
	Repl AVG	3.18	Repl AVG	14.01	Repl AVG	-19.64	Repl AVG	13.74
	Repl Sd	0.01	Repl SD	0.09	Repl SD	0.02	Repl SD	0.14
			N1 AVG	0.39	C6 AVG	-10.69	S1 AVG	0.54
Mar 4 Kidney Liver	AS AVG	5.07	AS AVG	-0.45	AS AVG	-25.81	AS AVG	5.96
	AS SD	0.06	AS SD	0.15	AS SD	0.09	AS SD	0.18
	Repl AVG	3.19	Repl AVG	14.07	Repl AVG	-19.41	Repl AVG	13.59
	Repl SD	0.00	Repl SD	0.06	Repl SD	0.35	Repl SD	0.32
			N1 AVG	0.37	C6 AVG	-10.76	S1 AVG	0.27
Mar 5 Lanugo Hair	AS AVG	5.12	AS AVG	-0.31	AS AVG	-25.81	AS AVG	5.91
	AS SD	0.12	AS SD	0.31	AS SD	0.11	AS SD	0.25
	Repl AVG	3.19	Repl AVG	14.22	Repl AVG	-19.63	Repl AVG	13.58
	Repl Sd	0.01	Repl SD	0.06	Repl SD	0.28	Repl SD	0.51
			N1 AVG	0.47	C6 AVG	-10.81	S1 AVG	0.17
		N1 SD	0.10	C6 SD	0.01	S1 SD	0.59	
All	C/N		δ15N		δ13C		δ34S	
	AS AVG	5.02	AS AVG	-0.52	AS AVG	-25.78	AS AVG	5.93
	AS SD	0.15	AS SD	0.42	AS SD	0.19	AS SD	0.62
	Repl AVG	3.23	Repl AVG	13.90	Repl AVG	-19.56	Repl AVG	13.53
	Repl SD	0.02	Repl SD	0.40	Repl SD	0.17	Repl SD	0.43
	STD AVG	-	STD AVG	0.39	STD AVG	-10.78	STD AVG	-0.09
		STD SD	0.07	STD SD	0.12	STD SD	0.51	

ANNEX to Chapter 4

1. SELECTION OF THE BEST TISSUE FOR HG STABLE ISOTOPES ANALYSIS

As we observed in [chapter 4](#), true seals tissues exhibit specific concentrations and proportions of Hg species (Mieiro et al., 2011; Pentreath, 1976), depending on several factors: tissue composition (proteins, lipids, carbohydrates), turnover rate, and food regime (Jardine et al., 2006; Maury-Brachet et al., 2006; Perga and Gerdeaux, 2005; Wang and Wong, 2003). Our findings confirm that in hooded seals this is equally valid for the analysis of Hg stable isotopes. For this reason, a multi-tissue approach might be the necessary approach in the assessment of Hg stable isotopes in a single organism, in order to get at the same time the information about Hg sources (Jardine et al., 2006; Tsui et al., 2019), internal processing (Kwon et al., 2016, 2012) and animal trophic ecology (Pinzone et al., 2021a). When such approach is not possible, few points should be considered for the selection of the right tissue to use.

1.1. Short-term *versus* long-term exposure studies

Because of their role in Hg internal metabolism, tissues like kidney and liver should be selected to study Hg accumulation rates and potential health effect. However, they might not be appropriate if we want to integrate a trophic analysis, for 2 reasons:

1. **Hg speciation.** In liver of ringed seals for example, MMHg and Hg²⁺ concentrations reach equilibrium sooner than HgSe because of their faster kinetics (Ewald et al., 2019). Despite constant internal demethylation rates, slow HgSe kinetics can result in highly variable Hg species composition. This reflects the comparatively short liver half-lives of Hg²⁺ (20 days) and MMHg (50 days) relative to HgSe (500 days) (Ewald et al., 2019). The large variability in Hg species profile in these tissues, could result in high heterogeneity of the isotopic results, complicating the interpretation of the data.
2. **Tissue turnover.** Since muscle and liver have different turnover rates, they integrate difference time period of Hg exposure and uptake by the organism of marine predators (Dietz et al., 2000; Lehnert et al., 2018). Specifically, liver represents Hg exposure throughout the life of an animal. Muscle on the other hand, has a turnover rate of few months (Ewald et al., 2019). In chapter 5, THg levels in muscle of true seals show that on the short-term, reliance on sympagic food webs in coastal areas might lead to higher Hg accumulation (Chapter 5, [§4.3](#)). The same measurement in another tissue could bring to another conclusion ([Chapter 3](#)). However, previous measurements of THg levels in livers of the same animals reported the highest concentrations in hooded seals compared to ringed seals (Pinzone et al., not published data; Dietz et al., 2019; Julshamn and Grahl-Nielsen, 2000; Rigét et al., 2011; Sonne et al., 2009b). This means that, if in the short-term

habitat use is the most important factor for Hg accumulation, on the long-term the situation might be different and the prey choice might represent the main route of entry of Hg in marine mammals.

1.2. Temporal studies

Nowadays, numerous temporal trend analyses are being conducted to study the impact of climate change on Hg sourcing and accumulation in Arctic predators (Dietz et al., 2021a; Mckinney et al., 2013; Rigét et al., 2011; Routti et al., 2019). In this regard, Hg concentrations and stable isotopes are compared from 1 year to the other over a series of 20 to 30 years (Bignert et al., 2004). Tissues with a higher fraction of iHg might integrate information of Hg accumulation over more than 1 year and could potentially mask the inter-annual variability in Hg levels in response of environmental changes. On the opposite side, a tissue like hair, presents a turnover so fast – two to three weeks during molting period – that integrate a very short period of time (Aubail et al., 2011). This could bring to a wrong interpretation of the intra-annual variability, when seals from the same year have been sampled before and after molting period (Peterson et al., 2016b).

In this situation, using a tissue less involved in the metabolization of Hg and with more homogenous iHg and MMHg concentrations, could be a better choice than kidney, liver or hair. The $\Delta^{199}\text{Hg}/\delta^{202}\text{Hg}$ ratios measured in captive hooded seals showed that the metabolization of Hg in liver, kidney and hair strongly modifies the information about Hg pathways in the environment, while in muscle it is conserved from diet to consumer (Chapter 4, Table 4.3). This indicates that measuring Hg stable isotopes in muscle could be more appropriate to trace Hg sources and trophic transfer within a single food web (e.g. secondary vs. tertiary consumer) or between different food webs (e.g. pelagic vs. coastal).

FIGURES

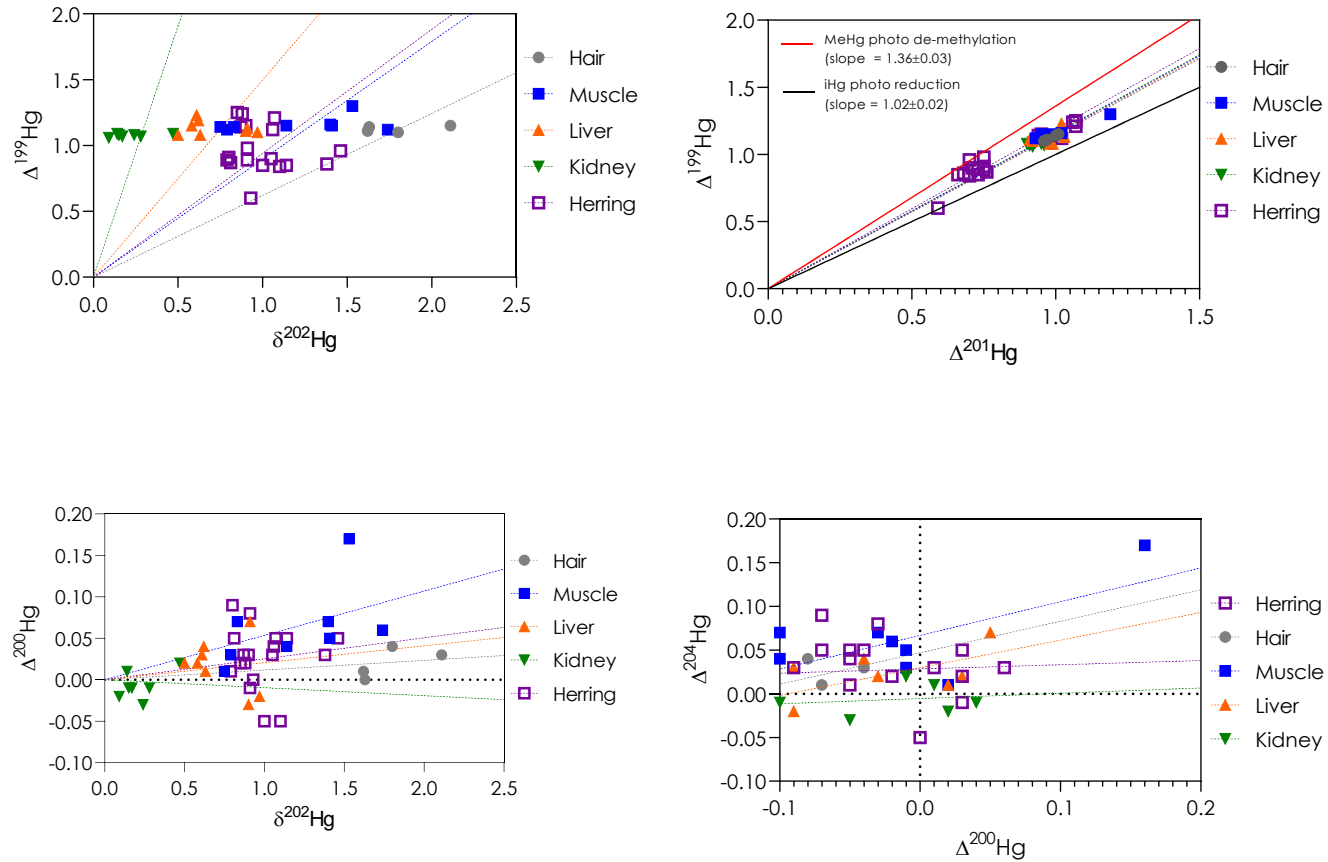


Figure A4.1. $\Delta^{199}\text{Hg}/\delta^{202}\text{Hg}$, $\Delta^{199}\text{Hg}/\Delta^{201}\text{Hg}$, $\Delta^{200}\text{Hg}/\delta^{202}\text{Hg}$ and $\Delta^{204}\text{Hg}/\Delta^{200}\text{Hg}$ slopes in hair (grey square), muscle (blue square), liver (orange triangle), kidney (green down-triangle) of hooded seals *C. cristata* and their prey, the herring *C. Harengus* (purple open square). Data are shown in per mill ‰.

TABLES

Table A4.1. Raw values of Hg stable isotopes MDF (expressed as δ) and MIF (expressed as Δ) for each analyzed sample. Letter a, b and c represents the replicates of a specific sample selected for internal calibration. Data are expressed in per mill ‰.

Organism	tissue	Sample	$\delta^{204}\text{Hg}$	$\delta^{202}\text{Hg}$	$\delta^{201}\text{Hg}$	$\delta^{200}\text{Hg}$	$\delta^{199}\text{Hg}$	$\Delta^{204}\text{Hg}$	$\Delta^{200}\text{Hg}$	$\Delta^{199}\text{Hg}$	$\Delta^{201}\text{Hg}$
Hooded seal	Liver	L1	0.83	0.58	1.46	0.31	1.30	-0.03	0.02	1.15	1.02
		L2a	0.82	0.61	1.48	0.34	1.39	-0.09	0.03	1.23	1.02
		L2b	0.89	0.62	1.48	0.35	1.35	-0.04	0.04	1.19	1.02
		L2c	0.77	0.50	1.35	0.27	1.20	0.03	0.02	1.08	0.98
		L3	1.41	0.91	1.72	0.53	1.36	0.05	0.07	1.13	1.03
		L4	1.17	0.90	1.59	0.42	1.33	-0.16	-0.03	1.11	0.91
		L5	1.35	0.97	1.65	0.46	1.34	-0.09	-0.02	1.10	0.92
	L6	0.97	0.63	1.47	0.33	1.24	0.02	0.01	1.08	0.99	
	Kidney	K1	0.30	0.24	1.13	0.09	1.14	-0.05	-0.03	1.08	0.95
		K2	0.45	0.28	1.12	0.13	1.15	0.04	-0.01	1.07	0.91
		K4	0.70	0.47	1.28	0.25	1.21	-0.01	0.02	1.09	0.93
		K5	0.12	0.15	1.02	0.07	1.12	-0.11	-0.01	1.08	0.90
		K6a	0.15	0.17	1.08	0.08	1.11	-0.10	-0.01	1.07	0.96
		K6b	0.21	0.14	1.03	0.08	1.12	0.01	0.01	1.09	0.92
		K6c	0.15	0.09	0.98	0.03	1.08	0.02	-0.02	1.06	0.92
	Muscle	M1	2.00	1.40	2.08	0.78	1.51	-0.10	0.07	1.16	1.02
		M2	2.58	1.74	2.24	0.93	1.56	-0.02	0.06	1.12	0.93
		M3	1.60	1.14	1.80	0.61	1.43	-0.10	0.04	1.15	0.95
		M4	2.45	1.53	2.35	0.94	1.69	0.16	0.17	1.30	1.19
		M5a	1.21	0.83	1.61	0.49	1.35	-0.03	0.07	1.14	0.98
		M5b	1.14	0.75	1.55	0.39	1.33	0.02	0.01	1.14	0.99
		M5c	1.17	0.79	1.56	0.43	1.32	-0.01	0.03	1.12	0.96
		M6	2.10	1.41	2.05	0.76	1.50	-0.01	0.05	1.15	0.99
	Hair	H1-5-6Pool	2.33	1.63	2.23	0.82	1.56	-0.11	0.00	1.14	1.00
		H2	2.35	1.62	2.18	0.82	1.51	-0.07	0.01	1.11	0.97
		H3	3.11	2.11	2.60	1.09	1.68	-0.04	0.03	1.15	1.01
		H4	2.61	1.80	2.32	0.95	1.55	-0.08	0.04	1.10	0.96
	Herring 2018	Muscle	C1	1.15	0.93	1.29	0.47	0.84	-0.24	0.00	0.60
C2			1.35	0.87	1.59	0.47	1.36	0.06	0.03	1.14	0.94
C3			1.25	0.85	1.71	0.45	1.47	-0.02	0.02	1.25	1.07
C5			1.52	1.10	1.53	0.50	1.12	-0.13	-0.05	0.84	0.70
C6			1.54	1.06	1.82	0.58	1.39	-0.05	0.04	1.12	1.02
C7			1.58	1.05	1.50	0.56	1.16	0.01	0.03	0.90	0.71
C8			1.74	1.14	1.59	0.63	1.14	0.03	0.05	0.85	0.73
C9a			1.13	0.79	1.35	0.40	1.09	-0.05	0.01	0.89	0.75
C9b			1.12	0.80	1.36	0.49	1.12	-0.07	0.09	0.91	0.75
C9c			1.14	0.81	1.37	0.45	1.07	-0.07	0.05	0.87	0.76
C10			1.33	0.88	1.72	0.46	1.46	0.03	0.02	1.24	1.06
C11			2.13	1.46	1.79	0.78	1.33	-0.04	0.05	0.96	0.70
C12			1.33	0.91	1.44	0.54	1.21	-0.03	0.08	0.98	0.75
C13			1.39	0.91	1.42	0.45	1.12	0.03	-0.01	0.89	0.73
C14			1.98	1.38	1.72	0.73	1.21	-0.09	0.03	0.86	0.68
C15	1.50	1.00	1.41	0.46	1.10	0.00	-0.05	0.85	0.66		
Herring 2012 – 2014	Muscle	CPool1	1.55	1.07	1.87	0.59	1.48	-0.05	0.05	1.21	1.07
		CPool2	1.14	0.90	1.63	0.48	1.38	-0.20	0.03	1.15	0.95

Table A4.2. $\Delta^{199}\text{Hg}/\Delta^{201}\text{Hg}$, $\Delta^{199}\text{Hg}/\delta^{202}\text{Hg}$, $\Delta^{200}\text{Hg}/\delta^{202}\text{Hg}$ and $\Delta^{200}\text{Hg}/\Delta^{204}\text{Hg}$ ratios, and $\delta^{202}\text{Hg}$ -TEF, $\Delta^{199}\text{Hg}$ -TEF, $\Delta^{201}\text{Hg}$ -TEF, $\Delta^{204}\text{Hg}$ -TEF and $\Delta^{200}\text{Hg}$ -TEF in tissues of hooded seal *C. cristata* and herring *C. harengus*. TEF (Trophic enrichment factor) values are calculated as the isotopic value (δ or Δ) measured in the tissue of the hooded seal minus the average of isotopic values (δ or Δ) found in herring (C1 to C15, plus Cpool1 and Cpool2).

Organism	tissue	Sample	$\Delta^{199}\text{Hg}/\Delta^{201}\text{Hg}$	$\Delta^{199}\text{Hg}/\delta^{202}\text{Hg}$	$\Delta^{200}\text{Hg}/\delta^{202}\text{Hg}$	$\Delta^{200}\text{Hg}/\Delta^{204}\text{Hg}$	$\delta^{202}\text{Hg}$ -TEF	$\Delta^{199}\text{Hg}$ -TEF	$\Delta^{201}\text{Hg}$ -TEF	$\Delta^{204}\text{Hg}$ -TEF	$\Delta^{200}\text{Hg}$ -TEF
Hooded seal	Liver	L1	1.13	0.50	0.04	-0.85	-0.42	0.18	0.21	0.02	0.00
		L2a	1.20	0.50	0.05	-0.31	-0.38	0.26	0.21	-0.05	0.00
		L2b	1.17	0.52	0.07	-1.02	-0.37	0.22	0.21	0.01	0.01
		L2c	1.10	0.46	0.04	0.71	-0.50	0.10	0.17	0.08	0.00
		L3	1.10	0.80	0.08	1.42	-0.09	0.16	0.22	0.10	0.05
		L4	1.21	0.81	-0.03	0.16	-0.10	0.13	0.10	-0.11	-0.05
		L5	1.19	0.88	-0.02	0.26	-0.03	0.13	0.11	-0.04	-0.05
	L6	1.09	0.58	0.02	0.51	-0.37	0.11	0.18	0.07	-0.01	
	Kidney	K1	1.14	0.22	-0.12	0.56	-0.76	0.11	0.14	0.00	-0.05
		K2	1.18	0.26	-0.04	-0.34	-0.72	0.10	0.10	0.08	-0.04
		K4	1.17	0.43	0.03	-1.59	-0.52	0.12	0.12	0.04	-0.01
		K5	1.19	0.14	-0.05	0.07	-0.84	0.11	0.09	-0.06	-0.03
		K6a	1.12	0.16	-0.04	0.07	-0.83	0.10	0.14	-0.05	-0.03
		K6b	1.18	0.12	0.07	1.48	-0.86	0.12	0.11	0.06	-0.02
		K6c	1.15	0.08	-0.17	-0.69	-0.91	0.08	0.11	0.07	-0.04
	Muscle	M1	1.13	1.21	0.05	-0.76	0.41	0.18	0.21	-0.05	0.05
		M2	1.20	1.55	0.03	-3.40	0.74	0.15	0.12	0.03	0.03
		M3	1.21	0.99	0.03	-0.39	0.14	0.17	0.14	-0.05	0.01
		M4	1.09	1.18	0.11	1.05	0.54	0.33	0.38	0.21	0.14
		M5a	1.16	0.73	0.08	-2.07	-0.16	0.17	0.17	0.02	0.04
		M5b	1.16	0.66	0.02	0.57	-0.24	0.17	0.17	0.07	-0.01
		M5c	1.17	0.70	0.04	-4.10	-0.21	0.15	0.15	0.04	0.01
	M6	1.16	1.23	0.03	-3.70	0.42	0.17	0.17	0.04	0.02	
	Hair	H1-5-6Pool	1.14	1.43	0.00	0.01	0.64	0.17	0.19	-0.06	-0.03
H2		1.15	1.46	0.00	-0.09	0.62	0.13	0.15	-0.02	-0.02	
H3		1.13	1.84	0.01	-0.70	1.11	0.17	0.20	0.01	0.00	
H4		1.14	1.64	0.02	-0.56	0.81	0.12	0.15	-0.03	0.02	
Herring 2018	Muscle	C1	1.02	1.54	0.00	-0.02	-	-	-	-	-
		C2	1.22	0.76	0.04	0.60	-	-	-	-	-
		C3	1.17	0.68	0.03	-1.16	-	-	-	-	-
		C5	1.21	1.31	-0.05	0.40	-	-	-	-	-
		C6	1.10	0.95	0.04	-0.98	-	-	-	-	-
		C7	1.26	1.17	0.03	2.35	-	-	-	-	-
		C8	1.17	1.34	0.05	1.55	-	-	-	-	-
		C9a	1.18	0.89	0.01	-0.16	-	-	-	-	-
		C9b	1.21	0.87	0.11	-1.19	-	-	-	-	-
		C9c	1.14	0.93	0.06	-0.68	-	-	-	-	-
		C10	1.17	0.71	0.03	0.89	-	-	-	-	-
		C11	1.38	1.52	0.03	-1.15	-	-	-	-	-
		C12	1.30	0.93	0.09	-2.24	-	-	-	-	-
		C13	1.22	1.02	-0.01	-0.42	-	-	-	-	-
		C14	1.26	1.60	0.03	-0.39	-	-	-	-	-
C15	1.29	1.18	-0.05	-	-	-	-	-	-		
Herring 2014	Muscle	CPool1	1.13	0.89	0.04	-1.02	-	-	-	-	-
		CPool2	1.21	0.79	0.03	-0.13	-	-	-	-	-

Table A4.3. THg, iHg and MMHg concentrations (in $\mu\text{g kg}^{-1}$ dw) and THg, iHg and MMHg. Measures were conducted for liver (**L**), muscle (**M**), kidney (**K**) and Hair (**H**) of hooded seals (*C. cristata*) and muscle (**M**) of their diet: the herring (**C**) fished in 2018. For each sample the number indicate the capital letter indicate the analyzed tissue, the number the analyzed seal and the letters a, b and c the replicate.

Organism	Tissue	Sample	THg	iHg	MMHg
Hooded seal	Liver	L1a	12624	9902	869
		L1b	-	9835	888
		L1c	-	10340	913
		L2a	10911	9024	852
		L2b	-	9054	882
		L2c	-	9681	880
		L3a	7708	8413	685
		L3b	-	8571	690
		L3c	-	9355	646
		L4a	6345	5543	566
		L4b	-	5567	562
		L4c	-	5527	562
		L5a	2674	2019	948
		L5b	-	1971	905
		L5c	-	1910	1014
		L6a	6989	4832	930
		L6b	-	4832	911
		L6c	-	4829	940
	Kidney	K1a	554	138	423
		K2b	-	133	412
		K3c	-	140	427
		K2a	348	74	270
		K2b	-	74	270
		K2c	-	77	272
		K3a	594	51	530
		K3b	-	63	526
		K3c	-	62	564
		K4a	480	107	362
		K4b	-	105	383
		K4c	-	104	366
		K5a	640	127	522
		K5b	-	119	550
		K5c	-	119	555
		K6a	627	101	588
		K6b	-	97	566
		K6c	-	94	570
	Muscle	M1a	3634	3066	528
		M2b	-	3176	526
		M3c	-	3156	496
M2a		5717	5068	566	
M2b		-	5354	552	
M2c		-	5389	530	
M3a		3531	2974	446	
M3b		-	3108	447	
M3c		-	3080	472	
M4a		7794	7360	389	
M4b		-	7363	383	
M4c		-	7206	354	
M5a		2427	1877	643	
M5b		-	1750	621	
M5c		-	1941	665	
M6a		9152	6024	652	
M6b		-	6015	707	
M6c		-	6271	693	
Hair	H1a	1257	145	1105	
	H2b	-	139	1162	
	H3c	-	147	1104	
	H2a	982	112	839	
	H2b	-	117	858	
	H2c	-	113	826	

		H3a	1130	78	1072
		H3b	-	80	1108
		H3c	-	74	1083
		H4a	622	93	531
		H4b	-	84	556
		H4c	-	95	541
		H5a	1592	138	1484
		H5b	-	134	1451
		H5c	-	135	1457
		H6a	1444	124	1351
		H6b	-	120	1365
		H6c	-	116	1358
		<hr/>			
		C1a	158	22	78
		C1b	-	22	78
		C1c	-	23	76
		C2a	116	14	105
		C2b	-	12	107
		C2c	-	13	103
		C3a	117	6	108
		C3b	-	9	121
		C3c	-	6	121
		C4a	119	4	44
		C4b	-	5	44
		C4c	-	4	41
		C5a	50	2	46
		C5b	-	3	51
		C5c	-	3	47
		C6a	171	16	159
		C6b	-	13	158
		C6c	-	14	160
		C7a	71	4	59
		C7b	-	4	64
		C7c	-	4	60
		C8a	62	6	56
		C8b	-	5	60
		C8c	-	5	60
		C9a	192	24	184
		C9b	-	16	182
		C9c	-	21	187
		C10a	166	11	157
		C10b	-	15	175
		C10c	-	13	154
		C11a	66	11	53
		C11b	-	11	56
		C11c	-	9	56
		C12a	188	17	169
		C12b	-	17	175
		C12c	-	17	171
		C13a	48	3	47
		C13b	-	4	49
		C13c	-	3	48
		C14a	87	6	74
		C14b	-	6	73
		C14c	-	6	74
		C15a	67	5	60
		C15b	-	5	64
		C15c	-	5	65
		<hr/>			
Herring 2018	Herring				

ANNEX to Chapter 5

$\Delta^{15}\text{N}$ AND $\Delta^{202}\text{Hg}$ INFER INTRA-SPECIFIC NICHE PARTITIONING IN HOODED SEALS

$\delta^{15}\text{N}$ values are strongly influenced by animals' metabolism and are found to increase from one trophic level to the next (Cantalapiedra-Hijar et al., 2015). Thus, they can be used as tracer of trophic position in addition to habitat use (McMahon et al., 2013b; Newsome et al., 2010). Contrasting literature exists on the occurrence of $\delta^{202}\text{Hg}$ trophic enrichment, reporting that it might happen exclusively only among top predators (Tsui et al., 2019). Moreover, we have previously shown that the extent of the $\delta^{202}\text{Hg}$ trophic enrichment might depend on the measured tissue as a result of the different spectrum of metabolic isotopic turnovers in an organism (Chapter 4, §4.2). What it is however certain, is that both $\delta^{15}\text{N}$ and $\delta^{202}\text{Hg}$ vary with the age of animals as a result of an ontogenetic shift in prey choice, habitat use and growth rates (Chapter 3 and 4; Bolea-Fernandez et al., 2019; Young et al., 2010). Therefore, the large spread of hooded seals' SEA along PC2 might be linked with shifts in diet and habitat use between age groups.

A second PCA and RDA were conducted for hooded seals only (Figure A5.2). The PCA loadings confirmed that circa 40 % of hooded seals variance was given by $\delta^{15}\text{N}$ and $\delta^{34}\text{S}$ values and circa 23 % by $\delta^{202}\text{Hg}$. The RDA showed that sex was the primary factor explaining the isotopic variability, followed weakly by age group. Satellite tracking studies have demonstrated how yearlings and subadult hooded seals tend to remain in strong association with the drift-ice of the Greenland Sea year-round, following its downward migration to the South of Greenland (Biuw et al., 2018; Folkow et al., 2010). Adult males and females instead, are believed to move northward after breeding, around the Fram Strait or Svalbard (Andersen et al., 2009; Folkow et al., 1996; Vacquie-Garcia et al., 2017). Our results show that adult females of hooded seals are characterized by isotopic values more similar to subadults. Specifically, adult females and subadults were characterized by higher values of $\delta^{34}\text{S}$ than adult males. The latter instead presented significantly higher $\delta^{15}\text{N}$ and $\delta^{202}\text{Hg}$ values. This suggests that **the trophic ecology of adult females of hooded seals resemble more that of subadults, rather than adult males.**

The hooded seal exhibits great sexual size dimorphism, with adult males being much bigger than females (Chapter 2, Table 2.1, §1). Therefore, a difference in habitat use and hunting strategies might occur. Sex differences in foraging behavior and diet are assumed to reflect differences in sex-specific costs of reproduction, or in the case of size dimorphism, effects of larger body size and intraspecific competition (Tucker et al., 2009). Even if telemetry data did not show any clear difference in movements between male and females hooded seals (Folkow and Blix, 1999); some indication of different mean dive depths in the post-breeding period exist (Andersen et al., 2013; Bajzak et al., 2009). Stomach content analysis showed some dietary differences with age but never between sexes (Haug et al., 2004; Potelev et al., 2014). However, this type of analysis allows only to study snapshots of the diet of an animal, because it is limited to prey ingested just before sampling (Matley et al.,

2015). Using another approach, Tucker and colleagues observed differences between male and female hooded seals' fatty acids (FA) profiles. Because FAs are deposited in predator adipose tissue in a predictable manner and there are limits on FA biosynthesis in higher order consumers, many FAs found in pinniped blubber can be attributed to dietary sources (Tucker et al., 2013). Their results strongly supported a diet segregation linked with sex in this species, confirming our results. The lower $\delta^{34}\text{S}$ and $\delta^{202}\text{Hg}$ values of hooded females and subadults might therefore indicate reliance on coastal and shallower food webs with respect to adult males. The higher $\delta^{15}\text{N}$ values found in adult hooded seal males could indicate reliance on deeper and higher trophic level prey such as the Greenland halibut or Atlantic cod.

FIGURES

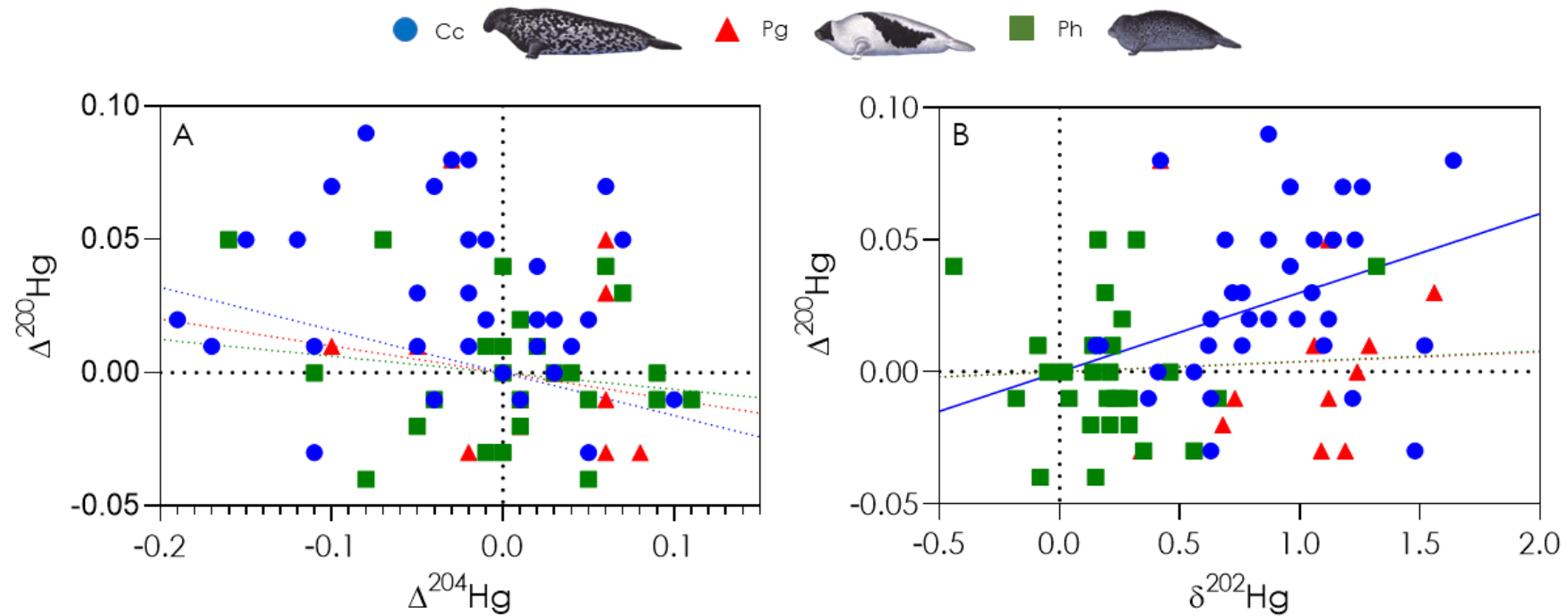


Figure A5.1. Hg even MIF biplots representing $\Delta^{200}\text{Hg}/\Delta^{204}\text{Hg}$ (A) and $\Delta^{200}\text{Hg}/\delta^{202}\text{Hg}$ (B) slopes for hooded (Cc), harp (Pg) and ringed seals (Ph) sampled between 2008 and 2019 along the Eastern coast of Greenland. Colors and shapes represent the species: blue circle = Cc, red triangle = Pg and green square = Ph. Dotted line represent not a significant linear regression fit, while straight lines represent a significant linear regression fit. The $\Delta^{200}\text{Hg}/\delta^{202}\text{Hg}$ line of Cc was the only significant one, with a slope of 0.03 ± 0.005 .

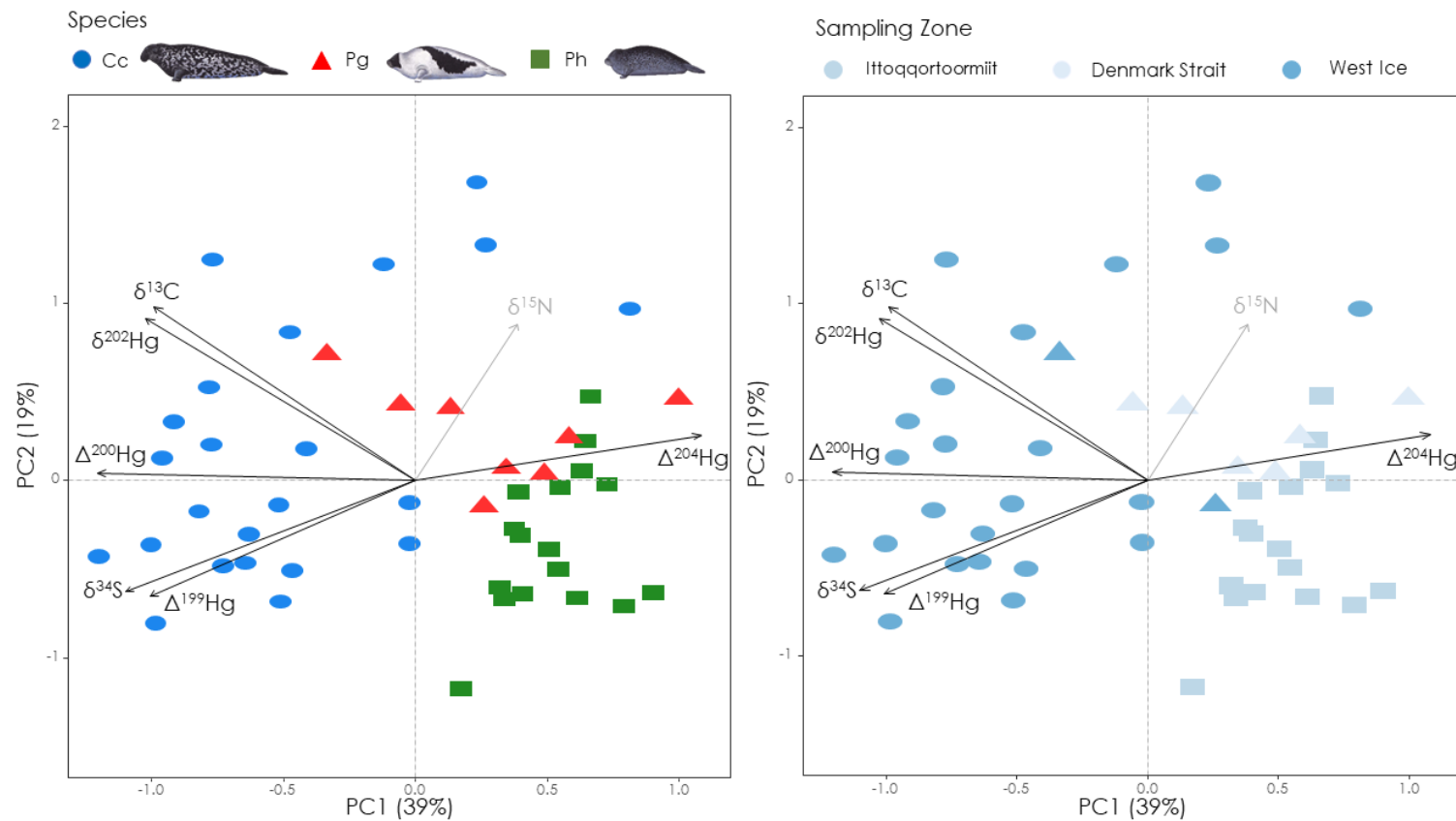


Figure A5.2. PCA scores biplot for hooded (Cc), harp (Pg) and ringed (Ph) seals multi-isotopic variance as explained by species (left) and sampling site (right). In the left figure the colors represent the species = blue: C), red: Pg, green: Ph. In the right figure the blue palette represents the sampling sites = West Ice: darkest blue, Ittoqqortoormiit: medium-blue, Denmark Strait: lightest blue. In both figures shapes indicate the species = Circle: Cc, triangles: Pg, square: Ph. As it can be observed the “West ice” points in the right figure overlap all (with the exception of one point) with the blue circles of the left figures (Cc). the same is observed for the “Ittoqqortoormiit” points on the right which overlap with all green squares (Ph) of the left figure.

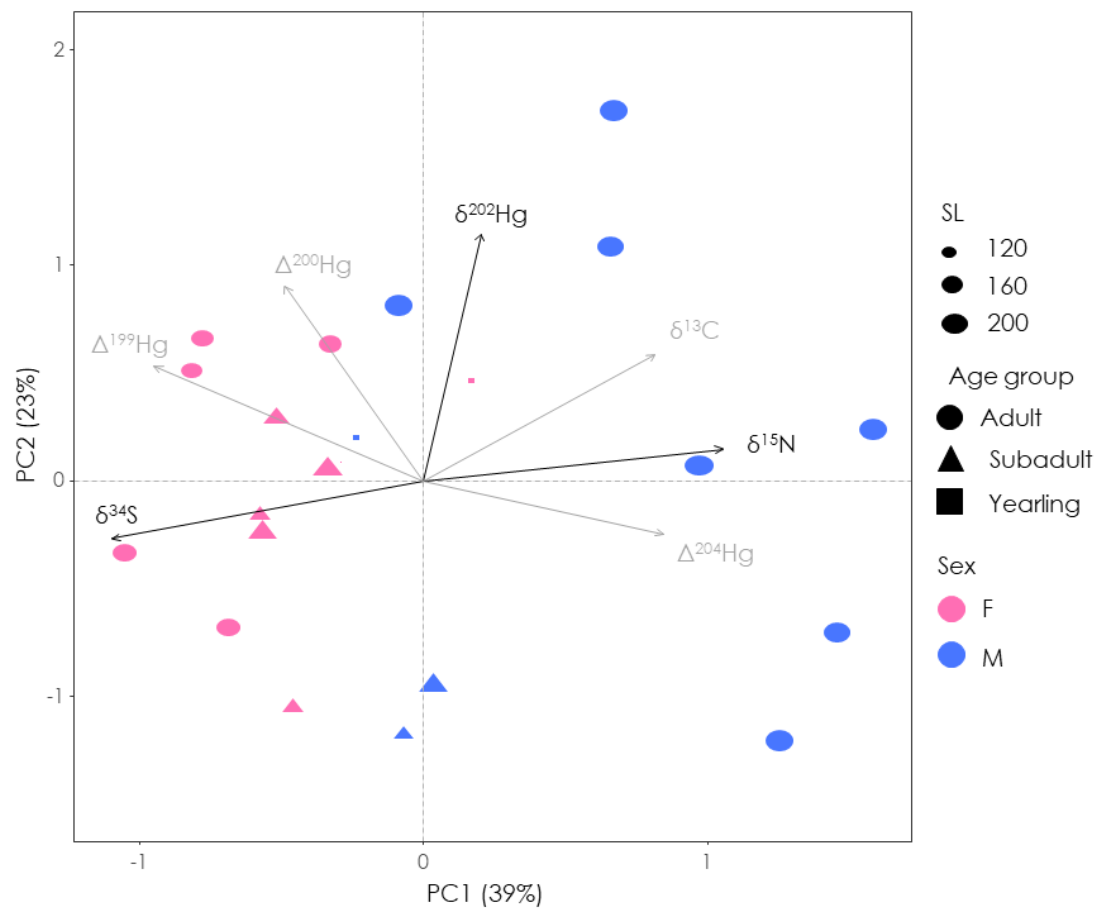


Figure A5.3. PCA scores biplot for hooded seal (*Cc*) exclusively. As showed by the legend the dimension of the shape indicates the standard length (SL) of the individual, the shape indicates the age group = circle: Adult, triangle: Subadult and square: Yearlings. All females are shown in pink, all males are shown in blue. The black arrows indicate the response variables that contribute the most to the variability along PC1 ($\delta^{34}\text{S}$ score = -1.09; $\delta^{15}\text{N}$ = 1.05) and PC2 ($\delta^{202}\text{Hg}$ = 1.14). Sex resulted the most important factor influencing hooded seals variance (adjusted R^2 = 0.35, F = 6.95, p = 0.001), followed by SL (adjusted R^2 = 0.23, F = 7.66, p = 0.004).

TABLES

Table A5.1. Spearman correlation matrices for all response variables measured in muscle tissue of hooded, harp and ringed seals from the East coast of Greenland from 2008 and 2019. Pairwise correlations are presented as Spearman rho values. Significant correlation is shown in yellow. Bold letters indicate a significance of $p < 0.0001$. Letters in italic indicate a significance of $p < 0.01$.

Ringed seal													
	$\delta^{13}\text{C}_{\text{corr}}$ (‰)	$d^{15}\text{N}$ (‰)	$d^{34}\text{S}$ (‰)	THg (ng g ⁻¹ dw)	$\delta^{202}\text{Hg}$ (‰)	$\Delta^{204}\text{Hg}$ (‰)	$\Delta^{201}\text{Hg}$ (‰)	$\Delta^{200}\text{Hg}$ (‰)	$\Delta^{199}\text{Hg}$ (‰)	$\Delta^{199}\text{Hg}/\Delta^{201}\text{Hg}$ g	$\Delta^{199}\text{Hg}/\delta^{202}\text{Hg}$	$\Delta^{200}\text{Hg}/\delta^{202}\text{Hg}$ g	$\Delta^{200}\text{Hg}/\Delta^{204}\text{Hg}$
$\delta^{13}\text{C}_{\text{corr}}$ (‰)	1	-0.19	-0.41	0.11	0.28	0.14	-0.06	0.17	-0.09	-0.06	0.08	0.02	0.22
$d^{15}\text{N}$ (‰)	-0.19	1	0.02	0.60	0.07	-0.19	-0.04	-0.11	-0.02	0.24	0.17	0.09	0.06
$d^{34}\text{S}$ (‰)	-0.41	0.02	1	0.02	-0.23	0.07	-0.20	-0.14	-0.13	0.25	0.23	-0.20	0.03
THg (ng.g ⁻¹ dw)	0.11	0.60	0.02	1	0.02	0.10	0.20	-0.14	0.31	0.28	-0.23	-0.33	0.27
$\delta^{202}\text{Hg}$ (‰)	0.28	0.07	-0.23	0.02	1	-0.10	0.05	-0.15	0.04	-0.05	-0.39	0.12	0.13
$\Delta^{204}\text{Hg}$ (‰)	0.14	-0.19	0.07	0.10	-0.10	1	0.10	0.00	0.03	-0.35	-0.31	0.16	-0.04
$\Delta^{201}\text{Hg}$ (‰)	-0.06	-0.04	-0.20	0.20	0.05	0.10	1	<i>0.47</i>	0.94	-0.03	0.06	<i>0.47</i>	0.11
$\Delta^{200}\text{Hg}$ (‰)	0.17	-0.11	-0.14	-0.14	-0.15	0.00	<i>0.47</i>	1	0.50	0.12	0.13	0.66	0.02
$\Delta^{199}\text{Hg}$ (‰)	-0.09	-0.02	-0.13	0.31	0.04	0.03	0.94	0.50	1	0.25	0.00	0.38	0.09
$\Delta^{199}\text{Hg}/\Delta^{201}\text{Hg}$	-0.06	0.24	0.25	0.28	-0.05	-0.35	-0.03	0.12	0.25	1	0.10	-0.25	0.01
$\Delta^{199}\text{Hg}/\delta^{202}\text{Hg}$	0.08	0.17	0.23	-0.23	-0.39	-0.31	0.06	0.13	0.00	0.10	1	0.14	-0.16
$\Delta^{200}\text{Hg}/\delta^{202}\text{Hg}$	0.02	0.09	-0.20	-0.33	0.12	0.16	<i>0.47</i>	0.66	0.38	-0.25	0.14	1	-0.25
$\Delta^{200}\text{Hg}/\Delta^{204}\text{Hg}$	0.22	0.06	0.03	0.27	0.13	-0.04	0.11	0.02	0.09	0.01	-0.16	-0.25	1
Harp seal													
	$\delta^{13}\text{C}_{\text{corr-Post et al}}$ (‰)	$d^{15}\text{N}$ (‰)	$d^{34}\text{S}$ (‰)	THg (ng g ⁻¹ dw)	$\delta^{202}\text{Hg}$ (‰)	$\Delta^{204}\text{Hg}$ (‰)	$\Delta^{201}\text{Hg}$ (‰)	$\Delta^{200}\text{Hg}$ (‰)	$\Delta^{199}\text{Hg}$ (‰)	$\Delta^{199}\text{Hg}/\Delta^{201}\text{Hg}$	$\Delta^{199}\text{Hg}/\delta^{202}\text{Hg}$	$\Delta^{200}\text{Hg}/\delta^{202}\text{Hg}$	$\Delta^{200}\text{Hg}/\Delta^{204}\text{Hg}$
$\delta^{13}\text{C}_{\text{corr}}$ (‰)	1	-0.47	0.09	0.08	-0.43	-0.44	0.16	-0.20	0.16	0.14	0.41	-0.30	0.10
$d^{15}\text{N}$ (‰)	-0.47	1	0.08	-0.33	-0.20	-0.17	-0.08	0.30	-0.03	-0.26	0.21	0.04	-0.40
$d^{34}\text{S}$ (‰)	0.09	0.08	1	-0.24	-0.01	-0.81	0.14	0.16	0.10	0.11	0.05	0.01	-0.42
THg (ng.g ⁻¹ dw)	0.08	-0.33	-0.24	1	-0.02	0.29	-0.30	-0.40	-0.29	0.40	-0.01	-0.18	0.21
$\delta^{202}\text{Hg}$ (‰)	-0.43	-0.20	-0.01	-0.02	1	-0.05	0.16	0.23	0.24	0.21	-0.99	0.61	0.53

$\Delta^{204}\text{Hg}(\text{‰})$	-0.44	-0.17	-0.81	0.29	-0.05	1	-0.29	-0.30	-0.30	-0.26	0.04	-0.11	0.13
$\Delta^{201}\text{Hg}(\text{‰})$	0.16	-0.08	0.14	-0.30	0.16	-0.29	1	0.63	0.98	-0.29	-0.20	0.42	0.06
$\Delta^{200}\text{Hg}(\text{‰})$	-0.20	0.30	0.16	-0.40	0.23	-0.30	0.63	1	0.58	-0.43	-0.31	0.96	0.09
$\Delta^{199}\text{Hg}(\text{‰})$	0.16	-0.03	0.10	-0.29	0.24	-0.30	0.98	0.58	1	-0.16	-0.26	0.40	0.12
$\Delta^{199}\text{Hg}/\Delta^{201}\text{Hg}$	0.14	-0.26	0.11	0.40	0.21	-0.26	-0.29	-0.43	-0.16	1	-0.14	-0.15	0.12
$\Delta^{199}\text{Hg}/\delta^{202}\text{Hg}$	0.41	0.21	0.05	-0.01	-0.99	0.04	-0.20	-0.31	-0.26	-0.14	1	-0.70	-0.60
$\Delta^{200}\text{Hg}/\delta^{202}\text{Hg}$	-0.30	0.04	0.01	-0.18	0.61	-0.11	0.42	0.96	0.40	-0.15	-0.70	1	0.47
$\Delta^{200}\text{Hg}/\Delta^{204}\text{Hg}$	0.10	-0.40	-0.42	0.21	0.53	0.13	0.06	0.09	0.12	0.12	-0.60	0.47	1
Hooded seal													
	$\delta^{13}\text{C}_{\text{corr-Post et al.}}(\text{‰})$	$d^{15}\text{N}(\text{‰})$	$d^{34}\text{S}(\text{‰})$	THg (ng g ⁻¹ dw)	$\delta^{202}\text{Hg}(\text{‰})$	$\Delta^{204}\text{Hg}(\text{‰})$	$\Delta^{201}\text{Hg}(\text{‰})$	$\Delta^{200}\text{Hg}(\text{‰})$	$\Delta^{199}\text{Hg}(\text{‰})$	$\Delta^{199}\text{Hg}/\Delta^{201}\text{Hg}$	$\Delta^{199}\text{Hg}/\delta^{202}\text{Hg}$	$\Delta^{200}\text{Hg}/\delta^{202}\text{Hg}$	$\Delta^{200}\text{Hg}/\Delta^{204}\text{Hg}$
$\delta^{13}\text{C}_{\text{corr.}}(\text{‰})$	1	0.7	-0.1	0.4	-0.1	0.0	0.0	0.1	0.1	0.2	-0.2	0.1	-0.1
$d^{15}\text{N}(\text{‰})$	0.7	1	-0.2	0.2	-0.1	0.1	-0.1	-0.2	-0.1	0.2	-0.2	-0.1	0.1
$d^{34}\text{S}(\text{‰})$	-0.1	-0.2	1	-0.1	-0.2	-0.4	0.1	0.0	0.2	0.1	0.3	0.1	-0.2
THg (ng g ⁻¹ dw)	0.4	0.2	-0.1	1	0.2	-0.2	-0.2	0.1	-0.2	0.1	-0.2	0.1	-0.1
$\delta^{202}\text{Hg}(\text{‰})$	-0.1	-0.1	-0.2	0.2	1	-0.1	0.3	0.4	0.1	-0.2	-0.7	0.1	0.0
$\Delta^{204}\text{Hg}(\text{‰})$	0.0	0.1	-0.4	-0.2	-0.1	1	-0.1	-0.1	-0.1	-0.1	-0.1	0.0	0.3
$\Delta^{201}\text{Hg}(\text{‰})$	0.0	-0.1	0.1	-0.2	0.3	-0.1	1	0.4	0.9	-0.5	0.2	0.3	0.0
$\Delta^{200}\text{Hg}(\text{‰})$	0.1	-0.2	0.0	0.1	0.4	-0.1	0.4	1	0.4	-0.1	-0.1	0.9	-0.3
$\Delta^{199}\text{Hg}(\text{‰})$	0.1	-0.1	0.2	-0.2	0.1	-0.1	0.9	0.4	1	-0.2	0.3	0.4	0.0
$\Delta^{199}\text{Hg}/\Delta^{201}\text{Hg}$	0.2	0.2	0.1	0.1	-0.2	-0.1	-0.5	-0.1	-0.2	1	0.2	-0.1	0.0
$\Delta^{199}\text{Hg}/\delta^{202}\text{Hg}$	-0.2	-0.2	0.3	-0.2	-0.7	-0.1	0.2	-0.1	0.3	0.2	1	0.1	0.1
$\Delta^{200}\text{Hg}/\delta^{202}\text{Hg}$	0.1	-0.1	0.1	0.1	0.1	0.0	0.3	0.9	0.4	-0.1	0.1	1	-0.3
$\Delta^{200}\text{Hg}/\Delta^{204}\text{Hg}$	-0.1	0.1	-0.2	-0.1	0.0	0.3	0.0	-0.3	0.0	0.0	0.1	-0.3	1

Table A5.2 Biplot scores for constrained (RDA) and unconstrained (PCA) response variables. The blue cells represent negative correlation; the yellow cells represent positive correlation. The color scaling shows the strength of the correlation with darker tones indicating stronger correlations. The values represent the strength of the correlation, the sign (positive or negative) represents the direction of the correlation.

Response Variable	Redundancy Analysis		Principal Component Analysis		
	RDA1	RDA2	PC1	PC2	PC3
$\delta^{13}\text{C}$	-0.56	-0.88	-0.99	0.98	-0.32
$\delta^{15}\text{N}$	0.36	-0.99	0.38	0.88	1.14
$\delta^{34}\text{S}$	-2.81	0.08	-1.10	-0.63	0.18
$\delta^{202}\text{Hg}$	-0.20	-0.43	-1.02	0.92	-0.15
$\Delta^{204}\text{Hg}$	0.05	0.002	1.08	0.26	0.38
$\Delta^{199}\text{Hg}$	-0.17	0.03	-1.01	-0.65	0.84
$\Delta^{200}\text{Hg}$	-0.02	-0.01	-1.20	0.04	0.22
Statistical results					
Eigenvalue	2.65	0.62	2.71	1.34	0.91
Explained proportion	0.57	0.13	0.39	0.19	0.13
Cumulative proportion	0.57	0.70	0.39	0.58	0.71
Cumulative Percentage	57 %	70 %	39 %	58 %	71 %

Table A5.3. Biplot scored for constraining variables (factors). The color scaling shows the strength of the correlation with darker tones indicating stronger correlations. The values represent the strength of the correlation, the sign (positive or negative) represents the direction of the correlation. The ANOVA permutation test results are reported. Bold numbers indicate significant correlation. Italic number indicates weak statistical significance.

	RDA1 scores	RDA2 scores	R	R adjusted	F	p value
Species~Pg	0.48	0.19	0.39	0.36	14.42	0.001
Species~Ph	0.35	0.42				
Age group~Subadult	-0.06	0.52	0.07	0.03	1.72	0.14
Age group~Yearling	-0.16	-0.14				
Sex~F	-0.24	0.39	0.11	0.07	2.67	0.03
Sex~M	0.30	-0.35				
SL	-0.04	-0.56	0.06	0.04	3.09	0.04
SZ~West Ice	-0.68	-0.51	0.39	0.37	14.8	0.001
SY	0.22	-0.50	0.02	0.02	4.44	<i>0.01</i>
SM	-0.21	0.40	0.02	0.02	3.4	0.10
BT	-0.27	0.12	0.05	0.03	2.39	0.08

Table A5.4. Calculated Layman and SIBER matrices for the modelled multivariate niches of hooded, harp and ringed seals sampled between 2008 and 2019 along the East coast of Greenland. SIBER ellipses were modelled using the PCA score values, therefore the presented results are dimensionless. N_{tot} = number of seals used for the calculation. SEA_B are represented as mode (95 % CI).

Calculated metrics	Hooded seal Cc ($N_{tot} = 23$)	Harp seal Pg ($N_{tot} = 7$)	Ringed seal Ph ($N_{tot} = 15$)
<i>Layman</i>			
Y_range	2.49	0.86	1.65
X_range	2.01	1.33	0.73
TA	2.90	0.50	0.56
CD	0.76	0.41	0.38
MNND	0.27	0.25	0.14
SDNND	0.14	0.12	0.11
<i>Geometric and Bayesian Standard ellipse</i>			
SEA	0.94	0.34	0.23
SEA _C	0.98	0.39	0.25
SEA _B	0.93 (0.60 – 1.41)	0.31 (0.14 – 0.68)	0.22 (0.14 – 0.37)

ANNEX to Chapter 6

1. APPLICATION OF LMMS FOR THE ANALYSIS OF Hg TEMPORAL TRENDS

The linear mixing models we applied in chapter 6 demonstrated to be a powerful tool to assess simultaneously the effect of multiple biotic and abiotic variables on THg temporal trends of Arctic seals. However, some problems aroused during the analysis of the models for hooded and ringed seals, which merit further consideration.

We generated an a priori list of candidate models containing all appropriate iterations of predictor variables and used the Akaike's information criterion corrected for small sample size (AICc) for the selection of most parsimonious models (Chapter 6, §2.5). In some cases, models that produced more significant coefficients and higher R^2 values, were not the most realistic with regards to the known Hg behavior in marine food webs. The results of such models seemed to be caused more by the type of input data, than the effective relationships between environmental variables and THg in nature. Such mismatch between expected and effective LMM trends might have been caused by:

1. **Multicollinearity between some explanatory variables.** Before running the LMMs, we calculated Pearson correlation matrices to check for correlation between all variables. This allowed to eliminate those variables strongly correlated with the others. We then scaled all predictor variables to further reduce collinearity. However such methods allow only to run multiple pairwise correlations, without considering all variables together (Akoglu, 2018). It is still possible that, when considered all together, some variables still correlated strongly. In this case, their contributions to the regression model would have be reported as minimal or insignificant. This may be due to their redundancy rather than a lack of causal importance (Buttigieg and Ramette, 2014).
2. **Absence of linear correlation.** When there is a large number of explanatory variables in the analysis, their "significance" should be interpreted with caution (Derksen and Keselman, 1992). Following from the logic of multiple testing, there is always a chance that the significance is due to chance alone (Whittingham et al., 2006). Using the right regression model is instrumental for a correct interpretation of the data. There are several type of correlations that could be tested between Hg and environmental proxies. In this work we fitted our models assuming simple linear regressions. However, such method needs several assumptions to be met to work properly (e.g. gaussian distribution, large N size and continuous sampling) (Harrell, 2001). The application of Generalized Additive Models (GAMs) allows fitting of large datasets with complicated interaction effects, non:parametric data and small N size of parameters (Drexler and Ainsworth, 2013). Considering the large set of ecological, environmental and biological proxies that we tested and

the large time gaps we had between sampling years, the use of GAMs at the place of simple LMMs would have been more appropriated (Denis et al., 2002).

Several statistical texts suggested that the addition or removal of variables should be guided by a priori field knowledge. Selection based solely on the statistical results should be handled with great care (Buttigieg and Ramette, 2014). The real-world "importance" of the explanatory variables in predicting the response variable goes beyond p-values and effect sizes. Thus, even if these variables are not the most prominent or significant predictors of the response, they may be the most important (Buttigieg and Ramette, 2014).

TABLES

Table A6.1. Raw values, yearly averages and 2 x Standard Deviation (2SD) of Hg stable isotope ratios for hooded seals *C. cristata*, harvested in the Greenland Sea from 1987 to 2019. Data are presented in δ notation (in per mill, ‰).

Year	$\delta^{202}\text{Hg}$	$\Delta^{199}\text{Hg}$	$\Delta^{200}\text{Hg}$	$\Delta^{201}\text{Hg}$	$\Delta^{204}\text{Hg}$	$\Delta^{199}\text{Hg}/\Delta^{201}\text{Hg}$
1987	0.87	0.86	0.05	0.70	-0.02	1.23
1987	0.76	0.78	0.03	0.61	-0.02	1.28
1987	0.15	0.95	0.01	0.72	0.04	1.31
1987	0.62	1.04	0.01	0.84	-0.17	1.24
1987	0.96	1.22	0.07	1.03	0.06	1.18
AVG	0.67	0.97	0.03	0.78	-0.02	1.25
2SD	0.63	0.34	0.06	0.33	0.18	0.10
2001	0.63	0.85	-0.03	0.68	-0.11	1.26
2001	0.17	0.91	0.01	0.79	-0.02	1.16
2001	0.72	0.79	0.03	0.60	-0.02	1.32
2001	1.14	1.16	0.05	0.93	-0.12	1.24
2001	0.42	1.16	0.08	0.99	-0.03	1.18
2001	0.37	0.97	-0.01	0.81	0.01	1.20
AVG	0.58	0.97	0.02	0.80	-0.05	1.23
2SD	0.68	0.31	0.08	0.30	0.11	0.12
2008	0.63	0.85	-0.03	0.68	-0.11	1.26
2008	1.10	1.08	0.01	0.84	0.02	1.29
2008	0.69	0.95	0.05	0.77	-0.01	1.23
2008	0.99	1.01	0.02	0.89	-0.01	1.14
AVG	0.85	0.97	0.02	0.79	-0.03	1.23
2SD	0.46	0.19	0.07	0.18	0.11	0.13
2017	1.12	0.67	0.02	0.50	0.03	1.33
2017	1.06	0.86	0.05	0.73	-0.15	1.17
2017	0.41	0.85	0.00	0.71	0.03	1.21
2017	0.63	0.71	0.02	0.60	0.05	1.20
AVG	0.81	0.77	0.02	0.63	-0.01	1.23
2SD	0.69	0.19	0.04	0.21	0.19	0.15
2018	1.18	0.80	0.07	0.71	-0.10	1.12
2018	0.76	0.95	0.01	0.82	-0.05	1.16
2018	0.87	0.97	0.09	0.78	-0.08	1.23
2018	0.79	0.95	0.02	0.69	-0.19	1.38
2018	1.26	1.09	0.07	0.89	-0.04	1.21
2018	1.52	0.94	0.01	0.79	-0.11	1.19
2018	1.05	0.96	0.03	0.80	-0.05	1.20
2018	0.96	1.12	0.04	0.95	0.02	1.18
2018	1.06	0.81	0.05	0.64	-0.10	1.27
2018	0.87	0.99	0.02	0.84	0.02	1.18

2018	1.22	0.86	-0.01	0.87	-0.04	0.99
AVG	1.05	0.95	0.04	0.80	-0.07	1.19
2SD	0.46	0.20	0.06	0.18	0.12	0.19
2019	1.64	0.87	0.08	0.84	-0.02	1.03
2019	0.56	0.36	0.00	0.29	0.00	1.28
2019	1.48	0.63	-0.03	0.52	0.05	1.22
2019	0.63	0.57	-0.01	0.51	0.10	1.13
2019	1.23	1.09	0.05	0.91	0.07	1.19
AVG	1.11	0.70	0.02	0.61	0.04	1.17
2SD	0.98	0.56	0.09	0.52	0.09	0.19

Table A6.2. Raw values, yearly averages and 2 x Standard Deviation (2SD) of Hg stable isotope ratios for ringed seals *P. hispida*, harvested in the Greenland Sea from 1987 to 2019. Data are presented in δ notation (in per mill, ‰).

Year	$\delta^{202}\text{Hg}$	$\Delta^{204}\text{Hg}$	$\Delta^{201}\text{Hg}$	$\Delta^{200}\text{Hg}$	$\Delta^{199}\text{Hg}$	$\Delta^{199}\text{Hg}/\Delta^{201}\text{Hg}$
1987	0.32	-0.07	0.76	0.05	1.01	1.34
1987	0.26	0.01	0.81	0.02	0.91	1.13
1987	0.46	0.03	0.88	0.00	1.11	1.26
1987	1.32	0.06	1.10	0.04	1.43	1.31
1987	0.16	-0.16	0.74	0.05	0.99	1.33
AVG	0.51	-0.03	0.86	0.03	1.09	1.27
2SD	0.94	0.18	0.29	0.04	0.41	0.17
2002	0.13	0.01	0.61	-0.02	0.88	1.44
2002	0.19	0.07	0.56	0.03	0.72	1.29
2002	0.29	0.09	0.54	-0.01	0.70	1.29
2002	0.14	-0.11	0.39	0.00	0.57	1.44
2002	0.04	-0.04	0.53	-0.01	0.79	1.48
AVG	0.16	0.01	0.53	0.00	0.73	1.39
2SD	0.18	0.17	0.16	0.03	0.23	0.18
2008	0.02	0.09	0.58	0.00	0.73	1.26
2008	-0.44	0.00	0.71	0.04	0.93	1.32
2008	-0.05	0.00	0.47	0.00	0.58	1.23
2008	-0.09	0.02	0.50	0.01	0.69	1.36
2008	0.21	0.04	0.59	0.00	0.75	1.27
2008	0.25	0.05	0.52	-0.01	0.66	1.26
AVG	-0.01	0.03	0.56	0.01	0.72	1.28
2SD	0.50	0.07	0.17	0.04	0.23	0.09
2016	-0.08	0.05	0.54	-0.04	0.69	1.27
2016	-0.18	0.11	0.72	-0.01	0.89	1.23
2016	0.22	0.00	0.84	0.01	1.08	1.29
2016	0.23	0.05	0.46	-0.01	0.60	1.29
2016	0.35	-0.01	0.55	-0.03	0.78	1.41
2016	0.14	-0.01	0.72	0.01	0.96	1.34
AVG	0.11	0.03	0.64	-0.01	0.83	1.31
2SD	0.40	0.10	0.28	0.04	0.36	0.12
2018	0.29	-0.05	0.42	-0.02	0.56	1.35
2018	0.56	0.00	0.72	-0.03	0.96	1.33
2018	0.15	-0.08	0.56	-0.04	0.68	1.21
2018	0.20	0.05	0.56	-0.01	0.69	1.23
2018	0.21	-0.05	0.47	-0.02	0.52	1.12
2018	0.66	0.01	0.34	-0.01	0.43	1.25
AVG	0.34	-0.02	0.51	-0.02	0.64	1.25
2SD	0.43	0.09	0.27	0.02	0.37	0.17

Table A6.3. Summary of top selected linear mixed effect models (LMMs) predicting **ringed seals** THg values in time. Akaike's Information Criterion corrected for small sample size (AICc) and Δ AICc were used to identify top model sets (Δ AICc values ≤ 2). Normalized Akaike weights (Weight) were used to assess individual model information content.

Model	Selected variables	AICc	Δ AICc	Weight
Base	Year + d15N	533.7	0.00	0.98
	d15N	541.8	8.11	0.02
Ecological	Year + d15N + d13C_corr	534.6	0.00	0.47
	Year + d15N + d34S	535.6	0.48	0.37
	Year + d15N + d34S + d13C_corr	536.5	2.04	0.17
Teleconnections	Year + d15N + d13C_corr + NAO	535.6	0.00	0.52
	Year + d15N + d13C_corr + winter AO	536.6	1.16	0.29
	Year + d15N + d13C_corr + winter AO + NAO	537.5	2.00	0.19
Climate	Year + d15N + d13C_corr + NAO + SAT	535.2	0.00	0.17
	Year + d15N + d13C_corr + NAO + SAT + SASIE	535.6	0.34	0.14
	Year + d15N + d13C_corr + NAO + SAT + GSSIE + SASIE	536.0	0.80	0.11
	Year + d15N + d13C_corr + NAO + SAT + SIFD (Ittoq.)	537.0	1.76	0.07
	Year + d15N + d13C_corr + NAO + GSSIE	537.0	1.81	0.07
	Year + d15N + d13C_corr + NAO + SAT + SIFD (Ittoq.) + SASIE	537.1	1.92	0.07
	Year + d15N + d13C_corr + NAO + SAT + GGSIE	537.3	2.12	0.06
	Year + d15N + d13C_corr + NAO + SAT + ASIE	537.4	2.39	0.08
	Year + d15N + d13C_corr + NAO + ASIE	537.5	2.33	0.05
	Year + d15N + d13C_corr + NAO + SIFD (Ittoq.)	537.6	2.39	0.05
	Year + d15N + d13C_corr + NAO + SAT + ASIE + SIFD (Ittoq.) + SASIE + GSIE	539.4	4.15	0.02
	Year + d15N + d13C_corr + NAO + SAT + ASIE + SAT + GSSIE	539.5	4.30	0.02
Diet	Year + d15N + d13C_corr + NAO + SAT + Gm	534.4	0.00	0.23
	Year + d15N + d13C_corr + NAO + SAT + Gm + Mv	535.0	0.56	0.17
	Year + d15N + d13C_corr + NAO + SAT + Rh	536.0	1.57	0.10
	Year + d15N + d13C_corr + NAO + SAT + Bs + Gm	536.0	1.64	0.10
	Year + d15N + d13C_corr + NAO + SAT + Gm + Rh	536.5	2.12	0.08
	Year + d15N + d13C_corr + NAO + SAT + Bs	536.6	2.24	0.07
	Year + d15N + d13C_corr + NAO + SAT + Bs + Mv	537.8	2.35	0.07
	Year + d15N + d13C_corr + NAO + SAT + Rh + Mv	536.9	2.48	0.07
	Year + d15N + d13C_corr + NAO + SAT + Mv	537.3	2.86	0.05
	Year + d15N + d13C_corr + NAO + SAT + Rh + Bs	538.1	3.73	0.03
	Year + d15N + d13C_corr + NAO + SAT + Rh + Bs + Gm + Mv	539.3	4.95	0.02

Table A6.4. Summary of top selected linear mixed effect models (LMMs) predicting **hooded seals** THg values in time. Akaike's Information Criterion corrected for small sample size (AICc) and Δ AICc were used to identify top model sets (Δ AICc values ≤ 2). Normalized Akaike weights (Weight) were used to assess individual model information content.

Model	Selected variables	AICc	delta	weight
Base	Year + d15N	351.0	0.00	0.63
	d15N	352.1	1.09	0.36
	Year	359.5	8.42	0.009
Ecology	Year + d15N + d13c_corr	343.7	0.00	0.71
	Year + d15N + d13C_corr + d34S	345.6	1.87	0.28
	Year + d15N + d34S	353.2	9.45	0.006
Teleconnections	Year + d15N + d13c_corr + AOw	344.6	0.00	0.48
	Year + d15N + d13c_corr + NAO	345.2	0.57	0.36
	Year + d15N + d13c_corr + NAO + AOw	346.8	2.12	0.16
Climate	Year + d15N + d13c_corr + AOw + GSSIE	342.9	0.00	0.29
	Year + d15N + d13c_corr + AOw + GSSIE + SAT	343.5	0.67	0.21
	Year + d15N + d13c_corr + AOw + SAT	343.8	0.96	0.18
	Year + d15N + d13c_corr + AOw + SASIE	344.6	1.75	0.12
	Year + d15N + d13c_corr + AOw + SASIE + SAT + GSSIE	345.2	2.36	0.09
	Year + d15N + d13c_corr + AOw + ASIE + SAT	345.5	2.61	0.08
	Year + d15N + d13c_corr + AOw + ASIE	346.8	3.96	0.04
Diet	Year + d15N + d13C_corr + AOw + GSSIE + Rh + Gm	326.6	0.00	0.91
	Year + d15N + d13C_corr + AOw + GSSIE + Rh	331.3	4.65	0.09

Table A6.5. Estimated regression parameters for the most parsimonious linear mixed-effect models (LMM) predicting ringed seals and hooded seals THg concentrations.

Species	Intercept	Predictor variables									df	AICc	weight
		$\delta^{13}\text{C}_{\text{corr}}$	$\delta^{15}\text{N}$	Atlantic cod	AOW	NAO	SAT	Year	GSSIE	Greenland halibut			
Ringed seal	-1.18E-16	-0.09	0.42	-0.15		0.13	-0.09	-0.11			7	534.4	0.23
Hooded seal	-0.03	0.46	0.09		-0.21		-0.60	-0.34	-1.13	0.13	9	320.1	0.60